Republic of Iraq
Ministry of Higher Education
and Scientific Research
University of Babylon
College of sciences for Women
Department of Chemistry

Study and Application of New Flow Injection Units

A Thesis

Submitted to the council of the College of Science for Women, University of Babylon, in Partial Fulfillment of the Requirements for the Degree of Master of Sciences in Chemistry

By

Lubna Raad Abid AL-Ameer AL-Hetty

B.Sc. Babylon University (2019)

Supervised by

Prof. Dr. Dakhil Nassir Taha Al-Zurgany

&

Asst. Prof. Dr. Kadhim Khalaf Hashim

2022 A.D **1444 AH**

Certification

I certify that this thesis entitled "**Study and Application of new Flow Injection Units**" was prepared under my supervision at the Department of Chemistry, College of Science for Woman, Babylon University, in partial requirements for the degree of Master of science in chemistry.

Signatures:

Name: **Dr. Dakhil Nassir Taha**

Title: Professor

Address: Department of Chemistry, College of Sciences for Women, Babylon University

Date: //2022

Name: **Dr. Kadhim Khalaf Hashim**

Title: Assist. Professor

Address: College of Environment Sciences, AlQasim Green University

Date: //2022

Signature:

Name: **Dr. Hazim Yahya Mohammed Ali**

Title: Assist. Professor

Address: Head of Department of Chemistry, College of Sciences for women, Babylon University

Date://2022

قال تعالى

بسم الله الرحمن الرحيم

﴿و يسألونك عَنِ الرُّوحِ قُلِ الرُّوحُ مِنْ أَمْرِ رَبِّي وَمَا أُوتِيتُم مِّن الْعِلْمِ إِلاَّ قَلِيلاً ۝وَلَئِن شِئْنَا لَنَذْهَبَنَّ بِالَّذِي أَوْحَيْنَا إِلَيْكَ ثُمَّ لاَ تَجِدُ لَكَ بِهِ عَلَيْنَا وَكِيلاً ۝إِلاَّ رَحْمَةً مِّن رَّبِّكَ إِنَّ فَضْلَهُ كَانَ عَلَيْكَ كَبِيراً ۝﴾

صدق الله العظيم

سورة الإسراء: الآيات 85-87

قال رسول الله ﷺ

"من سلك طريقا يلتمس فيه علما سهل الله له طريقا الى الجنة"

صدق رسول الله ﷺ

Dedication

Praise be to God and enough, and prayers are upon the beloved Prophet, his family, and those who are faithful.

I Dedicate my work first

To my parents...my role model in life, who have the first and last credit for achieving this achievement through their support and encouragement for my education.

- Then to the source of knowledge and the one who is serious about his hand, his ideas, and his methods of working for the recurring and renewed innovations of designs and ideas in a new dress and diligent scientific work to the wonderful spiritual father (the Iraqi scientist Professor Dr. Dakhil Nasser Taha Al-Zarqani).

- To the one who put the love of chemistry in me... to my role model, the sea of knowledge, humility, and good morals (Assistant Professor Dr. Fouad Fadel Muhammad Al-Qaim).

- And to the constant, encouraging, and supportive giver... I am proud to be one of his students in the graduation project for the bachelor's degree (Assistant Professor Dr. Hazim Yahya Al-Jubouri).

To my colleagues and comrades.

I dedicate this humble work to everyone who loves me for the sake of Allah and wishes me well

Researcher

Lubna Raad Abid Al- Ameer

Thanks, and appreciation

I thank God Almighty for enabling me to accomplish this thesis and thanking God Almighty is not complete except by thanking his servants who often helped me make this work appear this way...

*** It gives me great pleasure, as I finish writing my work, to extend my deepest thanks and great gratitude to my first supervisor and my esteemed professor (Professor Dr. Dakhil Nasser Taha) for his abundant knowledge and guidance, which eased the difficulties that I faced and the obstacles I encountered, starting from his proposal for the research project until the completion of the preparation of this thesis, may God reward him on my behalf with all the best.**

*** I would also like to thank the second supervisor (Assistant Professor Dr. Kazem Khalaf Al-Sultani) for his provision of equipment and continuous follow-up; may God reward him with good.**

*** I extend my sincere thanks and appreciation to the Head of the Chemistry Department, represented by (Assistant Professor Dr. Hazem Yahya Al-Jubouri) for allowing me the opportunity to complete my studies. I extend my heartfelt thanks to my honorable professors, in particular (Prof. Dr. Sadiq Abdul-Hussein, Dr. Ali Talib, and Dr. Noor Abdul-Razzak), and all the members of the Department of Chemistry for their cooperation with me and to everyone who offered me help.**

*** I also extend my heartfelt thanks to (Assistant Professor Dr. Ahmed Saleh Farhoud) for his moral and material help and assistance. May God make it in the balance of his good deeds and grant him all the best.**

Abstract

Chapter one is includes an introduction of the flow injection, the beginnings of the flow injection system and its techniques, as well as the dispersion in the analysis of the flow injection, the types of dispersion, the dispersion coefficient and methods for its calculation and the factors affecting the dispersion of the sample area. It also briefly introduces fluorescence and electronic transitions and gives an overview of the reagent 1,2-Naphthoquinone-4-Sulfonate, Mefenamic acid, and Procaine hydrochloride (brief introduction, chemical and physical properties, dosage forms, uses, and some applications), followed by the aim of the research project.

Chapter two includes a description of the instruments and chemicals used and the preparation methods.

Chapter three is contains two parts: The first part describes the components of the flow injection system, while the second part deals with the determination of Mefenamic acid, Procaine hydrochloride, and NQS, and this is done through two methods:

The first system is based on absorbance. This part includes a detailed study for determining Mefenamic acid by merging-zone FIA technique in pure form using the NQS reagent. The method is based on the reaction of Mefenamic acid and NQS in an alkaline medium (0.2M of NaOH) to form a reddish-brown complex. The physical and chemical conditions are studied and improved. The graph of the linear calibration curve in the range (1-20) ppm with the correlation coefficient r = 0.9999, and the relative standard deviation percentile RSD % is 1.23 for a concentration of 13 ppm at the optimum conditions, 6 replicate measurements were carried out for the determined concentration.

Then Mefenamic acid is determined using the Reverse-contentious FIA technique in its pure form using the NQS reagent. The physical and chemical conditions are studied and improved. The graph of the linear calibration curve in the range (1-30) ppm with correlation coefficient r = 0.9869, and the relative standard deviation percentile RSD % is 0.5 for a concentration of 30 ppm at the optimum conditions, 6 replicate measurements were carried out for the determined concentration

After that, the same interaction is studied in the traditional method, and the obtained results are compared with the two developed methods. Each way show advantages. The graph of the linear calibration curve is in the range (0.5-10) ppm with a correlation coefficient r = 0.9997, and the relative standard deviation percentile RSD % is 0.072 for a concentration of 7 ppm.

The second system is based on fluorescence, this system include four different reactions that are studied:

1- Determining Procaine hydrochloride by merging-zone FIA technique in pure form in aqueous solutions. The physical and chemical conditions are studied and improved. The graph of the linear calibration curve with a range of (1-100) ppm with a correlation coefficient of r = 0.9986 and the relative standard deviation percentile RSD % is 2.008 for a concentration of 70 ppm.

2- Determining NQS by merging-zone FIA technique in pure form in aqueous solutions. The physical and chemical conditions are studied and improved. The graph of the linear calibration curve in the range (5-50) ppm with the correlation coefficient of r = 0.9976 and the relative standard deviation percentile RSD % is 1.941 for a concentration of 30 ppm

3- Determining Mefenamic acid by the traditional method in pure form using the NQS reagent. The process is based on the reaction of Mefenamic acid and NQS in an alkaline medium (NaOH) to form a reddish-brown complex that reduces or quenches the fluorescence luster of the NQS reagent. The graph of the linear calibration curve is in the range (1-100) ppm with a correlation coefficient of r=0.9993.

4- Determining Mefenamic acid by the traditional method in its pure form in aqueous solutions, as the MA in the pure state gives a fluorescence emission spectrum at 295.2 nm. The graph of the linear calibration curve is in the range (1-100) ppm with the correlation coefficient r=0.9988.

List of Content

List of Tables

List of Figures

List of Schemes

List of Abbreviations

Shorten	Full name
B.D.H	British Drug Houses
CFIA	Continuous flow injection analysis
D	Dispersion coefficient
DPV	Differential Pulse Voltammetry
EI	Enzymatic Inhibition
FIA	flow injection analysis
HC	Holding coil
HPLC	High-performance liquid chromatography
IR	Infrared
IUPAC	International Union of Pure and Applied Chemistry
MCFA/ MSFA	Mono-segmented continuous flow analysis
MEA	Mefenamic acid
MSFIA	Multi-syringe flow injection analysis
NMR	Nuclear Magnetic Resonance
NQS	1,2-Naphthoquinone-4-Sulfonic Acid Sodium Salt
NSAIDs	Non-steroidal anti-inflammatory drugs
pH	Acidic function
rFIA	Reverse flow injection analysis
RP-HPLC	Reversed Phase Liquid Chromatographic
S.D.I	state drug industry
SCFA	Segmented continuous flow analysis

Shorten	Full name
SERS	Surface-Enhanced Raman Scattering
SFA	Segmented flow analysis
SFIA	Stop-flow injection analysis
SIA	Sequential injection analysis
SIA-CL	Sequential Injection Analysis Chemiluminescence
SPCE	Screen-Printed Carbon Electrode
TNS	Transient Neurologic Symptoms
UV-Vis	Ultraviolet-visible spectroscopy

Chapter One

Introduction and Literature Review

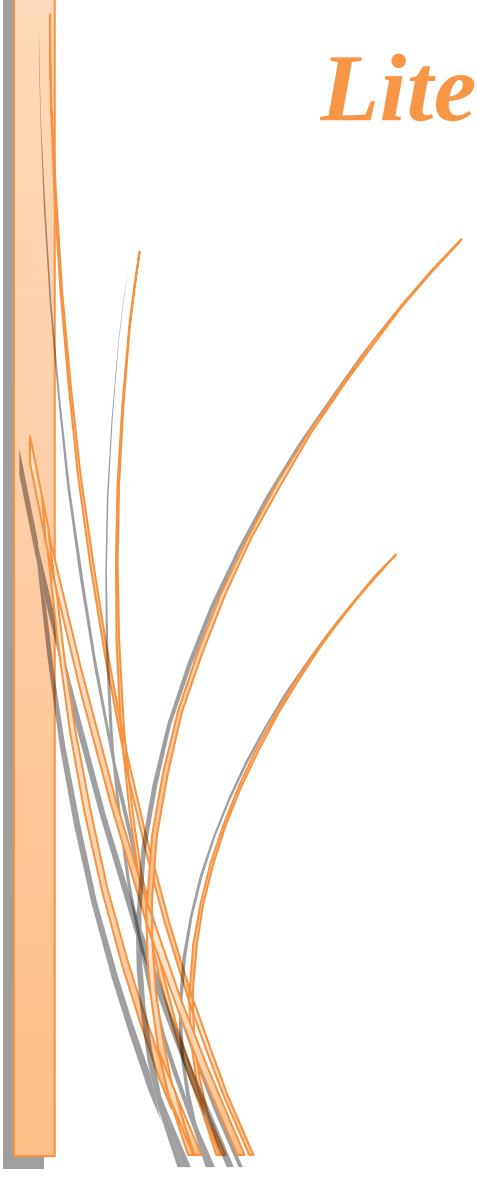

1. Introduction

1.1 Flow Analysis

Flow examination refers to the common name for all investigative techniques that rely on introducing a sample into a flowing liquid, it is referred to as the carrier stream through aspiration or injection into the medium [1].

Flow analysis can be divided into two categories based on two fundamental ideas [2]. It is possible to divide samples into two categories: those introduced continuously and those presented discretely, and those raised in a segmented or an unsegmented manner depending on the flowing media [3-5], as illustrated in Figure [1.1].

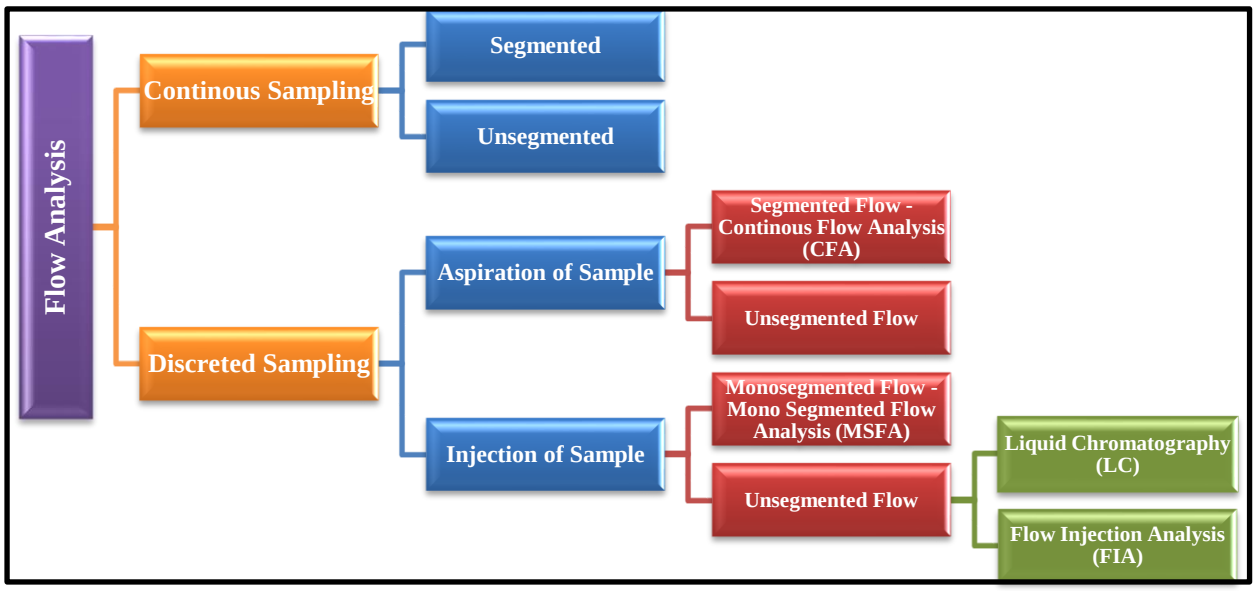

Figure [1.1]: Organization of flow analysis techniques by IUPAC guidelines

The applications of this technique include pharmaceutical analyses [6, 7], insecticide screenings [8, 9], cosmetics evaluations [10-12], and more. In flow injection analysis, many distinct advantages set it apart. These advantages are:

1. They convert open-system reactions (open cups) to closed-system responses.
2. It can reduce the analysis time by substituting mechanical processes instead of manual ones, such as mixing and separating, as it can quickly model at 120 analyzes per hour.
3. Its modern devices are characterized by being small in size.
4. The devices have a speedy response, as the time is between 5 and 200 seconds.
5. The injected sample volume is between 10 and 200 microliters and is not a consuming material. This technique does not require more than half a milliliter of the reagent solution at each analysis.
6. Personal errors are minimal compared to other techniques.
7. This technique appears in high congruence and repetition in the readings.
8. FA is combined with other analytical methods.

1.1.1 Beginnings of Flow Injection Analysis

Even though flow analysis has been around since the 1940s, it is still relatively new. In 1957, Skeggs' seminal work presented the general technique of segmented continuous flow analysis (SCFA) through air-segmented streams, which was later combined with other detection procedures such as redox potential, pH, turbidity, and spectrophotometric absorbance of radiation, as well as the elimination of the sampling stage of the analyzed material [3, 13-15]. These advancements laid the groundwork for the introduction of flow analysis in 2000 . This technique restricts sample longitudinal dispersion along the flow stream, which minimizes sample contact and allows for a more extended residence period of the sample, hence boosting sensitivity and allowing for comparatively slow reactions. However, any air bubbles injected into the liquid stream must be eliminated

before the test[16]. To avoid detection errors, aspirating the bubbles before detection is usual, as shown in Figure [1.2].

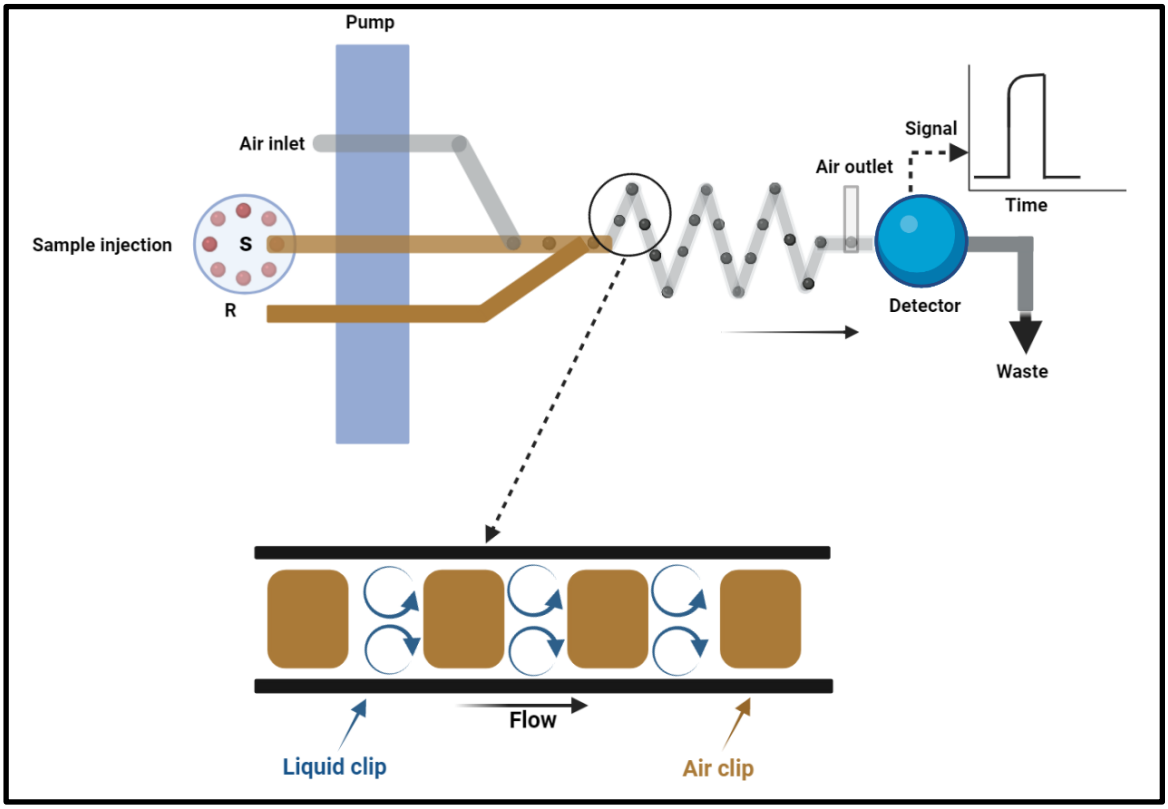

Figure [1.2]: The parts of the SFA analyzer and its mechanics

There are many disadvantages that have been identified from the use of this technique. These are:

1. It isn't easy to control the size of air bubbles.
2. The flow is irregular due to air pressure and rough paths of bubbles.
3. Emptying the air bubbles is required before they reach the cell.
4. The difficulty of completely controlling the movement of the carrier current.
5. The bubble analysis device is large and complex.

In the literature, it is noted that the new idea of continuous flow analysis was simultaneously patented in 1975 by Ruzicka and Hansen in Denmark and Stewart in the United States [4].

A continuous flow injection analysis (CFIA) manifold injects a liquid sample into a non-segmented continuous carrier stream of a suitable liquid using a (CFIA) manifold. This equipment is simple, affordable, and has a high sample rate and dependability while still being easy to use. The residence time of the model in a non-segmented stream is much less than the residence time in an air-segmented system. Following that, several other highly competitive flow injection instruments were created and deployed to various applications in the following years.

The FIA device, which has a column as part of its design, appears superficially to be the HPLC device, with the likeness and convergence in flow velocity and size being preserved in the rest of the device (pump, valve, detector, and recorder) as shown in Figure [1.3]. Because the fluid in HPLC requires a strong thrust force through the column material, the pressure in HPLC is 70 atmospheres, whereas, in FIA, it is 0.5 atmospheres, as a simple peristaltic pump (i.e., a pump with no valves) is used. While these techniques have different purposes, the most significant difference is their focus. FIA is meant to find the most important number of samples with the fewest reagents and sample solutions, while HPLC is about separating and estimating several components in one model.

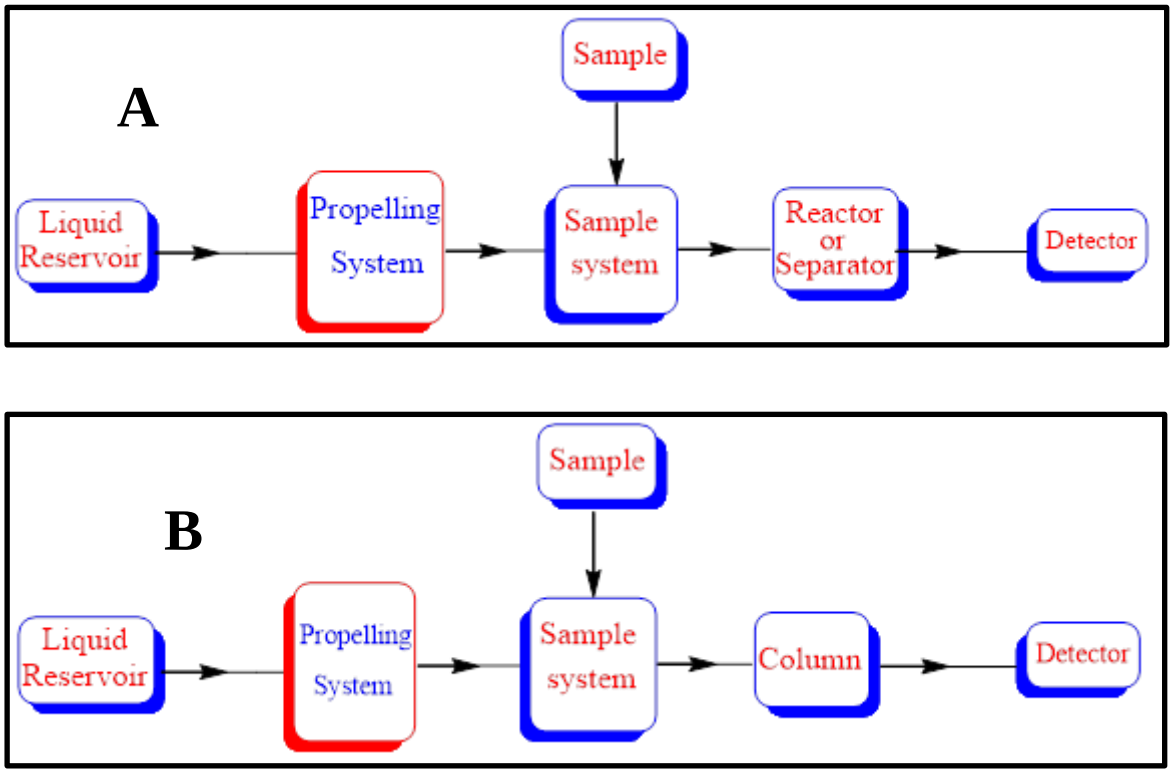

Figure [1.3]: Similarity between (A) FIA. and (B) HPLC.

1.1.2 Technical Modes of Flow Injection Analysis

1.1.2.1 Merging Zones Technique

Bergamin and colleagues were the first to propose merging zones in 1978 . In this way, the problem of continuous flow injection instruments was avoided, which used the reagent endlessly even when there was no sample to analyze. Even though volumes at the CFIA do not exceed a few hundred microliters, the merging zones technique resulted in considerable cost savings, and notably for expensive chemicals such as phenol. This method must inject each sample and reagent separately into the carrier stream, which is accomplished using a twofold injection valve. As a result, the sample-reagent zone is produced, and the sample is then transferred to the detector for analysis[17], as shown in Figure [1.4].

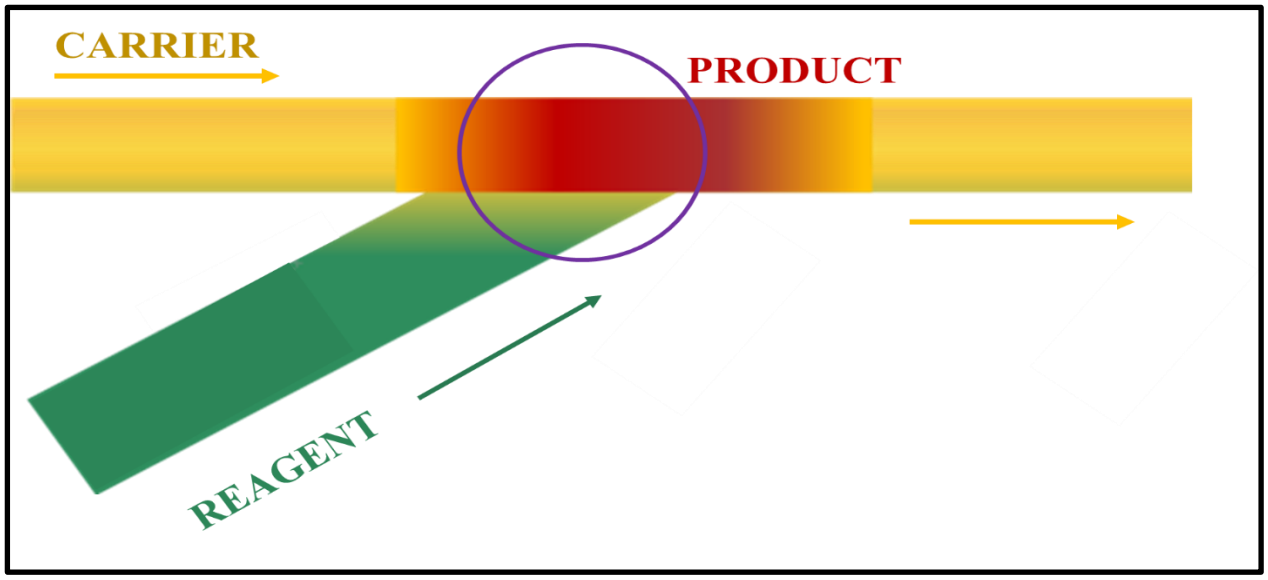

Figure [1.4]: Merging zone technique

1.1.2.2 Stop-Flow Injection Analysis

In 1979, Ruzicka and Hansen proposed stop-flow injection analysis (SFIA) to detect glucose and urea levels in blood serum samples . The injection process is identical to that used in FIA, except that when the sample/reagent zone reaches the flow cell, the carrier stream is terminated, and the flow cell is closed. Selecting and regulating the stopping time improves sensitivity while simultaneously reducing dispersion by extending the residence time of slow reactions without increasing the length of the reaction coil. The waste generation, enabling kinetic studies across a wide range of concentrations and wavelengths, reducing reagent use and waste generation, and enabling kinetic studies across a wide range of concentrations and wavelengths[18], as shown in Figure [1.5].

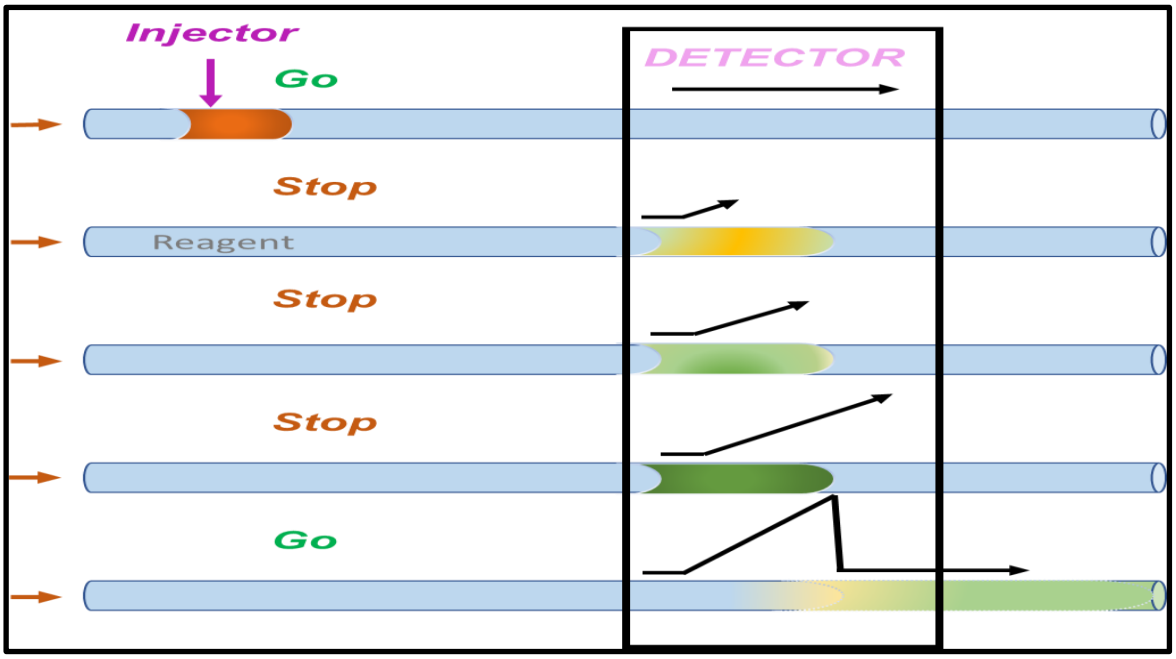

Figure [1.5]: Stop Flow Injection Analysis

1.1.2.3 Reversed Flow Injection Analysis

Johnson and Petty first proposed this technique in 1982 as an early attempt to detect the amount of phosphate in seawater by injecting the reagent into the water . rFIA was utilized, which is a reversed FIA technique. The sample was pumped continuously rather than through a carrier, and a premixed reagent was injected instead of a page; this is partly because dispersion in rFIA is lower than in traditional FIA, which reduces the diluting impact and increases insensitivity[19].

When the reagents used are expensive, and the model is cheap and available in large quantities, it is preferable to reverse the injection process. In rFIA, the reagent solution is injected into the sample solution, as the latter becomes the conductive current. This technology is characterized by being economical because the used detector is small. Still, this technology is flawed as it consumes the sample solution. The valves need a cleaning process at each

analysis, which causes time consumption and reduces the number of analyzed samples.

1.1.2.4 Mono-segmented Flow Analysis

To increase the sample rate and sensitivity of continuous flow measurements, Pasquini and de Oliviera developed mono-segmented continuous flow analysis (MCFA) or (MSFA) in 1985 . The sample zone must be injected between two bubbles of air or inert gas to prevent it from being scattered by the carrier solution. In the absence of chemical reaction or sufficient residence time for the response to approach equilibrium without axial dispersion between the sample/reagent zone and carrier, this technique provides measurements that can be made without interference [20].

1.1.2.5 Sequential Injection Analysis

Ruzicka and Marshall introduced sequential injection analysis in 1990 by publishing the first description (SIA) . The SIA technique is based on the sequential sample injection and reagent into a holding coil and toward the pump via a selection valve. After that, the flow is reversed to propel the piece and reagent-distributed zones through the reaction coil and detector before being changed again [21], as shown in Figures [1.6] and [1.7].

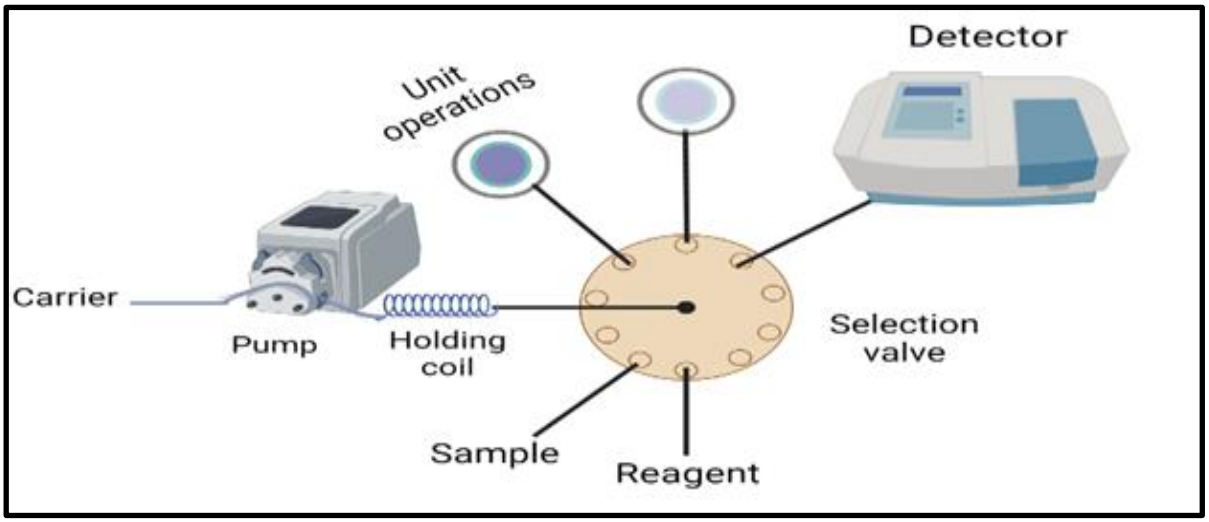

Figure [1.6]: The manifold of Sequential Injection Analysis

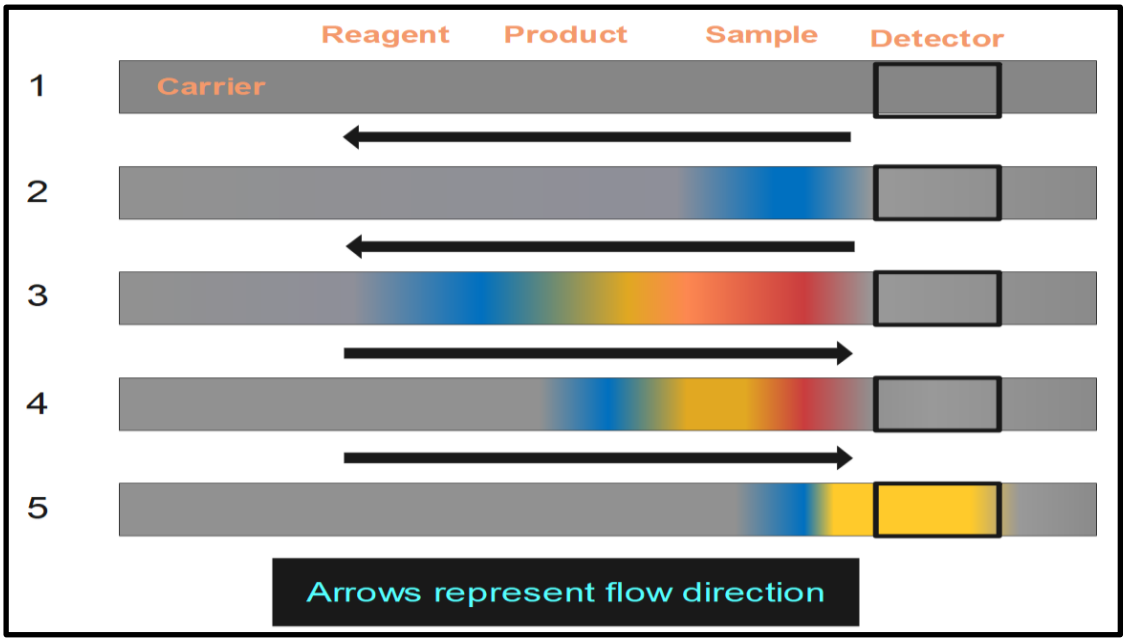

Figure [1.7]: The SIA method is composed of the following steps: (1) satisfying the holding coil (HC) with carrier solution, (2) aspirating the reagent into the HC, (3) aspirating the sample into the HC, (4) fraternization to generate a sample/reagent zone, and (5) measuring the product zone at the detector.

In addition to versatility and comprehensive computer interoperability, SIA offers excellent sample throughput and lower reagent and sample use than other systems.

1.1.2.6 Analyses of Injections Using Multiple Syringes

The multi-syringe flow injection analysis (MSFIA) technique was developed in 1999 as a very speedy and resilient solution for automating many procedures that combined the advantages of both the FIA and SIA techniques. Automatic flow injection systems of this type comprise an auto burette equipped with four syringes for injection. Peristaltic pumps move different liquids at high flow rates, comparable to how they work. Each syringe's head is equipped with a two-way commutation valve, which allows for coupling the needle to the manifold lines of the solution reservoir as desired [22].

1.1.3 Dispersion in FIA

Controlling the dispersion of the sample is one of the principles of FIA, so when designing any FIA system, attention is focused on two things: the amount of the original sample solution that is diluted by diffusion on its way towards the detector and the time it takes for the sample area to cut the distance from the injection valve to the sensor. Distribution occurs at the convergence of two liquids of different concentrations, as the internal penetration of the molecules of a fluid occurs through another fluid in contact with it, which is called dispersion. It contributes to the interaction between the sample material and the detector, increasing insensitivity. Also, it causes the occurrence of a mitigation process that, in turn, reduces sensitivity and increases the breadth of the top area. It is concluded that the dominant chemical reaction causes an increase in sensitivity with an increase in dispersion [23]. Still, sometimes dilution is the main influencing factor, which leads to a decrease in the method's

sensitivity, so it is necessary to control and balance the effects of the chemical reaction and the dilution process.

1.1.3.1 Dispersion Types

A- Axial Dispersion: occurs in the current flow direction and leads to attenuation and widening at the top, more significant than radial dispersion. The axial distribution clearly shows its effect in straight pipes, as shown in Figure [1.8], and the axial dispersion is called laminar flow [24].

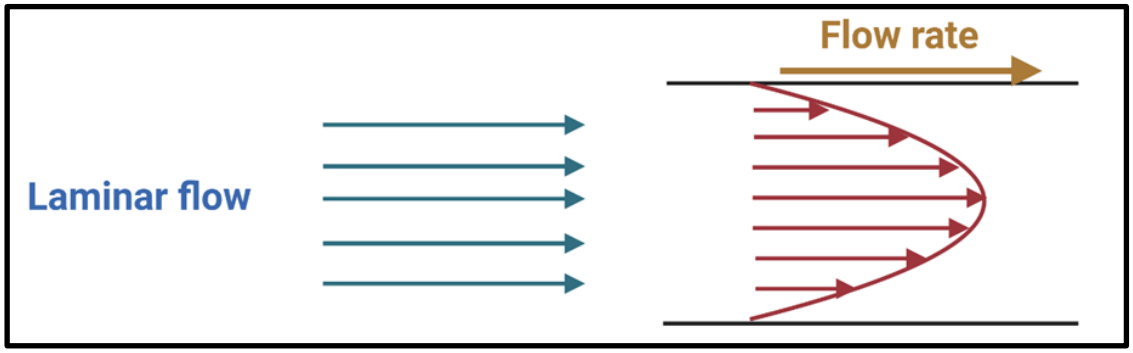

Figure [1.8]: Axial dispersion

B- Radial Dispersion: is produced by the effect of the current flowing, which is usually directed towards the walls, so it causes mixing to occur with the least amount of dilution and expansion in the area of the top. Using coiled tubes and reactors, the bends in the flow path cause greater sensitivity and narrow, sharp peaks. Figure [1.9] shows the flow path's radial dispersion resulting from hooks [25].

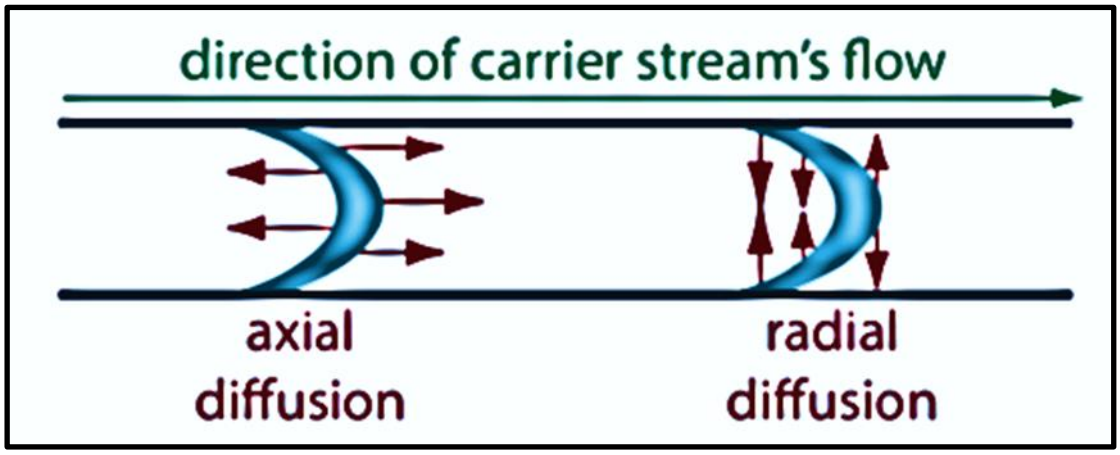

Figure [1.9]: Type of dispersion

1.1.3.2 Dispersion coefficient

The dispersion coefficient (D) is distinct as the ratio between the concentration before and after dilution as shown in Figure [1.10] [26-29].

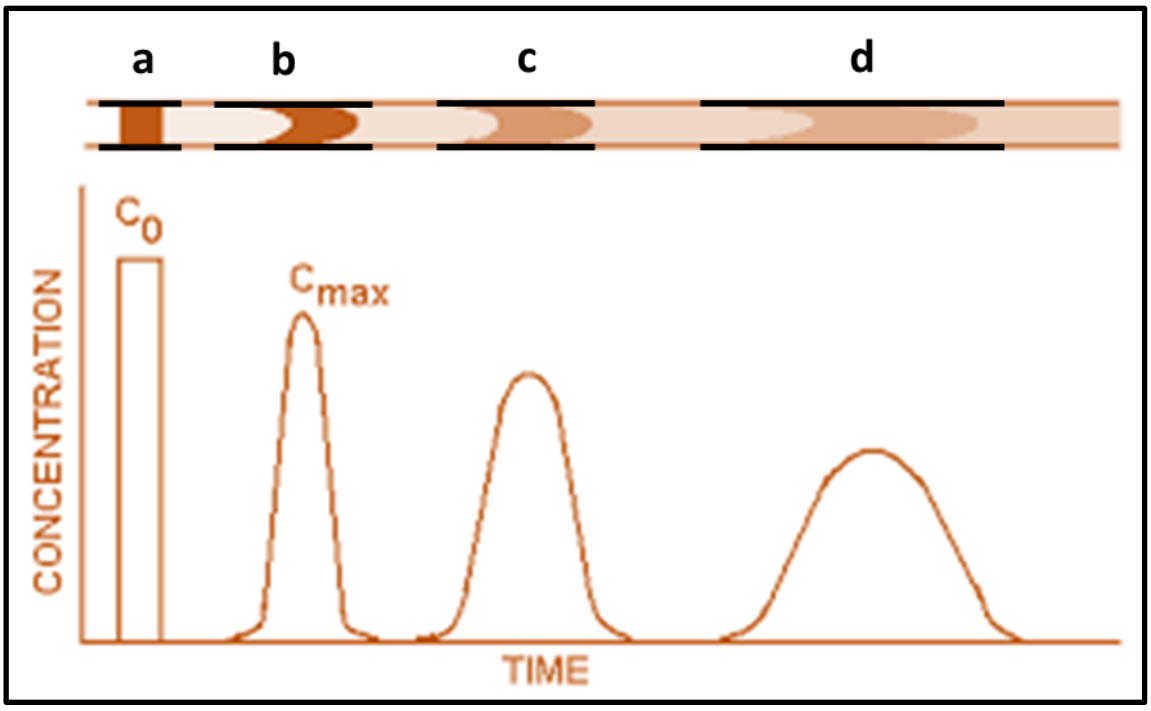

Figure [1.10]: Effect of dispersion on the shape of a sample's flow profile at different times during a flow injection analysis; (a) at injection valve before flow at the manifold ((t_o=0)), (b) when convection dominates dispersion

($((t_1>t_o))$), (c) when convection and diffusion contribute to dispersion($((t_2>t_1))$); and (d) when diffusion dominates dispersion ($((t_2>>))$). (Co= Conc. in injected volume, C= peak conc. at detector).

The dispersion coefficient is given by Equation [1.1].

$$D = C^o / C_{max} = H^o / H_{max} = A^o / A_{max} \ldots\ldots\ldots\ldots\ldots [1.1]$$

C_{max} Concentration after dilution in the recorded curve

C^o Original concentration of the injected form solution

H_{max}, H^o When dealing with the height of the summit as a reading

A_{max}, A^o When dealing with absorbance as a reading

The FIA regulations give dispersion three categories [30-34]**:**

1- When 3 > D > 1, the scattering is low or limited. It is preferred to achieve high analytical sensitivity in coordination with detectors with high sensitivity, such as ionic selective electrodes, atomic spectroscopy, and electrical conductivity.
2- When 10 > D > 3 the classification is as medium dispersion. It is commonly used whenever a special mixing process is required for the sample area with the detector, such as spectroscopic methods.
3- As for the high dispersion systems when D > 10, they are used in cases where parts require intense mixing of the sample area with the reagents, such as flow-injection adjustments and slow reactions that require a long time to complete the response.

1.1.3.3 Method for Calculating the Dispersion Coefficient

The dispersion coefficient is measured by comparing the response resulting from two cases [35, 36]

1- Mixing the sample solution at a specific concentration with the reacting solutions and injecting the resulting solution into the system as the resulting curve reaches a steady-state, which is °H, which is proportional to the concentration of the solution original °C, this response is free from dispersal effects.
2- The other case includes injecting the sample with the same concentration into the line of the carrier solution and recording the response H_{max} is proportional to the concentration C_{max}, as the effect of dispersion emerges, as the reaction here is less than continuous response (°C) and the value of D is calculated through Equation [1.1].

1.1.3.4 Factors Affecting the Dispersion of the Sample Area

The degree of dispersion and the height of the recorded peak is determined by several factors, including the injected sample and the flow channels' geometry, lengths, and flow velocity [37].

1.1.3.4.1 Injected Sample Volume

The injected model is one of the critical factors affecting the dispersion process. It increases the sensitivity size (peak height) as the size of the injected sample increases. Still, with larger volumes of samples, there will be no complete dispersion of the model in the reagent solution; as the increase in the example is relative to a decrease in sensitivity and an increase in time, the

detector may cause a broad peak or may cause a double in height and increase time to analyze necessary [38].

1.1.3.4.2 Volume of Reagents

The change in the volume of reagents through changing the lengths of the model connections plays an essential role in the effect on dispersion and, therefore, sensitivity, which increases directly with the size of the detector to increase the distribution of the sensor in the model. Still, the high volumes when reading the model cause distortion and a double peak. Still, the single-channel system means that the detector is the carrier solution, so the sensor size is ineffective. The latter does not apply to the single-channel system that operates with the inverse gastric injection technique, as the size of the detector becomes the effect mentioned previously [39].

1.1.3.4.3 Engineering Formation of Pipes

Reaction coils and coil-shaped tubes are preferred over straight lines, and this is to increase the degree of mixing with radial dispersion using secondary flow events as a result of centrifugal forces when the solution passes through the twisted areas, and this leads to a radial mixing in the size of the injected sample and thus reduces the axial dispersion [40].

1.1.3.4.4 Dimensions of the Reaction Coil

The scattering of the sample area upsurges with the increase in the internal diameters of the reaction coil, tubes, and channels, as the value of samples and D, is directly proportional to the square of the pipe diameter, so doubling the pipe diameter increases the volume the required reagents are four times. The dispersion of the sample area increases with the increase in the

distance it travels. With the rise in the length of the tubes, the time for diffusion increases, while there is less time for diffusion to occur in short-length tubes. In addition, increasing the length of the coil delays the analysis time, therefore, the number of samples is localized in a specific time, so it is preferable to use smaller lengths. When the output is formed at speed, sometimes it utilizes a high reaction coil lengths case. It is essential when the reaction needs time to complete (slow responses). The latter increases the reaction coil's length to increase the peak's height [41].

1.1.3.4.5 Flow Rate

Ruzica and Hansen explain that dispersal incidence is less at slow flow velocities. Decreasing the flow velocity increases the retention time of the sample before it is transferred to the detector. In this case, the model and sensor interaction reach equilibrium. Then the response will be higher at lower flow velocities. Higher velocities reduce sensitivity than lower velocities. A broad, double, distorted peak appears, increasing the analysis time and thus reducing the number of samples. The proportion of materials mixing and spreading among them may be slow, with an increase in speed. In the loop, the mixing increases at a specific time and, therefore, the height of the top gains [42].

1.1.3.4.6 The Degree of Mixing of Solutions

The mixing ratio of one substance solution varies with another when the sample solution mixes with the reagent quickly; this means that the dispersion is fast and a rapid response appears, but when the mixing is ventilated, the distribution is slow; also, this requires changing other factors that affect mixing and thus dispersion, such as velocity, temperature and length interaction file [43].

1.1.3.4.7 Concentration of Reagents

The reagent concentration is one factor that affects the scattering area and thus sensitivity. Low concentrations from the detector compared to the model's attention gives a low sensitivity. Still, increasing the engagement increases the sensitivity (Peak height). When all the sample quantity is reacted and converted into a product, the reagent concentration increase becomes non-existent effective. The high concentrations of the reagent 1 x 10^{-3} molar in the single-channel system in which the solution is the detector is the carrier current working to produce a noise more significant than the baseline. Therefore, it is preferable to use very dilute concentrations of 1 x 10^{-5} molar so that the noise of the detector signal does not interfere with the peak signal [44].

1.1.4 Components of Flow Injection Units:[45]

1. The pump propels the carrier stream through a narrow tube.
2. Connection tubes.
3. An injection port (injection valve) introduces a minor discrete sample or standard into the carrier stream.
4. Reaction coil: A sample processing step is responsible for the mixing of reagents, samples, and standards, the dilution of the piece, and the enrichment of models for trace study.
5. Detector: important to measure response.

1.2. Fluorescence

At ambient temperature, most molecules are at their lowest vibrational level, known as the ground electronic state, and are promoted to excited states due to light. Simple illustrations of molecule absorption to produce the first, S1,

or second, S2, excited states are shown in the following diagrams in Figure [1.11] [46].

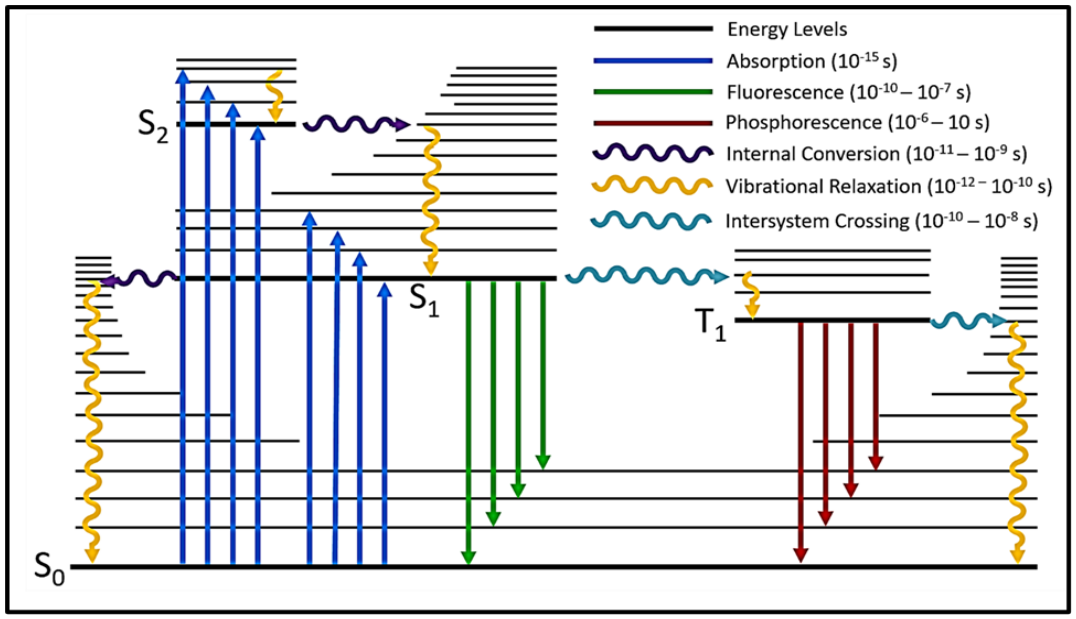

Figure [1.11]: Transitions that contribute to the formation of absorption and fluorescence emission spectra [47, 48]

Excitation can cause the molecule to vibrate at one of the vibrational sub-levels associated with each electronic state, depending on the nature of the excitation. Because the energy is absorbed in discrete quanta, distinct absorption bands are expected to be formed. As previously stated, the simplified picture above does not consider the rotational levels associated with each vibrational level, which generally increases the number of possible absorption bands to the point where individual transitions become challenging to resolve. As a result, most compounds, except those with local rotational levels, have broad absorption spectra (for example, planar and aromatic compounds). After absorbing energy and attaining one of the higher vibrational frequencies of the excited state, the molecule loses all of its surplus vibrational energy due to a collision with another molecule. It decays to the vibrational level that corresponds to the excited state's lowest vibrational level. As a bonus, virtually

every molecule with an electronic structure more significant than the second undergoes internal conversion and transitions with the same energy from its lowest vibrational level to a higher vibrational level of a lower excited state. For the molecules to achieve the lowest vibrational level of their initial excited state, they must continue to lose energy. The molecule can then return to any of the vibrational vibrations of the ground state, generating energy in the form of fluorescence. The quantum efficiency of the solution will be maximized if this step is repeated for all molecules that have absorbed light. If the alternative path is never used, the quantum efficiency of the alternative way will be less than one, and it may even be close to zero. The 0 - 0 transition, which connects the lowest vibrational level of the ground electronic state to the lowest vibrational level of the first excited state, happens in both absorption and emission processes and can be used to distinguish between the two types of methods [49]. All other absorption transitions take significantly more energy than fluorescence emission transitions. Therefore, it may be expected that the emission spectrum will overlap the absorption spectrum at the wavelength associated with the zero-to-zero transition and that the remainder of the emission spectrum will be either lower in energy or longer in wavelength than the absorption spectrum [50] Figure [1.12].

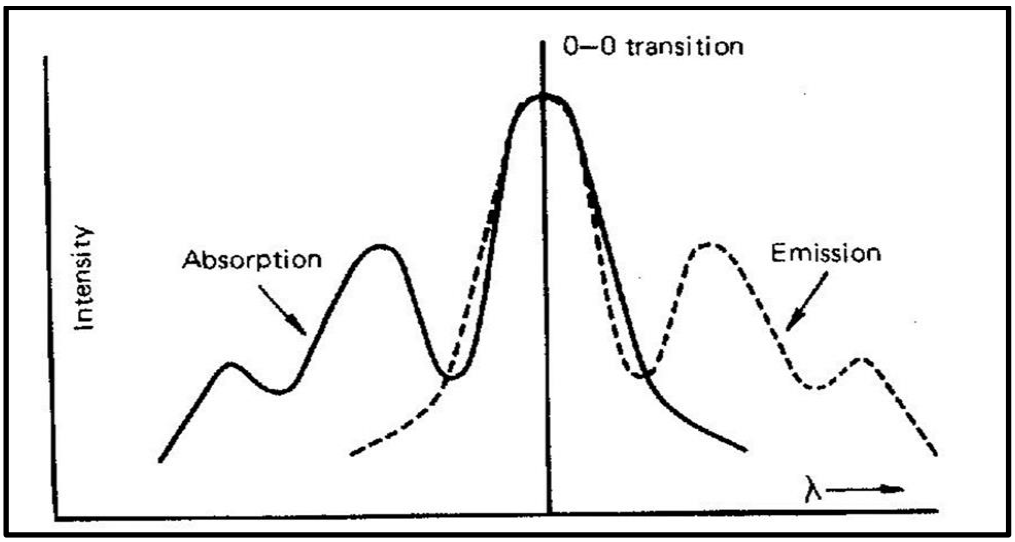

Figure [1.12]: Idealized Absorption and Emission Spectra [51]

The absorption and emission spectra coincide strictly at the spectrum's 0-0 transitions. The discrepancy signifies little energy lost due to the absorbing molecule's interaction with the solvent molecules in the surrounding environment. Due to the energy absorption necessary to reach the initial excited state, the molecule's structure is mostly unaffected. Accordingly, the ground and first excited states have a comparable distribution of vibrational levels. The energy discrepancies between emission and absorption bands will equal their energy disparities [52]. There are numerous instances where the emission spectra are the inverse of the absorption spectra. Because fluorescence emission always originates at the lowest vibrational level of the first excited state, the shape of the emission spectrum remains constant regardless of the wavelength of the stimulating light. The emission spectrum depicts how much light is emitted compared to the excitation wavelength. It is necessary to vary the wavelength of the exciting light while simultaneously charting the emission from the sample as a function of the wavelength of the exciting light to acquire the excitation spectrum. The corrected excitation spectrum is a plot of emission vs. excitation wavelength produced when the intensity of the exciting light remains constant while the wavelength of the light changes.

The quantum efficiency of complex compounds is not dependent on the wavelength of light used, which is valid for the vast majority of such compounds. Except for molecules with a high molecular extinction coefficient, the emission will be proportional to their molecular extinction coefficient. In other words, a substance's corrected excitation spectrum will be similar to its absorption spectrum if the substance does not have a high molecular extinction coefficient [53-55].

1.3. 1,2-Naphthoquinone-4-Sulfonate:

Inorganic amines and amino acids are being determined analytically utilizing 1,2-Naphthoquinone-4-sulfonate (NQS), which is increasingly being used in conjunction with ultraviolet/visible (UV-Vis) spectrophotometric detection methods [56-58]. In 1922, Folin proposed using of NQS as a reagent for the calorimetric determination of amino acids. Initial experiments resulted in the development of an amino acid identification method, in which amino groups are coupled with NQS in an alkaline solution to produce vibrantly colored molecules. Numerous studies have used the reagent to determine the presence of amines, and reddish dyes have been extracted into chloroform using the same method. The quantitative analysis of phenethylamine compounds was carried out using NQS [59]. Extraction of the reaction products was accomplished by thin-layer chromatography [60], which was followed by analysis utilizing a range of techniques, including elemental analysis, nuclear magnetic resonance (NMR), infrared (IR), and mass spectrometry [61] as shown in Figure [1.13].

Figure [1.13]: Image of NQS in nature and Chemical Structure

1.4 Drugs

1.4.1 Mefenamic Acid (MA)

1.4.1.1 Brief Introduction of Mefenamic Acid (MA):

Mefenamic acid, an anthranilic acid derivative, is a non-steroidal anti-inflammatory medication (NSAID) that belongs to the fenamate class [62]. It has a short plasma half-life of 2 hours. Non-steroidal anti-inflammatory drugs are classified into eight classes based on their structural similarities. Among these classes, anthranilic acid derivatives play a significant role. Mefenamic acid treats various types of discomfort, including menstrual cramps. It acts as an anti-inflammatory, analgesic, and antipyretic. Mefenamic, like other NSAIDs, is non-selective. It inhibits the two cyclooxygenase isoforms (COX-1 and COX-2), inhibiting the metabolism of cellular arachidonic acid (AA) and upregulating prostaglandin production, resulting in an increase in vascular permeability, edema, hyperalgesia, pyrexia, and inflammation [63-66]. IUPAC Name: N-(2,3-dimethyl phenyl)-2-aminobenzoic acid. Molecular Formula: $C_{15}H_{15}NO_2$ Figure [1.14]

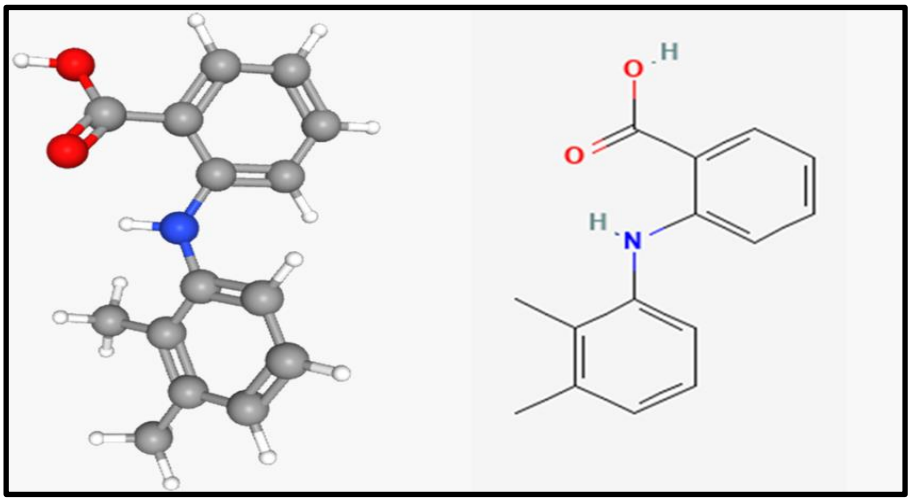

Figure [1.14]: The Chemical Structure of Mefenamic Acid.

1.4.1.2 Chemical and Physical Properties of Mefenamic Acid[65]

- Trade name: Ponstel, Ponstan, many others.
- Molecular Weight: 241.285 g/mol.
- State: Solid (i.e., a white crystalline powder).
- Solubility: It dissolves in dilute solutions of alkali hydroxides. Practically insoluble in water, slightly soluble in ethanol (96 percent), and methylene chloride.
- Pka= 4.2 (at 25℃).
- Elimination half-life: 2–4 hours.
- Melting point= 230 °C.

1.4.1.3 Dosage Forms of Mefenamic Acid [66]

MEF is available in the market as:

- Capsule.
- Tablet.

1.4.1.4 Usage of Mefenamic Acid

Relieve mild to moderate pain, including menstrual pain [63].

1.4.2. Procaine Hydrochloride

1.4.2.1 Brief Introduction of Procaine HCl

Caine is a short-acting ester local anesthetic which is used as a substitute for cocaine as a spinal aesthetic in the early twentieth century. It is also one of the earliest spinal aesthetics, having replaced cocaine as the preferred spinal aesthetic in the early twentieth century. However, due to concerns regarding lidocaine and transient neurologic symptoms (TNS), Procaine has been re-

evaluated as a fast-acting local aesthetic option. However, this medication is not widely used because it has a higher failure rate than lidocaine, causes significantly more nausea, and requires a longer recovery. 135 If used, it is often administered as a hyperbaric drug in dosages ranging from 50 to 200 mg at a 10 percent concentration [67-69]. IUPAC Name**:** 2-(diethylamino) ethyl4-aminobenzoate; hydrochloride. Molecular Formula: $C_{13}H_{21}ClN_2O_2$ Figure [1.15].

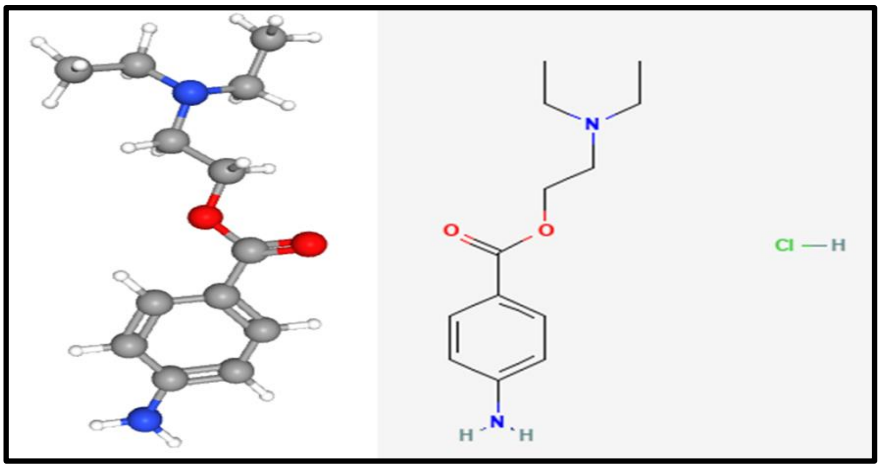

Figure [1.15]: The Chemical Structure of Procaine

1.4.2.2 Chemical and Physical Properties of Procaine [69]

- Trade name: Novocain or Neocene.
- Molecular Weight: 272.77 g/mole.
- State: Solid (i.e., a white crystalline powder).
- Solubility: It dissolves well in water and less in alcohol and is insoluble in ether.
- Elimination half-life: 40–84 seconds.
- Melting point: 155-175 °C.

1.4.2.3 Dosage Forms of Procaine

Procaine is available in the market as a capsule, tablet, and injection.

1.4.2.4 Using of Procaine:

- Local an aesthesia.
- To treat many diseases:
  - Fat.
  - Subscription.
  - Orgasm.
  - Cancer diseases.

1.5 Literature Review of the Analytical Method Used for the Determination of Mefenamic Acid and Procaine HCl

Table [1.1] below represents different methods that are used to determine Mefenamic Acid and Procaine hydrochloride.

Table [1.1]: Different Methods used to Determine Mefenamic Acid and Procaine Hydrochloride

	Reagent	λ_{max} nm	Technology	LOD mg L^{-1}	LOQ mg L^{-1}	R^2	Range mg L^{-1}	RSD	Slope	Recovery %	Ref.
Mefenamic acid	Potassium ferricyanide	465	FI Spectrophotometric	—	—	0.9998	1.00-100	0.82	1.68 $\times 10^{-2}$	—	[70]
	—	280	HPLC	15	25	0.998	25 – 4000 ng/mL	10.6 %	0.0003	110±7.5	[71]
	Ce (IV)	Ex 255 Em 354	Spectrofluorimetric	0.009	—	—	0.03 – 1.5	1.72 %	—	102–109	[72]
	—	300	HPLC	1.5	5.9	0.998	50 – 250	0.090	1.77	99.61	[73]
	—	—	potentiometric	6.2×10^{-7}	—	0.998	10^{-6}– 10^{-2}	1.5	58.9 ± 0.7	100.14	[74]
	Chloranil	540	spectrophotometric	2.16	7.15	0.9996	10 – 60	—	2.4×10^{-2}	—	[75]
	Ferric chloride with o-phenanthroline	510	Indirect Spectrophotometric	0.065	0.195	0.9993	0.4 – 2.0	<2.0	0.048	100 ± 0.92	[76]
	EEM	460	spectrofluorimetric	0.32	—	0.995	0.66 – 10.00	—	—	109.0	[77]

	Reagent	λ_{max} nm	Technology	LOD mg L^{-1}	LOQ mg L^{-1}	R^2	Range mg L^{-1}	RSD	Slope	Recovery %	Ref.
Mefenamic acid	—	220	RP-HPLC	0.39	1.2	0.999	100 – 300	—	866.4	99.7 – 102.2	[78]
	NQS	450	spectrophotometric	0.189	—	0.9995	0.5 – 10.0	1.29– 2.14	0.1409	99.80 – 100.80	[79]
	Astrafloxin	533	extraction – spectrophotometric	0.72	—	0.9988	2.0 – 21.0	—	0.1443	—	[80]
	—	280	extraction and HPLC	0.075	—	0.989	0.7– 100	4.2	—	—	[81]
	—	225	TLC-densitometric RP-HPLC-DAD	—	—	0.9999 , 0.9997	0.3–2 , 7–50	1.134 , 1.389	5207 , 117.11	99.558 ± 0.928 , 99.52 ± 0.346	[82]
	—	282	Developed HPLC	4.88	14.78	0.9999	1.29 – 806	1.07	0.2064	101.10 ± 1.56	[83]
	—	—	Voltametric	1.94 nM	—	0.990	1x 10^{-8} – 3x10^{-6} M	3.7375	—	96.35	[84]
	Metol	533	Spectrophotometric	0.03 mg/ml	0.1 mg/ml	0.9949	2.4 – 24	0.4	—	100.01	[85]

	Reagent	λ_{max} nm	Technology	LOD mg L^{-1}	LOQ mg L^{-1}	R^2	Range mg L^{-1}	RSD	Slope	Recovery %	Ref.
Procaine hydrochloride	4-dimethylaminocinnamaldehyde	547.5	stopped-flow	—	—	0.998	0.5 – 20	0.73	8.41×10^{-3}	—	[86]
	acetone and aged	Ex 402 Em 494	Spectrofluorimetric	7.7	—	0.999	0 –250	2.16	—	—	[87]
	p-dimethylaminobenzalhyde	455	Spectrophotometric	0.1	—	0.9994	0.2–15	1.7	—	92.0–110.0	[88]
	KMnO4	> 390	SIA-CL	0.3	—	0.9998	0.5–50	3.6	—	—	[89]
	pumice modified carbon paste electrode	—	DPV	5.0×10^{-8} M	—	0.995	9.0×10^{-7} – 2.6×10^{-5} M	3.2	5.062×10^{3}	95.2–104.8	[90]
	NQS	484	Spectrophotometric	0.28	—	0.9996	30 – 100	—	19.23	98.0 – 105.2	[91]

	Reagent	λ_{max} nm	Technology	LOD mg L^{-1}	LOQ mg L^{-1}	R^2	Range mg L^{-1}	RSD	Slope	Recovery %	Ref.
Procaine hydrochloride	fluorescamine	Ex 400 Em 494	sequential injection fluorometric	2.6	—	0.9980	10–200	2.1	—	—	[92]
	—	—	FIA using SPCE	6.0×10^{-6} M	—	0.9997	9.0×10^{-6}– 1.0×10^{-4} M	3.2	—	94.8 – 102.3	[93]
	H_2O_2	550	UV-Vis (EI)	3.80×10^{-8} M	—	0.9783	1.50×10^{-7}– 4.15×10^{-6} M	3.05	—	—	[94]
	Phenol	450	Spectrophotometric	1.2931	4.3103	0.9983	2–22	1.651	0.0798	99.82–101.50	[95]
	potassium peroxymonosulfate	—	polarographic	6×10^{-6}	1.9×10^{-6}	0.9996	1×10^{-6}– 5×10^{-5}	1.13	9.1×10^{4}	—	[96]
	Ag-Np	633	SERS	1×10^{-11} M	—	0.9994	10^{-7}– 10^{-10} M	—	216.12	—	[97]

1.5 The Current Work Aims at:

1. Designing new flow injection units to determination Mefenamic acid, Procaine hydrochloride, and NQS.
2. It is determining the optimum conditions for the reaction and studying the physical with chemical variables affecting the estimation, such as Flow rate, Reaction Coil, pH, Volume of buffer, and reagent concentration.
3. Calculating the sampling rate, dispersion coefficient, dead volume, and repeatability.
4. Mefenamic acid, Procaine, and NQS are determined from their aqueous solutions by spectrophotometric with FIA, batch spectrophotometric method, and Spectrofluorimetric.

Chapter Two

Chemicals and Apparatus

2. Chemicals and Apparatus

2.1. Tools and Apparatus used

Several techniques and tools are used in the current study, most of which are listed in Table [2.1].

Table [2.1]: Devices Used in the Study and their Manufacturers

No.	Instrument	Model	Company supplied
1	[1]BioLogic QuadTec UV-Vis Detector	130200	BIO-RAD, U.S.A.
2	[1]Spectrophotometer	PD-303	APEL, Japan
3	[1]Competence Analytical Balance	CPA2P	SARTORIUS, Germany
4	[1]Peristaltic pump	Rabbit Peristaltic Pump	RAININ, France
5	[1]Rotary 6- port injection valve	7725i	RHEODYNE, U.S.A.
6	[1]Reaction coil	Teflon tube	__
7	[1]Connection tubes	silicone rubber	__
8	[1]Data Acquisition	USB3253	ZIAD, China
9	[1]Power Transformer	__	ANLIXUM, China
10	[1]Fluorescence Detector	LC 240	PERKIN ELMER, U.K.

No.	Instrument	Model	Company supplied
11	[1]Scanning Fluorescence Detector	474	Waters, Japan
12	[2]Fluorescence Spectrometer	FS-2	Scinco, China

2.2. Chemical Reagents

2.2.1. Chemicals Preparation

All chemicals and reagents used in this project were analytical grade reagents. Table [2.2] tabulates the main chemicals used throughout this project work as a standard stock solution. Other standard solutions were prepared by subsequent dilution of the stock solution.

Table [2.2]: The Main Chemicals and Reagents Throughout this Research Work

Name	Formula	Purity %	M.wt (g/mol)	Company Supplier	Remarks
Potassium dihydrogen phosphate	KH_2PO_4	99.0	136	(B.D.H)	Dissolved in distilled water
Boric acid	H_3BO_3	99.9	61.83	(B.D.H)	Dissolved in distilled water
Potassium chloride	KCl	99.9	74.55	(B.D.H)	Dissolved in distilled water

[1] University of Babylon / College of Science for Women-Department of Chemistry.
[2] University of Babylon / College of Science for Women-Department of Laser Physics.

Name	Formula	Purity %	M.wt (g/mol)	Company Supplier	Remarks
Potassium hydroxide	KOH	99.9	56.1	(B.D.H)	Dissolved in distilled water
Sodium hydroxide	NaOH	98.0	40	Loba Chemie	Standardized with HCl
1,2-Naphthoquinone-4-Sulfonic Acid Sodium Salt (N.Q.S.)	$C_{10}H_5NaO_5S$	97.0	260	Sigma-Aldrich	Dissolved in distilled water
Mefenamic acid (MA)	$C_{15}H_{15}NO_2$	99.7	241	(S.D.I)	Dissolves in dilute solutions of alkali hydroxides
Procaine	$C_{13}H_{20}N_2O_2$	99.6	272.7	(S.D.I)	Dissolved in distilled water

2.2.2. Sample Preparation

2.2.2.1. Sample Preparation of Mefenamic Acid 250ppm

A standard drug was prepared by dissolving 25mg (0.025gm) of MA. in 25mL distilled water and diluting it to 100ml in a volumetric flask with distilled water. Subsequent dilutions were freshly prepared working solutions.

2.2.2.2. Sample Preparation of Procaine Hydrochloride 250ppm

A standard drug was prepared by dissolving 25mg (0.025gm) of Procaine HCl in 25mL distilled water and diluting it to 100ml in a volumetric flask with distilled water. Subsequent dilutions were freshly prepared working solutions.

2.2.2.3. 1,2-Naphthoquinone-4-Sulfonic Sodium Salt (NQS) 100 ppm Solution

A stock solution was freshly prepared by dissolving 5mg (0.005gm) of the reagent in 50mL of distilled water.

2.2.2.4. Sodium Hydroxide 0.2M Solution

It was prepared by dissolving 1.6gm of sodium hydroxide in 25ml of distilled water and diluting to 200mL in a volumetric flask with distilled water.

2.2.2.5. Potassium Chloride 0.2M Solution

A standard solution was prepared by dissolving 2.858gm in 20ml of distilled water and diluting it to 200mL in a volumetric flask with distilled water.

2.2.2.6. Boric Acid 0.2M Solution

A standard solution was prepared by dissolving 1.2366gm in 25ml of distilled water and diluting it to 100mL in a volumetric flask with distilled water.

2.2.2.7. Sodium Hydroxide – Boric Acid (buffer solution) (pH~9)

It was prepared by dissolving 0.6gm of boric acid in 50mL distilled water and mixing with 4.15mL sodium hydroxide (0.2M). Then the solution was diluted with distilled water to the mark in a 100mL volumetric flask [98].

2.2.2.8. Boric Acid – Potassium Chloride – Sodium Hydrochloride (buffer solution) (pH~10)

It was prepared by mixing 25mL boric acid (0.2M) with 25mL potassium chloride (0.2M) and adding 21.85mL sodium hydroxide (0.2M), and then the solution was diluted with distilled water to the mark in a 100mL volumetric flask [99].

2.2.2.9. Sodium hydroxide – Potassium chloride (buffer solution) (pH~12)

It was prepared by mixing 50mL potassium chloride (0.2M) with 24mL sodium hydroxide (0.2M). Then the solution was diluted with distilled water to the mark in a 100mL volumetric flask [100].

2.2.2.10. Sodium hydroxide – Potassium chloride (buffer solution) (pH~13)

It was prepared by mixing 25mL potassium chloride (0.2M) with 65mL sodium hydroxide (0.2M). The solution was diluted with distilled water to the mark in a 100mL volumetric flask [101].

Chapter Three

Results and Discussion

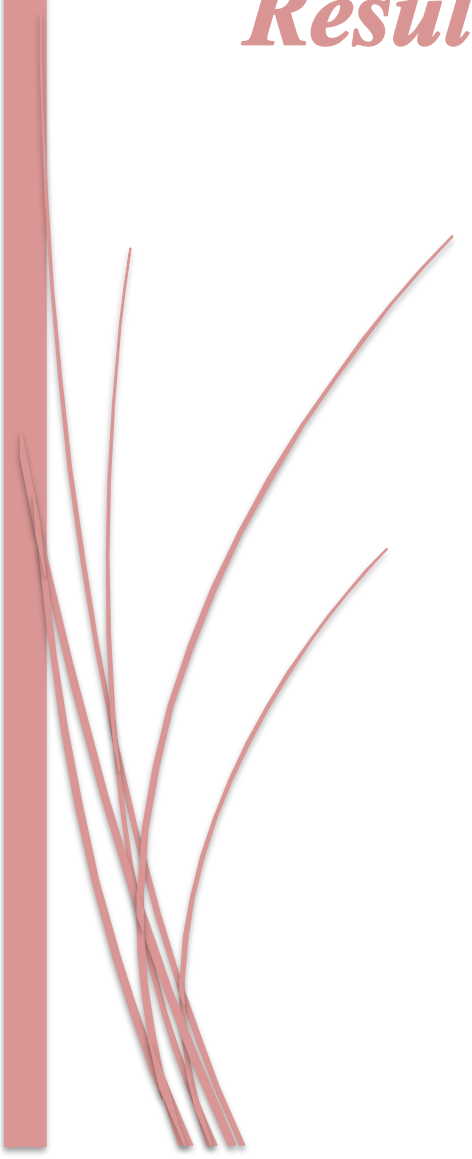

3. Results and Discussion

3.1. Design of Flow Injection Units

Continuous flow injection analysis systems consist of essential parts: fluid pumping system, coils, measuring devices, reading system, and injection unit. In general, the flow injection system used in this research consists of the following parts:

3.1.1. Peristaltic Pump

The first stage starts by operating the multi-channel peristaltic pump, as shown in Figure [3.1] and Scheme [3.1], which works to pump the transporting solution to the unit passing through the injection valve to the cell, as the system tubes and coils are filled with the transporting solution. The reading considers the transport solution as a reference (blank).

Figure [3.1]: Rabbit Peristaltic Pump (RAININ)

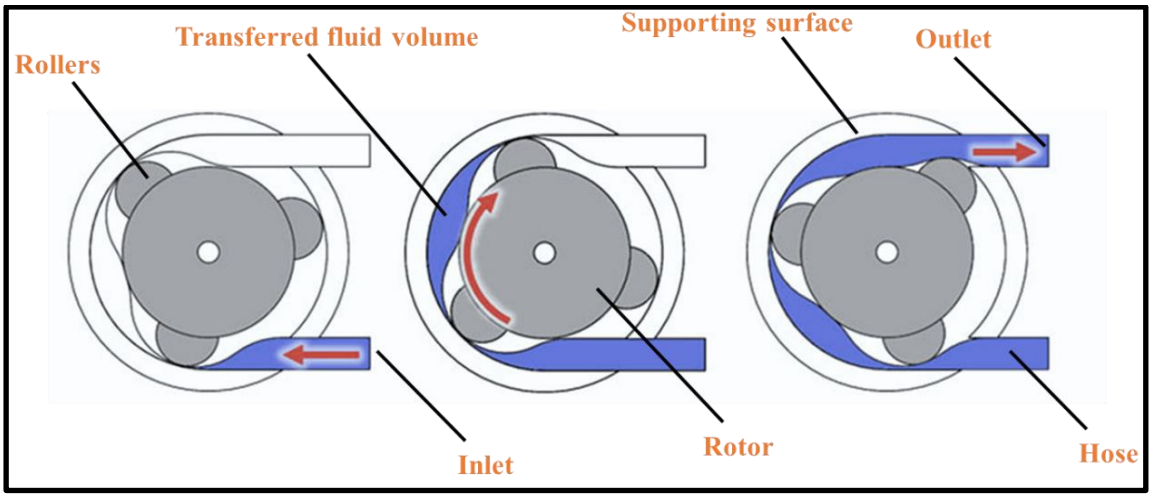

Scheme [3-1]: The Movement of Fluid within the Parts of the Peristaltic Pump

The pump contains a lever that causes speed control through numbers recorded on it that change mechanically with the movement of the lever, and these numbers start from 1 to 10. Still, it is correct to deal with the speed with the volume that is pumped per minute because peristaltic pumps are manufactured in different shapes and designs. The volume descending from the designed unit was collected during a fixed time of 1 minute to deal with the flow rate in units (ml) per minute for each digital speed of the pump, as shown in Table [3.1].

Table [3.1]: The Amount of Flow Velocity Per Velocity of the Pump

Flow rate (mL/min)	The volume descending from the system(mL) in one minute	Speed recorded on the pump
0.5	**0.5**	**1**
1.0	**1.0**	**2**
1.5	**1.5**	**3**
2.0	**2.0**	**4**
2.5	**2.5**	**5**
3.0	**3.0**	**6**
3.5	**3.5**	**7**
4.0	**4.0**	**8**
4.5	**4.5**	**9**
5.0	**5.0**	**10**

3.1.2. Injection Valve

The second phase includes loading the reagent or sample (depending on the technique used) in the hexagonal injection unit shown in Figure [3.2].

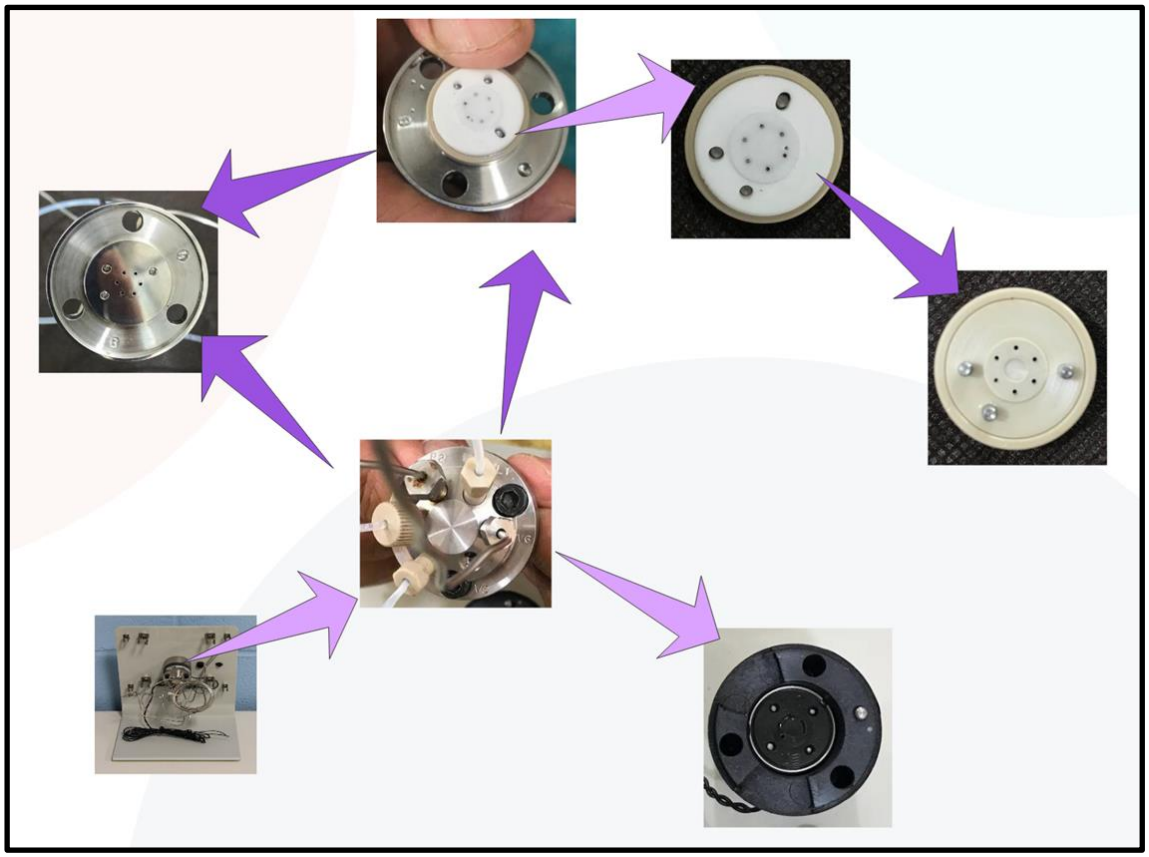

Figure [3.2]: How to Choose the Appropriate Holes for the Sample Loop from the Six Holes of the Valve, and Holes 1 and 4 were selected.

This stage is represented by the entry of the reagent or sample into the loop of the injection unit, as the direction of filling the reagent connection or the sample is from one external movement (load) No. (1) » (2) » (3) » (6) and surplus to the waste as shown in Scheme [3-2] [A].

After the loading process is completed, the direction of the valve is changed in such a way that the carrier solution pushes the reagent or sample that was loaded in the loop; the direction of injection is No. (4) » (3) » (6) » (5), where this change in the direction of the valve leads to the flow towards the reaction coil as the materials mix and the reaction product is formed as shown in Scheme [3-2] [B].

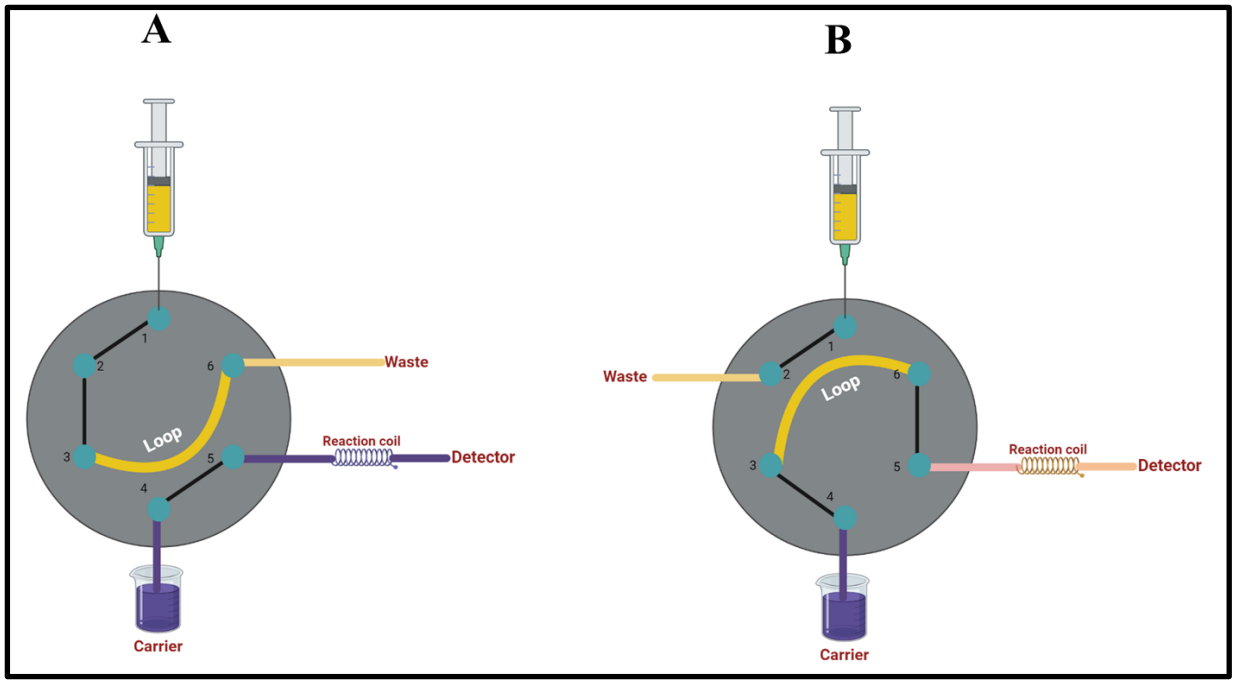

Scheme [3-2]: (A) Loading and (B) Injection Process in the Injection Unit

3.1.3. Reaction Coil

The amount of volume accommodated by the different lengths of the reaction coils used in the system was also calculated by the cylinder volume equation $\boldsymbol{v=r^2\pi h}$., e.g., a Teflon tube of ID=1 mm, r=0.5 mm=0.05 cm Figure [3.3] and Table [3.2].

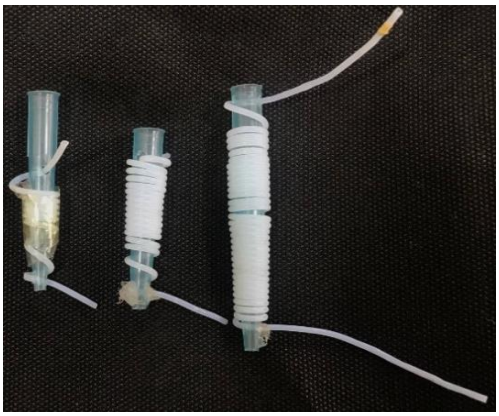

Figure [3.3]: A Collection of Reaction Coils has Variable Lengths

Table [3.2]: The Volume of each Reaction Coil

Volume (µL)	Length of reaction coil (cm)
196.25	**25**
392.50	**50**
588.75	**75**
785.00	**100**

3.1.4. Data Acquisition

Unlike previous instruments, the new one employs a novel, constructed, in-lab planned, and in-lab managed G-Chrome flow-injection software as shown in Figure [3.4] to determine the spectroscopic approach. This system is straightforward to use, and data transmission is automatic. Due to the internal architecture of the software utilized in this technique, injecting the sample and then repeating it at an intersection or modifying the sample is straightforward. Additionally, it was discovered that the data acquired was accurate and equivalent to that produced using more complex instruments. This system is differentiated by its cost and convenience of use, high degree of flexibility, precision, and control over the results, and, most crucially, the analyst's ability to build and improve the system and approach.

Figure [3.4]: Data Acquisition (ZIAD Model USB3253)

The overall structure of the designed systems, in general, is given in Figure [3.5].

Figure [3.5]: The Whole Setup of the Manifold System for the Measuring Absorbance and Fluorescence Response of Different Analytes.

3.2. Techniques used for the Determination of Amino Drugs and the Reagent. Scheme [3.3].

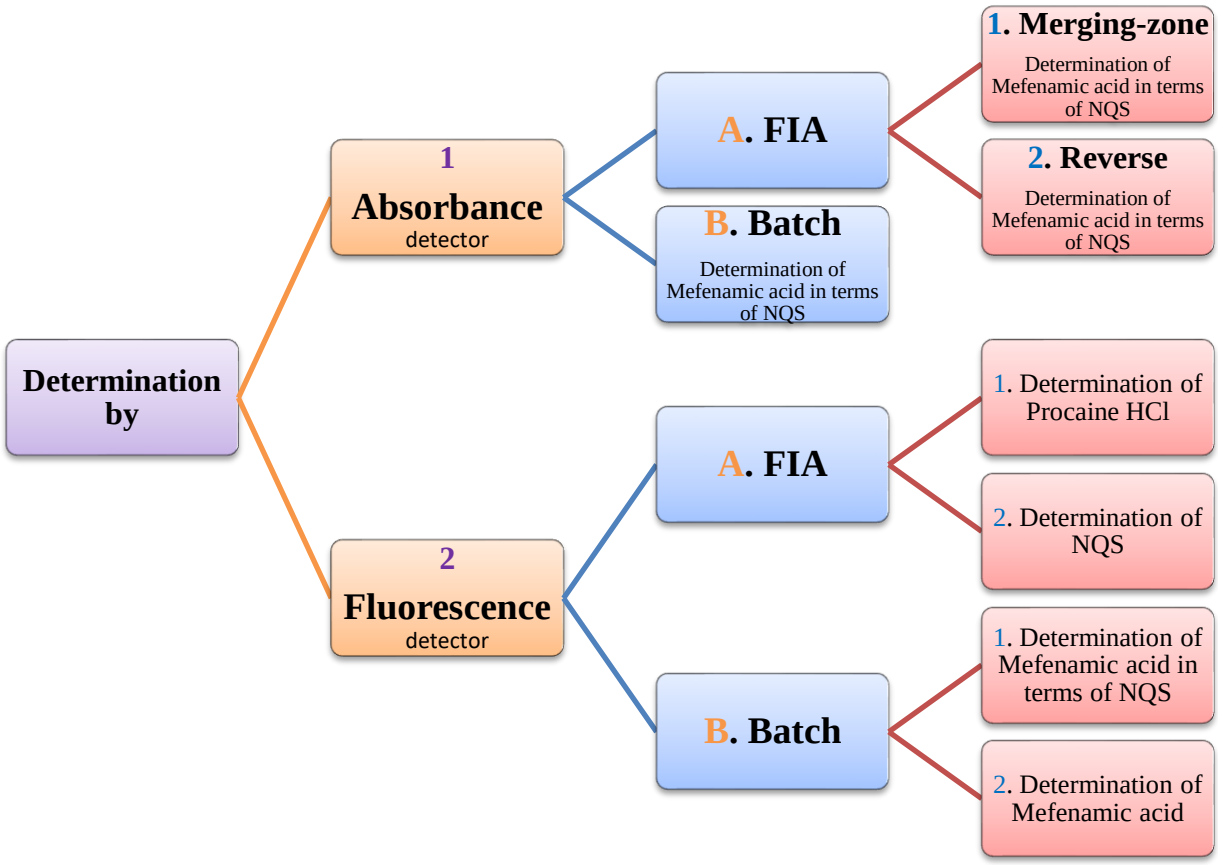

Scheme [3.3]: Different Techniques for Determination of Amino Drugs and Reagent

3.2.1.A. Determination of Mefenamic Acid in Terms of NQS Using FIA

It was decided to use Accumulate Peak Analysis (APA) because of its precision, quick analysis, and ability to graph data. The data produced from the technique were screened and compared to the standard solution with the help of an equation that was expressly created for this purpose. This step will aid the analyst in understanding the parameters that influence the performance of the analysis during the next stage.

The method depends on the electrophilic aromatic substitution reaction between Mefenamic Acid and NQS in the alkaline medium, as shown in Scheme [3.4]**.**

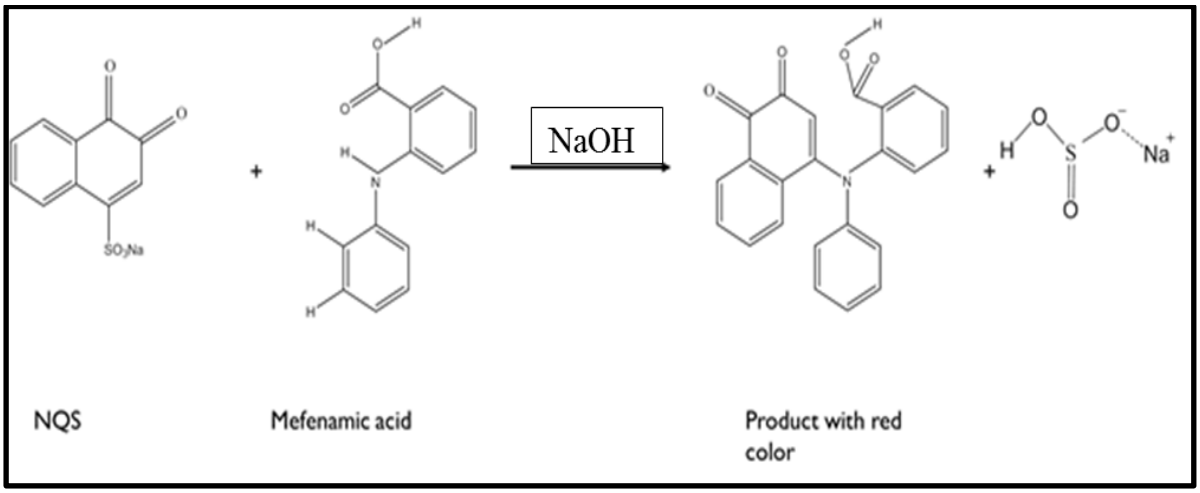

Scheme [3.4]: Reaction between NQS and Mefenamic acid

3.2.1.A.a. Determining the Maximum Wavelength (λmax)

The wavelength of maximum absorption of MA with an NQS reagent was scanned using a UV Vis spectrophotometer. A UV-Vis spectrum of NQS solution showed a maximum absorption peak at 380 nm. Adding an appropriate volume from the previous solution in a convenient concentration to the alkaline

MA solution will produce a reddish-brown reaction product with a new characteristic peak at 477 nm, as shown in Figure [3.6] and Table [3.3]. The new peak exists due to the formation complex between MA and NQS solutions.

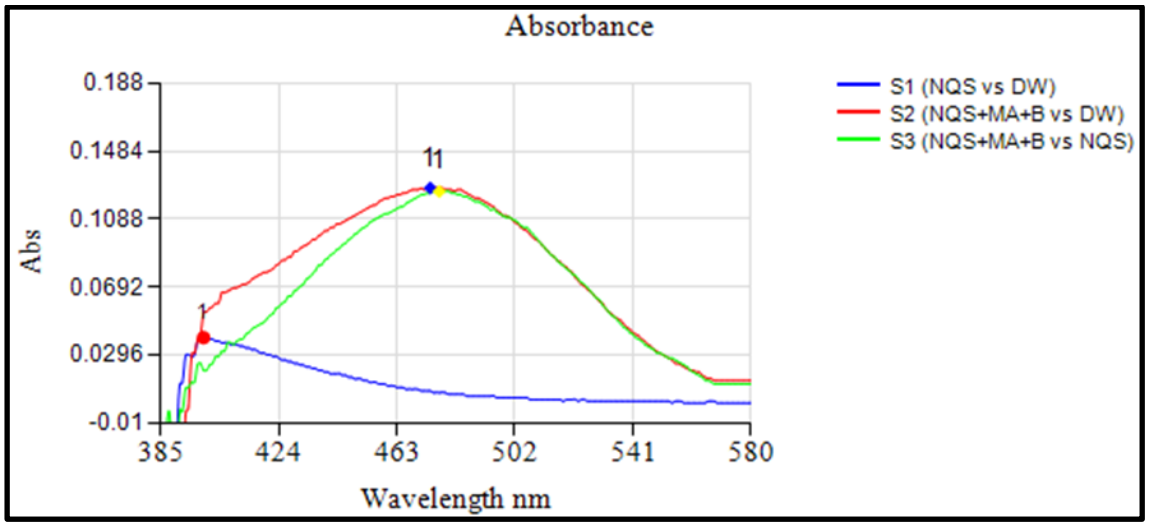

Figure [3.6]: UV- absorbance scanning spectrum for 10 ppm NQS solution (blue line), the reaction product between 10 ppm MA and 10 ppm NQS in an alkaline medium against distilled water (red line), and the reaction product between 10 ppm MA and 10 ppm NQS in an alkaline medium against absorption of 10 ppm NQS solution as a blank solution (green line).

Table [3.3]: Result of Lambda max

Lembda	S1	Lembda	S2	Lembda	S3
399	0.04	474	0.127	477	0.125

3.2.1.A.1. Merging Zone Method

A single parameter was changed in the FIA unit as shown in scheme [3.5] to optimize the experimental conditions. The effect on the absorbance of the colored species was monitored to identify the best possible testing conditions.

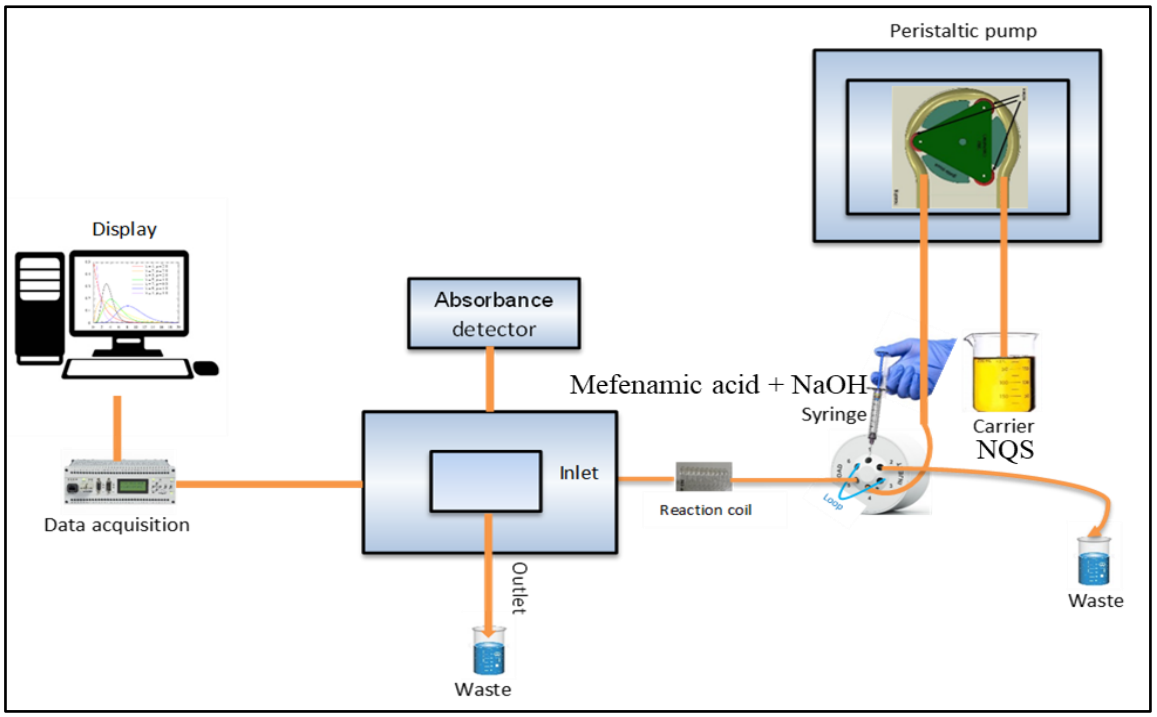

Scheme [3.5]: Design of Merging Zone -FIA with an Absorbance Detector

3.2.1.A.1.1. The Influence of Flow Rate:

The effect of the flow rate and the selection of the optimum speed for the system interaction was studied. The results in Figure [3.7] show the impact of the pump speed on the response value (peak height) at the conditions mentioned below, as it is noted that the response decreases by increasing the pump speed from 1 to 6, and this matches the theoretical foundations of the effect of speed on response. The third speed with a response rate of 0.148 is preferred over the fourth, fifth, and sixth speeds with a response rate of 0.146, 0.133, and 0.130, respectively, for being the highest value. In addition to that, the third speed is preferable to the slower speeds. However, speeds 1 and 2 have the same response rate, which is 0.152, which is the highest response than the third speed (0.148), the shape of the peaks for those low speeds is wide and double-topped and not ideal; either the shape of the peak of the third speed, which has a flow rate of 1.5 ml per minute, is the best because it is sharp and uniform, as the third speed gives the best mixing of the reaction materials.

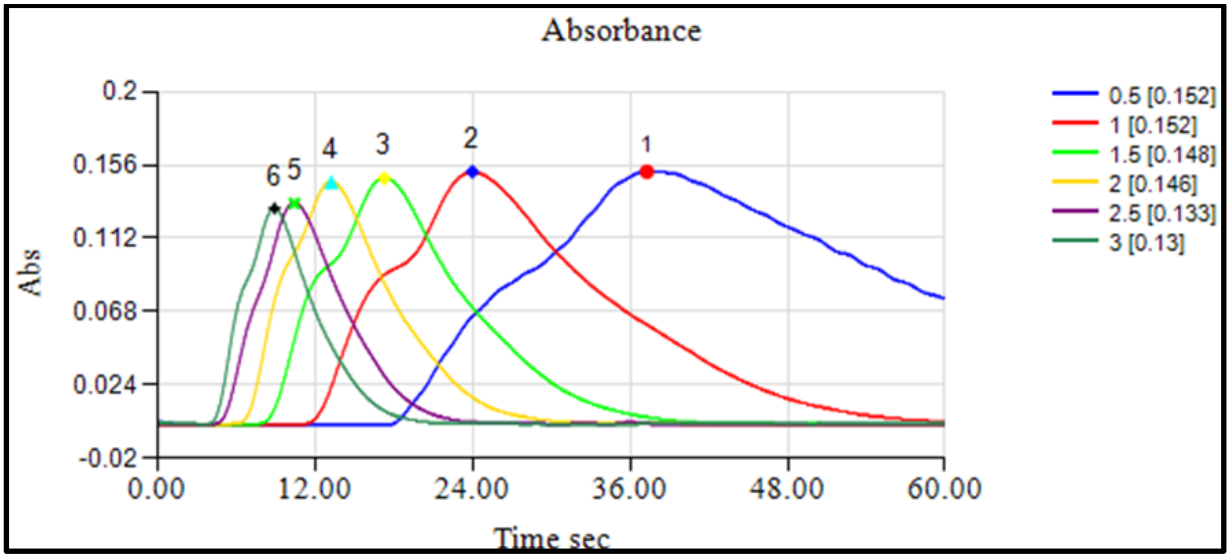

Figure [3.7]: Shows the effect of flow rate on the absorption peak height when, MA conc. = 20 ppm, NQS conc. = 50 ppm, reaction coil length = zero, used alkaline medium = buffer solution, pH value= 12, at room temperature.

These results match what other researchers have stated [70]. It was found that increasing the flow rate reduces the response. It was also found that the shape of the peak at low speeds is wide, double in height, and distorted, but the peak is sharp and uniform at high rates. It can be said that the peak is double because of speed in the mixing process, where the spread is irregular and areas are formed where the mixing is high, and the other is low.

3.2.1.A.1.2. The Effect of the Mixing Coil Length

The reaction coil length effect on the peak height was investigated using varying lengths of reaction coil ranging from 0 to 100 cm. The results show the highest absorbency value and the best shape for the peak obtained after eliminating the double-top peak (which indicates that the mixing was not complete) was when using a reaction coil with a length of 25 cm that; the peak height increases with the increase of the reaction coil length up to 25 cm as shown in Figure [3.8]. At longer lengths, the peak height will decrease due to the dilution process accompanying the reaction coil that has a longer length.

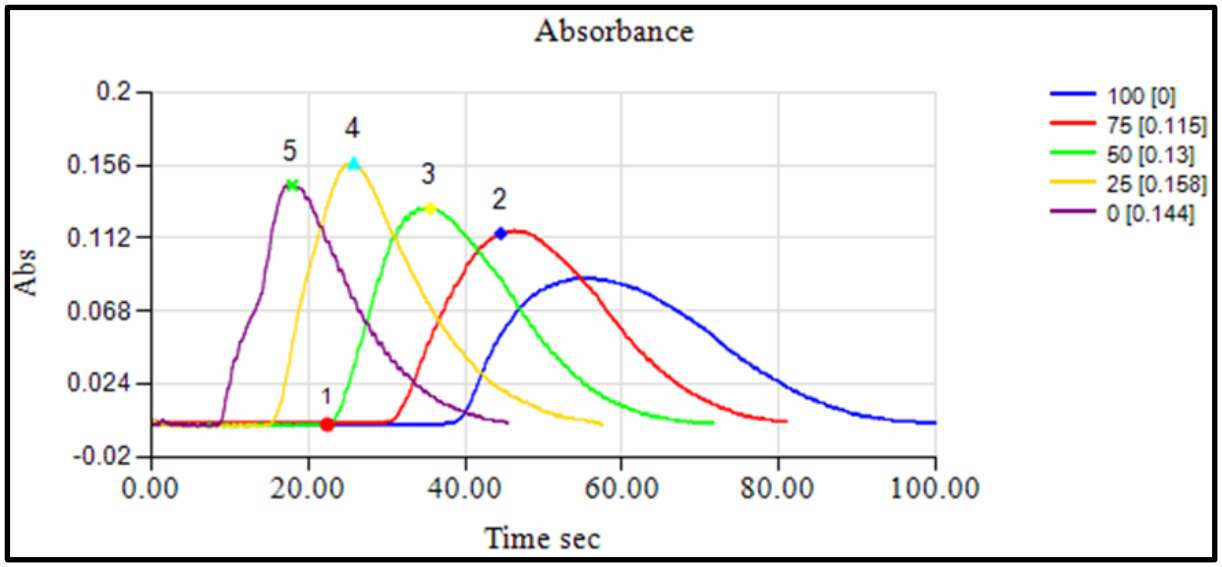

Figure [3.8]: This shows the effect of the reaction coil on the absorption peak height when MA conc. = 20 ppm, NQS conc. = 50 ppm, used alkaline medium = buffer solution, pH value= 12, at room temperature.

3.2.1.A.1.3. The Effect of the Alkaline Type and the Quantity Added

Different alkaline types were tested as alkaline mediums like sodium hydroxide and buffer solutions pH (9-12). The results indicate that the solution resulting from using sodium hydroxide will give the highest absorption peak, as shown in Figure [3.9].

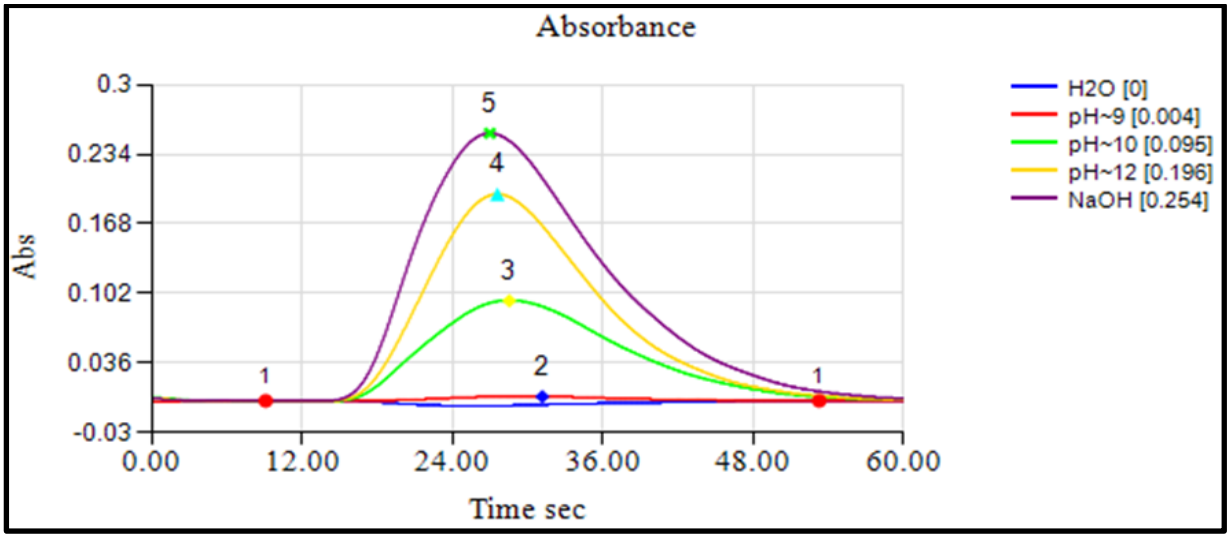

Figure [3.9]: The Influence of the alkaline type when MA conc. = 20 ppm, NQS conc. = 50 ppm, reaction coil length = 25 cm at room temperature

The influence of various volumes added 0.05 to 0.2 mL of the 0.2M from sodium hydroxide solution on the formation of the reaction product has been studied. The results show that the optimum volume of sodium hydroxide solution added into the 20 mL from 20 ppm of MA is 0.1 mL, as shown in Figure [3.10]. This volume of the NaOH solution achieves the best homogeneous merging zone between MA and NQS solutions and shows the highest peak; therefore, 0.1 mL has been chosen as the optimum alkaline medium volume in subsequent experiments.

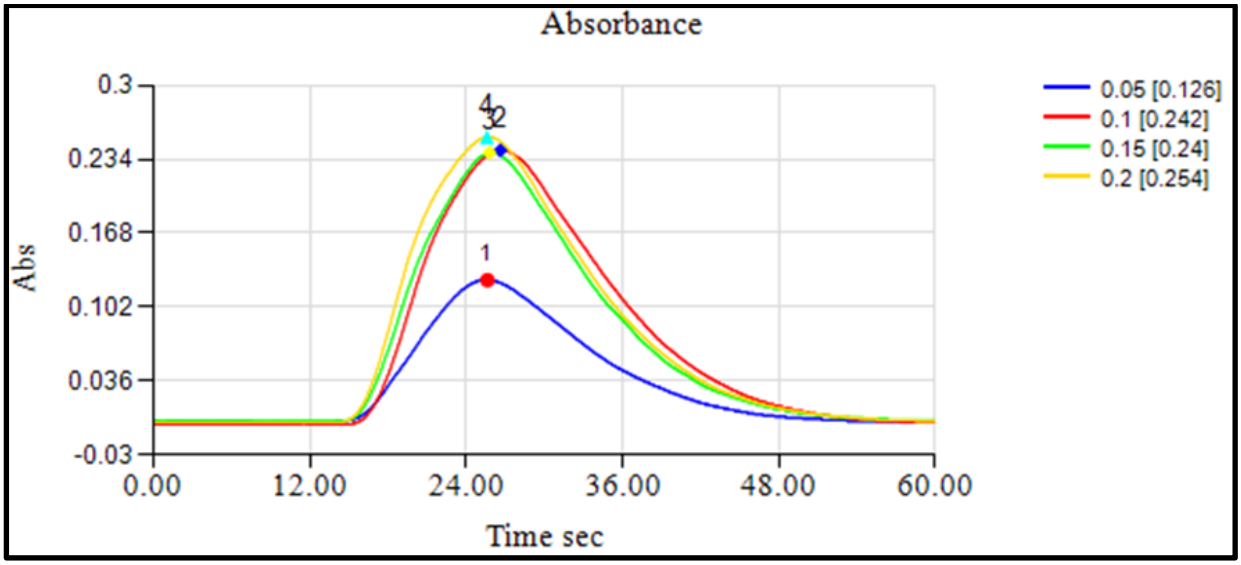

Figure [3.10]: The effect of 0.2M NaOH volume on the absorption peak height when MA conc. = 20 ppm, NQS conc. = 50 ppm, reaction coil length = 25 cm at room temperature

3.2.1.A.1.4. Effect of NQS Concentration

The influence of NQS concentration has been studied in the range of 10 - 100 ppm. The best peak height was observed when using 50 ppm of NQS for the complex formation, as shown in Figure [3.11].

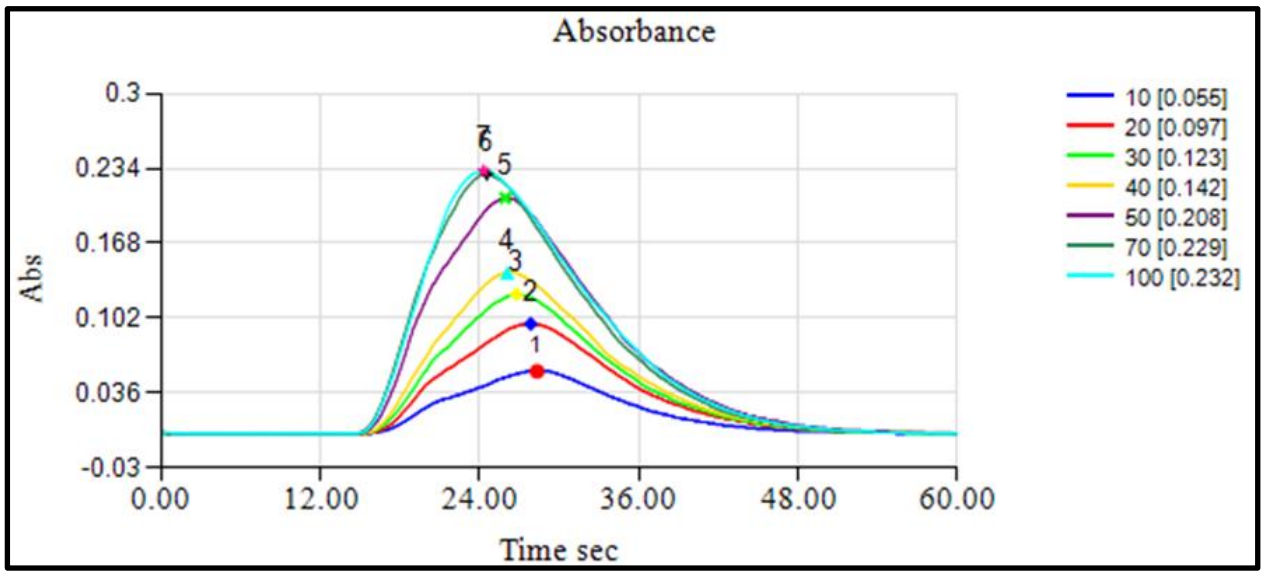

Figure [3.11]: The influence of NQS concentration on the absorption peak height when MA conc. = 20 ppm, reaction coil length = 25 cm, 0.2M NaOH = 0.1 mL to 20 mL MA at room temperature.

Although the response rate increases with the increasing concentration of the reagent, the best concentration was chosen as 50 ppm because high concentrations of the reagent show a deviation in the shape of the peak (the reagent between two regions of the reaction product formation), and it is also preferable to use dilute concentrations of the reagent to ensure that the signal of the concentration of the reagent does not interfere with the signal of the reaction product.

3.2.1.A.1.5. General Procedures and the Calibration Curve

According to the optimum conditions, MA was quantitatively determined. The calibration curve was prepared at 477 nm by organizing a series of MA solutions with different concentrations and analyzing each employing the FIA system. The absorption peak height value of the formed complex was plotted against the concentration. The suggested method allows for the determination of MA in the range of (1-20) ppm, as shown in Figures [3.12] and [3.13].

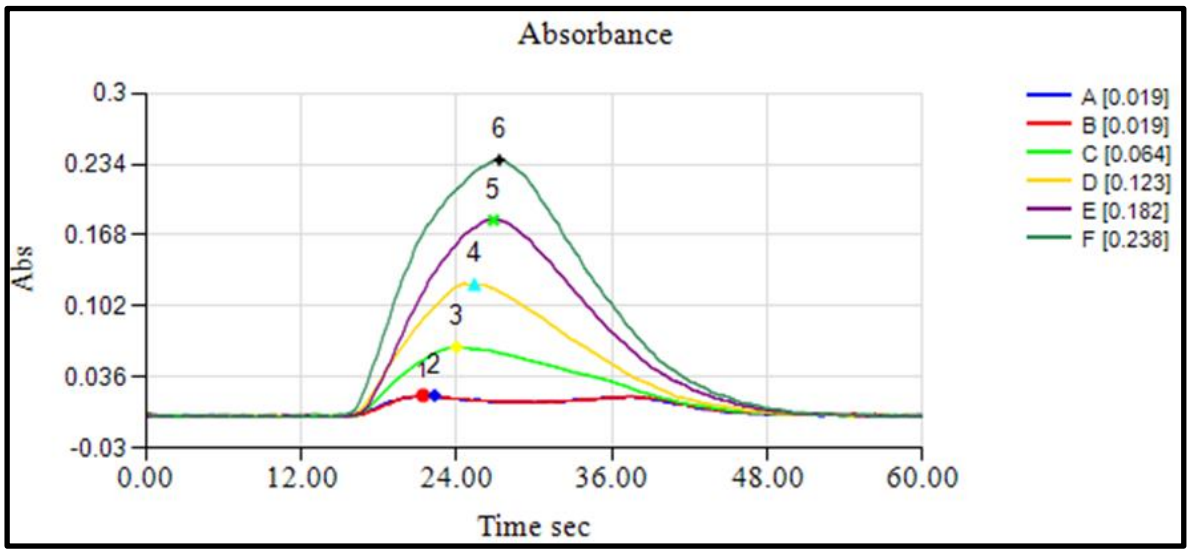

Figure [3.12]: Absorption Spectra of Mefenamic Acid.

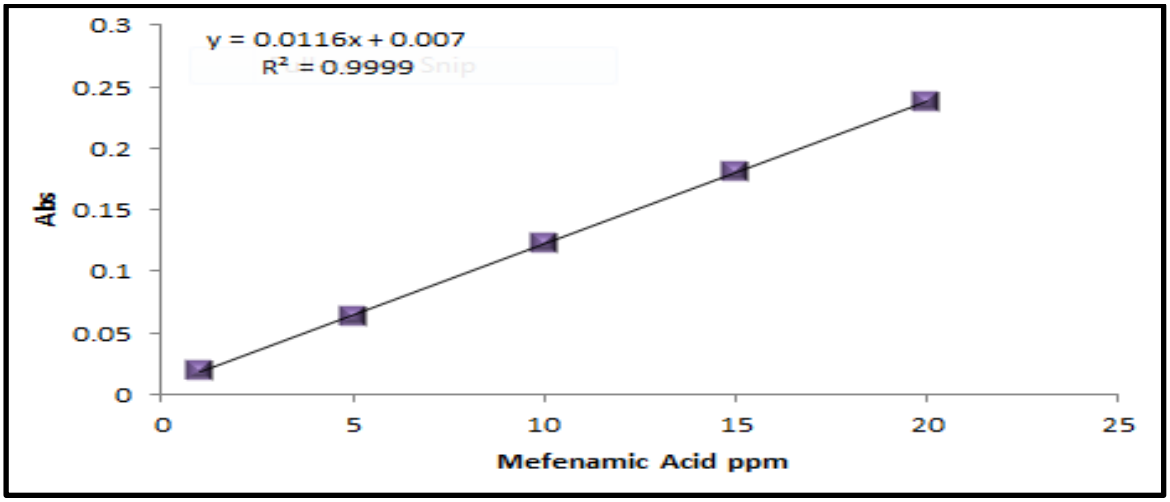

Figure [3.13]: Calibration Curve of Mefenamic Acid

The sensitivity of the suggested method represented as detection limit (LOD) and quantitation limit (LOQ) has been estimated to be equal to 0.021 and 0.071 ppm, respectively, as shown in Table [3.4].

Table [3.4]: The effect of MA conc. on the absorption peak height when, NQS conc. = 50 ppm, reaction coil length = 25 cm, 0.2M NaOH = 0.1 mL to 20 mL MA at room temperature

Mefenamic acid ppm	Abs	QR
1	0.019	0.019
1	0.019	0.019
5	0.064	0.065
10	0.123	0.123
15	0.182	0.181
20	0.238	0.239

SD = 0.0009
LOD=0.021
LOQ=0.071

3.2.1.A.1.6. Repeatability

The relative standard deviation (RSD %) represents the precision of the proposed method has been studied utilizing 13 ppm of MA solution. At the optimum conditions, 6 replicate measurements were carried out for the determined concentration and recorded as shown in Figure [3.14] and Table [3.5]. The standard deviation value is equal to 0.0019, and the relative standard deviation value is equal to 1.237, indicating the high precision of the suggested method.

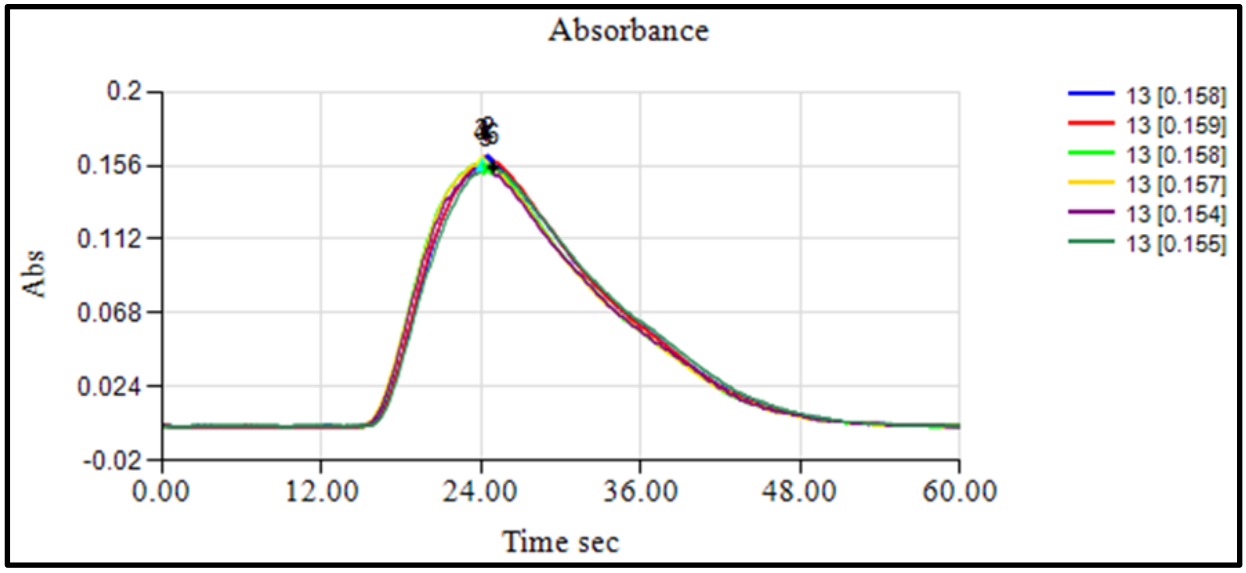

Figure [3.14]: Repeatability of 13 ppm MA Solution by Merging Zone –FIA

Table [3. 5]: Repeatability results for 13 ppm MA solution by Merging zone -FIA

Sample No.	1	2	3	4	5	6	Mean	SD	RSD%
Abs.	0.158	0.159	0.158	0.157	0.154	0.155	0.157	0.0019	1.237

3.2.1.A.1.7. Dead Volume

The quality of the obtained results was examined by performing the dead volume experiment. This experiment includes three steps: in the first step, water instead of MA was loaded in the valve loop after mixing with NaOH, and in the second step, water instead of the carrier solution represented the NQS. In the third step, water was used instead of NaOH and loaded into the valve loop after mixing with MA. The response to the three experiments was confirmed and was zero, indicating no dead volume, Figure [3.15].

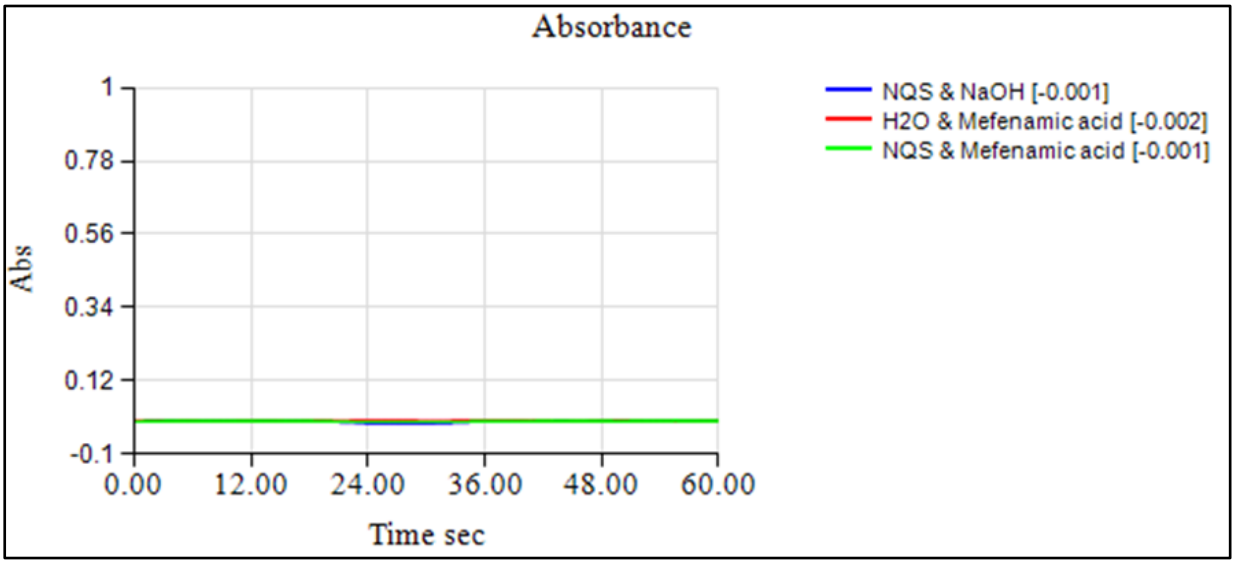

Figure [3.15]: The Dead Volume of MA

3.2.1.A.1.8. The Determination of Dispersion

The dispersion coefficient (dilution factor D) was studied to illustrate the dispersion process extent within the flow injection system from the injection point at the valve to the detecting point at the detector. The dispersion coefficient can be calculated through Equation [1.1] and its equal 1.11.

The dispersion coefficient was studied using one concentration of MA solution within the calibration curve range (20 ppm). In the first step, the reaction between the MA alkaline solution and the NQS solution was implemented inside the FIA system under the defined optimum conditions by measuring the peak height that represents the peak height with the dilution process (H max). In the second step, the reaction between the MA alkaline solution and the NQS solution in appropriate volumes was implemented in a glass beaker and passed the final solution through the system, then measuring the absorption peak height that takes the plateau shape with a constant height value with the time that represents the peak height without the dilution process (H°). The obtained results are displayed in Figure [3.16].

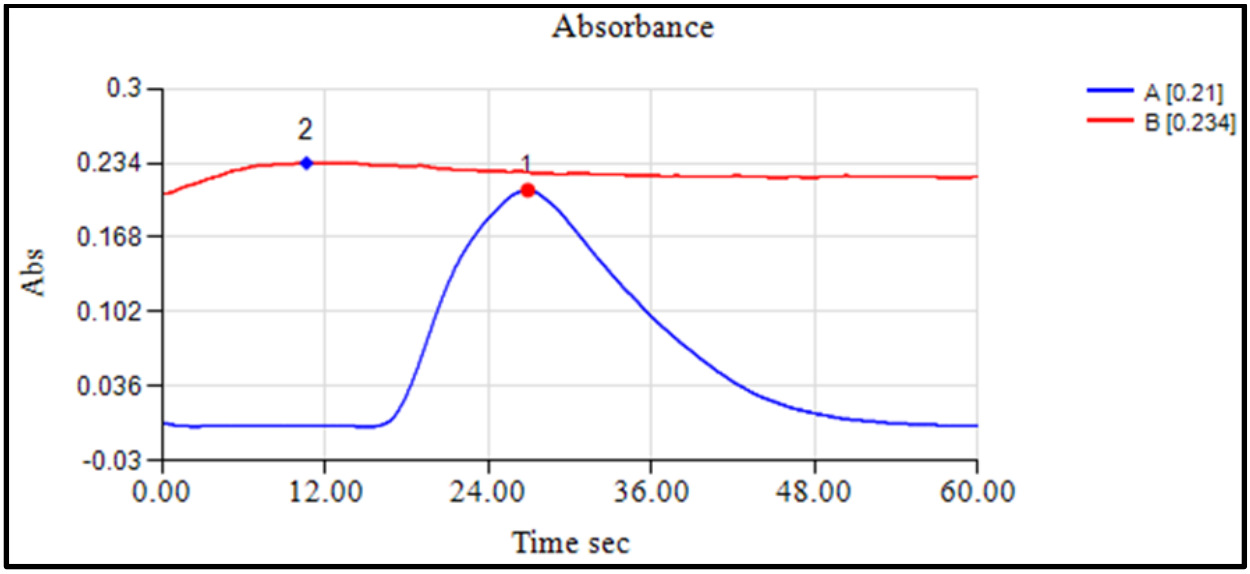

Figure [3.16]: Dispersion Coefficient Study Results for MA Determination FIA System

3.2.1.A.1.9. Calculating the Sampling Frequency of the FIA System for MA Determination by NQS

According to the optimum conditions, the sampling frequency of the MA determination by the FIA system has been calculated by accounting for the

consumed time from the injection moment to the moment when the absorption peak reaches its maximum height; the practical frequency is 120 samples per hour.

3.2.1.A.1.10. In Aqueous Solutions, MA can be Determined as follows

Three aqueous solutions were prepared and considered solutions of unknown concentration; then, the absorbance was measured according to the optimum conditions, as shown in Fig. [3.17]. Then the solutions' concentration was determined by setting each solution's absorbance on the straight line of the previous calibration curve, as shown in Fig. [3.18] and Table [3.6]. The value of the resulting solutions from the calibration curve was very close to the prepared solutions, considering the preparation errors.

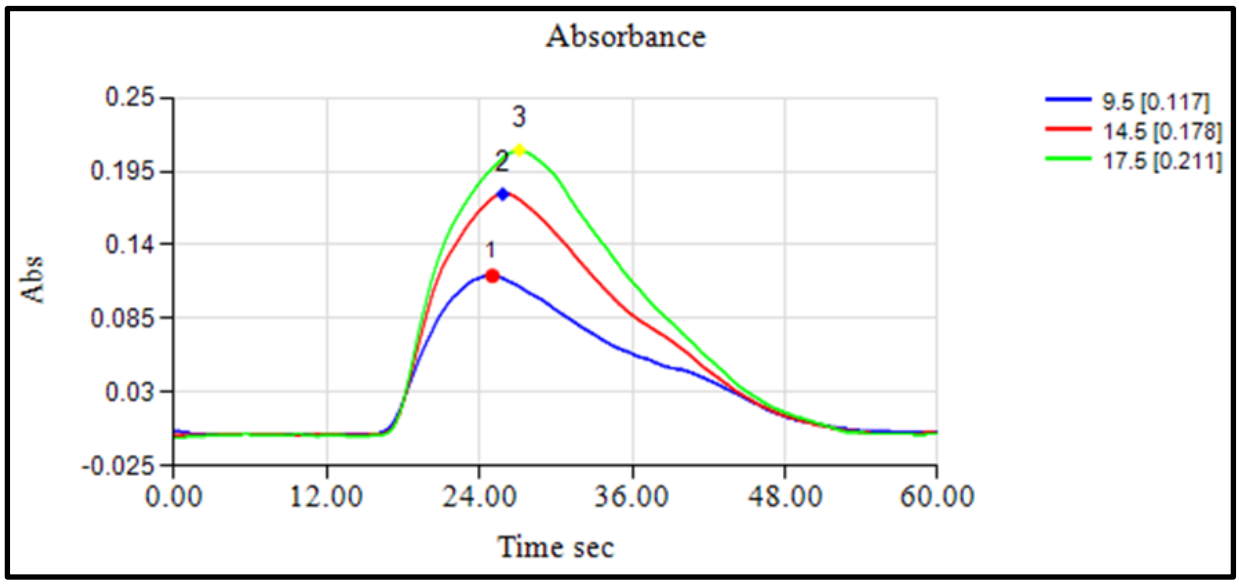

Figure [3.17]: The Spectrum of Possible Applications

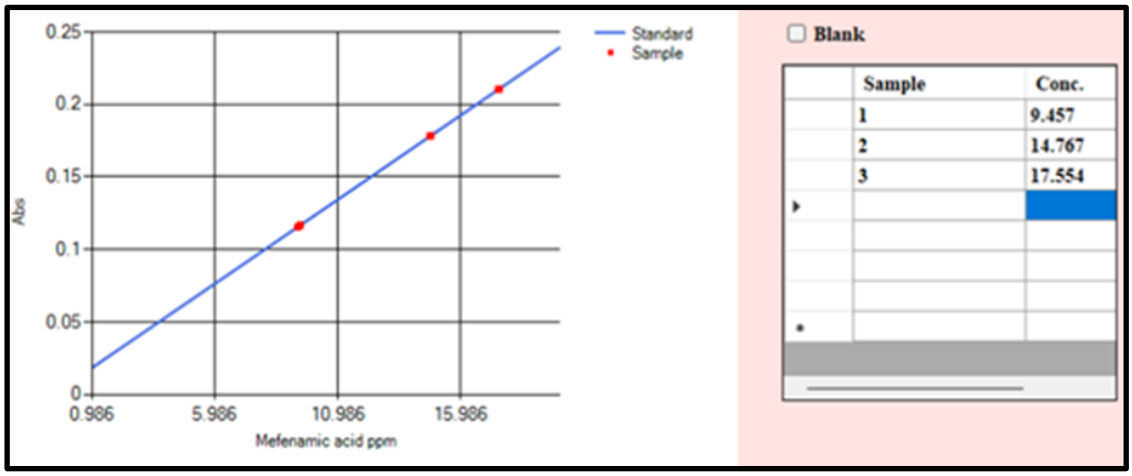

Figure [3.18]: Determination of Unknown Aqueous Solutions

Table [3.6]: Value of Sample Application

Index	Taken	Founded	Peak Height	Recovery
1	9.5	9.457	0.117	99.547
2	14.5	14.767	0.178	101.8
3	17.5	17.554	0.211	100.3

3.2.1.A.2. Reverse – Continuous FIA

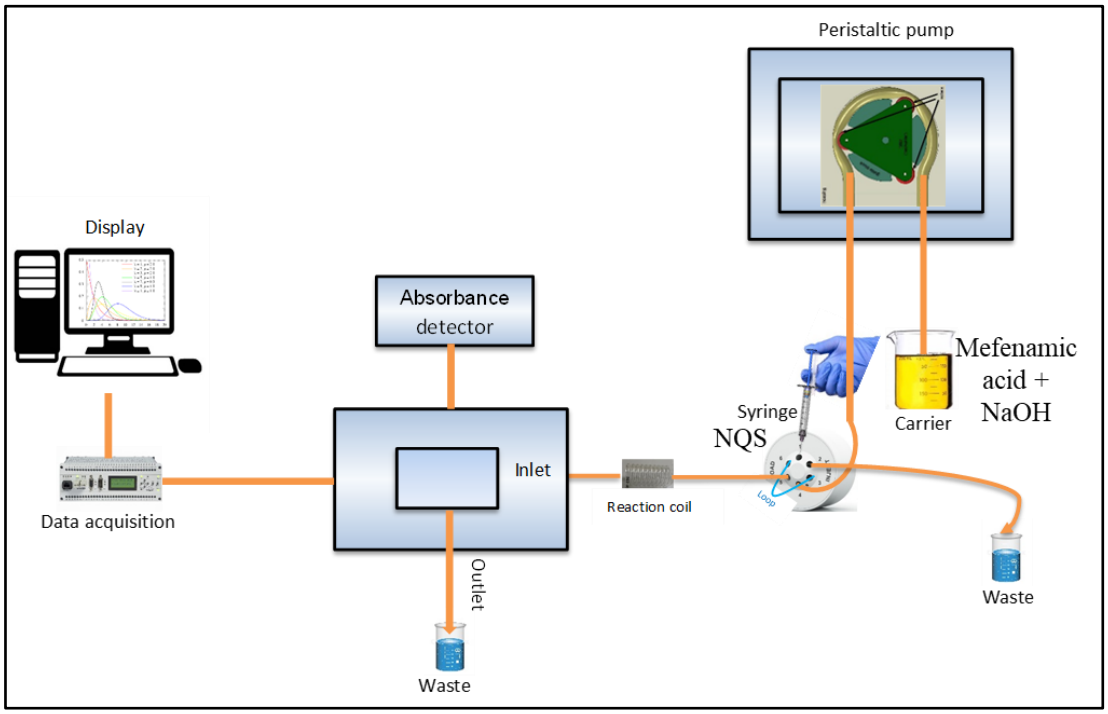

Scheme [3.6]: Design of Reverse – Continuous FIA with Absorbance Detector

3.2.1.A.2.1. The Influence of Flow Rate:

The effect of the flow rate and the selection of the optimum speed for the system interaction was studied. The results in Figure [3.19] show the effect of the pump speed on the response value (peak height) at the conditions mentioned below, as it is noted that the response decreases by increasing the pump speed from 1 to 5, and this matches the theoretical foundations of the effect of speed on response. The third speed with a response rate of 0.16 is preferred over the fourth and fifth speeds with a response rate of 0.151 and 0.144, respectively, for being the highest value. Also, the third speed is preferable to the slower speeds. However, speed 2 have a response rate of 0.165, which is higher than the third speed (0.16), the shape of the peak for those low speed is wide and double-topped, and not ideal; either the form of the peak of the third speed, which has a flow rate of 1.5 ml per minute, is the best because it is sharp and uniform, as the third speed gives the best mixing of the reaction materials.

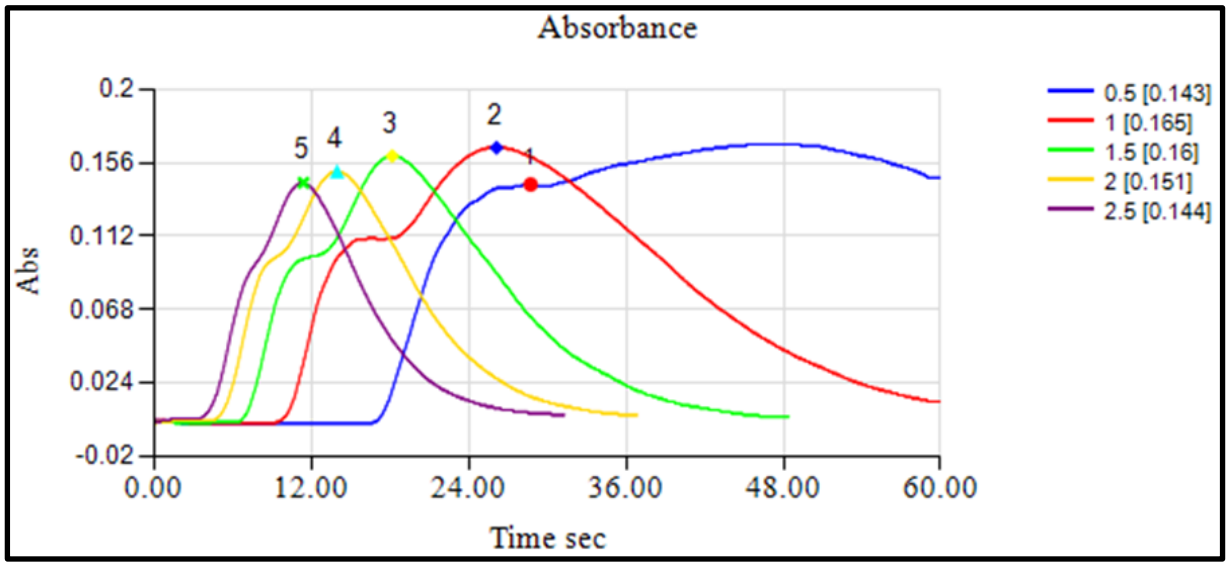

Figure [3.19]: The Effect of Flow Rate on the Absorption Peak Height when, MA conc. = 30 ppm, NQS conc. = 50 ppm, reaction coil length = zero, used alkaline medium = buffer solution, pH value= 12, at room temperature.

3.2.1.A.2.2. The Effect of the Length of the Mixing Coil

The reaction coil length effect on the peak height was investigated using varying lengths of reaction coil ranging from 0 to 100 cm. The results show the highest absorbency value and the best shape for the peak obtained after eliminating the double-top peak (which indicates that the mixing was not complete) was when using a reaction coil with a length of 75 cm that; the peak height increases with the increase of the reaction coil length up until to 75 cm as shown in Figure [3.20]. At longer lengths, the peak height will decrease due to the dilution process accompanying the reaction coil that has a longer length.

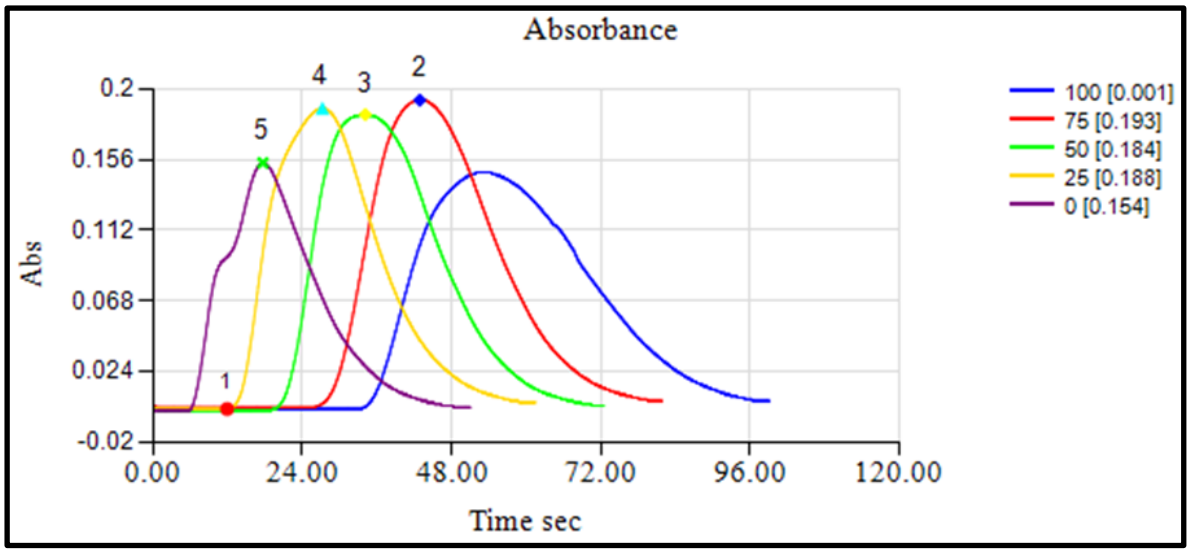

Figure [3.20]: The Effect of the Reaction Coil on the Absorption Peak Height when MA conc. = 30 ppm, NQS conc. = 50 ppm, used alkaline medium = buffer solution, pH value= 12, at room temperature.

3.2.1.A.2.3. The Effect of the Alkaline Type and the Quantity Added

Different alkaline types were tested as alkaline mediums like sodium hydroxide and buffer solutions pH (9-12). The results indicate that the solution

resulting from using sodium hydroxide will give the highest absorption peak, as shown in Figure [3.21].

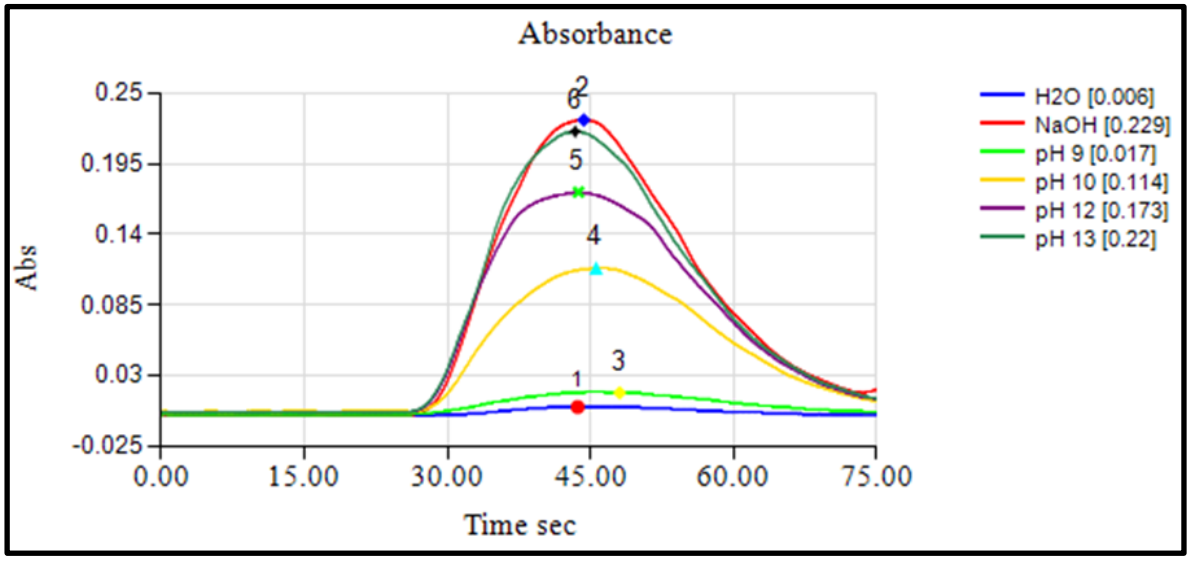

Figure [3.21]: The Influence of the Alkaline Type when MA conc. =30 ppm, NQS conc. = 50 ppm, reaction coil length = 75 cm at room temperature

The influence of various volumes added 0.05 to 0.2 mL of the 0.2 M from sodium hydroxide solution on the formation of the reaction product has been studied. The results show that the optimum volume of sodium hydroxide solution added into the 20 mL from 30 ppm of MA is 0.15 mL, as shown in Figure [3.22]. This volume of the NaOH solution achieves the best homogeneous merging zone between MA and NQS solutions and shows the highest peak; therefore, 0.15 mL has been chosen as the optimum alkaline medium volume in subsequent experiments.

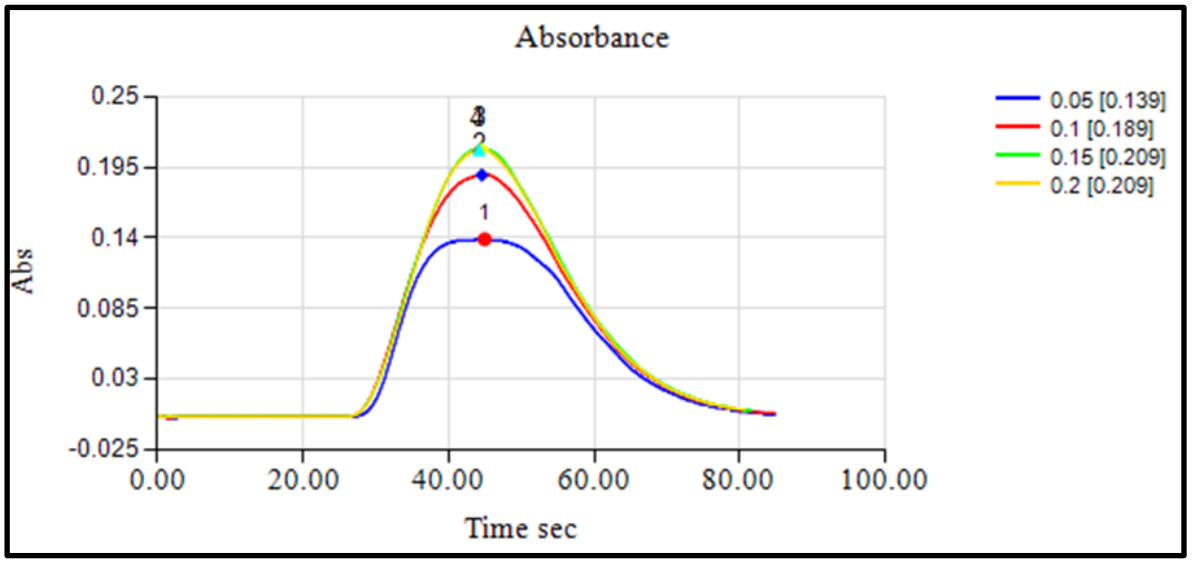

Figure [3.22]: The Effect of NaOH Volume on the Absorption Peak Height when MA conc. =30 ppm, NQS conc. = 50 ppm, reaction coil length = 75 cm at room temperature.

3.2.1.A.2.4. Effect of NQS Concentration

The influence of NQS concentration has been studied in the range of 10 - 100 ppm. The best peak height was observed when using 50 ppm of NQS for the complex formation, as shown in Figure [3.23].

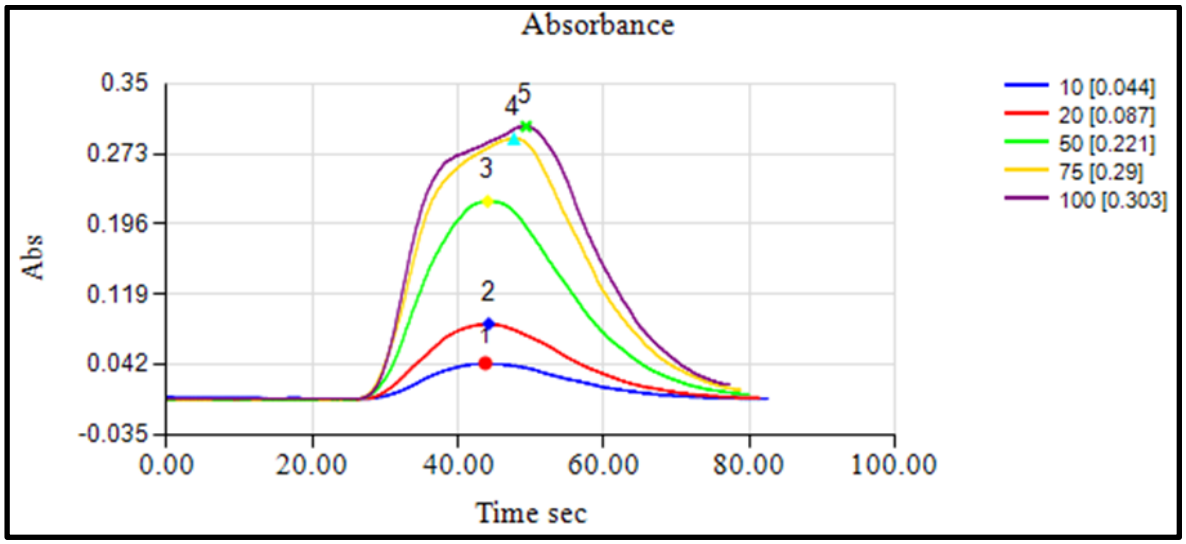

Figure [3.23]: The Influence of NQS Concentration on the Absorption Peak Height when MA conc. = 30 ppm, reaction coil length = 75 cm, NaOH = 0.15 mL to 20 mL MA at room temperature.

Although the response rate increases with the increasing concentration of the reagent, the best concentration was chosen as 50 ppm because high concentrations of the reagent show a deviation in the shape of the peak (the reagent between two regions of the reaction product formation), and it is also preferable to use dilute concentrations of the reagent to ensure that the signal of the concentration of the reagent does not interfere with the signal of the reaction product.

3.2.1.A.2.5. General Procedures and the Calibration Curve

According to the optimum conditions, MA was quantitatively determined. The calibration curve was prepared at 477 nm by preparing a series of MA solutions with different concentrations and analyzing each employing the FIA system. The absorption peak height value of the formed complex was plotted against the concentration. The suggested method allows for the determination of MA in the range of (1-30) ppm, as shown in Figures [3.24] and [3.25].

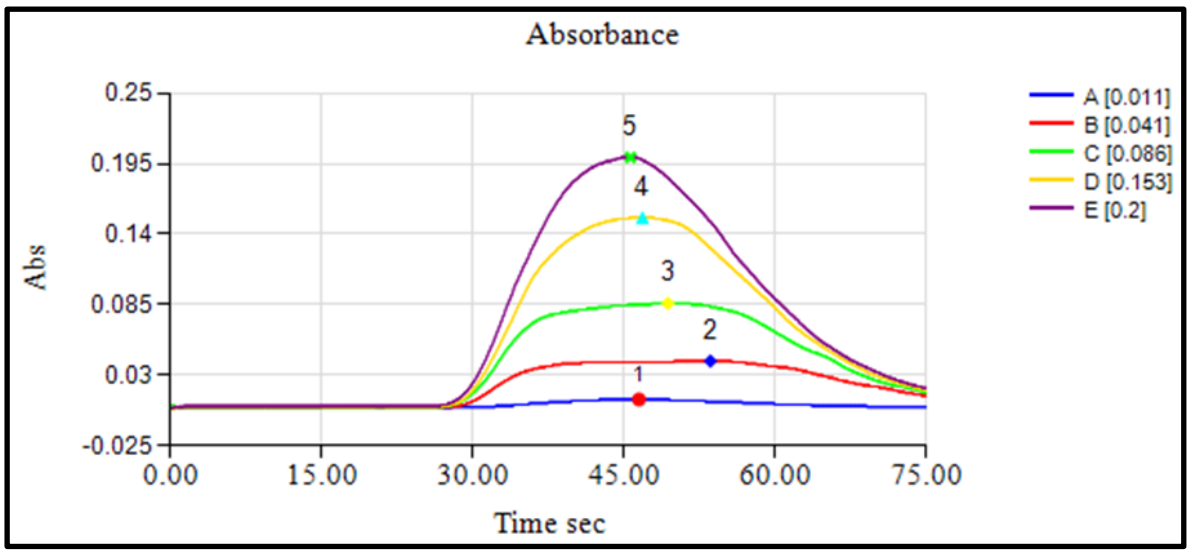

Figure [3.24]: Absorption Spectra of MA by Reverse – Continuous FIA

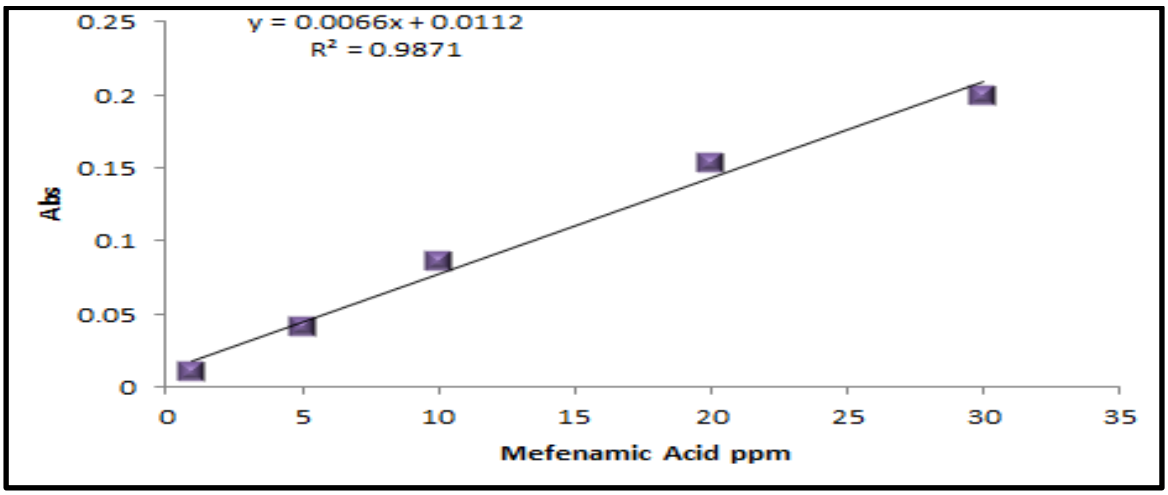

Figure [3.25]: Calibration Curve of MA

The sensitivity and correlation coefficient are shown in Table [3.7].

Table [3.7]: The Effect of MA conc. on the Absorption Peak Height when, NQS conc. = 50 ppm, reaction coil length = 75 cm, NaOH = 0.15 mL to 20 mL MA at room temperature

MA ppm	Abs	QR
1	0.011	0.018
5	0.041	0.044
10	0.086	0.077
20	0.153	0.143
30	0.2	0.209

3.2.1.A.2.6. Repeatability

The relative standard deviation (RSD %) represents the precision of the proposed method has been studied utilizing 30 ppm of MA solution. At the optimum conditions, 6 replicate measurements were carried out for the determined concentration and recorded as shown in Figure [3.26] and Table

[3.8]. The standard deviation value is equal to 0.0019, and the relative standard deviation value is equal to 0.586, indicating the high precision of the suggested method.

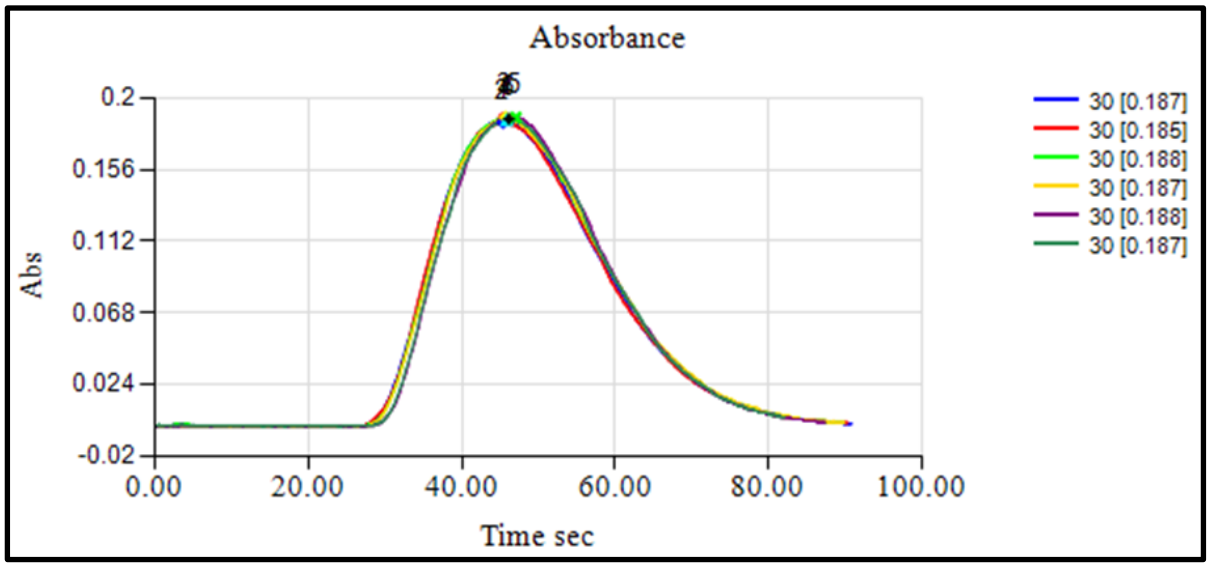

Figure [3.26]: Repeatability of 30 ppm MA Solution by Reverse – Continuous FIA

Table [3.8]: Repeatability Results for 30 ppm MA Solution by Reverse – Continuous FIA

Sample No.	1	2	3	4	5	6	Mean	SD	RSD%
Abs.	0.187	0.185	0.188	0.187	0.188	0.187	0.187	0.0011	0.586

3.2.1.A.2.7. Dead Volume

The quality of the obtained results was examined by performing the dead volume experiment. This experiment includes two steps: in the first step, water instead of NQS was loaded in the valve loop, and in the second step, water instead of the carrier solution represented the mixture of MA and NaOH. The

response to the two experiments was confirmed and was zero, indicating no dead volume, as shown in Figure [3.27].

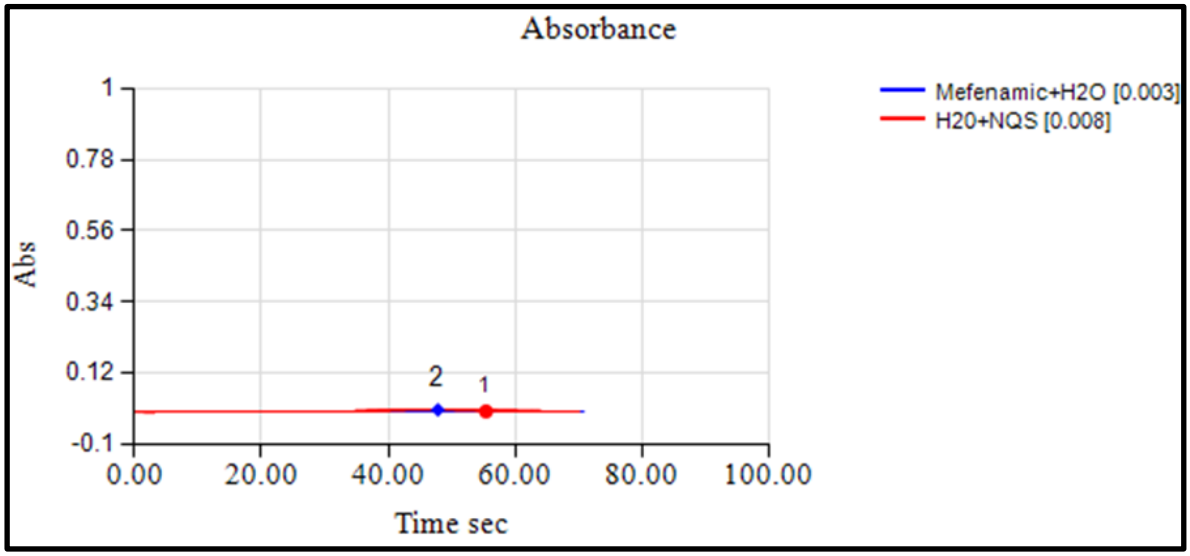

Figure [3.27]: The Dead Volume of MA

3.2.1.A.2.8. The Determination of Dispersion

The dispersion coefficient (dilution factor D) was studied to illustrate the dispersion process extent within the flow injection system from the injection point at the valve to the detecting point at the detector. The dispersion coefficient can be calculated through Equation [1.1] and its equal 1.17.

The dispersion coefficient was studied using one concentration of MA solution within the calibration curve range (30 ppm). In the first step, the reaction between the MA alkaline solution and the NQS solution was implemented inside the FIA system under the defined optimum conditions by measuring the peak height that represents the peak height with the dilution process (H_{max}). In the second step, the reaction between the MA alkaline solution and the NQS solution in appropriate volumes was implemented in a glass beaker and passed the final solution through the system, then measuring

the absorption peak height that takes the plateau shape with a constant height value with the time that represents the peak height without the dilution process (H°). And the obtained results are displayed in Figure [3.28].

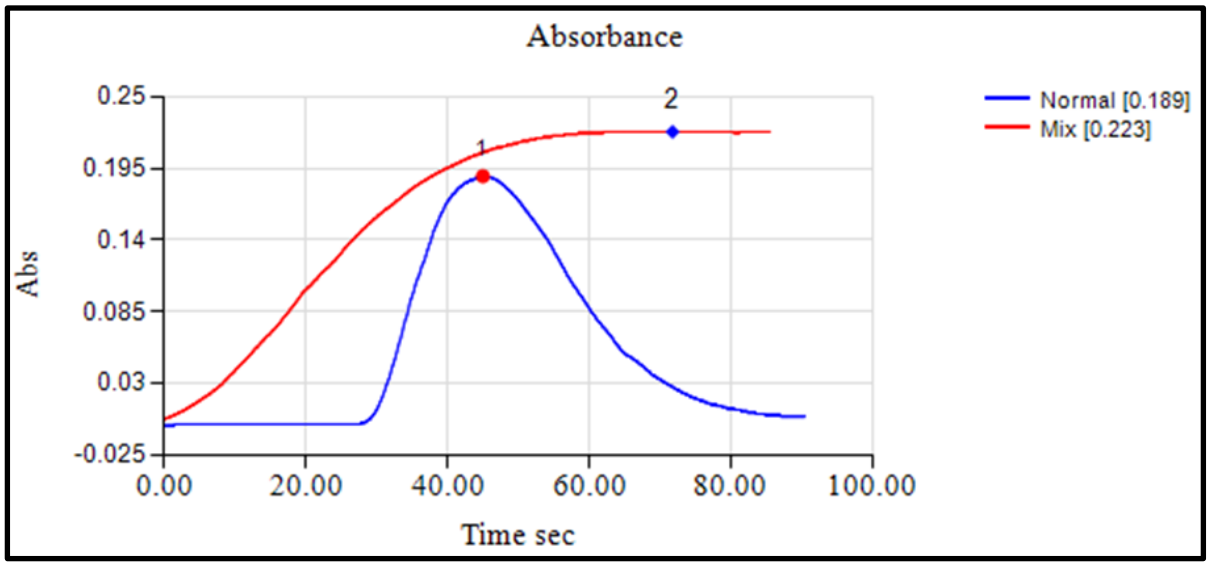

Figure [3.28]: Dispersion Coefficient Study Results for MA Determination FIA System

3.2.1.A.2.9. In Aqueous Solutions, MA can be Determined as follows

Two aqueous solutions were prepared and considered solutions of unknown concentration; then, the absorbance was measured according to the optimum conditions, as shown in Figure [3.29]. Then the solutions' concentration was determined by setting each solution's absorbance on the straight line of the previous calibration curve, as shown in Figure [3.30] and Table [3.9]. The value of the resulting solutions from the calibration curve was very close to the prepared solutions, considering the preparation errors.

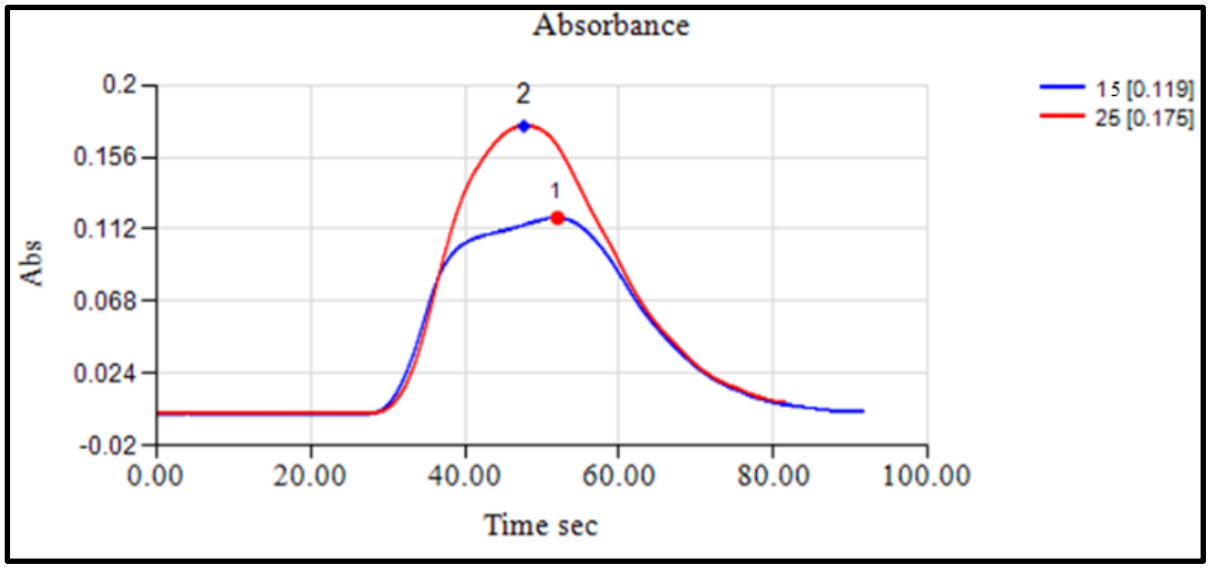

Figure [3.29]: The Spectrum of Possible Applications

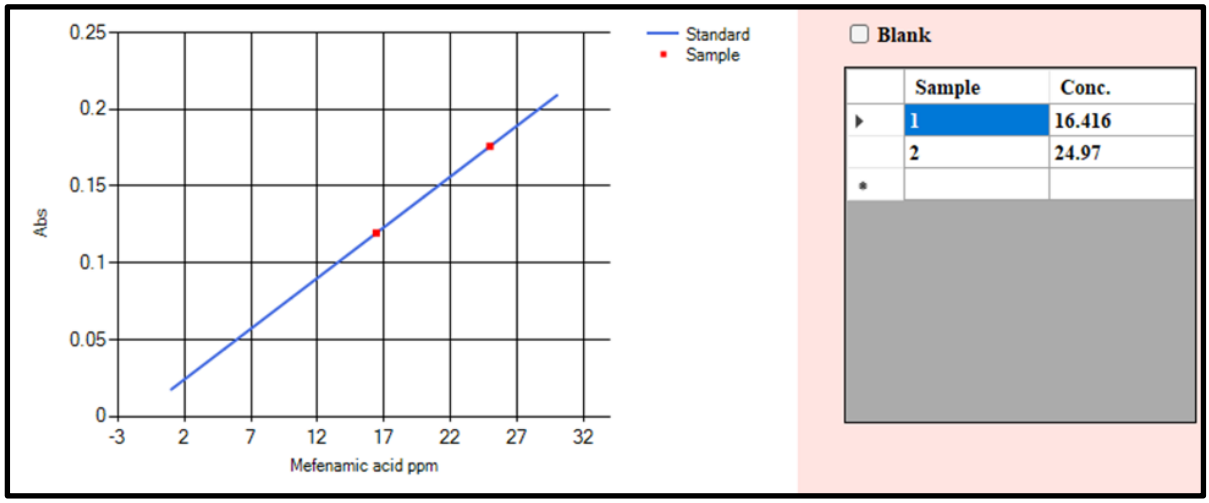

Figure [3.30]: Determination of Unknown Aqueous Solutions

Table [3.9]: Value of Sample Application

Index	Sample ppm (Taken)	MA ppm (Founded)	Peak Height	Recovery
1	15	16.358	0.119	109
2	25	24.889	0.175	99.6

3.2.1.B.1. The Calibration Curve of MA Determination by NQS in the Basic Medium Using the Spectrophotometric Method (Batch method)

The calibration curve of the MA determination method at 477 nm was plotted under the optimum conditions by preparing a series of MA solutions having different concentrations and analyzing each in triplicate, then drawing the reaction product absorbance against the corresponding MA concentration.

The suggested method allows for determining the MA in the linearity range of (0.5-10) ppm, as shown in Table [3.10] and Figure [3.31].

Table [3.10]: The effect of MA concentration on the absorption value when, MA volume = 1mL, NQS conc. = 50 ppm, NQS volume = 1 mL, used base type = NaOH, Base conc. = 0.2M, Base volume = 0.1 mL, at room temperature.

MA conc. ppm	Abs. 1	Abs. 2	Abs. 3	Absorbance means	SD	RSD%
0.5	0.063	0.063	0.062	0.0626	0.00047	0.752
2	0.187	0.186	0.186	0.186	0.00047	0.253
4	0.371	0.371	0.37	0.3706	0.00047	0.127
7	0.654	0.653	0.653	0.653	0.00047	0.072
10	0.919	0.919	0.918	0.9186	0.00047	0.051

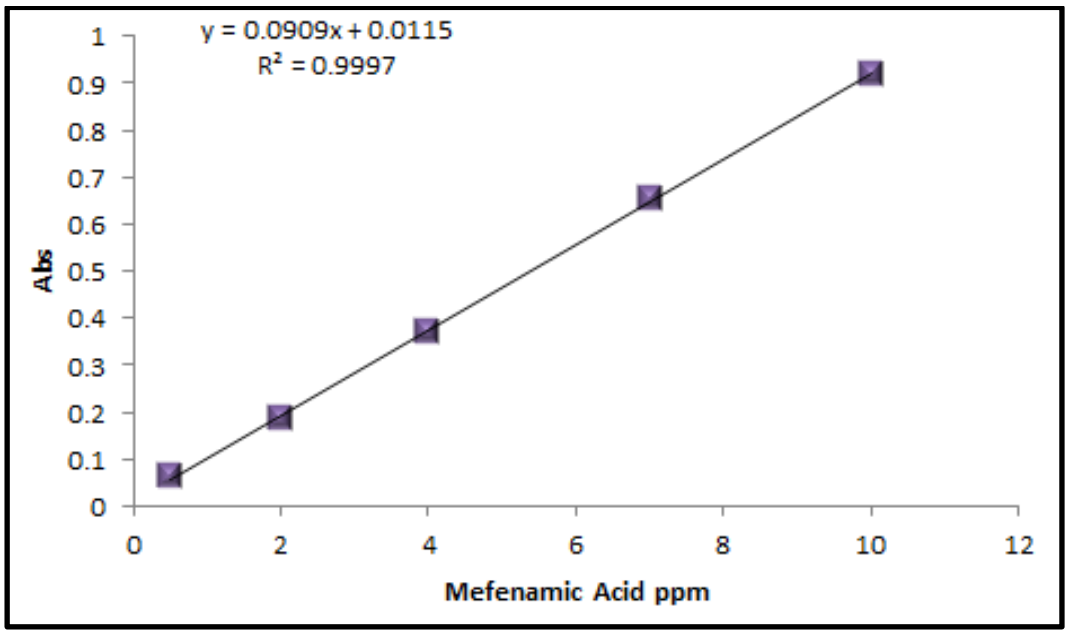

Figure [3.31]: Calibration Curve of MA by Batch Method

3.2.1.B.2. In Aqueous Solutions, MA can be Determined as follows

Three aqueous solutions of unknown concentration were measured, and then their concentration was determined after measuring the absorbance and determined on the calibration curve, as shown in Table [3.11] and Figure [3.32].

Table [3.11]: The Value of the Sample Application

Index	Sample (taken)ppm	Mefenamic acid (founded)ppm	Absorbance	Recovery
1	2	2.2	0.205	110
2	5	5.1	0.476	102
3	6.5	6.7	0.624	103

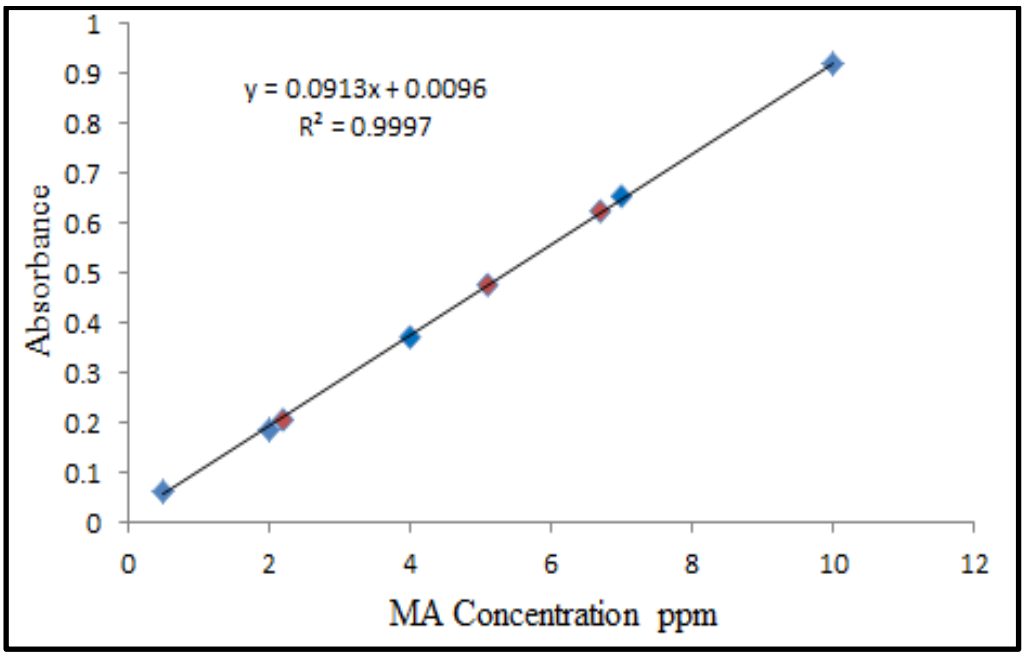

Figure [3.32]: Determination of Unknown Aqueous Solutions

3.2.2.A.1. Spectrofluorometric Method to Determine Procaine Hydrochloride by Merging-Zone FIA

A single parameter was changed to optimize experimental conditions, and the effect on the fluorescence of the species was monitored to identify the best possible testing conditions for the experiment, see Scheme [3.7].

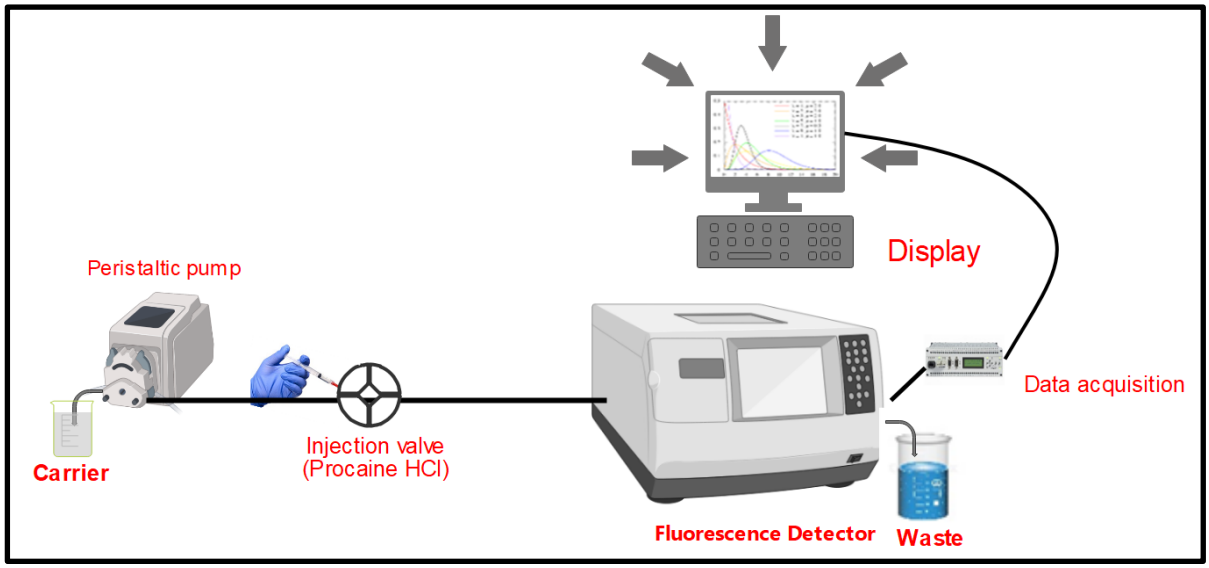

Scheme [3.7]: Design of Merging-Zone FIA with Fluorescence Detector

3.2.2.A.1.1. Determining the Maximum Ex and Em to Procaine HCl

A maximum emission of Procaine was scanned by using a fluorescence spectrophotometer. The fluorescence spectrum of Procaine showed a maximum excitation peak at 285 nm and a maximum emission peak at 362 nm, as shown in Figure [3.33] and Table [3.12].

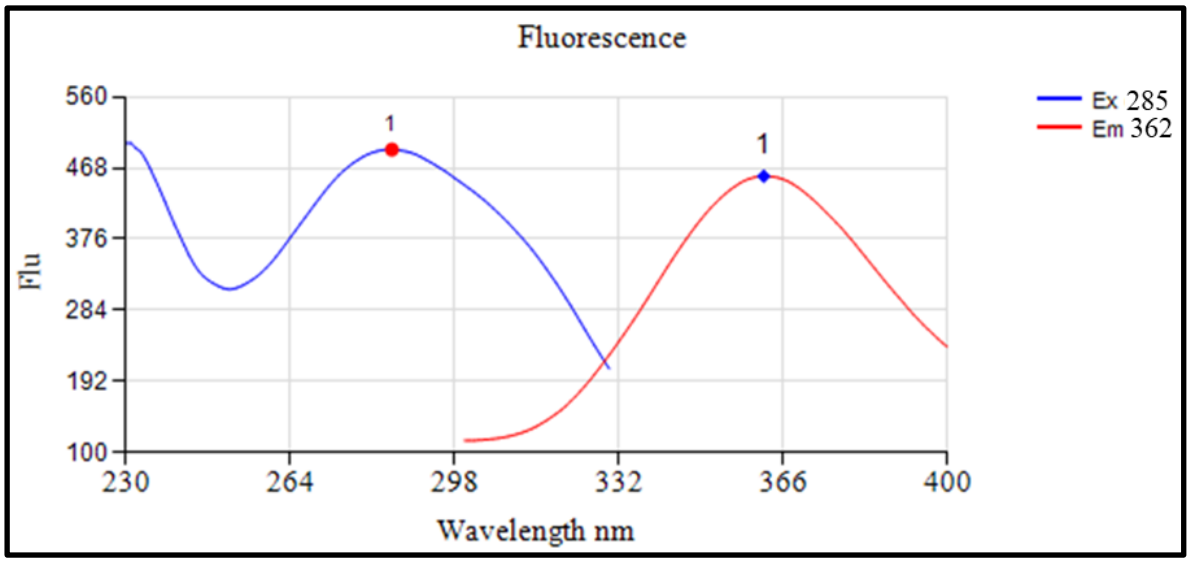

Figure [3.33]: Typical Scanning Fluorescence Spectrum for 300 ppm Procaine Standard of Excitation Spectral (blue line) and Emission Spectral Response (red line) Dissolved in Distilled Water

Table [3.12]: Result of Lambda Max

INDEX	Lembda	Ex
1	285	491.916

INDEX	Lembda	Em
1	362	457.393

3.2.2.A.1.2. The Influence of Flow Rate:

The effect of the flow rate and the selection of the optimum speed for the system interaction was studied. The results in Figure [3.34] show the effect of the pump speed on the response value (peak height) at the conditions mentioned below, as it is noted that the response decreases by increasing the pump speed from 1 to 5, and this matches the theoretical foundations of the effect of speed on response. The third speed, with a response rate of 112.106, is preferred over the fourth and fifth speeds for being the highest value. Also, the third speed is preferable to the slower speeds; although speeds 1 and 2 have the highest response than the third speed, the shape of the peak for those low speeds is broad and not ideal; either the form of the peak of the third speed, which has a flow rate of 1.5 ml per minute, is the best because it is sharp and uniform.

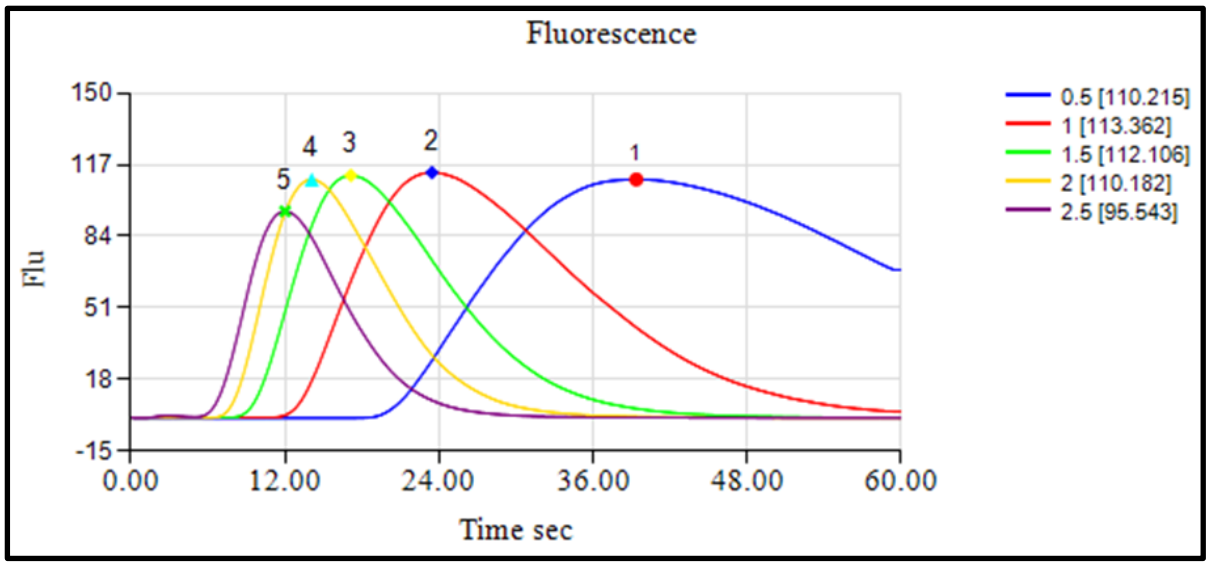

Figure [3.34]: Effect of Flow Rate on the Fluorescence Peak Height when, Procaine conc. = 70 ppm, reaction coil length = zero, at room temperature.

3.2.2.A.1.3. General Procedures and the Calibration Curve

Procaine was quantitatively determined, and the calibration curve was prepared at Ex 285 nm and Em 362 nm by preparing a series of Procaine solutions with different concentrations and analyzing each employing the FIA system. The fluorescence peak height value was plotted against the concentration. The suggested method allows for the determination of Procaine in the range of (1-100) ppm, as shown in Figures [3.35] and [3.36] and Table [3.13].

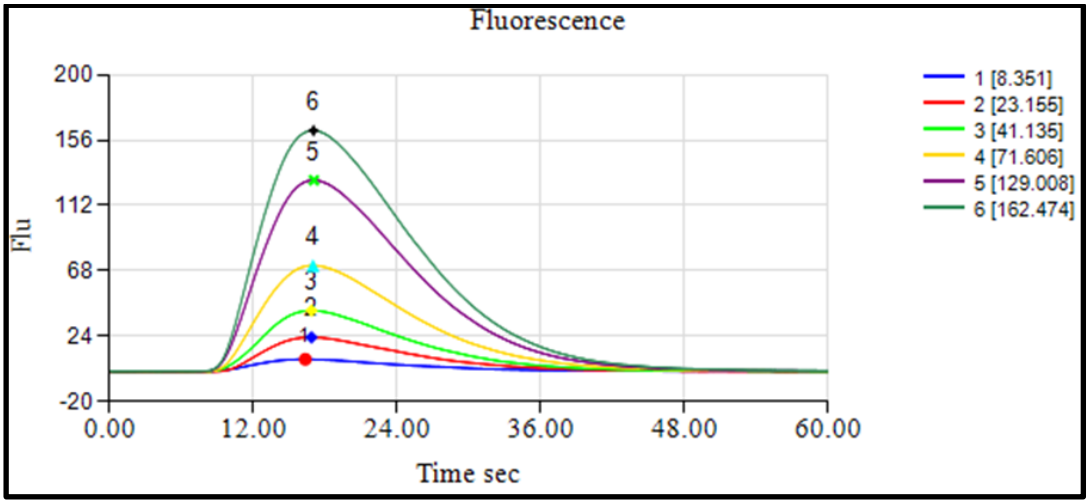

Figure [3.35]: Fluorescence Spectra of Procaine by Merging-Zone FIA

Table [3.13]: The Effect of Procaine conc. on the Fluorescence Peak Height when, flow rate = 1.5 mL/min, carrier = distilled water, reaction coil length = zero, at room temperature

Index	Sample	Procaine HCl ppm	Peak Height
1	1	1	8.351
2	2	5	23.155
3	3	10	41.135
4	4	50	71.606
5	5	75	129.008
6	6	100	162.474

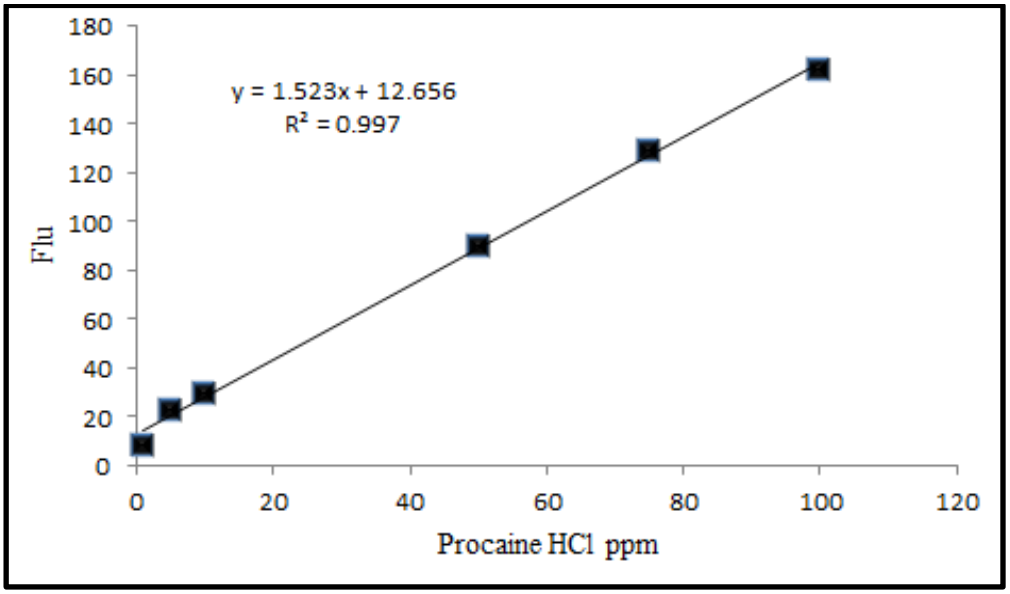

Figure [3.36]: Calibration Curve of Procaine

3.2.2.A.1.4. Repeatability

The relative standard deviation (RSD %) represents the precision of the proposed method has been studied utilizing 70 ppm of Procaine solution. At the optimum conditions, 4 replicate measurements were carried out for the determined concentration and recorded as shown in Figure [3.37] and Table [3.14]. The standard deviation value is equal to 2.378, and the relative standard deviation value is equal to 2.008, indicating the high precision of the suggested method.

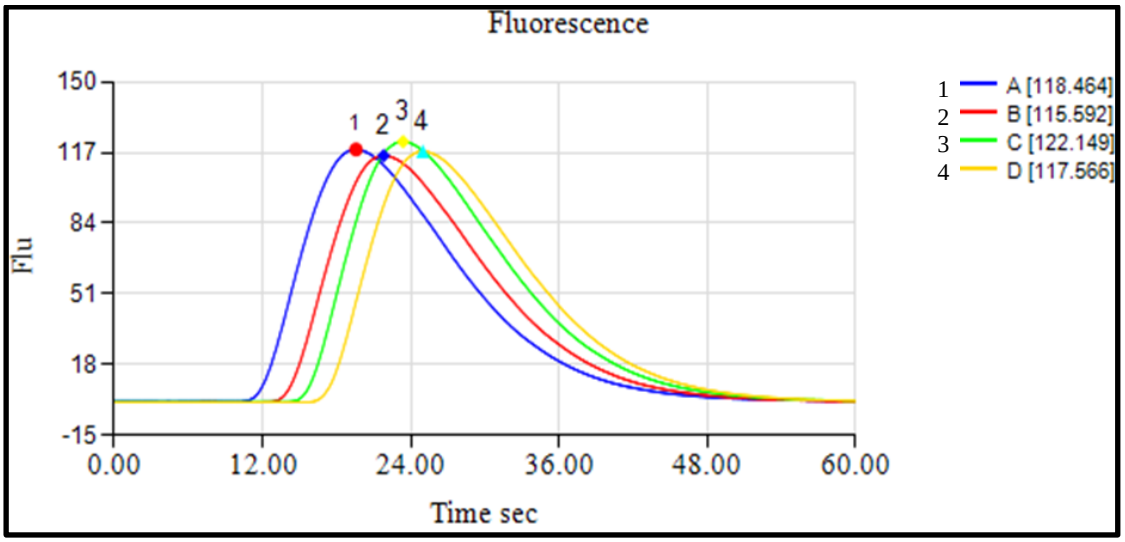

Figure [3.37]: Depicted the Repeatability of Procaine

Table [3.14]: Repeatability Results for 70 ppm Procaine Solution by Merging-Zone FIA

Sample No.	1	2	3	4	Mean	SD	RSD%
Flu.	118.464	115.592	122.149	117.566	118.443	2.378	2.008

3.2.2.A.1.5 The Determination of Dispersion

The dispersion coefficient (dilution factor D) was studied to illustrate the dispersion process extent within the flow injection system from the injection point at the valve to the detecting point at the detector. The dispersion coefficient can be calculated through Equation [1.1] and its equal 1.651.

The dispersion coefficient was studied by using one concentration of procaine solution within the calibration curve range (80 ppm). In the first step, the procaine solution was implemented inside the FIA system under the defined optimum conditions by measuring the peak height that represents the peak height with the dilution process (H max). In the second step, the procaine solution was implemented in a glass beaker and passed the solution through the system, then measuring the fluorescence peak height that takes the plateau shape with a constant height value with the time representing the peak height without the dilution process (H°). The obtained results are displayed in Figure [3.38].

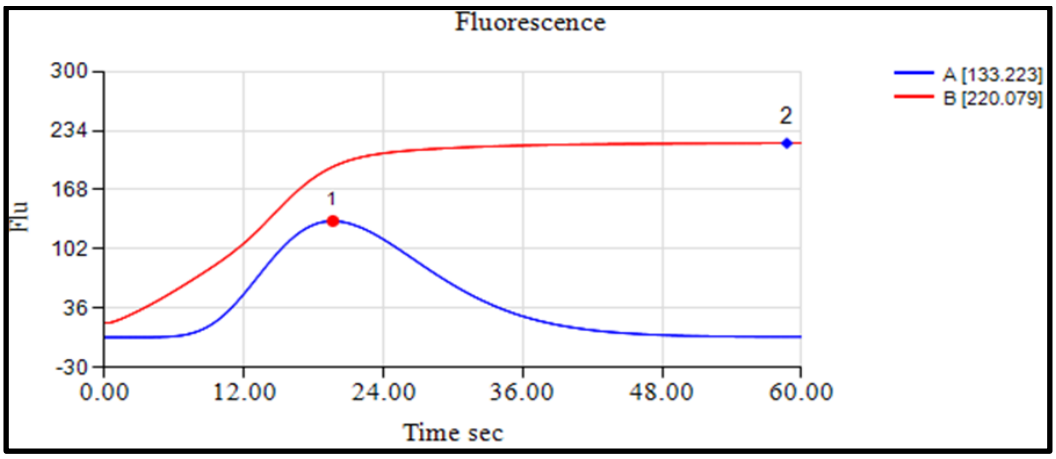

Figure [3.38]: Dispersion Coefficient Study Results for Procaine Determination Merging-Zone FIA

3.2.2.A.1.6. Application in Aqueous Solutions

Three aqueous solutions were prepared and considered solutions of unknown concentration; then, the fluorescence was measured according to the optimum conditions, as shown in Figure [3.39]. Then the solutions' concentration was determined by setting each solution's fluorescence on the straight line of the previous calibration curve, as shown in Figure [3.40] and Table [3.15]. The value of the resulting solutions from the calibration curve was very close to the prepared solutions, considering the preparation errors.

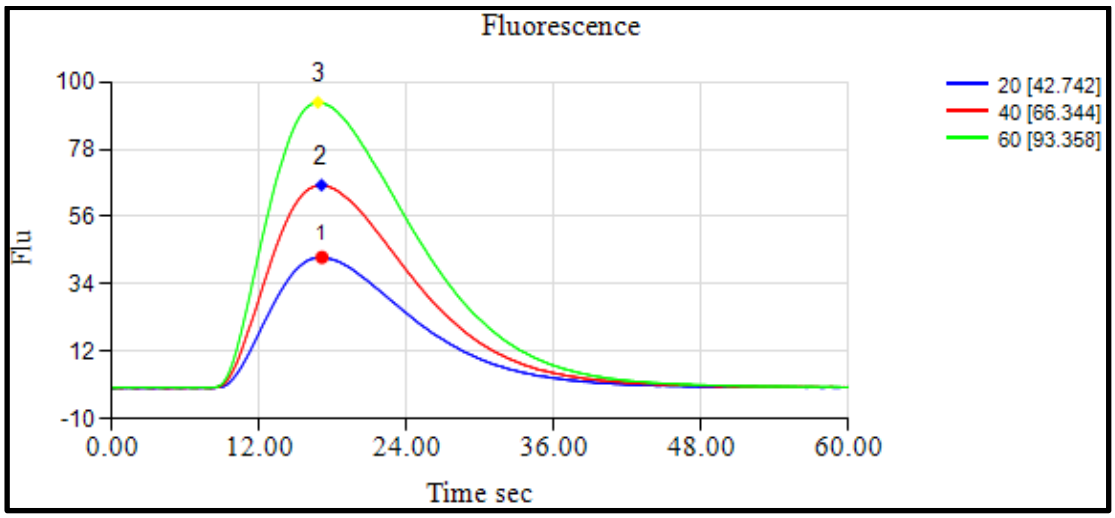

Figure [3.39]: The Spectrum of Possible Applications

Table [3.15]: Value of Sample Application

Index	Sample (taken)	Procaine (founded)	Peak Height	Recovery
1	20	20	42.742	100
2	40	36.5	66.344	91
3	60	54.6	93.358	91

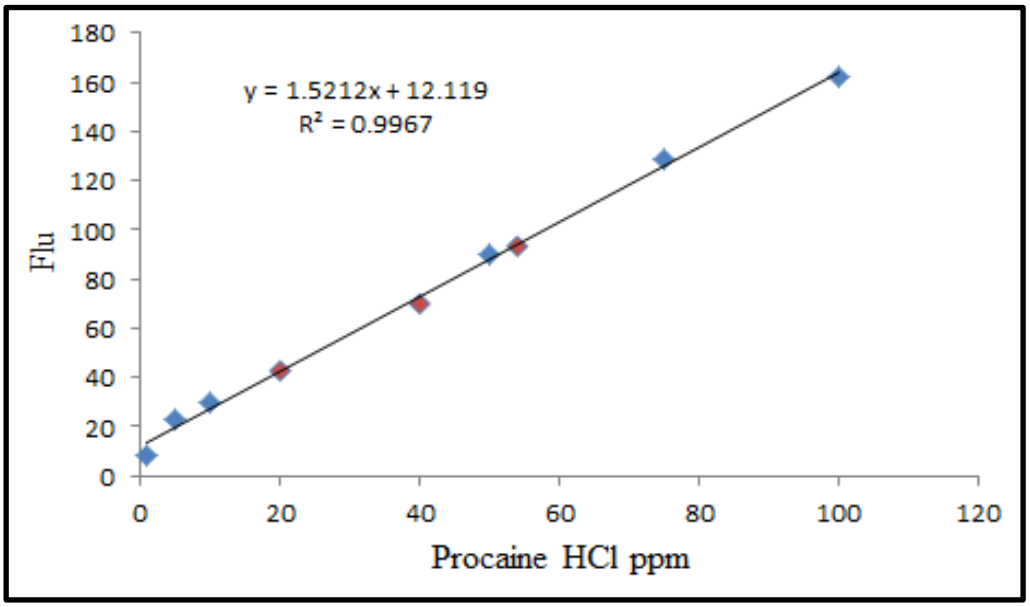

Figure [3.40]: Determination of Unknown Aqueous Solutions

3.2.2.A.2. Spectrofluorometric Method to Determine NQS by Merging-Zone FIA

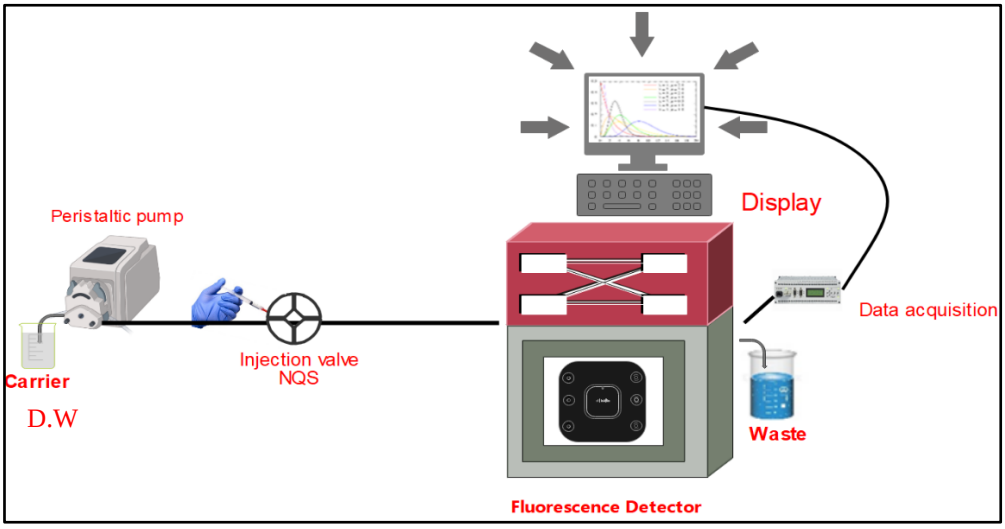

Scheme [3.8]: Design of Merging-Zone FI Unit with Fluorescence Detector

3.2.2.A.2.1. Determining the Maximum Ex and Em to NQS

A maximum emission of NQS was scanned using a fluorescence spectrophotometer. The fluorescence spectrum of NQS showed a maximum excitation peak at 469 nm and a maximum emission peak at 543 nm, as shown in Figure [3.41] and Table [3.16].

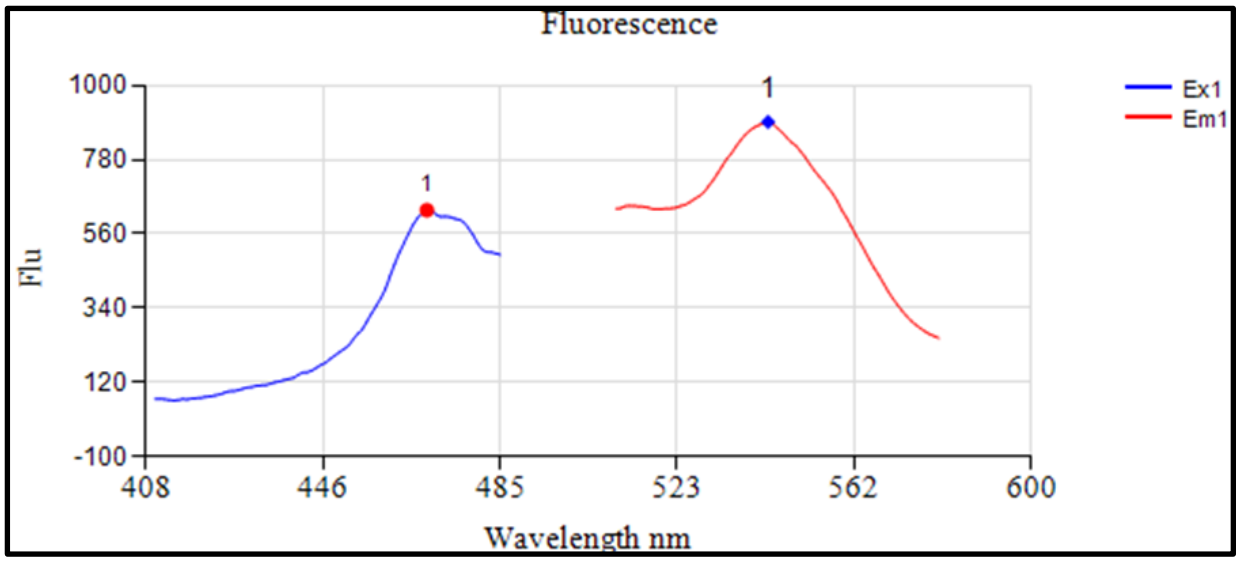

Figure [3.41]: Typical Scanning Fluorescence Spectrum for 80 ppm NQS Standard of Excitation Spectral (blue line) and Emission Spectral Response (red line) Dissolved in Distilled Water

Table [3.16]: Result of Lambda Max

Lembda	Ex1	Lembda	Em1
469	630.21	543	892.058

3.2.2.A.2.2. General Procedures and the Calibration Curve

NQS was quantitatively determined, and the calibration curve was prepared at Ex 469 nm and Em 543 nm by preparing a series of NQS solutions with different concentrations and analyzing each employing the FIA system. The fluorescence peak height value was plotted against the concentration Figure [3.42]. The suggested method allows for the determination of NQS in the range of (5-50) ppm, as shown in Table [3.17] and Figure [3.43].

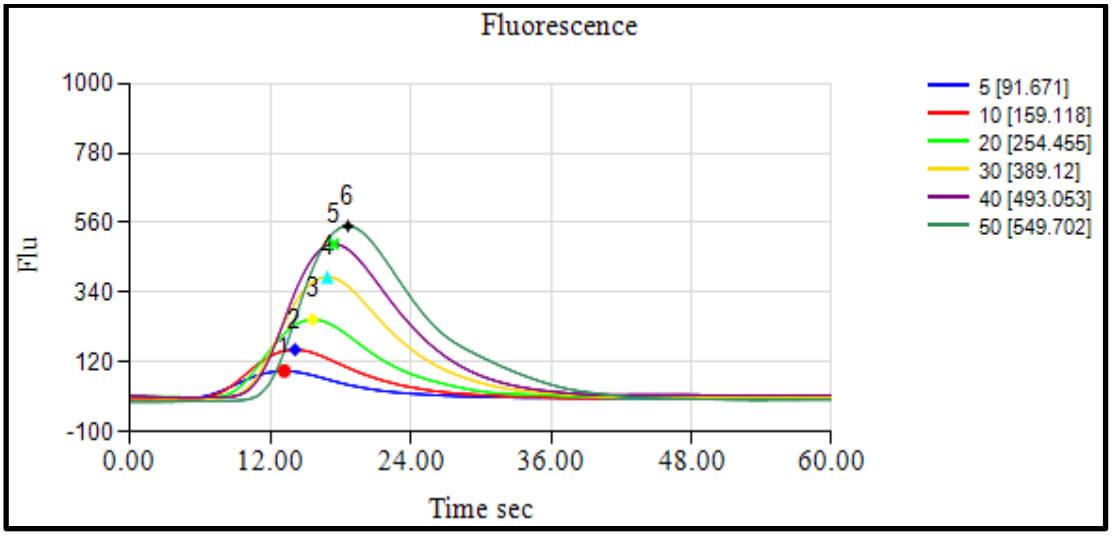

Fig. [3.42]: Fluorescence Spectra of NQS by Merging-Zone FIA

Table [3.17]: The Effect of NQS conc. on the Fluorescence Peak Height when, flow rate = 1.5 mL/min, carrier = distilled water, reaction coil length = zero, at room temperature

Index	Sample	test ppm	Peak Height
1	1	5	91.671
2	2	10	159.118
3	3	20	254.455
4	4	30	389.12
5	5	40	493.053
6	6	50	549.702

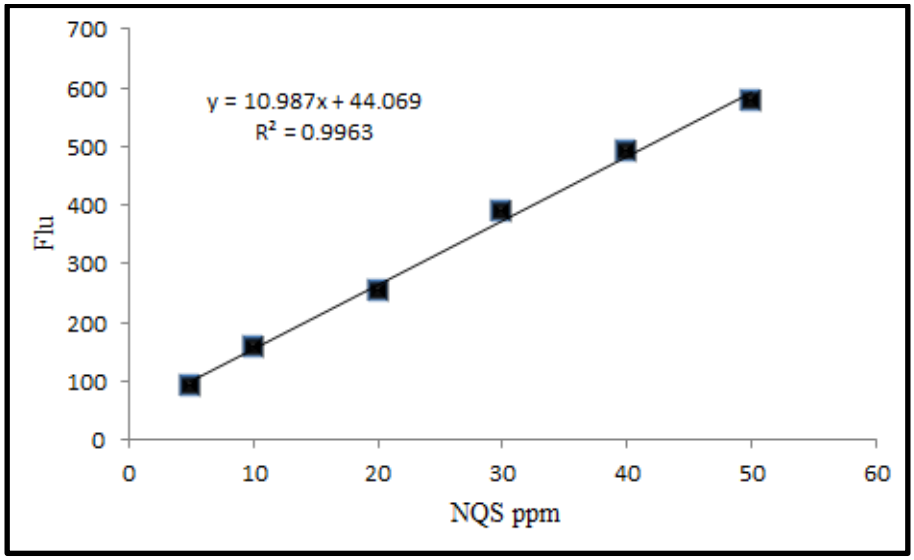

Figure [3.43]: Calibration Curve of NQS

3.2.2.A.2.3. Repeatability

The relative standard deviation (RSD %) representing the precision of the proposed method has been studied utilizing 30 ppm of NQS solution. At the optimum conditions, 6 replicate measurements were carried out for the determined concentration and recorded as shown in Figure [3.44] and Table [3.18]. The standard deviation value is equal to 7.862, and the relative standard deviation value is equal to 1.941, indicating the high precision of the suggested method.

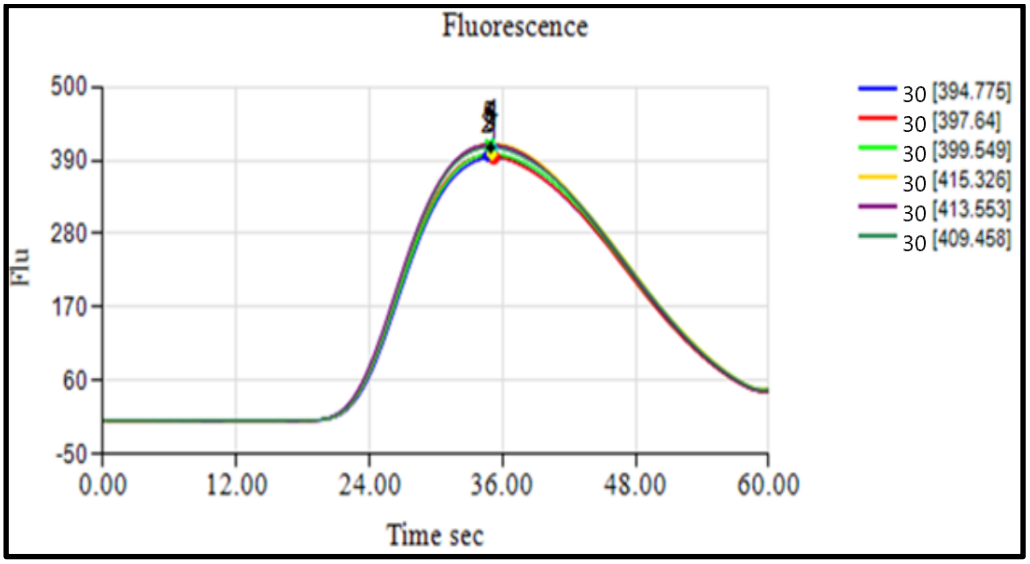

Figure [3.44]: Repeatability of 30 ppm for NQS Solution by Merging-Zone FIA

Table [3.18]: Repeatability Results for 30 ppm NQS Solution by Merging-Zone FIA

Sample No.	1	2	3	4	5	6	Mean	SD	RSD%
Flu.	395	398	400	415	414	409	405	7.862	1.941

3.2.2.A.2.4. Application in aqueous solutions

Three aqueous solutions were prepared and considered solutions of unknown concentration; then, the fluorescence was measured according to the optimum conditions, as shown in Figure [3.45]. Then the solutions' concentration was determined by setting each solution's fluorescence on the straight line of the previous calibration curve, as shown in Figure [3.46] and Table [3.19]. The value of the resulting solutions from the calibration curve was very close to the prepared solutions, considering the preparation errors.

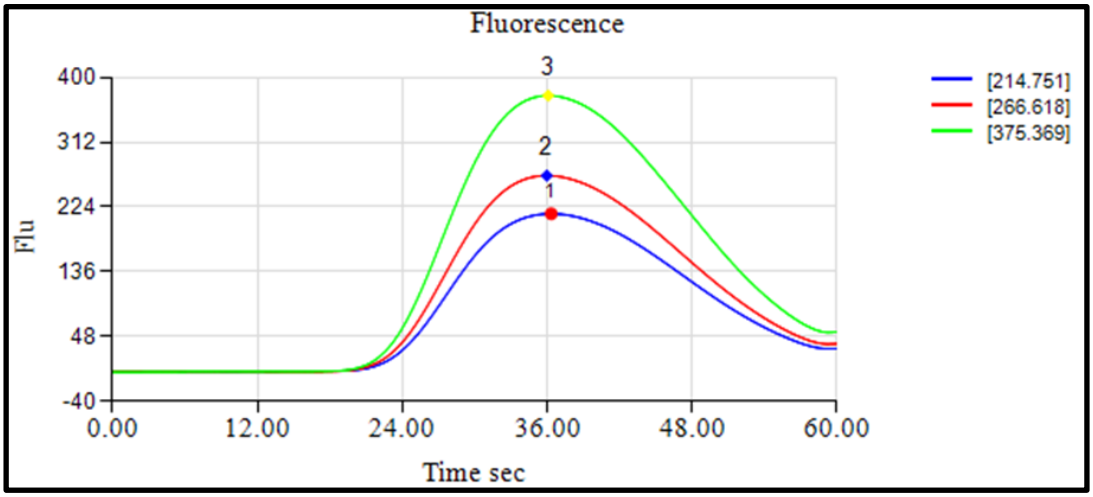

Figure [3.45]: The Spectrum of Possible Applications

Table [3.19]: Value of Sample Application

Index	Sample (taken)ppm	NQS (founded)ppm	Peak Height	Recovery
1	15	15.34	214.751	102
2	20	20.987	266.618	104
3	30	30.03	375.369	100

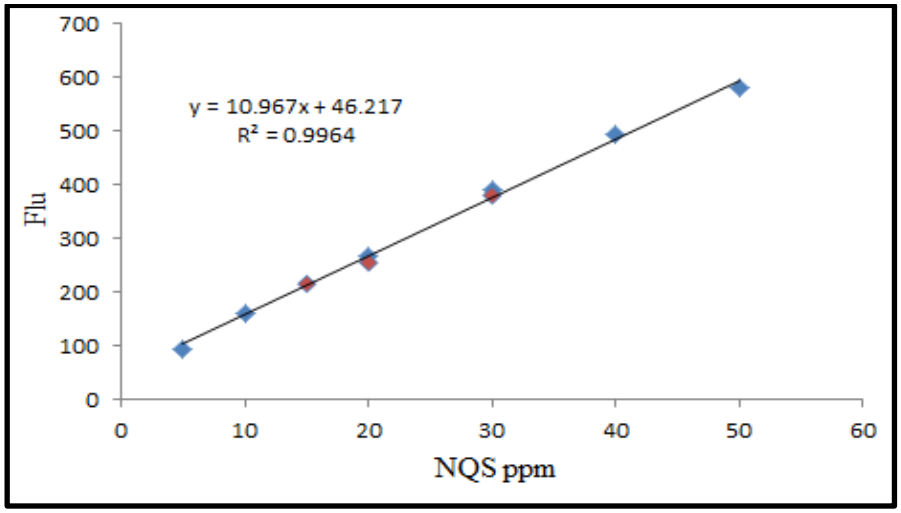

Figure [3.46]: Determination of Unknown Aqueous Solutions

3.2.2.B.1. Batch Spectrofluorometric Method to Determine MA in Terms of NQS

3.2.2.B.1.1. Determining the Maximum Ex &Em to NQS

A maximum emission of 100 ppm NQS was scanned using a fluorescence spectrophotometer. The fluorescence spectrum of NQS showed a maximum emission peak at 477.42 nm, as shown in Figure [3.47].

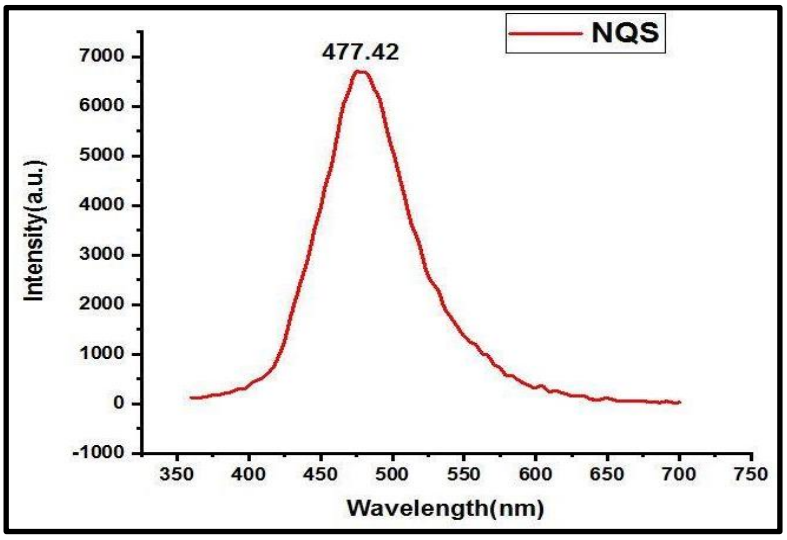

Figure [3.47]: A Maximum Fluorescence Emission Spectrum of NQS

3.2.2.B.1.2. General Procedures and the Calibration Curve

MA was quantitatively determined, and the calibration curve was prepared at Em 477 nm by preparing a series of MA solutions with different

concentrations and analyzing each after mixing with base and reagent. The fluorescence peak height value was plotted against the concentration Figure [3.48]. The suggested method allows for the determination of MA in the range of (1-100) ppm, as shown in Table [3.20] and Figure [3.49].

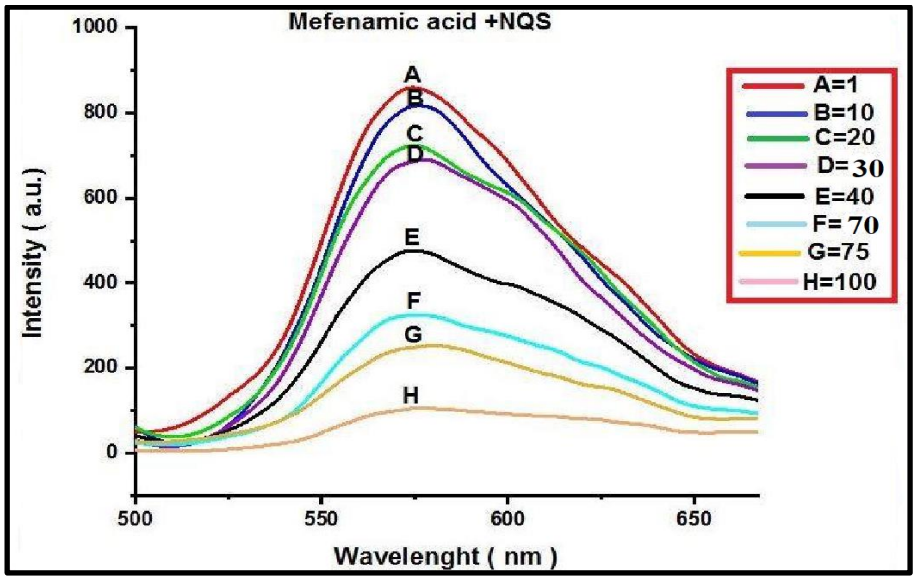

Figure [3.48]: Fluorescence Spectra of MA in Terms of NQS

Table [3.20]: The Effect of MA Conc. on the Fluorescence Peak Height when, NQS conc. = 50 ppm, volume of alkaline medium = 0.1 mL of 0.2 M from NaOH, at room temperature

Index	MA concentration(ppm)	Peak Hight
A	1	880
B	10	805
C	20	730
D	25	690
E	40	590
F	70	330
G	75	290
H	100	90

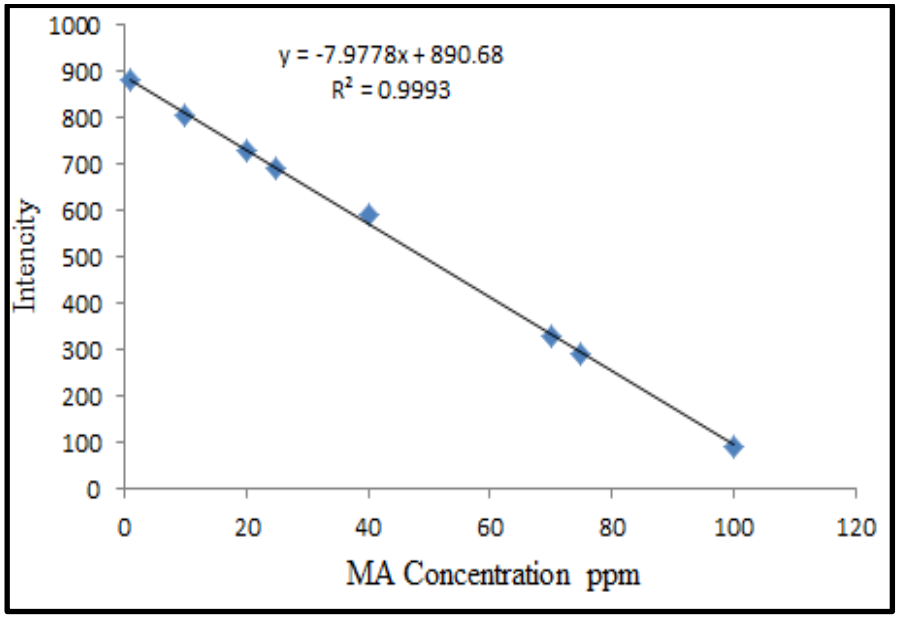

Figure [3.49]: Calibration Curve of MA

3.2.2.B.1.3. Application in aqueous solutions

Three aqueous solutions were prepared and considered solutions of unknown concentration; then, the fluorescence was measured according to the optimum conditions, then the solutions' concentration was determined by setting each solution's fluorescence on the straight line of the previous calibration curve, as shown in Table [3.21] and Figure [3.50]. The value of the resulting solutions from the calibration curve was very close to the prepared solutions, considering the preparation errors.

Table [3.21]: Value of Sample Application

Index	Sample (taken)ppm	MA (founded)ppm	Peak Height	Recovery
1	35	33.4	600	103
2	40	40.9	590.7	101
3	75	77.5	290.41	99

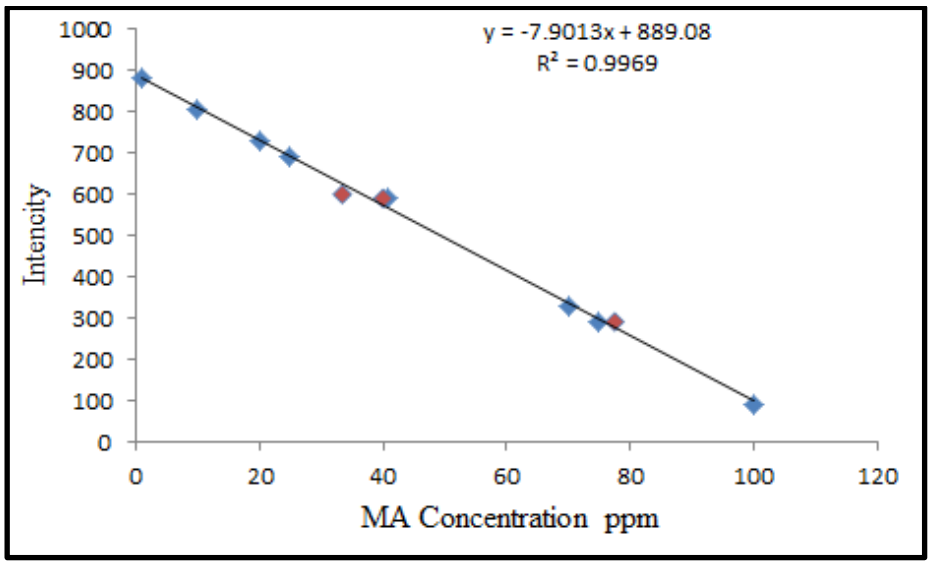

Figure [3.50]: Determination of Unknown Aqueous Solutions

3.2.2.B.2. Batch Spectrofluorometric Method to Determine MA

3.2.2.B.2.1. Determine the Maximum Em of MA

A maximum emission of 100 ppm MA was scanned using a fluorescence spectrophotometer. The fluorescence spectrum of MA showed a maximum emission peak at 295.2 nm, as shown in Figure [3.51].

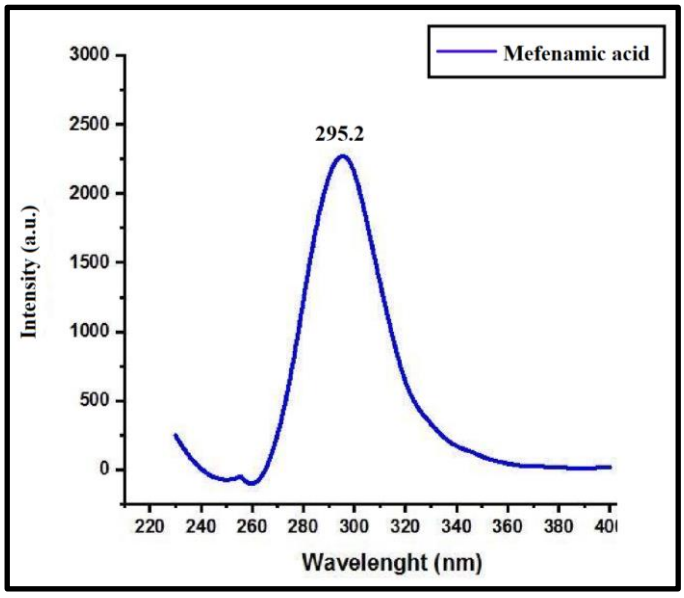

Figure [3.51]: A Maximum Fluorescence Emission Spectrum of MA

3.2.2.B.2.2. General Procedures and the Calibration Curve

MA was quantitatively determined, and the calibration curve was prepared at Em 295.2 nm by preparing a series of MA solutions with different concentrations and analyzing each. The fluorescence peak height value was plotted against the concentration Figure [3.52]. The suggested method allows for the determination of MA in the range of (1-100) ppm, as shown in Table [3.22] and Figure [3.53].

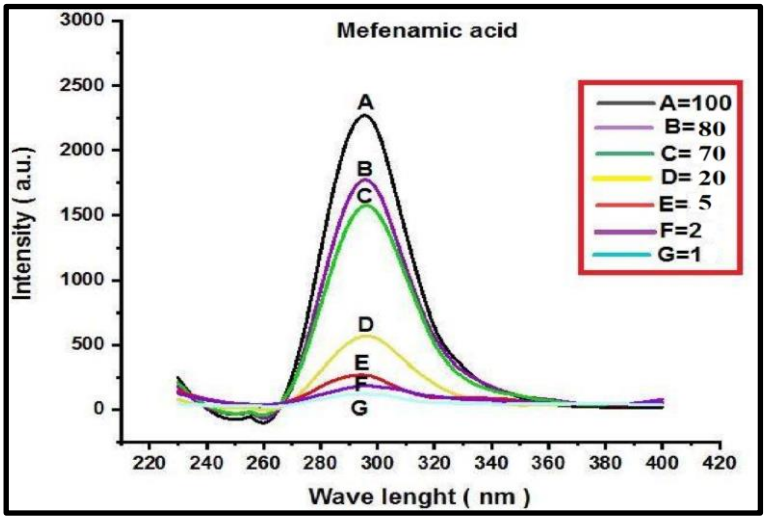

Figure [3.52]: Fluorescence Spectra of MA

Table [3.22]: The Effect of MA Conc. on the Fluorescence Peak Height at room temperature

Index	MA concentration(ppm)	Peak Height
G	1	130
F	2	195
E	5	250
D	20	600
C	70	1600
B	80	1800
A	100	2300

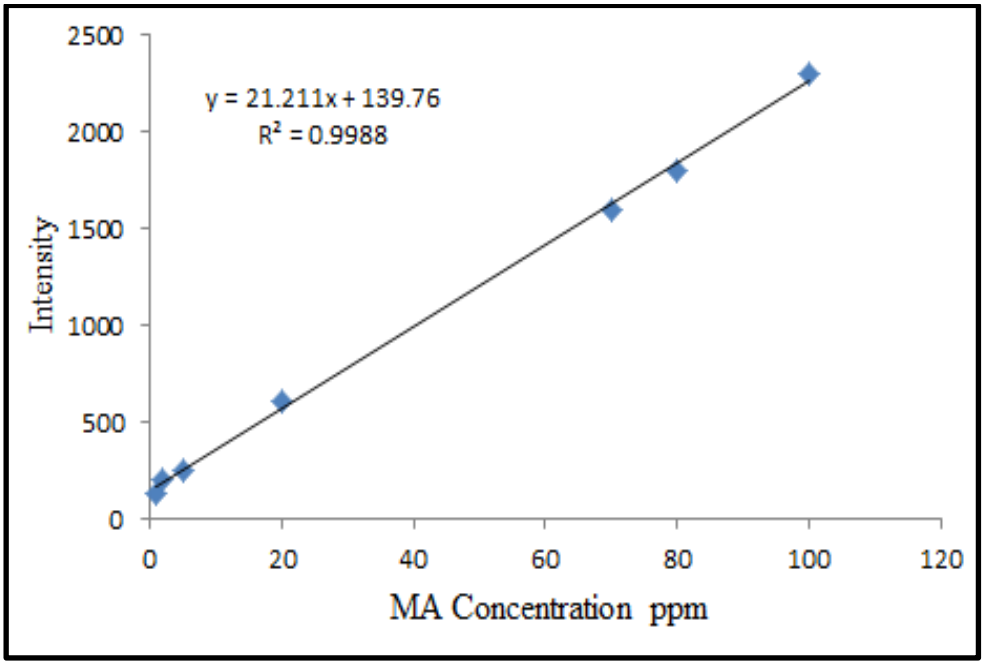

Figure [3.53]: Calibration Curve of MA

3.2.2.B.2.3. Application in aqueous solutions

Three aqueous solutions were prepared and considered solutions of unknown concentration; then, the fluorescence was measured according to the optimum conditions, then the solutions' concentration was determined by setting each solution's fluorescence on the straight line of the previous calibration curve, as shown in Table [3.23] and Figure [3.54]. The value of the resulting solutions from the calibration curve was very close to the prepared solutions, considering the preparation errors.

Table [3.23]: Value of Sample Application

Index	Sample (taken)ppm	MA (founded)ppm	Peak Height	Recovery
1	35	33.4	850.89	95
2	55	40.9	1255.42	98
3	90	77.5	2051.6	101

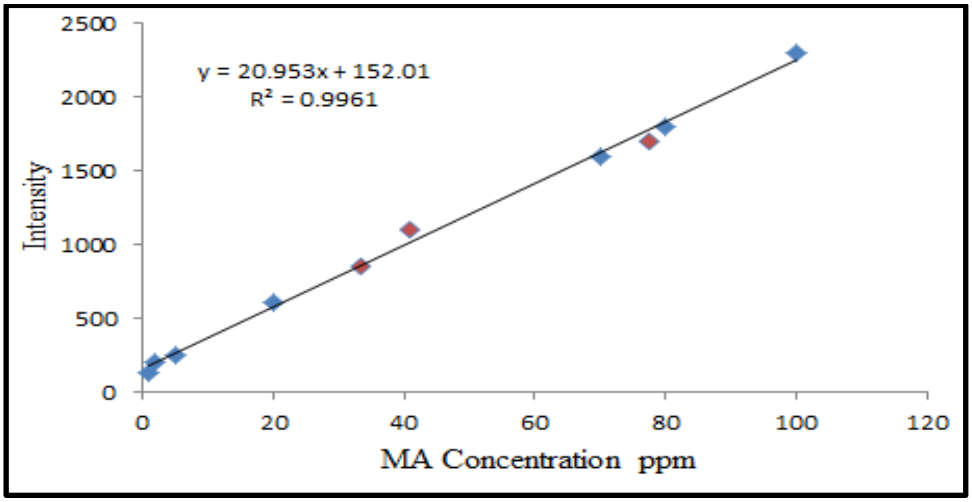

Figure [3.54]: Determination of Unknown Aqueous Solutions

3.3 results of the research and their comparison with previous studies

Table [3.24]: The results of this research

	Method	Reagent	Rang ppm	R^2	Slop	RSD%	Recovery	λ_{max}
Mefenamic acid	Merging zone - FIA	NQS	1-20	0.9999	0.012	1.237	99.5-101.8	477
	Reverse -FIA	NQS	1-30	0.9869	0.007	0.586	99.6-109	477
	Batch	NQS	0.5-10	0.9997	0.0912	0.072	102-110	477
	Fluorescence (Batch)	NQS	1-100	0.9993	7.997	—	99-103	Em(NQS) 477.42
	Fluorescence (Batch) Direct	—	1-100	0.9988	21.211	—	95-101	Em(MA) 295.2
Procaine HCl	Fluorescence + Merging FIA	NQS	1-100	0.9986	1.519	2	91-100	Em(NQS) 362
NQS	Fluorescence + Merging FIA	NQS	5-50	0.9976	10.961	1.941	100-104	Em 573

From the Table [3.24] we note that the MA determination methods have certain properties that are characterized by their range, RSD%, and R. In general, flow injection methods are characterized by low sample size and modeling speed while fluorescence methods are characterized by a wide range.

The RSD%, sensitivity and range of the both merging zone and reverse methods are better than those found in the literature [72, 73, 75-79]in the MA's determination.

As for the determination of procaine, the method is better in terms of range, RSD% and sensitivity compared to [86, 88, 89, 91, 94, 95].

3.4. Conclusions:

1. Amino drugs and reagents under study can be determined using the spectral methods, which can be combined with the flow injection technique. The study has shown that all systems designed are highly efficient.
2. The determination of MA, Procaine and the reagent (NQS) in the flow injection unit is characterized by the rate in analysis and high sensitivity in determination and wide range of concentrations, which is one of the preferred advantages in analytical chemistry.
3. The flow injection system is characterized by not consuming chemicals in large quantities, as it is characterized by the use of tiny volumes and low concentrations of both the reagent and the carrier solution mixture, as well as the small sample size
4. Other benefits of the new systems were high selectivity and recovery, good repeatability, fair relative standard deviation values, high sampling rate, good precision and accuracy, and dead volume equal to zero.
5. The linearity range of the calibration graph is different with the difference in the flow injection or batch system for the same reaction.
6. The proposed methods were applied to determine MA, Procaine, and NQS from aqueous solutions.
7. The fluorescence estimation method is characterized by its wide range and high sensitivity
8. Both NQS and MA reagents were determined by fluorescence using aqueous solutions without needing expensive reagents.

3.5. Recommendations

1-Determining other amino drugs using this technique

2-By FIA methods, other reagents can be identified

3-It is possible to use the UV area directly to identify amino drugs through these systems

4-Linking these techniques to HPLC technology and estimating amino drugs through it

5-Through the results, fluorescence can be linked to the flow injection to determine the amino drugs and organic reagents capable of interacting with primary and secondary amines.

Reference

Reference:

1. van der LINDEN, W.E., Classification and definition of analytical methods based on flowing media (IUPAC Recommendations 1994). Pure and applied chemistry, 1994. 66(12): p. 2493-2500.

2. Tóth, K.S., K Kutner, Wlodzimierz Fehér, Zs Lindner, Erno, Electrochemical detection in liquid flow analytical techniques: Characterization and classification (IUPAC Technical Report). Pure and Applied Chemistry, 2004. 76(6): p. 1119-1138.

3. Skeggs, L.T., An automatic method for colorimetric analysis. American journal of clinical pathology, 1957. 28: p. 311-322.

4. Ruzicka, J.H., EH, Anal Chim Acta 78: 145; Danish Patent Application No. 4846/84, Sept 1974. US Patent, 1975. 4.

5. Růžička, J.S., JWB, Flow injection analysis: Part II. Ultrafast determination of phosphorus in plant material by continuous flow spectrophotometry. Analytica Chimica Acta, 1975. 79: p. 79-91.

6. Soto, C.S., Renato Contreras, David Poza, Cristián Orellana, Sandra Olivares-Rentería, Georgina A, Flow Injection Analysis (FIA) with Thermal Lens Spectrometry (TLS) for the Rapid Determination of Cefoperazone in Urine and Water. Analytical Letters, 2022. 55(12): p. 1932-1944.

7. Setayeshfar, I.R., Hamid Reza Khani, Omid, Application of flow injection analysis-solid phase extraction based on ion-pair formation for selective preconcentration of trace amount of anti-HIV drug. Microchemical Journal, 2022. 177: p. 107245.

8. Ghosh, S.A., Samar Sami Bornman, Charné Apollon, Wilgince Hussien, Aya Misbah Badawy, Ahmed Emad Amer, Mohamed Hussein Kamel, Manar Bakr Mekawy, Eman Ahmed Bedair, Heba, The application of rapid test paper technology for pesticide detection in horticulture crops: a comprehensive review. Beni-Suef University Journal of Basic and Applied Sciences, 2022. 11(1): p. 1-28.

9. Sanches, A.M.C.P., Maiyara Matos, Roberto Tarley, César R Teixeira Medeiros, Roberta A, Flow Injection Analysis System Coupled to Chronoamperometry and Boron-Doped Diamond Electrode for Determination of Synthetic Hormones 17α-Ethinylestradiol and Cyproterone Acetate. Analytical Letters, 2022: p. 1-17.

10. Oyella, D., Assessment of hydroquinone in selected cosmetic products sold on the market within Kampala. 2022, Makerere university.

11. Trojanowicz, M.P., Marta, Flow-Injection Methods in Water Analysis—Recent Developments. Molecules, 2022. 27(4): p. 1410.

12. Negrete, M.A.A.W., Kazimierz Barrientos, Eunice Yanez Escobosa, Alma Rosa Corrales Donis, Israel Enciso Wrobel, Katarzyna, Determination of chromium (III) picolinate in dietary supplements by flow injection-electrospray ionization-tandem mass spectrometry, using cobalt (II) picolinate as internal standard. Talanta, 2022. 240: p. 123161.

13. Betteridge, D.R., J, The determination of glyosbol in water by flow-injection analysis-a novel way of measuring viscosity. Talanta, 1976. 23(5): p. 409-410.

14. Hansen, E.H.R., Jaromir, Flow injection analysis: Part VI. The determination of phosphate and chloride in blood serum by dialysis and sample dilution. Analytica Chimica Acta, 1976. 87(2): p. 353-363.

15. Dutt, V.E.M., Horacio A, Repetitive determination of isonicotinic acid hydrazide in flow-through systems by series reactions. Analytical Chemistry, 1977. 49(6): p. 776-779.

16. Troanowicz, M., Flow Injection Analysis, Instrumentations and applications. 1st. Edition, World Scientific Publishing USA, 2000.

17. Zagatto, E.K., FJ Reis, BF, Merging zones in flow injection analysis: Part 1. Double proportional injector and reagent consumption. Analytica Chimica Acta, 1978. 101(1): p. 17-23.

18. Ruzicka, J.H., EH Ghose, Animesh K Mottola, HA, Enzymic determination of urea in serum based on pH measurement with the flow injection method. Analytical Chemistry, 1979. 51(2): p. 199-203.

19. Johnson, K.S.P., Robert L, Determination of nitrate and nitrite in seawater by flow injection analysis 1. Limnology and Oceanography, 1983. 28(6): p. 1260-1266.

20. Pasquini, C.D.O., Walace A, Monosegmented system for continuous flow analysis. Spectrophotometric determination of chromium (VI), ammonia and phosphorus. Analytical Chemistry, 1985. 57(13): p. 2575-2579.

21. Ruzicka, J.M., Graham D, Sequential injection: a new concept for chemical sensors, process analysis and laboratory assays. Analytica Chimica Acta, 1990. 237: p. 329-343.

22. Martín, V.C.E., Jose Manuel, Multicommutated Flow Injection Analysis, Multisyringe Flow Injection Analysis, and Multipumping Flow Systems. Flow Injection Analysis of Food Additives, 2015. 1: p. 79.

23. Trojanowicz, M., Advances in flow analysis. 2008: John Wiley & Sons.

24. Sherritt, R.G.C., Jamal Mehrotra, Anil K Behie, Leo A, Axial dispersion in the three-dimensional mixing of particles in a rotating drum reactor. Chemical Engineering Science, 2003. 58(2): p. 401-415.

25. Ingram, A.S., JPK Parker, DJ Fan, Xianfeng Forster, RG, Axial and radial dispersion in rolling mode rotating drums. Powder technology, 2005. 158(1-3): p. 76-91.

26. Kato, T.K., Yasushi Nishimura, Masayuki, Temperature dependence of chromatic dispersion in various types of optical fiber. Optics Letters, 2000. 25(16): p. 1156-1158.

27. Aubin, J.P., L Xuereb, Catherine Gourdon, Christophe, Effect of microchannel aspect ratio on residence time distributions and the axial dispersion coefficient. Chemical Engineering and Processing: Process Intensification, 2009. 48(1): p. 554-559.

28. Njeng, A.B.V., Stéphane Clausse, Marc Dirion, J-L Debacq, Marie, Effect of lifter shape and operating parameters on the flow of materials in a pilot rotary kiln: Part I. Experimental RTD and axial dispersion study. Powder Technology, 2015. 269: p. 554-565.

29. Wells, M.S., DE, The effects of crossing trajectories on the dispersion of particles in a turbulent flow. Journal of fluid mechanics, 1983. 136: p. 31-62.

30. Rastegar, S.O.G., Tingyue, Empirical correlations for axial dispersion coefficient and Peclet number in fixed-bed columns. Journal of Chromatography A, 2017. 1490: p. 133-137.

31. Parsaie, A.H., Amir Hamzeh, Predicting the longitudinal dispersion coefficient by radial basis function neural network. Modeling earth systems and environment, 2015. 1(4): p. 1-8.

32. Rubio, F.C.M., A Sánchez García, MC Cerón Camacho, F García Grima, E Molina Chisti, Y, Mixing in bubble columns: a new approach for characterizing dispersion coefficients. Chemical Engineering Science, 2004. 59(20): p. 4369-4376.

33. Liu, H., Predicting dispersion coefficient of streams. Journal of the Environmental Engineering Division, 1977. 103(1): p. 59-69.

34. Caldeweyher, E.B., Christoph Grimme, Stefan, Extension of the D3 dispersion coefficient model. The Journal of chemical physics, 2017. 147(3): p. 034112.

35. Jiemchooroj, A.N., Patrick Sernelius, Bo E, Complex polarization propagator method for calculation of dispersion coefficients of extended π-conjugated systems: The C 6 coefficients of polyacenes and C 60. The Journal of chemical physics, 2005. 123(12): p. 124312.

36. Ruiz-Capillas, C.N., Leo ML, Flow injection analysis of food additives. Vol. 1. 2015: CRC Press.

37. Ruzicka, J.H., Elo Harald, Flow injection analysis. Vol. 104. 1988: John Wiley & Sons.

38. Weng Larsen, S.L., Claus, Critical factors influencing the in vivo performance of long-acting lipophilic solutions—impact on in vitro release method design. The AAPS journal, 2009. 11(4): p. 762-770.

39. Lapa, R.A.L., José LFC Reis, Boaventura F Santos, João LM Zagatto, Elias AG, Multi-pumping in flow analysis: concepts, instrumentation, potentialities. Analytica Chimica Acta, 2002. 466(1): p. 125-132.

40. Whitson, M., Glossary of fusion energy. 1985, USDOE Office of Scientific and Technical Information, Oak Ridge, TN.

41. Kovacev, N.L., Sheng Zeraati-Rezaei, Soheil Hemida, Hassan Tsolakis, Athanasios Essa, Khamis, Effects of the internal structures of monolith ceramic substrates on thermal and hydraulic properties: additive manufacturing, numerical modelling and experimental testing. The International Journal of Advanced Manufacturing Technology, 2021. 112(3): p. 1115-1132.

42. Osborne, O.D.P., Allan Lenehan, Claire E, A simple colorimetric FIA method for the determination of pyrite oxidation rates. Talanta, 2010. 82(5): p. 1809-1813.

43. Bourne, J.K., F Rys, P, Mixing and fast chemical reaction—I: Test reactions to determine segregation. Chemical Engineering Science, 1981. 36(10): p. 1643-1648.

44. Zagatto, E.A.G.A., MAZ Jacintho, Antonio Octavio Mattos, IL, Compensation of the Schlieren effect in flow-injection analysis by using dual-wavelength spectrophotometry. Analytica Chimica Acta, 1990. 234: p. 153-160.

45. Shiundu, P.M., Automated methods development in flow injection analysis. 1991.

46. Hammond, G.S.T., Nicholas J, Organic Photochemistry: The study of photochemical reactions provides new information on the excited states of molecules. Science, 1963. 142(3599): p. 1541-1553.

47. Wachtler, M.S., Adolfo Gatterer, Karl Fritzer, Harald P Ajo, David Bettinelli, Marco, Optical properties of rare-earth ions in lead germanate glasses. Journal of the American Ceramic Society, 1998. 81(8): p. 2045-2052.

48. Bejaoui, S.M., Xavier Desgroux, Pascale Therssen, Eric, Laser induced fluorescence spectroscopy of aromatic species produced in atmospheric sooting flames using UV and visible excitation wavelengths. Combustion and Flame, 2014. 161(10): p. 2479-2491.

49. Cartwright, D.C., Vibrational populations of the excited states of N2 under auroral conditions. Journal of Geophysical Research: Space Physics, 1978. 83(A2): p. 517-531.

50. Vandewal, K.B., J Nikolis, VC, How to determine optical gaps and voltage losses in organic photovoltaic materials. Sustainable Energy & Fuels, 2018. 2(3): p. 538-544.

51. Fan, C.H.S., Peipei Su, Tsu-Hui Cheng, Chien-Hong, Host and dopant materials for idealized deep-red organic electrophosphorescence devices. Advanced Materials, 2011. 23(26): p. 2981-2985.

52. Dorenbos, P., The 4fn↔ 4fn− 15d transitions of the trivalent lanthanides in halogenides and chalcogenides. Journal of luminescence, 2000. 91(1-2): p. 91-106.

53. Ishida, H.T., Seiji Hasegawa, Yasuchika Katoh, Ryuzi Nozaki, Koichi, Recent advances in instrumentation for absolute emission quantum yield measurements. Coordination chemistry reviews, 2010. 254(21-22): p. 2449-2458.

54. Würth, C.G., Markus Pauli, Jutta Spieles, Monika Resch-Genger, Ute, Relative and absolute determination of fluorescence quantum yields of transparent samples. Nature protocols, 2013. 8(8): p. 1535-1550.

55. Brouwer, A.M., Standards for photoluminescence quantum yield measurements in solution (IUPAC Technical Report). Pure and Applied Chemistry, 2011. 83(12): p. 2213-2228.

56. Al-Tamimi, S.A.A.-M., Norah Sultan Abdulaziz Aly, Fatma Ahmed, Utility of Spectroscopic Studies for Quantification of Cefditoren Pivoxil in Commercial Samples. Journal of the Chemical Society of Pakistan, 2021. 43(4).

57. Kazemipour, M.F., Iman Ansari, Mehdi, Gabapentin Determination in Human Plasma and Capsule by Coupling of Solid Phase Extraction, Derivatization Reaction, and UV-Vis Spectrophotometry. Iranian Journal of Pharmaceutical Research: IJPR, 2013. 12(3): p. 247.

58. Elbashir, A.A.A., Abir Abdalla Ali Ahmed, Shazalia M Aboul-Enein, Hassan Y, 1, 2-Naphthoquinone-4-sulphonic acid sodium salt (NQS) as an analytical reagent for the determination of pharmaceutical amine by

spectrophotometry. Applied Spectroscopy Reviews, 2012. 47(3): p. 219-232.

59. Hashimoto, Y.E., Masaru Tominaga, Keiko Inuzuka, Shigeko Moriyasu, Masataka, Quantitative analysis of phenethylamine derivatives by thin layer chromatography. Determination of psychotropic drugs and ephedra bases. Microchimica Acta, 1978. 70(5): p. 493-504.

60. Farrell, B.J., TM, An investigation of high-performance liquid chromatographic methods for the analysis of amphetamines. Journal of Chromatography B: Biomedical Sciences and Applications, 1983. 272: p. 111-128.

61. Darwish, I.A.A., Heba H Amer, Sawsan M Al-Rayes, Lama I, Spectrophotometric study for the reaction between fluvoxamine and 1, 2-naphthoquinone-4-sulphonate: Kinetic, mechanism and use for determination of fluvoxamine in its dosage forms. Spectrochimica Acta Part A: Molecular and Biomolecular Spectroscopy, 2009. 72(4): p. 897-902.

62. Choi, K.C., Jung-Kap Yoo, Gyurng-Soo, Spectrophotometric determination of amantadine sulfate after ion-pairing with methyl orange. Archives of Pharmacal Research, 1991. 14(4): p. 285-289.

63. de Abajo, F.J.R., Luis Alberto García Montero, Dolores, Association between selective serotonin reuptake inhibitors and upper gastrointestinal bleeding: population based case-control study. Bmj, 1999. 319(7217): p. 1106-1109.

64. Kuznetsova, L.A.C., W Terence, Applications of ultrasound streaming and radiation force in biosensors. Biosensors and Bioelectronics, 2007. 22(8): p. 1567-1577.

65. J, d.A.F., Effects of selective serotonin reuptake inhibitors on platelet function. Drugs & aging, 2011. 28(5): p. 345-367.

66. Sowjanya, K.T., JC Gurupadayya, BM Indupriya, M, Spectrophotometric determination of pregabalin using Gibb's and MBTH reagent in pharmaceutical dosage form. Der Pharma Chemica, 2011. 3(1): p. 112-122.

67. Steindler, A.L., JV, Differential diagnosis of pain low in the back: allocation of the source of pain by the procaine hydrochloride method. Journal of the American Medical Association, 1938. 110(2): p. 106-113.

68. Outland, T.H., CR, The use of procaine hydrochloride as a therapeutic agent. Journal of the American Medical Association, 1940. 114(14): p. 1330-1333.

69. Chapman, C.C., P Nielsen, IL Sitaram, BR Huntington, PJ, The role of procaine in adverse reactions to procaine penicillin in horses. Australian veterinary journal, 1992. 69(6): p. 129-133.

70. García, S.S.-P., Concepción Albero, Isabel García, Concepción, Flow-injection spectrophotometric determination of diclofenac or mefenamic acid in pharmaceuticals. Microchimica Acta, 2001. 136(1): p. 67-71.

71. Rouini Mohammad-Reza Asadipour Ali Ardakani, Y.H.A., Fakhredin, Liquid chromatography method for determination of mefenamic acid in human serum. Journal of Chromatography B, 2004. 800(1-2): p. 189-192.

72. Ahad, B.-T., A Simple Spectrofluorimetric Method for Determination of Mefenamic Acid in Pharmaceutical Preparation and Urine. Bulletin of the Korean Chemical Society, 2006. 27.

73. Jaiswal, Y.T., Gokul Surana, Sanjay, Application of HPLC for the simultaneous determination of ethamsylate and mefenamic acid in bulk drugs and tablets. Journal of liquid chromatography & related technologies, 2007. 30(8): p. 1115-1124.

74. Santini, A.P., Helena Redigolo Pezza, Leonardo, Development of a potentiometric mefenamate ion sensor for the determination of mefenamic acid in pharmaceuticals and human blood serum. Sensors and Actuators B: Chemical, 2007. 128(1): p. 117-123.

75. Raza, A., Spectrophotometric determination of mefenamic acid in pharmaceutical preparations. Journal of Analytical Chemistry, 2008. 63(3): p. 244-247.

76. M Al-mufty, Z.R.A., Nief, Indirect spectrophotometric method for the determination of mefenamic acid in pharmaceutical formulations. Rafidain journal of science, 2009. 20(6): p. 39-47.

77. Madrakian, T.A., Abbas Mohammadnejad, Masoumeh, Second-order advantage applied to simultaneous spectrofluorimetric determination of paracetamol and mefenamic acid in urine samples. Analytica chimica acta, 2009. 645(1-2): p. 25-29.

78. Havaldar, F.H.V., Dharmendra L, Simultaneous determination of paracetamol, acetyl salicylic acid, mefenamic acid and cetirizine dihydrochloride in the pharmaceutical dosage form. E-Journal of Chemistry, 2010. 7(S1): p. S495-S503.

79. Dikran, S.B.M., Ala Karim al-Jabburi, Muin Iskandar Nasir, Ahmad Saib, Spectrophotometric determination of mefenamic acid in pharmaceutical preparations. Ibn al-Haitham Journal for Pure and Applied Science, 2014(Vol. 27, Issue 3 (31 Dec. 2014), pp.339-349, 11 p.): p. 11.

80. Kormosh, Z.A.M., O. Yu Bazel', Ya R., Extraction-spectrophotometric determination of mefenamic acid in pharmaceutical preparations. Journal of Analytical Chemistry, 2014. 69(10): p. 960-964.

81. Kahkha, M.R.R.K., Massoud Afarani, Mahdi Shafiee Sepehri, Zahra, Determination of mefenamic acid in urine and pharmaceutical samples by HPLC after pipette-tip solid phase microextraction using zinc sulfide modified carbon nanotubes. Analytical Methods, 2016. 8(30): p. 5978-5983.

82. Morcoss, M.M.A., Nada S Ali, Nouruddin W Elsaady, Mohammed T, Different chromatographic methods for simultaneous determination of mefenamic acid and two of its toxic impurities. Journal of chromatographic science, 2017. 55(7): p. 766-772.

83. ATIPAIRIN, A.S., SOMCHAI, DETERMINATION OF MEFENAMIC ACID IN A TOPICAL EMULGEL BY A VALIDATED HPLC METHOD. International Journal of Applied Pharmaceutics, 2019: p. 86-90.

84. Malode, S.J.S., Nagaraj P Kulkarni, Raviraj M, Voltammetric detection and determination of mefenamic acid at silver-doped TiO2 nanoparticles modified electrode. Materials Today: Proceedings, 2019. 18: p. 671-678.

85. Rashad, I.Q.B., Mohsin Hamza. Spectrophotometric Determination of Mefenamic acid using Metol reagent by Oxidative Coupling Reaction. in

IOP Conference Series: Materials Science and Engineering. 2021. IOP Publishing.

86. Carmona, M.S., Manuel Pérez-Bendito, Dolores, A selective and sensitive kinetic method for the determination of procaine and benzocaine in pharmaceuticals. Journal of pharmaceutical and biomedical analysis, 1992. 10(2-3): p. 145-152.

87. Carretero, A.S.C.-B., C Peinado, S Fernández El Bergmi, R Gutiérrez, A Fernández, Fluorimetric determination of procaine in pharmaceutical preparations based on its reaction with fluorescamine. Journal of pharmaceutical and biomedical analysis, 1999. 21(5): p. 969-974.

88. Liu, L.D.L., Yuan Wang, Huai You Sun, Yue Ma, Li Tang, Bo, Use of p-dimethylaminobenzalhyde as a colored reagent for determination of procaine hydrochloride by spectrophotometry. Talanta, 2000. 52(6): p. 991-999.

89. Paseková, H.P., Miroslav, Determination of procaine, benzocaine and tetracaine by sequential injection analysis with permanganate-induced chemiluminescence detection. Talanta, 2000. 52(1): p. 67-75.

90. Wang, C.Y.H., Xiao Ya Di Jin, Gen Leng, Zong Zhou, Differential pulse adsorption voltammetry for determination of procaine hydrochloride at a pumice modified carbon paste electrode in pharmaceutical preparations and urine. Journal of pharmaceutical and biomedical analysis, 2002. 30(1): p. 131-139.

91. Xu, L.X.S., Yun Xiu Wang, Huai You Jiang, Ji Gang Xiao, Yan, Spectrophotometric determination of procaine hydrochloride in pharmaceutical products using 1, 2-naphthoquinone-4-sulfonic acid as the

chromogenic reagent. Spectrochimica Acta Part A: Molecular and Biomolecular Spectroscopy, 2003. 59(13): p. 3103-3110.

92. Chen, X.-W.S., Xin Wang, Jian-Hua, A sequential injection fluorometric procedure for the determination of procaine in human blood and pharmaceuticals. Analytical and bioanalytical chemistry, 2006. 385(4): p. 737-741.

93. Bergamini, M.F.S., André L Stradiotto, Nelson R Zanoni, Maria Valnice B, Flow injection amperometric determination of procaine in pharmaceutical formulation using a screen-printed carbon electrode. Journal of pharmaceutical and biomedical analysis, 2007. 43(1): p. 315-319.

94. Chen, Y.-H.T., Feng-Shou Song, Mao-Ping, Spectrophotometric determination of procaine hydrochloride with hemoglobin as catalyst. Journal of analytical chemistry, 2009. 64(4): p. 366-370.

95. Al-Uzri, W.A., Spectrophotometric Determination of Procaine Hydrochloride in Pharmaceutical Preparations via Diazotization-Coupling Reaction with Phenol. Asian Journal of Chemistry, 2015. 27(12).

96. Plotycya, S.S., Oksana Pysarevska, Solomiya Blazheyevskiy, Mykola Dubenska, Liliya, A new approach for the determination of benzocaine and procaine in pharmaceuticals by single-sweep polarography. International Journal of Electrochemistry, 2018. 2018.

97. Abdulazeez, I.P., Saheed A Saleh, Tawfik A Al-Saadi, Abdulaziz A, Spectroscopic, DFT and trace detection study of procaine using surface-

enhanced Raman scattering technique. Chemical Physics Letters, 2019. 730: p. 617-622.

98. Bülbül, B.B., Seda, Developing of buffer-precipitation method for lead metaborate (Pb (BO2)(2) center dot H2O) nanostructures. 2020.

99. Attia, K.A.E.-O., Ahmed Ramzy, Sherif Abdelazim, Ahmed H Hasan, Mohamed A Abdel-Kareem, Rady F, Simultaneous determination of elbasvir and grazoprevir in their pharmaceutical formulation by synchronous fluorescence spectroscopy coupled to dual wavelength method. Spectrochimica Acta Part A: Molecular and Biomolecular Spectroscopy, 2021. 248: p. 119157.

100. Chayavanich, K.T., Pattara Imyim, Apichat, Biocompatible film sensors containing red radish extract for meat spoilage observation. Spectrochimica Acta Part A: Molecular and Biomolecular Spectroscopy, 2020. 226: p. 117601.

101. Aupoil, J.C., Jean-Baptiste de Lacaillerie, Jean-Baptiste d'Espinose Poulesquen, Arnaud, Interplay between silicate and hydroxide ions during geopolymerization. Cement and Concrete Research, 2019. 115: p. 426-432.

الخلاصة

الفصل الاول تضمن مقدمة عن حقن الجريان ،بدايات نظام حقن الجريان وتقنياته فضلاً عن التشتت في تحليل حقن الجريان ،انواع التشتت ،معامل التشتت وطرق حسابه و العوامل المؤثرة على تشتت منطقة العينة . يصف ايضاً مقدمه موجزه عن الفلورية والانتقالات الإلكترونية بالإضافة الى نظره عامه عن الكاشفNQS و كل من Mefenamic acid و Procaine hydrochloride (مقدمة موجزه ،الخصائص الكيميائية والفيزيائية ، اشكال الجرعات ، الاستخدامات و بعض التطبيقات) متبوعة بأهداف من مشروع البحث.

بينما الفصل الثاني يتضمن وصف للأجهزة و المواد الكيميائية المستخدمة وطرائق تحضيرها

اما الفصل الثالث يحتوي على جزئيين : يصف الجزء الاول مكونات منظومة حقن الجريان بينما يتناول الجزء الثاني تقدير كل من Mefenamic acid ,Procaine hydrochloride and NQS ويتم ذلك من خلال نظامين:

النظام الاول : بالاعتماد على الامتصاصية تضمن هذا الجزء دراسة تفصيلية كامله لتقدير Mefenamic acid بتقنية merging-zone FIA بالصورة النقية باستخدام الكاشف NQS واستندت الطريقة على تفاعل Mefenamic acid و NQS في وسط قاعدي (هيدروكسيد الصوديوم) لتكوين معقد بني محمر . تمت دراسة المتغيرات الفيزيائية و الكيميائية وتحسينها . كما كان الرسم البياني لمنحني المعايرة الخطي بمدى ppm(1-20) مع معامل الارتباط 9999. 0= r والانحراف المعياري النسبي المئوي RSD % 1.23 لتركيز 13 ppm

ثم تم تقدير Mefenamic acid بتقنية Reverse-contentious FIA بالصورة النقية باستخدام الكاشف NQS. تمت دراسة المتغيرات الفيزيائية و الكيميائية وتحسينها . كما كان الرسم البياني لمنحني المعايرة الخطي بمدى ppm(1-30) مع معامل الارتباط 9869. 0= r والانحراف لمعياري النسبي المئوي RSD % 0.5 لتركيز 30 ppm

بعد ذلك تمت دراسة نفس التفاعل في الطريقة التقليدية وقورنت النتائج المتحصل عليها مع الطريقتان المطورتان وتبين لكل طريقه مزايا حيث كان الرسم البياني لمنحني المعايرة الخطي بمدى ppm(10-0.5) مع معامل الارتباط 9997. 0= r والانحراف لمعياري النسبي المئوي RSD % اقل من 0.072 لتركيز 7 ppm.

النظام الثاني : بالاعتماد على الفلورية تضمن هذا النظام اربع تفاعلات مختلفة تم دراستها

1- تقدير Procaine hydrochloride بتقنية merging-zone FIA بالمحاليل المائية . تمت دراسة المتغيرات الفيزيائية و الكيميائية وتحسينها . كما كان الرسم البياني لمنحني المعايرة الخطي بمدى (1-100)ppm مع معامل الارتباط r =0 .9986 والانحراف لمعياري النسبي المئوي RSD % 2.008 لتركيز70 ppm .

2- تقدير NQS بتقنية merging-zone FIA بالمحاليل المائية . تمت دراسة المتغيرات الفيزيائية و الكيميائية وتحسينها . كما كان الرسم البياني لمنحني المعايرة الخطي بمدى (5-50)ppm مع معامل الارتباط r =0 .9976 والانحراف لمعياري النسبي المئوي RSD % 1.941 لتركيز30 ppm.

3- تقدير Mefenamic acid بالطريقة التقليدية باستخدام الكاشف NQS واستندت الطريقة على تفاعل Mefenamic acid و NQS في وسط قاعدي (هيدروكسيد الصوديوم) لتكوين معقد بني محمر يعمل على تقليل او اخماد بريق فلورة الكاشف NQS كان الرسم البياني لمنحني المعايرة الخطي بمدى (1-100)ppm مع معامل الارتباط r=0.9993 .

4- تقدير Mefenamic acid بالطريقة التقليدية في محاليله المائية حيث ان MA في الحالة النقية يعطي طيف انبعاث فلوريه عند nm295.2 كان الرسم البياني لمنحني المعايرة الخطي بمدى (1-100)ppm مع معامل الارتباط r=0.9988 .

جمهورية العراق
وزارة التعليم العالي والبحث العلمي
جامعة بابل – كلية العلوم للبنات
قسم الكيمياء

دراسة و تطبيق منظومات حقن جرياني جديدة

رسالة
مقدمة الى مجلس كلية العلوم للبنات -جامعة بابل
كجزء من متطلبات نيل درجة الماجستير في الكيمياء

بواسطة

لبنى رعد عبد الامير الهيتي

بكالوريوس علوم كيمياء – جامعة بابل (2019)

إشراف

أ.د.داخل ناصر طه الزرقاني

و

أ.م.د.كاظم خلف هاشم

2022 م

1443 هـ

الخلاصة

الفصل الاول تضمن مقدمة عن حقن الجريان ،بدايات نظام حقن الجريان وتقنياته فضلاً عن التشتت في تحليل حقن الجريان ،انواع التشتت ،معامل التشتت وطرق حسابه و العوامل المؤثرة على تشتت منطقة العينة . يصف ايضاً مقدمه موجزه عن الفلورية والانتقالات الإلكترونية بالإضافة الى نظره عامه عن الكاشف NQS و كل من Mefenamic acid و Procaine hydrochloride (مقدمة موجزه ،الخصائص الكيميائية والفيزيائية ، اشكال الجرعات ، الاستخدامات و بعض التطبيقات) متبوعة بأهداف من مشروع البحث.

بينما الفصل الثاني يتضمن وصف للأجهزة و المواد الكيميائية المستخدمة وطرائق تحضيرها

اما الفصل الثالث يحتوي على جزئيين : يصف الجزء الاول مكونات منظومة حقن الجريان بينما يتناول الجزء الثاني تقدير كل من Procaine hydrochloride and NQS, Mefenamic acid ويتم ذلك من خلال نظامين:

النظام الاول : بالاعتماد على الامتصاصية تضمن هذا الجزء دراسة تفصيلية كامله لتقدير Mefenamic acid بتقنية merging-zone FIA بالصورة النقية باستخدام الكاشف NQS واستندت الطريقة على تفاعل Mefenamic acid و NQS في وسط قاعدي (هيدروكسيد الصوديوم) لتكوين معقد بني محمر . تمت دراسة المتغيرات الفيزيائية و الكيميائية وتحسينها . كما كان الرسم البياني لمنحني المعايرة الخطي بمدى (1-20)ppm مع معامل الارتباط 9999. 0= r والانحراف المعياري النسبي المئوي 1.23 % RSD لتركيز 13 ppm

ثم تم تقدير Mefenamic acid بتقنية Reverse-contentious FIA بالصورة النقية باستخدام الكاشف NQS. تمت دراسة المتغيرات الفيزيائية و الكيميائية وتحسينها . كما كان الرسم البياني لمنحني المعايرة الخطي بمدى (1-30)ppm مع معامل الارتباط 9869. 0= r والانحراف لمعياري النسبي المئوي 0.5 % RSD لتركيز 30 ppm

بعد ذلك تمت دراسة نفس التفاعل في الطريقة التقليدية وقورنت النتائج المتحصل عليها مع الطريقتان المطورتان وتبين لكل طريقه مزايا حيث كان الرسم البياني لمنحني المعايرة الخطي بمدى (0.5-10)ppm

مع معامل الارتباط 9997. 0= r والانحراف لمعياري النسبي المئوي RSD % اقل من 0.072 لتركيز 7 ppm.

النظام الثاني : بالاعتماد على الفلورية تضمن هذا النظام اربع تفاعلات مختلفة تم دراستها

1- تقدير Procaine hydrochloride بتقنية merging-zone FIA بالمحاليل المائية . تمت دراسة المتغيرات الفيزيائية و الكيميائية وتحسينها . كما كان الرسم البياني لمنحني المعايرة الخطي بمدى (1-100)ppm مع معامل الارتباط 9986. 0= r والانحراف لمعياري النسبي المئوي RSD % 2.008 لتركيز70 ppm .

2- تقدير NQS بتقنية merging-zone FIA بالمحاليل المائية . تمت دراسة المتغيرات الفيزيائية و الكيميائية وتحسينها . كما كان الرسم البياني لمنحني المعايرة الخطي بمدى (5-50)ppm مع معامل الارتباط 9976. 0= r والانحراف لمعياري النسبي المئوي RSD % 1.941 لتركيز30 ppm.

3- تقدير Mefenamic acid بالطريقة التقليدية باستخدام الكاشف NQS واستندت الطريقة على تفاعل Mefenamic acid و NQS في وسط قاعدي (هيدروكسيد الصوديوم) لتكوين معقد بني محمر يعمل على تقليل او اخماد بريق فلورة الكاشف NQS كان الرسم البياني لمنحني المعايرة الخطي بمدى (1-100)ppm مع معامل الارتباط r=0.9993 .

4- تقدير Mefenamic acid بالطريقة التقليدية في محاليله المائية حيث ان MA في الحالة النقية يعطي طيف انبعاث فلوريه عند nm295.2 كان الرسم البياني لمنحني المعايرة الخطي بمدى (1-100)ppm مع معامل الارتباط r=0.9988 .

Chapter Two

Chemicals and Apparatus

2. Chemicals and Apparatus

2.1. Tools and Apparatus used

Several techniques and tools are used in the current study, most of which are listed in Table [2.1].

Table [2.1]: Devices Used in the Study and their Manufacturers

No.	Instrument	Model	Company supplied
1	[1]BioLogic QuadTec UV-Vis Detector	130200	BIO-RAD, U.S.A.
2	[1]Spectrophotometer	PD-303	APEL, Japan
3	[1]Competence Analytical Balance	CPA2P	SARTORIUS, Germany
4	[1]Peristaltic pump	Rabbit Peristaltic Pump	RAININ, France
5	[1]Rotary 6- port injection valve	7725i	RHEODYNE, U.S.A.
6	[1]Reaction coil	Teflon tube	__
7	[1]Connection tubes	silicone rubber	__
8	[1]Data Acquisition	USB3253	ZIAD, China
9	[1]Power Transformer	__	ANLIXUM, China
10	[1]Fluorescence Detector	LC 240	PERKIN ELMER, U.K.

No.	Instrument	Model	Company supplied
11	[1]Scanning Fluorescence Detector	474	Waters, Japan
12	[2]Fluorescence Spectrometer	FS-2	Scinco, China

2.2. Chemical Reagents

2.2.1. Chemicals Preparation

All chemicals and reagents used in this project were analytical grade reagents. Table [2.2] tabulates the main chemicals used throughout this project work as a standard stock solution. Other standard solutions were prepared by subsequent dilution of the stock solution.

Table [2.2]: The Main Chemicals and Reagents Throughout this Research Work

Name	Formula	Purity %	M.wt (g/mol)	Company Supplier	Remarks
Potassium dihydrogen phosphate	KH_2PO_4	99.0	136	(B.D.H)	Dissolved in distilled water
Boric acid	H_3BO_3	99.9	61.83	(B.D.H)	Dissolved in distilled water

[1] University of Babylon / College of Science for Women-Department of Chemistry.
[2] University of Babylon / College of Science for Women-Department of Laser Physics.

Name	Formula	Purity %	M.wt (g/mol)	Company Supplier	Remarks
Potassium chloride	KCl	99.9	74.55	(B.D.H)	Dissolved in distilled water
Potassium hydroxide	KOH	99.9	56.1	(B.D.H)	Dissolved in distilled water
Sodium hydroxide	NaOH	98.0	40	Loba Chemie	Standardized with HCl
1,2-Naphthoquinone-4-Sulfonic Acid Sodium Salt (N.Q.S.)	$C_{10}H_5NaO_5S$	97.0	260	Sigma-Aldrich	Dissolved in distilled water
Mefenamic acid (MA)	$C_{15}H_{15}NO_2$	99.7	241	(S.D.I)	Dissolves in dilute solutions of alkali hydroxides
Procaine	$C_{13}H_{20}N_2O_2$	99.6	272.7	(S.D.I)	Dissolved in distilled water

2.2.2. Sample Preparation

2.2.2.1. Sample Preparation of Mefenamic Acid 250ppm

A standard drug was prepared by dissolving 25mg (0.025gm) of MA. in 25mL distilled water and diluting it to 100ml in a volumetric flask with distilled water. Subsequent dilutions were freshly prepared working solutions.

2.2.2.2. Sample Preparation of Procaine Hydrochloride 250ppm

A standard drug was prepared by dissolving 25mg (0.025gm) of Procaine HCl in 25mL distilled water and diluting it to 100ml in a volumetric flask with distilled water. Subsequent dilutions were freshly prepared working solutions.

2.2.2.3. 1,2-Naphthoquinone-4-Sulfonic Sodium Salt (NQS) 100 ppm Solution

A stock solution was freshly prepared by dissolving 5mg (0.005gm) of the reagent in 50mL of distilled water.

2.2.2.4. Sodium Hydroxide 0.2M Solution

It was prepared by dissolving 1.6gm of sodium hydroxide in 25ml of distilled water and diluting to 200mL in a volumetric flask with distilled water.

2.2.2.5. Potassium Chloride 0.2M Solution

A standard solution was prepared by dissolving 2.858gm in 20ml of distilled water and diluting it to 200mL in a volumetric flask with distilled water.

2.2.2.6. Boric Acid 0.2M Solution

A standard solution was prepared by dissolving 1.2366gm in 25ml of distilled water and diluting it to 100mL in a volumetric flask with distilled water.

2.2.2.7. Sodium Hydroxide – Boric Acid (buffer solution) (pH~9)

It was prepared by dissolving 0.6gm of boric acid in 50mL distilled water and mixing with 4.15mL sodium hydroxide (0.2M). Then the solution was diluted with distilled water to the mark in a 100mL volumetric flask [98].

2.2.2.8. Boric Acid – Potassium Chloride – Sodium Hydrochloride (buffer solution) (pH~10)

It was prepared by mixing 25mL boric acid (0.2M) with 25mL potassium chloride (0.2M) and adding 21.85mL sodium hydroxide (0.2M), and then the solution was diluted with distilled water to the mark in a 100mL volumetric flask [99].

2.2.2.9. Sodium hydroxide – Potassium chloride (buffer solution) (pH~12)

It was prepared by mixing 50mL potassium chloride (0.2M) with 24mL sodium hydroxide (0.2M). Then the solution was diluted with distilled water to the mark in a 100mL volumetric flask [100].

2.2.2.10. Sodium hydroxide – Potassium chloride (buffer solution) (pH~13)

It was prepared by mixing 25mL potassium chloride (0.2M) with 65mL sodium hydroxide (0.2M). The solution was diluted with distilled water to the mark in a 100mL volumetric flask [101].

Chapter Three

Results and Discussion

3. Results and Discussion

3.1. Design of Flow Injection Units

Continuous flow injection analysis systems consist of essential parts: fluid pumping system, coils, measuring devices, reading system, and injection unit. In general, the flow injection system used in this research consists of the following parts:

3.1.1. Peristaltic Pump

The first stage starts by operating the multi-channel peristaltic pump, as shown in Figure [3.1] and Scheme [3.1], which works to pump the transporting solution to the unit passing through the injection valve to the cell, as the system tubes and coils are filled with the transporting solution. The reading considers the transport solution as a reference (blank).

Figure [3.1]: Rabbit Peristaltic Pump (RAININ)

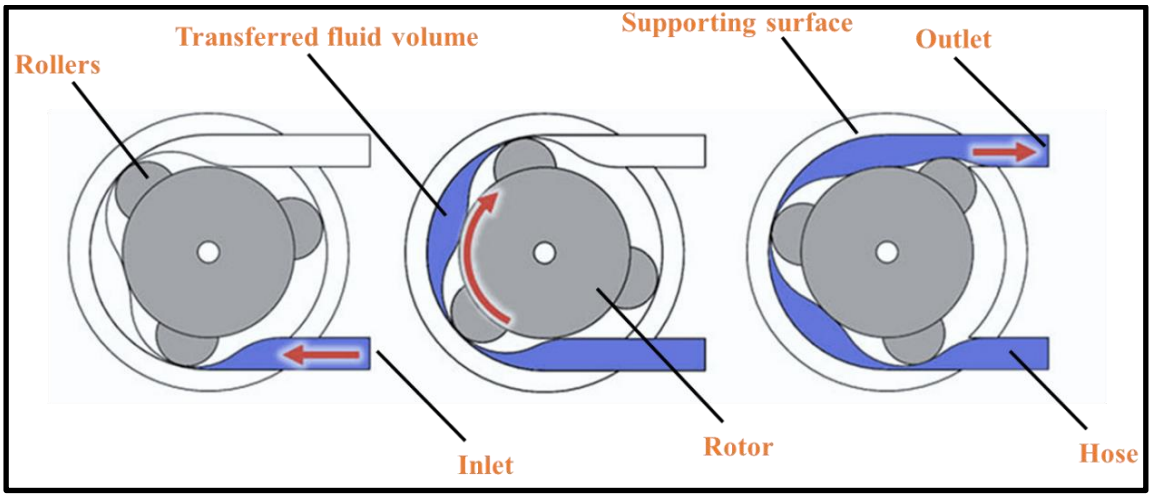

Scheme [3-1]: The Movement of Fluid within the Parts of the Peristaltic Pump

The pump contains a lever that causes speed control through numbers recorded on it that change mechanically with the movement of the lever, and these numbers start from 1 to 10. Still, it is correct to deal with the speed with the volume that is pumped per minute because peristaltic pumps are manufactured in different shapes and designs. The volume descending from the designed unit was collected during a fixed time of 1 minute to deal with the flow rate in units (ml) per minute for each digital speed of the pump, as shown in Table [3.1].

Table [3.1]: The Amount of Flow Velocity Per Velocity of the Pump

Flow rate (mL/min)	The volume descending from the system(mL) in one minute	Speed recorded on the pump
0.5	**0.5**	**1**
1.0	**1.0**	**2**
1.5	**1.5**	**3**
2.0	**2.0**	**4**
2.5	**2.5**	**5**
3.0	**3.0**	**6**
3.5	**3.5**	**7**
4.0	**4.0**	**8**
4.5	**4.5**	**9**
5.0	**5.0**	**10**

3.1.2. Injection Valve

The second phase includes loading the reagent or sample (depending on the technique used) in the hexagonal injection unit shown in Figure [3.2].

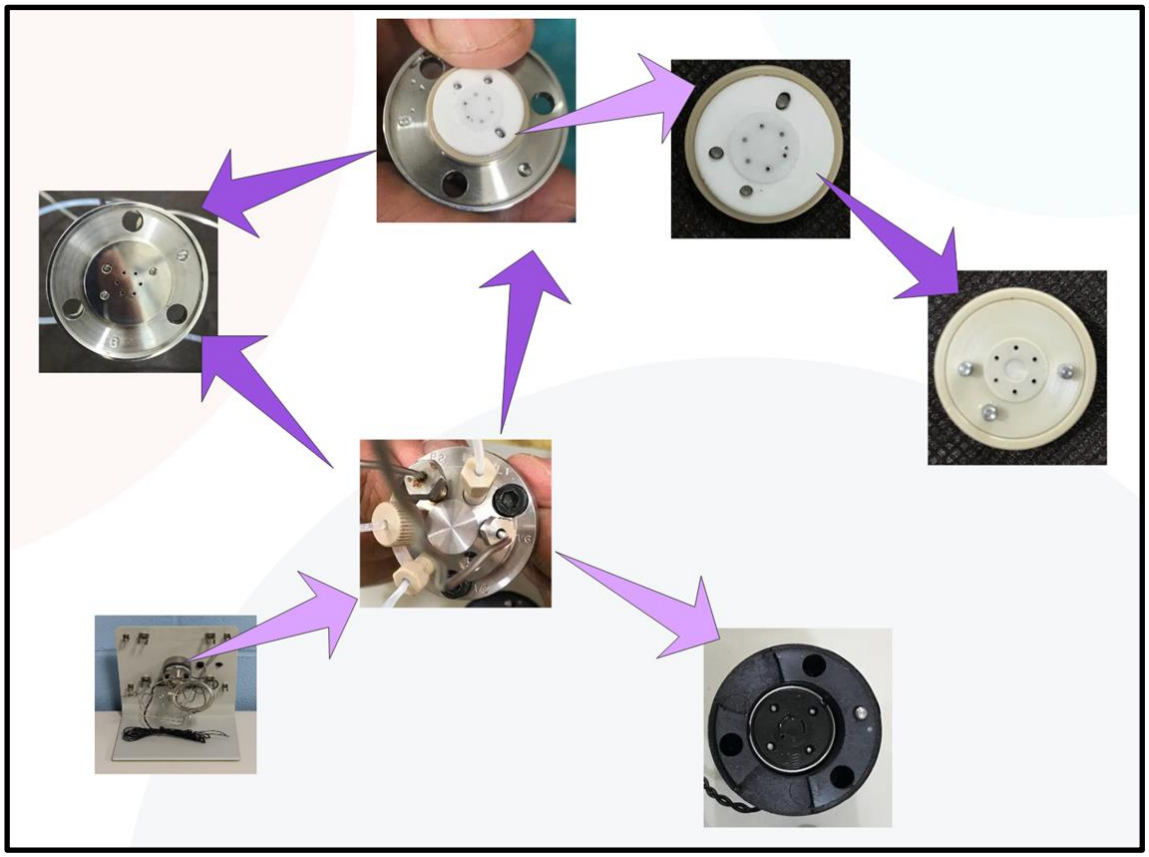

Figure [3.2]: How to Choose the Appropriate Holes for the Sample Loop from the Six Holes of the Valve, and Holes 1 and 4 were selected.

This stage is represented by the entry of the reagent or sample into the loop of the injection unit, as the direction of filling the reagent connection or the sample is from one external movement (load) No. (1) » (2) » (3) » (6) and surplus to the waste as shown in Scheme [3-2] [A].

After the loading process is completed, the direction of the valve is changed in such a way that the carrier solution pushes the reagent or sample that was loaded in the loop; the direction of injection is No. (4) » (3) » (6) » (5), where this change in the direction of the valve leads to the flow towards the reaction coil as the materials mix and the reaction product is formed as shown in Scheme [3-2] [B].

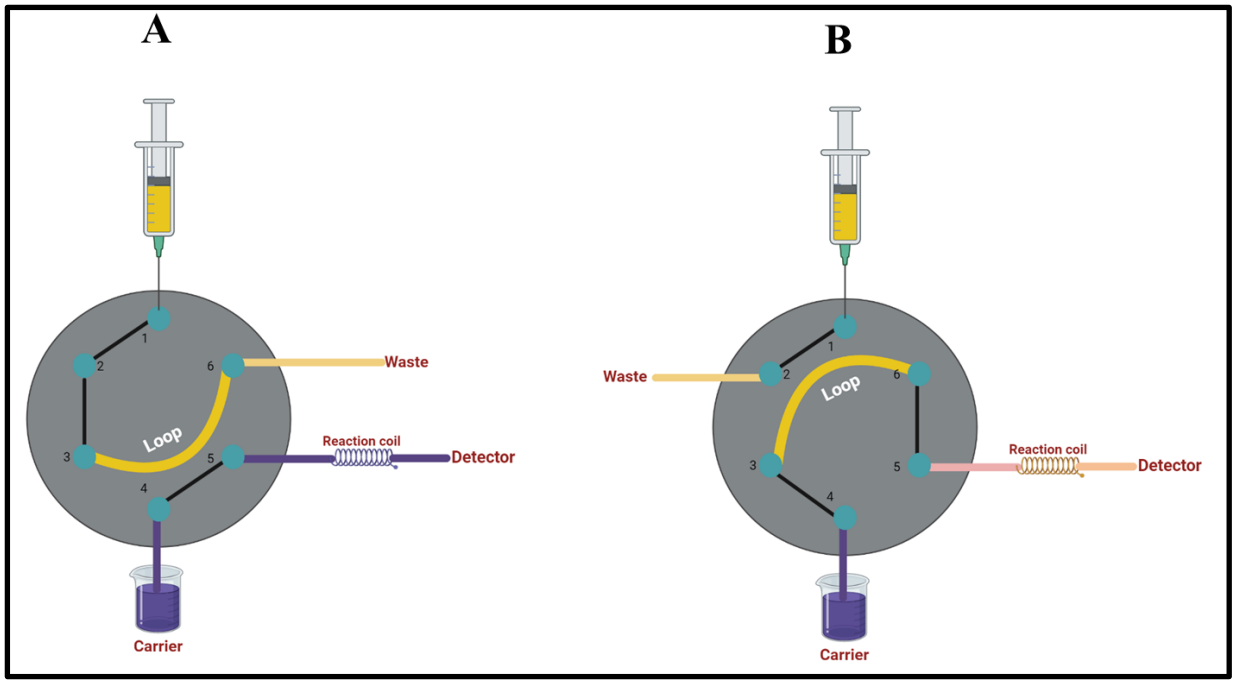

Scheme [3-2]: (A) Loading and (B) Injection Process in the Injection Unit

3.1.3. Reaction Coil

The amount of volume accommodated by the different lengths of the reaction coils used in the system was also calculated by the cylinder volume equation $\boldsymbol{v=r^2\pi h}$., e.g., a Teflon tube of ID=1 mm, r=0.5 mm=0.05 cm Figure [3.3] and Table [3.2].

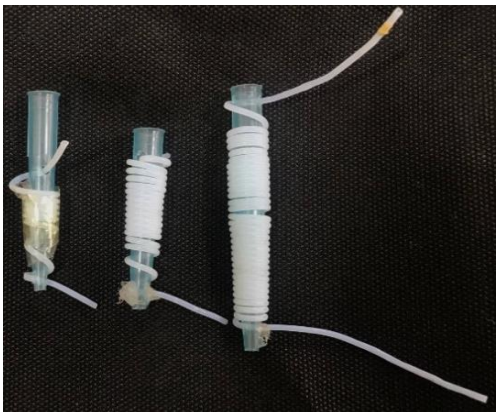

Figure [3.3]: A Collection of Reaction Coils has Variable Lengths

Table [3.2]: The Volume of each Reaction Coil

Volume (µL)	Length of reaction coil (cm)
196.25	**25**
392.50	**50**
588.75	**75**
785.00	**100**

3.1.4. Data Acquisition

Unlike previous instruments, the new one employs a novel, constructed, in-lab planned, and in-lab managed G-Chrome flow-injection software as shown in Figure [3.4] to determine the spectroscopic approach. This system is straightforward to use, and data transmission is automatic. Due to the internal architecture of the software utilized in this technique, injecting the sample and then repeating it at an intersection or modifying the sample is straightforward. Additionally, it was discovered that the data acquired was accurate and equivalent to that produced using more complex instruments. This system is differentiated by its cost and convenience of use, high degree of flexibility, precision, and control over the results, and, most crucially, the analyst's ability to build and improve the system and approach.

Figure [3.4]: Data Acquisition (ZIAD Model USB3253)

The overall structure of the designed systems, in general, is given in Figure [3.5].

Figure [3.5]: The Whole Setup of the Manifold System for the Measuring Absorbance and Fluorescence Response of Different Analytes.

3.2. Techniques used for the Determination of Amino Drugs and the Reagent. Scheme [3.3].

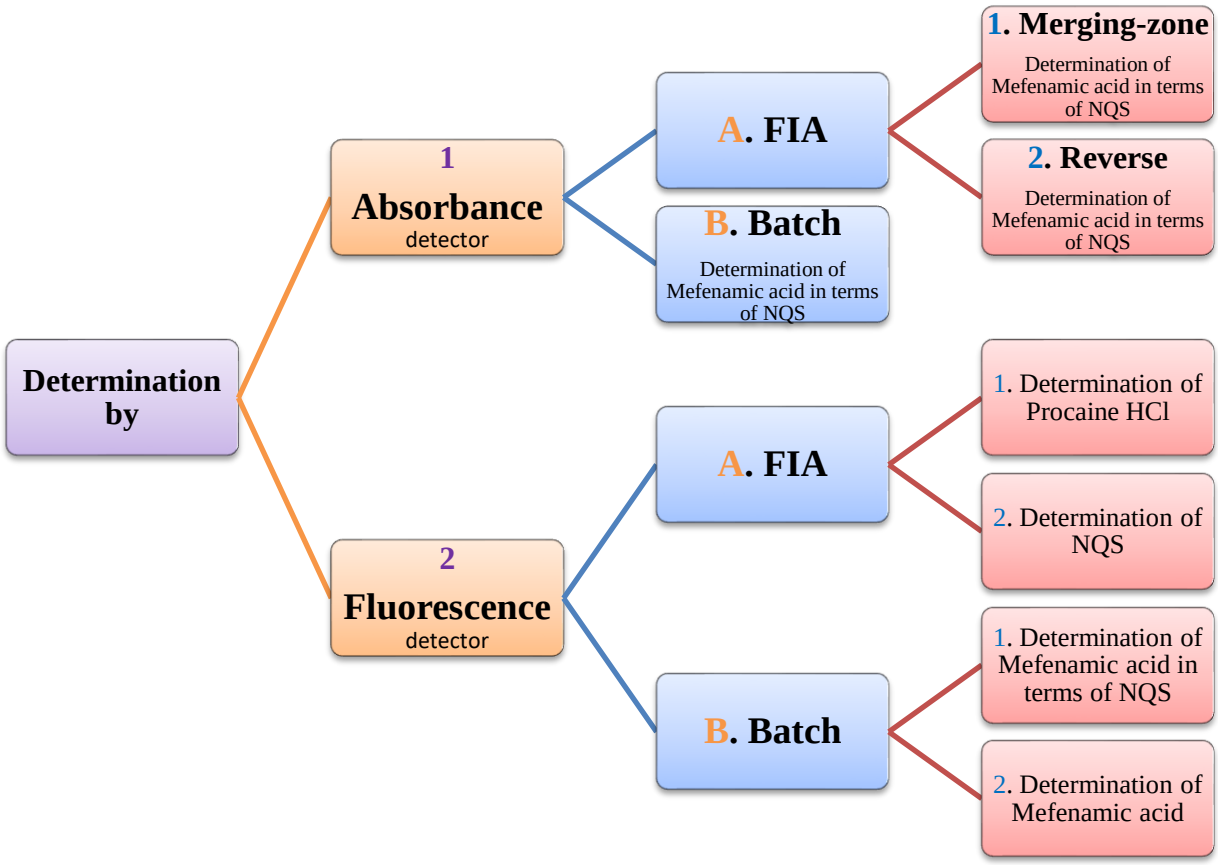

Scheme [3.3]: Different Techniques for Determination of Amino Drugs and Reagent

3.2.1.A. Determination of Mefenamic Acid in Terms of NQS Using FIA

It was decided to use Accumulate Peak Analysis (APA) because of its precision, quick analysis, and ability to graph data. The data produced from the technique were screened and compared to the standard solution with the help of an equation that was expressly created for this purpose. This step will aid the analyst in understanding the parameters that influence the performance of the analysis during the next stage.

The method depends on the electrophilic aromatic substitution reaction between Mefenamic Acid and NQS in the alkaline medium, as shown in Scheme [3.4]**.**

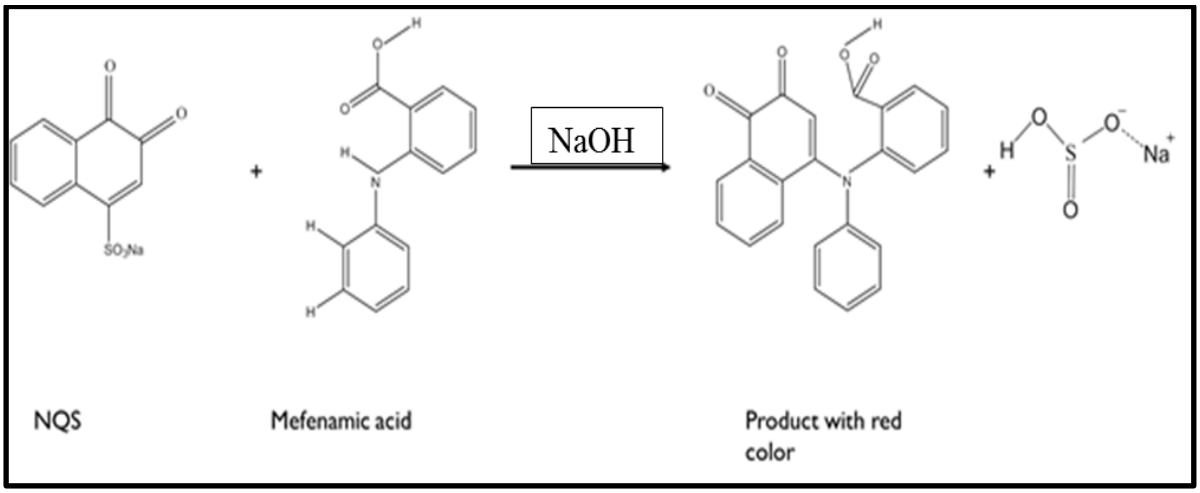

Scheme [3.4]: Reaction between NQS and Mefenamic acid

3.2.1.A.a. Determining the Maximum Wavelength (λmax)

The wavelength of maximum absorption of MA with an NQS reagent was scanned using a UV Vis spectrophotometer. A UV-Vis spectrum of NQS solution showed a maximum absorption peak at 380 nm. Adding an appropriate volume from the previous solution in a convenient concentration to the alkaline

MA solution will produce a reddish-brown reaction product with a new characteristic peak at 477 nm, as shown in Figure [3.6] and Table [3.3]. The new peak exists due to the formation complex between MA and NQS solutions.

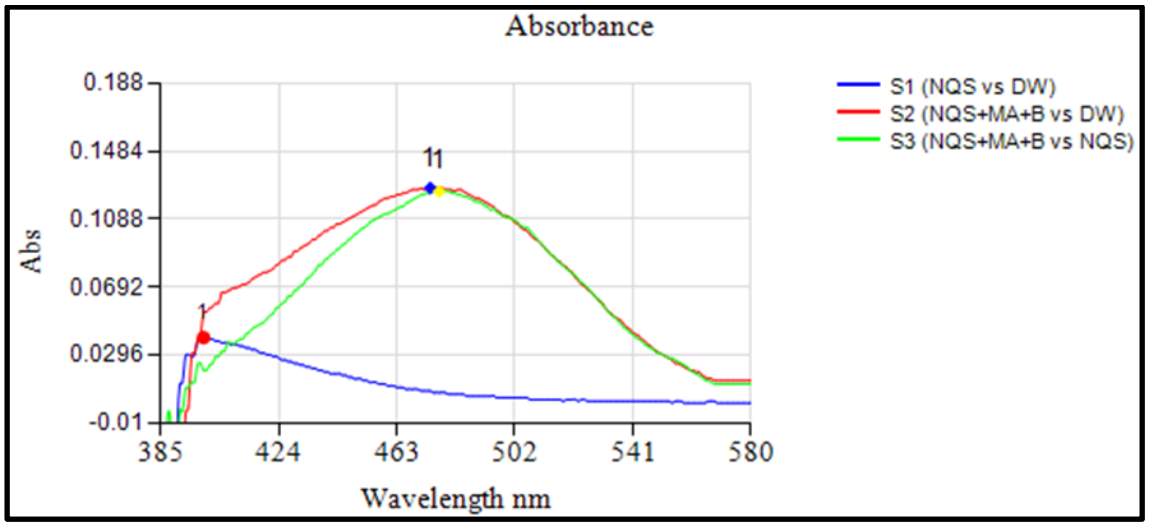

Figure [3.6]: UV- absorbance scanning spectrum for 10 ppm NQS solution (blue line), the reaction product between 10 ppm MA and 10 ppm NQS in an alkaline medium against distilled water (red line), and the reaction product between 10 ppm MA and 10 ppm NQS in an alkaline medium against absorption of 10 ppm NQS solution as a blank solution (green line).

Table [3.3]: Result of Lambda max

Lembda	S1	Lembda	S2	Lembda	S3
399	0.04	474	0.127	477	0.125

3.2.1.A.1. Merging Zone Method

A single parameter was changed in the FIA unit as shown in scheme [3.5] to optimize the experimental conditions. The effect on the absorbance of the colored species was monitored to identify the best possible testing conditions.

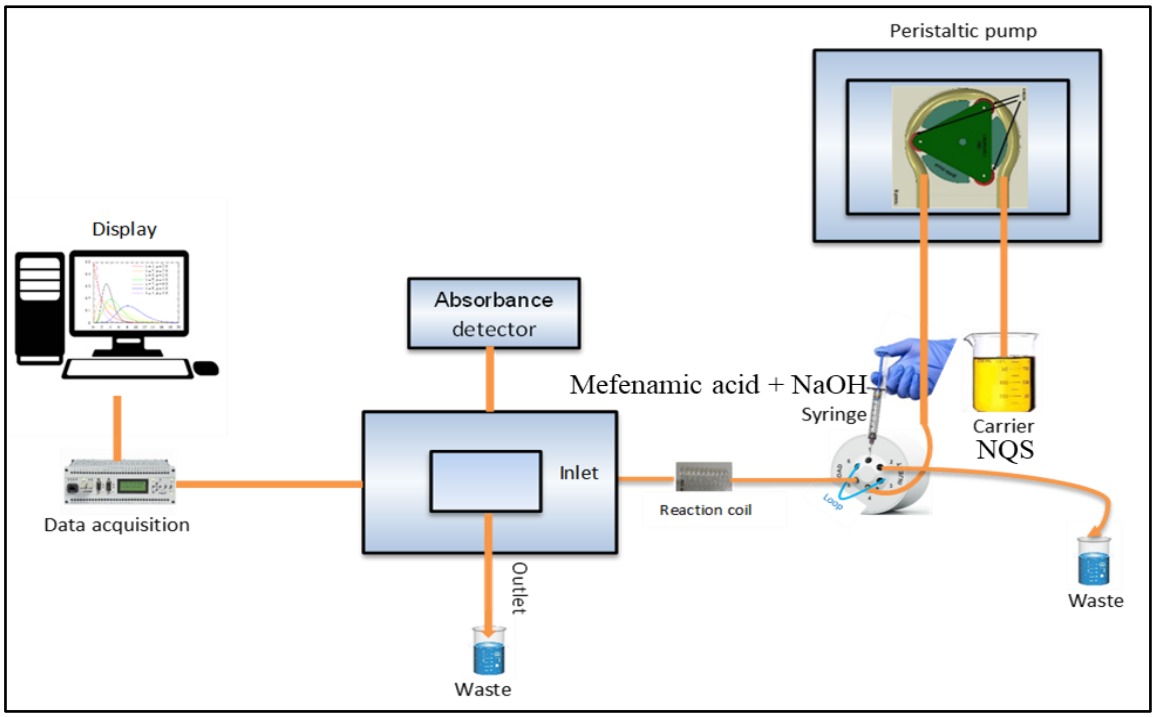

Scheme [3.5]: Design of Merging Zone -FIA with an Absorbance Detector

3.2.1.A.1.1. The Influence of Flow Rate:

The effect of the flow rate and the selection of the optimum speed for the system interaction was studied. The results in Figure [3.7] show the impact of the pump speed on the response value (peak height) at the conditions mentioned below, as it is noted that the response decreases by increasing the pump speed from 1 to 6, and this matches the theoretical foundations of the effect of speed on response. The third speed with a response rate of 0.148 is preferred over the fourth, fifth, and sixth speeds with a response rate of 0.146, 0.133, and 0.130, respectively, for being the highest value. In addition to that, the third speed is preferable to the slower speeds. However, speeds 1 and 2 have the same response rate, which is 0.152, which is the highest response than the third speed (0.148), the shape of the peaks for those low speeds is wide and double-topped and not ideal; either the shape of the peak of the third speed, which has a flow rate of 1.5 ml per minute, is the best because it is sharp and uniform, as the third speed gives the best mixing of the reaction materials.

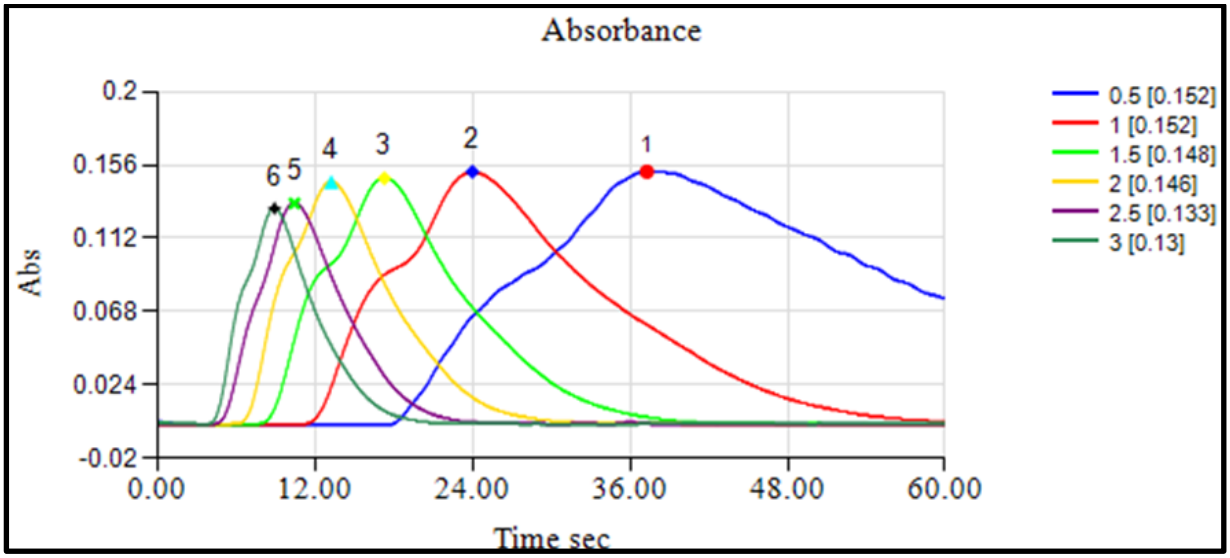

Figure [3.7]: Shows the effect of flow rate on the absorption peak height when, MA conc. = 20 ppm, NQS conc. = 50 ppm, reaction coil length = zero, used alkaline medium = buffer solution, pH value= 12, at room temperature.

These results match what other researchers have stated [70]. It was found that increasing the flow rate reduces the response. It was also found that the shape of the peak at low speeds is wide, double in height, and distorted, but the peak is sharp and uniform at high rates. It can be said that the peak is double because of speed in the mixing process, where the spread is irregular and areas are formed where the mixing is high, and the other is low.

3.2.1.A.1.2. The Effect of the Mixing Coil Length

The reaction coil length effect on the peak height was investigated using varying lengths of reaction coil ranging from 0 to 100 cm. The results show the highest absorbency value and the best shape for the peak obtained after eliminating the double-top peak (which indicates that the mixing was not complete) was when using a reaction coil with a length of 25 cm that; the peak height increases with the increase of the reaction coil length up to 25 cm as shown in Figure [3.8]. At longer lengths, the peak height will decrease due to the dilution process accompanying the reaction coil that has a longer length.

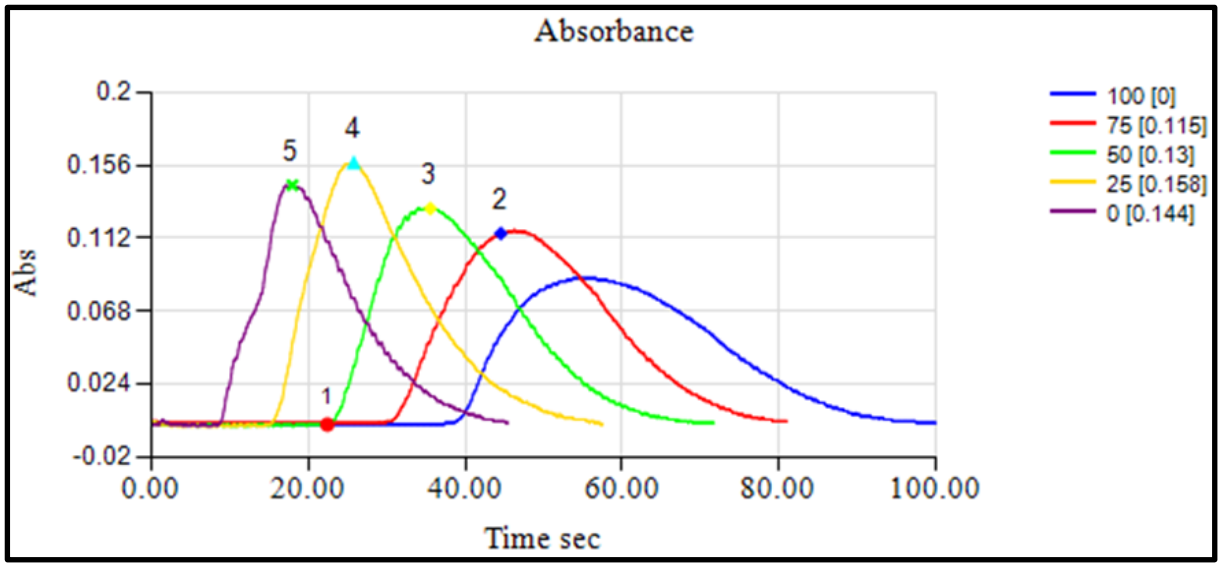

Figure [3.8]: This shows the effect of the reaction coil on the absorption peak height when MA conc. = 20 ppm, NQS conc. = 50 ppm, used alkaline medium = buffer solution, pH value= 12, at room temperature.

3.2.1.A.1.3. The Effect of the Alkaline Type and the Quantity Added

Different alkaline types were tested as alkaline mediums like sodium hydroxide and buffer solutions pH (9-12). The results indicate that the solution resulting from using sodium hydroxide will give the highest absorption peak, as shown in Figure [3.9].

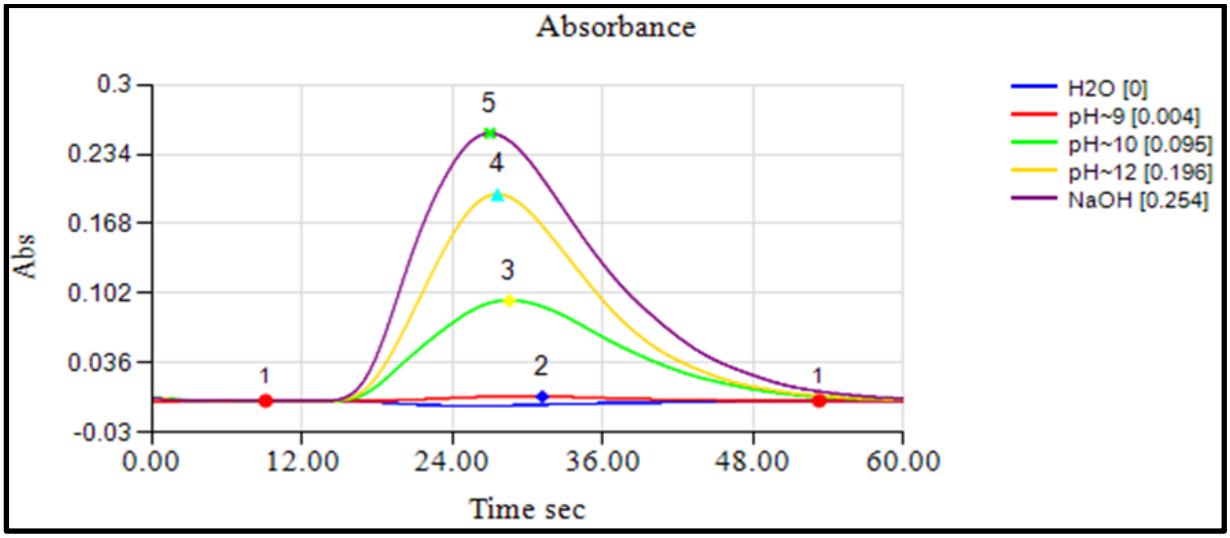

Figure [3.9]: The Influence of the alkaline type when MA conc. = 20 ppm, NQS conc. = 50 ppm, reaction coil length = 25 cm at room temperature

The influence of various volumes added 0.05 to 0.2 mL of the 0.2M from sodium hydroxide solution on the formation of the reaction product has been studied. The results show that the optimum volume of sodium hydroxide solution added into the 20 mL from 20 ppm of MA is 0.1 mL, as shown in Figure [3.10]. This volume of the NaOH solution achieves the best homogeneous merging zone between MA and NQS solutions and shows the highest peak; therefore, 0.1 mL has been chosen as the optimum alkaline medium volume in subsequent experiments.

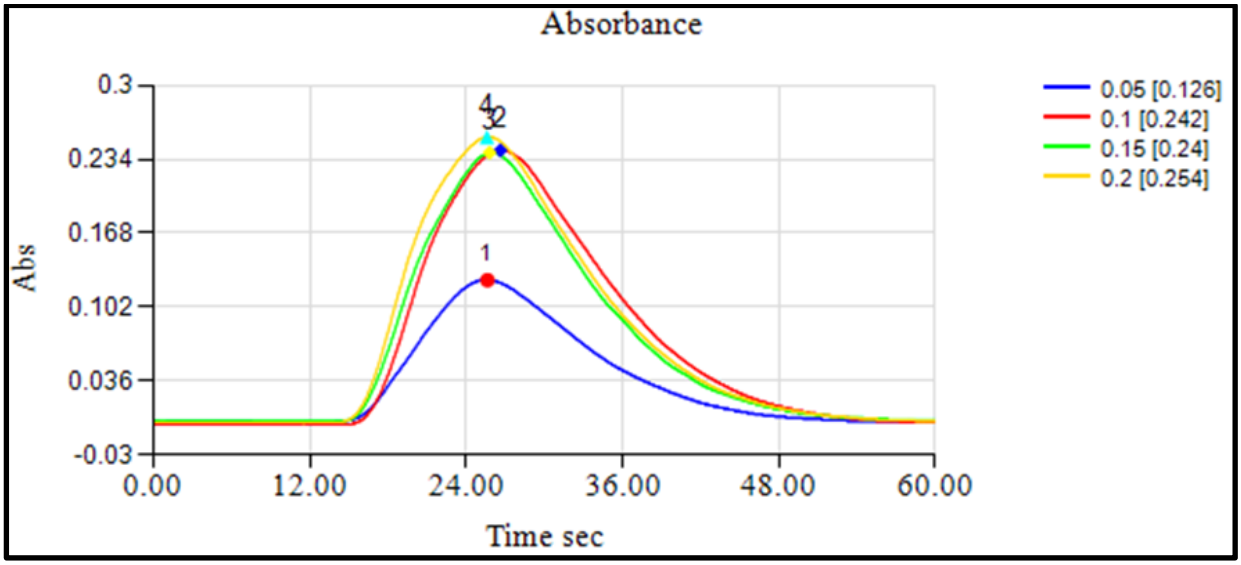

Figure [3.10]: The effect of 0.2M NaOH volume on the absorption peak height when MA conc. = 20 ppm, NQS conc. = 50 ppm, reaction coil length = 25 cm at room temperature

3.2.1.A.1.4. Effect of NQS Concentration

The influence of NQS concentration has been studied in the range of 10 - 100 ppm. The best peak height was observed when using 50 ppm of NQS for the complex formation, as shown in Figure [3.11].

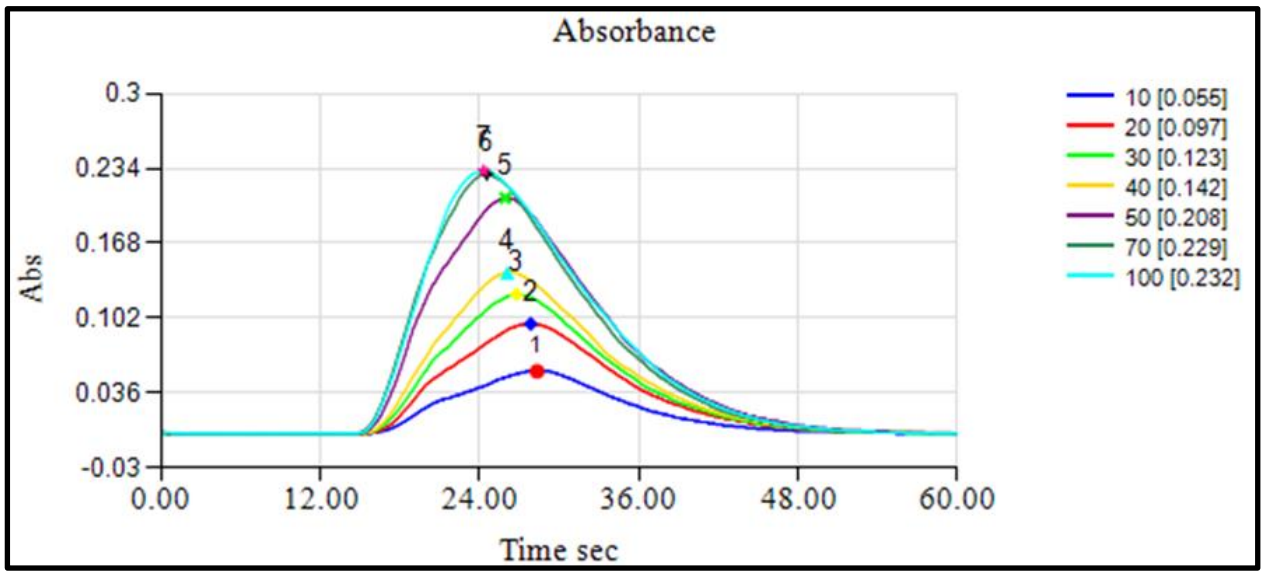

Figure [3.11]: The influence of NQS concentration on the absorption peak height when MA conc. = 20 ppm, reaction coil length = 25 cm, 0.2M NaOH = 0.1 mL to 20 mL MA at room temperature.

Although the response rate increases with the increasing concentration of the reagent, the best concentration was chosen as 50 ppm because high concentrations of the reagent show a deviation in the shape of the peak (the reagent between two regions of the reaction product formation), and it is also preferable to use dilute concentrations of the reagent to ensure that the signal of the concentration of the reagent does not interfere with the signal of the reaction product.

3.2.1.A.1.5. General Procedures and the Calibration Curve

According to the optimum conditions, MA was quantitatively determined. The calibration curve was prepared at 477 nm by organizing a series of MA solutions with different concentrations and analyzing each employing the FIA system. The absorption peak height value of the formed complex was plotted against the concentration. The suggested method allows for the determination of MA in the range of (1-20) ppm, as shown in Figures [3.12] and [3.13].

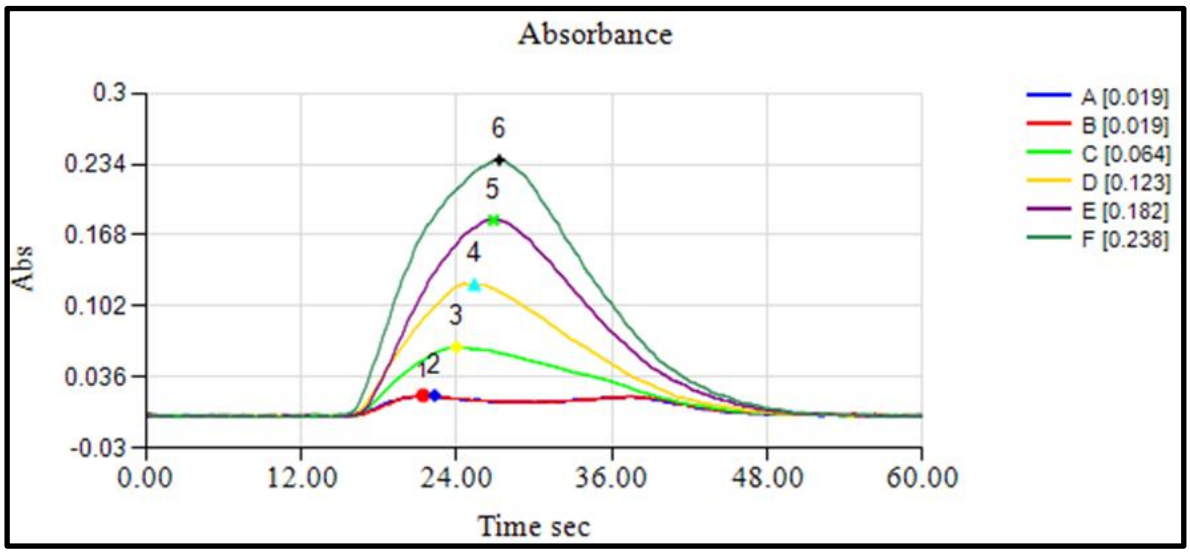

Figure [3.12]: Absorption Spectra of Mefenamic Acid.

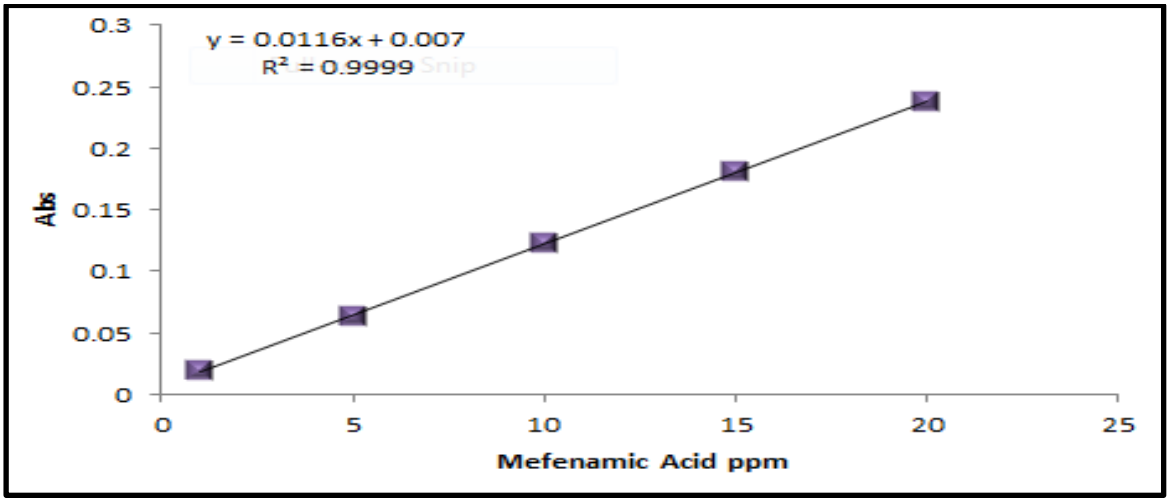

Figure [3.13]: Calibration Curve of Mefenamic Acid

The sensitivity of the suggested method represented as detection limit (LOD) and quantitation limit (LOQ) has been estimated to be equal to 0.021 and 0.071 ppm, respectively, as shown in Table [3.4].

Table [3.4]: The effect of MA conc. on the absorption peak height when, NQS conc. = 50 ppm, reaction coil length = 25 cm, 0.2M NaOH = 0.1 mL to 20 mL MA at room temperature

Mefenamic acid ppm	Abs	QR
1	0.019	0.019
1	0.019	0.019
5	0.064	0.065
10	0.123	0.123
15	0.182	0.181
20	0.238	0.239

SD = 0.0009
LOD=0.021
LOQ=0.071

3.2.1.A.1.6. Repeatability

The relative standard deviation (RSD %) represents the precision of the proposed method has been studied utilizing 13 ppm of MA solution. At the optimum conditions, 6 replicate measurements were carried out for the determined concentration and recorded as shown in Figure [3.14] and Table [3.5]. The standard deviation value is equal to 0.0019, and the relative standard deviation value is equal to 1.237, indicating the high precision of the suggested method.

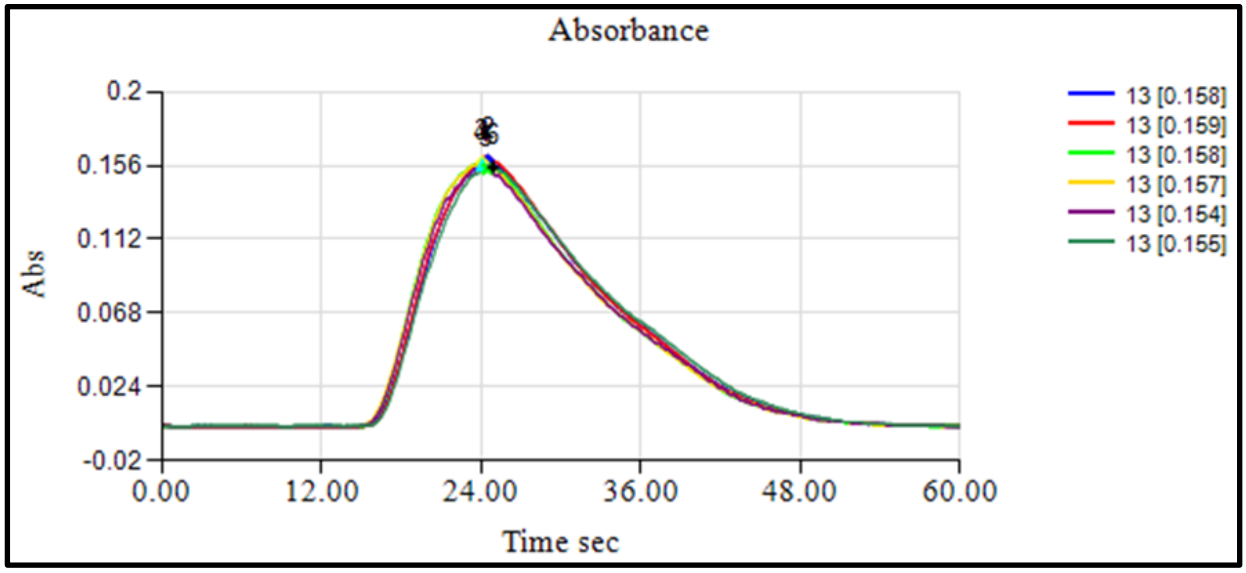

Figure [3.14]: Repeatability of 13 ppm MA Solution by Merging Zone –FIA

Table [3. 5]: Repeatability results for 13 ppm MA solution by Merging zone -FIA

Sample No.	1	2	3	4	5	6	Mean	SD	RSD%
Abs.	0.158	0.159	0.158	0.157	0.154	0.155	0.157	0.0019	1.237

3.2.1.A.1.7. Dead Volume

The quality of the obtained results was examined by performing the dead volume experiment. This experiment includes three steps: in the first step, water instead of MA was loaded in the valve loop after mixing with NaOH, and in the second step, water instead of the carrier solution represented the NQS. In the third step, water was used instead of NaOH and loaded into the valve loop after mixing with MA. The response to the three experiments was confirmed and was zero, indicating no dead volume, Figure [3.15].

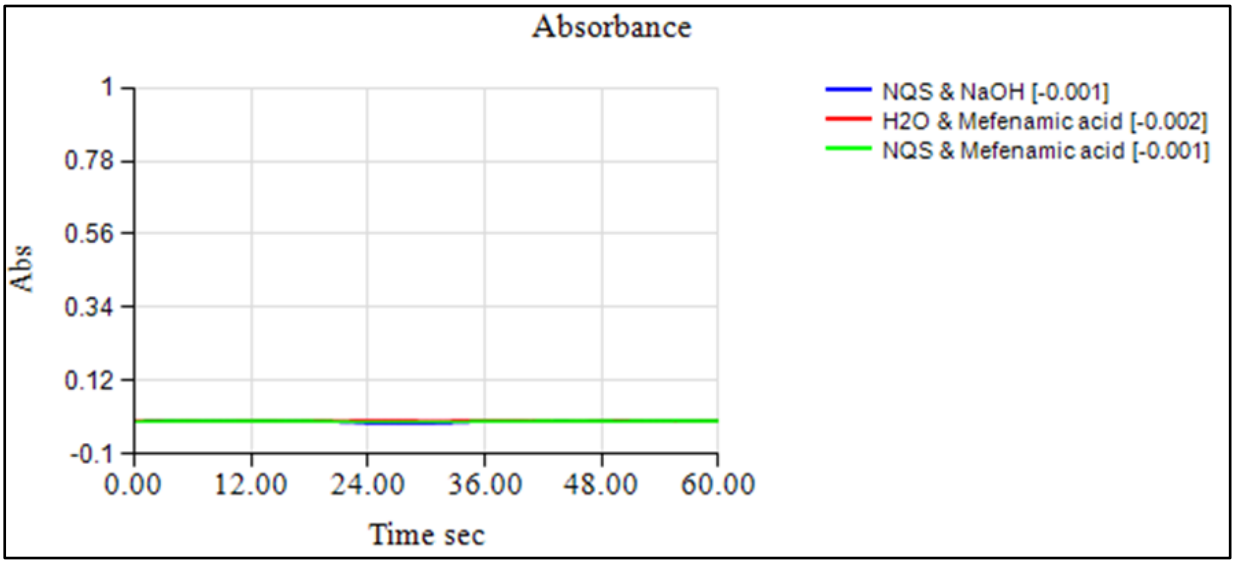

Figure [3.15]: The Dead Volume of MA

3.2.1.A.1.8. The Determination of Dispersion

The dispersion coefficient (dilution factor D) was studied to illustrate the dispersion process extent within the flow injection system from the injection point at the valve to the detecting point at the detector. The dispersion coefficient can be calculated through Equation [1.1] and its equal 1.11.

The dispersion coefficient was studied using one concentration of MA solution within the calibration curve range (20 ppm). In the first step, the reaction between the MA alkaline solution and the NQS solution was implemented inside the FIA system under the defined optimum conditions by measuring the peak height that represents the peak height with the dilution process (H max). In the second step, the reaction between the MA alkaline solution and the NQS solution in appropriate volumes was implemented in a glass beaker and passed the final solution through the system, then measuring the absorption peak height that takes the plateau shape with a constant height value with the time that represents the peak height without the dilution process (H°). The obtained results are displayed in Figure [3.16].

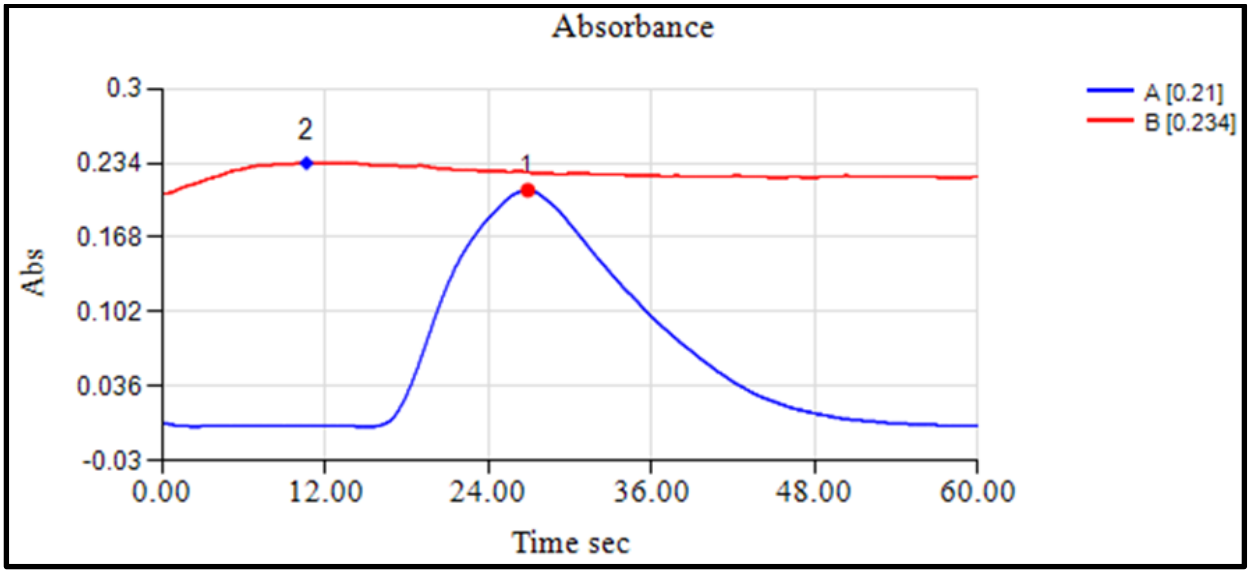

Figure [3.16]: Dispersion Coefficient Study Results for MA Determination FIA System

3.2.1.A.1.9. Calculating the Sampling Frequency of the FIA System for MA Determination by NQS

According to the optimum conditions, the sampling frequency of the MA determination by the FIA system has been calculated by accounting for the

consumed time from the injection moment to the moment when the absorption peak reaches its maximum height; the practical frequency is 120 samples per hour.

3.2.1.A.1.10. In Aqueous Solutions, MA can be Determined as follows

Three aqueous solutions were prepared and considered solutions of unknown concentration; then, the absorbance was measured according to the optimum conditions, as shown in Fig. [3.17]. Then the solutions' concentration was determined by setting each solution's absorbance on the straight line of the previous calibration curve, as shown in Fig. [3.18] and Table [3.6]. The value of the resulting solutions from the calibration curve was very close to the prepared solutions, considering the preparation errors.

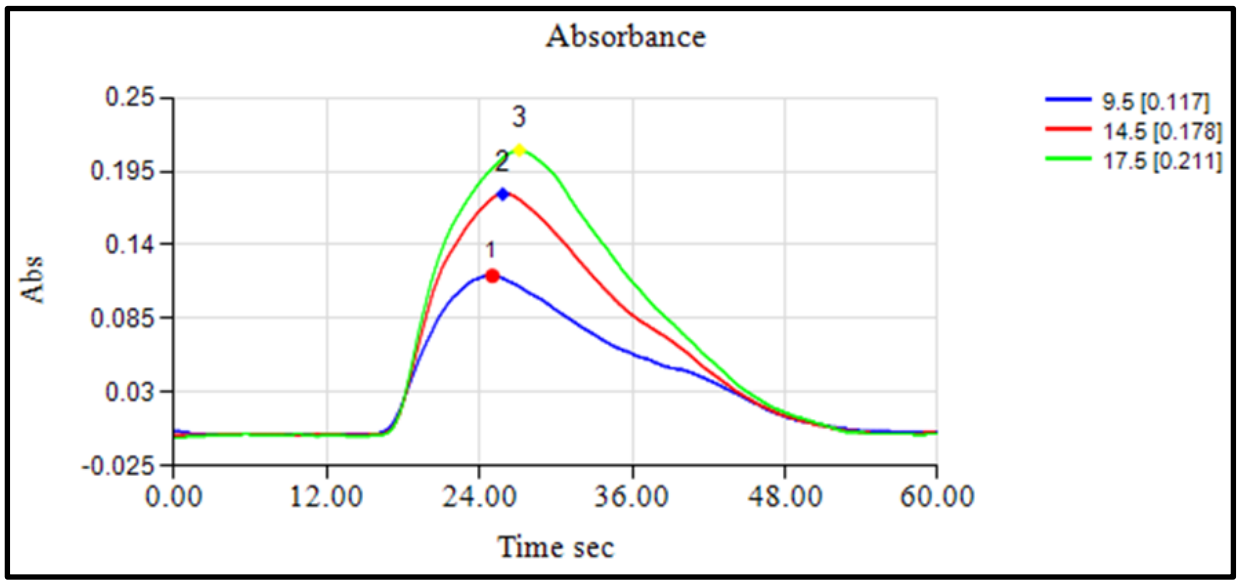

Figure [3.17]: The Spectrum of Possible Applications

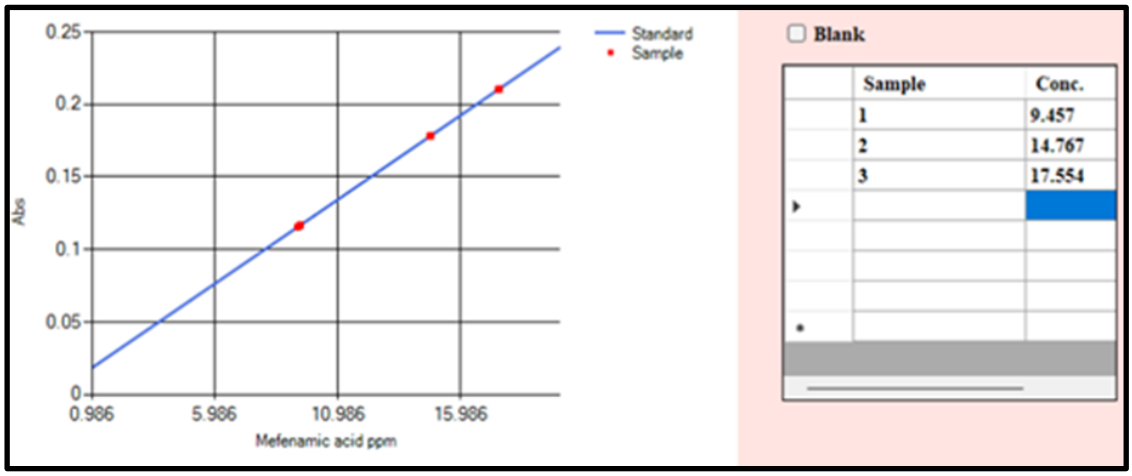

Figure [3.18]: Determination of Unknown Aqueous Solutions

Table [3.6]: Value of Sample Application

Index	Taken	Founded	Peak Height	Recovery
1	9.5	9.457	0.117	99.547
2	14.5	14.767	0.178	101.8
3	17.5	17.554	0.211	100.3

3.2.1.A.2. Reverse – Continuous FIA

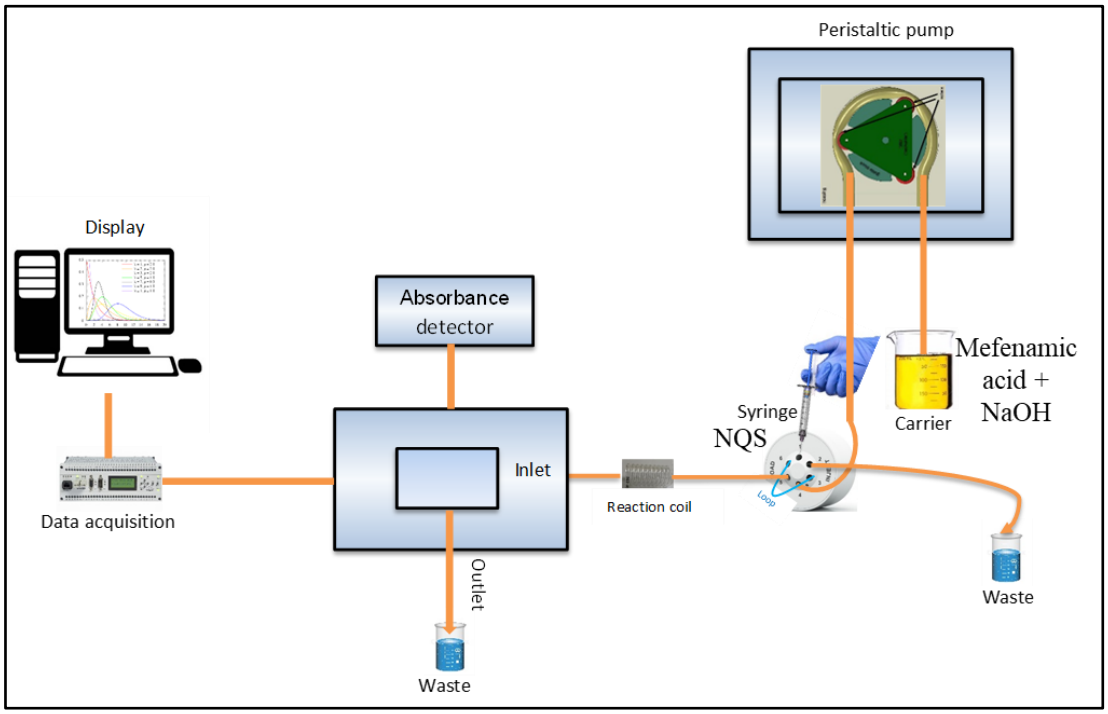

Scheme [3.6]: Design of Reverse – Continuous FIA with Absorbance Detector

3.2.1.A.2.1. The Influence of Flow Rate:

The effect of the flow rate and the selection of the optimum speed for the system interaction was studied. The results in Figure [3.19] show the effect of the pump speed on the response value (peak height) at the conditions mentioned below, as it is noted that the response decreases by increasing the pump speed from 1 to 5, and this matches the theoretical foundations of the effect of speed on response. The third speed with a response rate of 0.16 is preferred over the fourth and fifth speeds with a response rate of 0.151 and 0.144, respectively, for being the highest value. Also, the third speed is preferable to the slower speeds. However, speed 2 have a response rate of 0.165, which is higher than the third speed (0.16), the shape of the peak for those low speed is wide and double-topped, and not ideal; either the form of the peak of the third speed, which has a flow rate of 1.5 ml per minute, is the best because it is sharp and uniform, as the third speed gives the best mixing of the reaction materials.

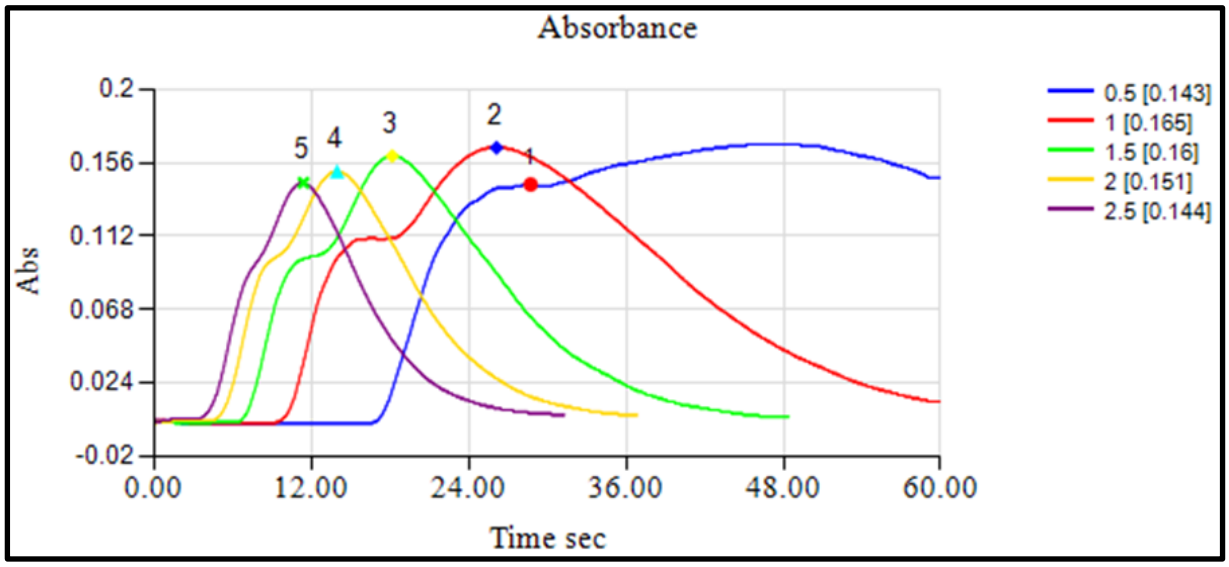

Figure [3.19]: The Effect of Flow Rate on the Absorption Peak Height when, MA conc. = 30 ppm, NQS conc. = 50 ppm, reaction coil length = zero, used alkaline medium = buffer solution, pH value= 12, at room temperature.

3.2.1.A.2.2. The Effect of the Length of the Mixing Coil

The reaction coil length effect on the peak height was investigated using varying lengths of reaction coil ranging from 0 to 100 cm. The results show the highest absorbency value and the best shape for the peak obtained after eliminating the double-top peak (which indicates that the mixing was not complete) was when using a reaction coil with a length of 75 cm that; the peak height increases with the increase of the reaction coil length up until to 75 cm as shown in Figure [3.20]. At longer lengths, the peak height will decrease due to the dilution process accompanying the reaction coil that has a longer length.

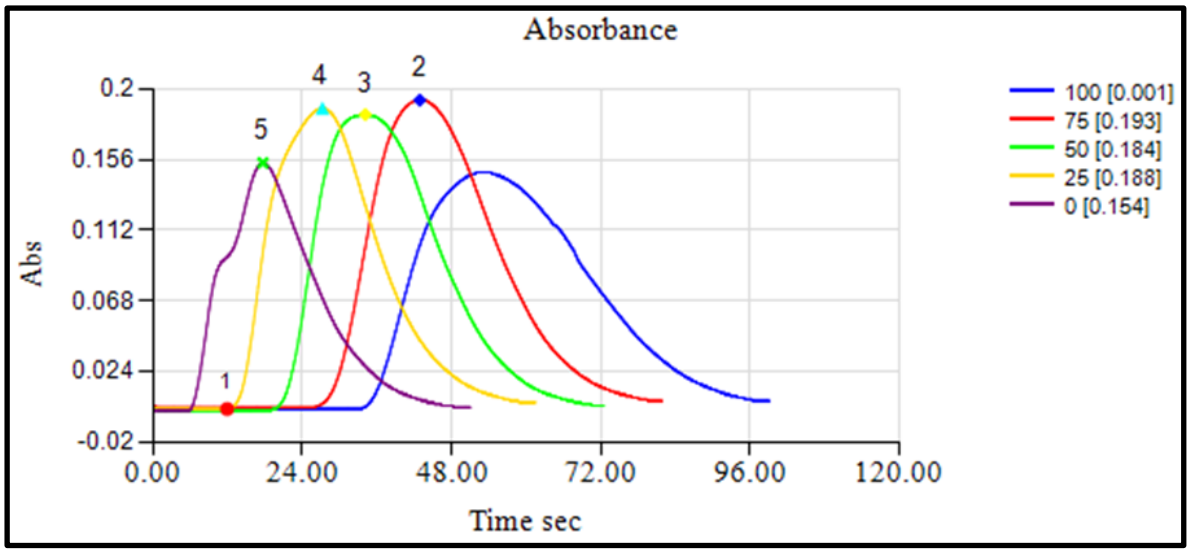

Figure [3.20]: The Effect of the Reaction Coil on the Absorption Peak Height when MA conc. = 30 ppm, NQS conc. = 50 ppm, used alkaline medium = buffer solution, pH value= 12, at room temperature.

3.2.1.A.2.3. The Effect of the Alkaline Type and the Quantity Added

Different alkaline types were tested as alkaline mediums like sodium hydroxide and buffer solutions pH (9-12). The results indicate that the solution

resulting from using sodium hydroxide will give the highest absorption peak, as shown in Figure [3.21].

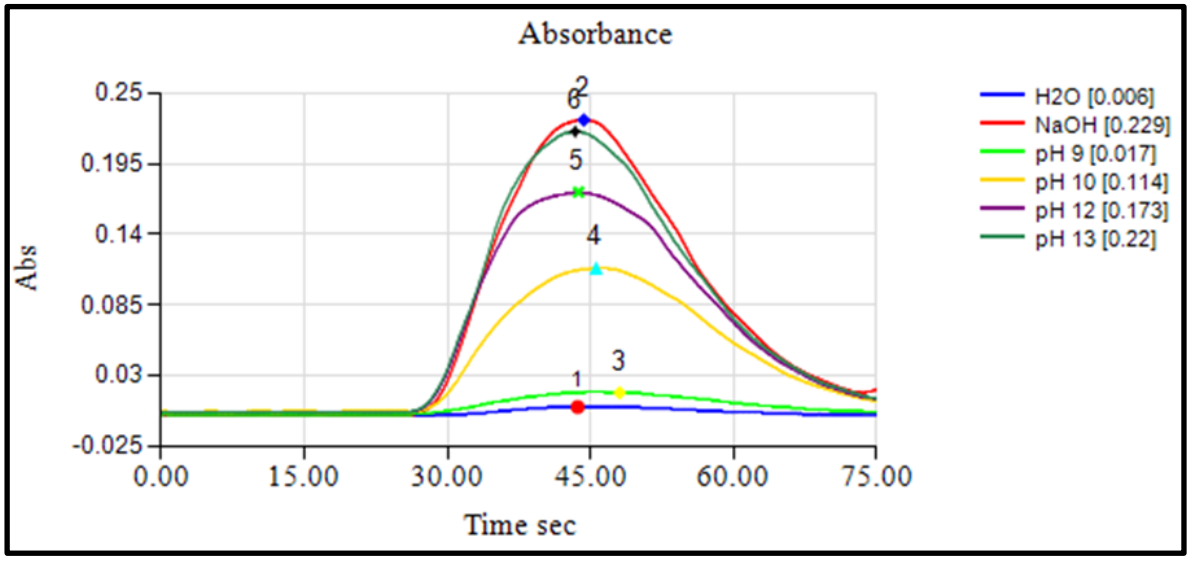

Figure [3.21]: The Influence of the Alkaline Type when MA conc. =30 ppm, NQS conc. = 50 ppm, reaction coil length = 75 cm at room temperature

The influence of various volumes added 0.05 to 0.2 mL of the 0.2 M from sodium hydroxide solution on the formation of the reaction product has been studied. The results show that the optimum volume of sodium hydroxide solution added into the 20 mL from 30 ppm of MA is 0.15 mL, as shown in Figure [3.22]. This volume of the NaOH solution achieves the best homogeneous merging zone between MA and NQS solutions and shows the highest peak; therefore, 0.15 mL has been chosen as the optimum alkaline medium volume in subsequent experiments.

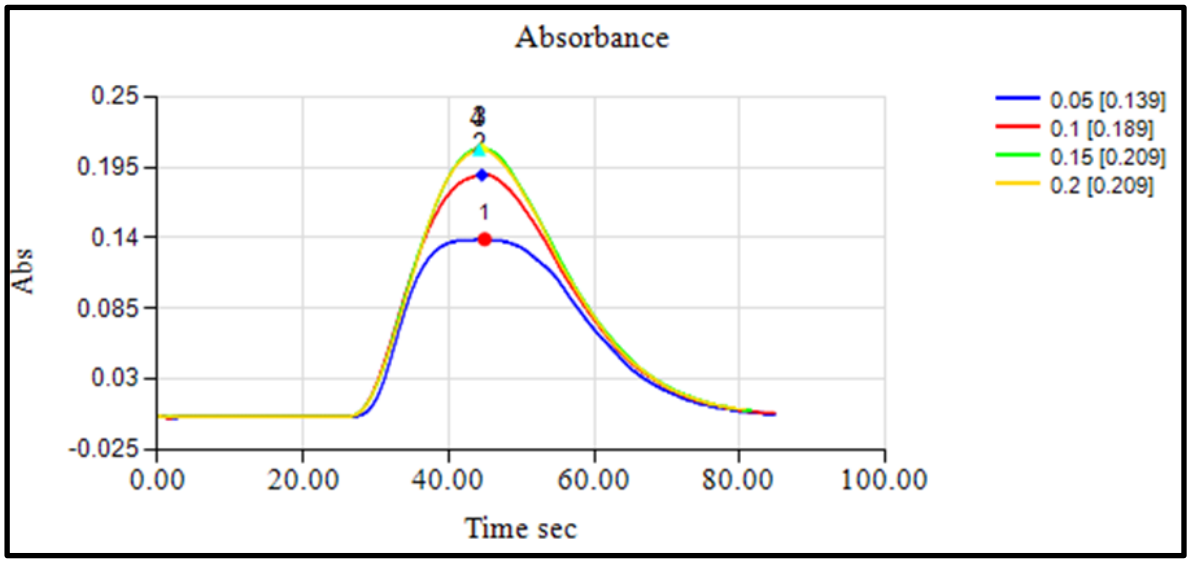

Figure [3.22]: The Effect of NaOH Volume on the Absorption Peak Height when MA conc. =30 ppm, NQS conc. = 50 ppm, reaction coil length = 75 cm at room temperature.

3.2.1.A.2.4. Effect of NQS Concentration

The influence of NQS concentration has been studied in the range of 10 - 100 ppm. The best peak height was observed when using 50 ppm of NQS for the complex formation, as shown in Figure [3.23].

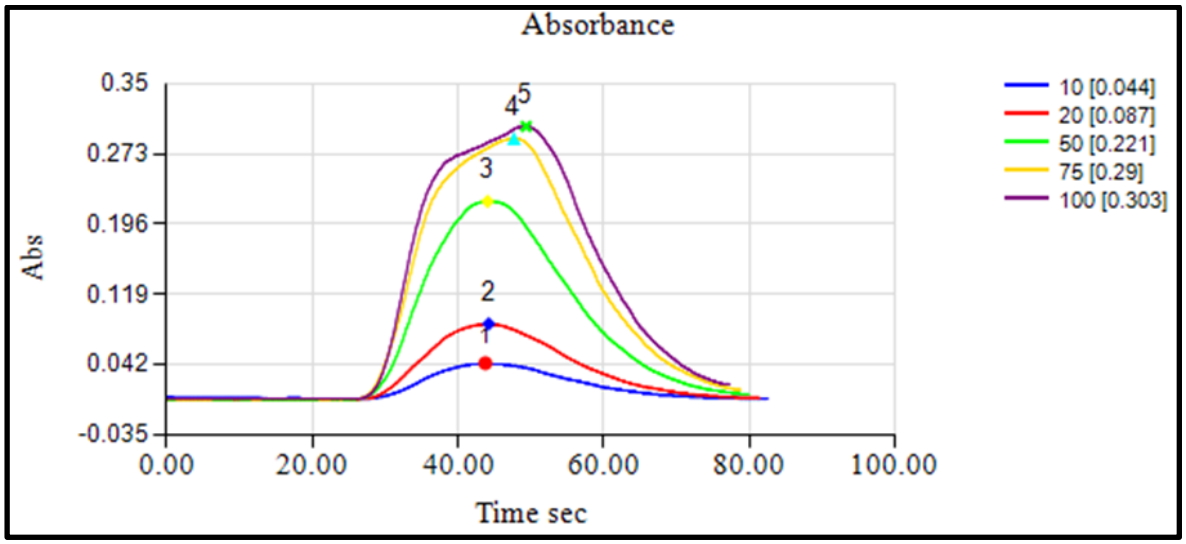

Figure [3.23]: The Influence of NQS Concentration on the Absorption Peak Height when MA conc. = 30 ppm, reaction coil length = 75 cm, NaOH = 0.15 mL to 20 mL MA at room temperature.

Although the response rate increases with the increasing concentration of the reagent, the best concentration was chosen as 50 ppm because high concentrations of the reagent show a deviation in the shape of the peak (the reagent between two regions of the reaction product formation), and it is also preferable to use dilute concentrations of the reagent to ensure that the signal of the concentration of the reagent does not interfere with the signal of the reaction product.

3.2.1.A.2.5. General Procedures and the Calibration Curve

According to the optimum conditions, MA was quantitatively determined. The calibration curve was prepared at 477 nm by preparing a series of MA solutions with different concentrations and analyzing each employing the FIA system. The absorption peak height value of the formed complex was plotted against the concentration. The suggested method allows for the determination of MA in the range of (1-30) ppm, as shown in Figures [3.24] and [3.25].

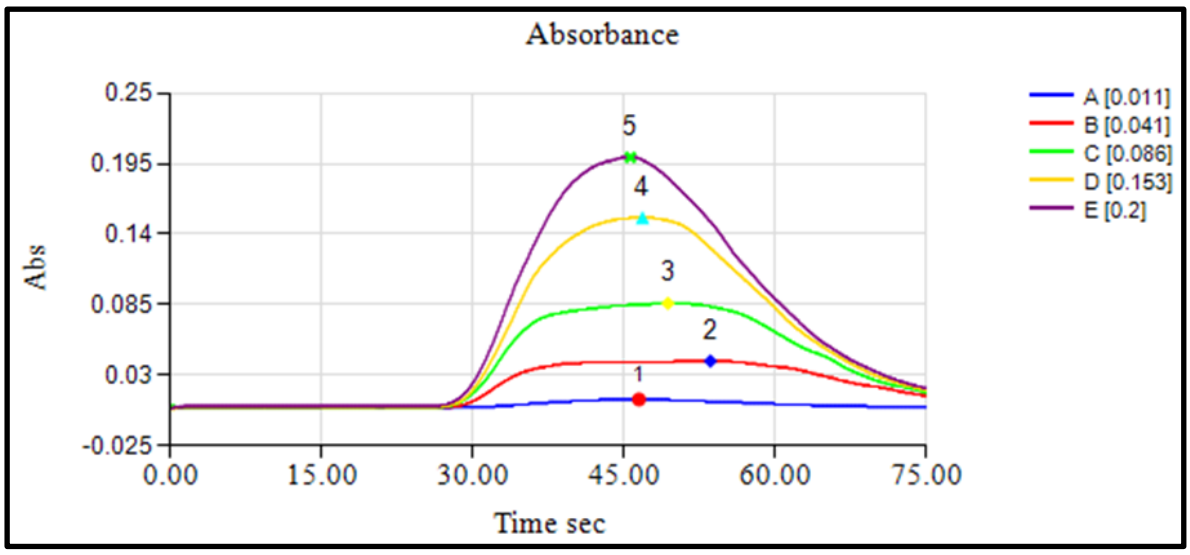

Figure [3.24]: Absorption Spectra of MA by Reverse – Continuous FIA

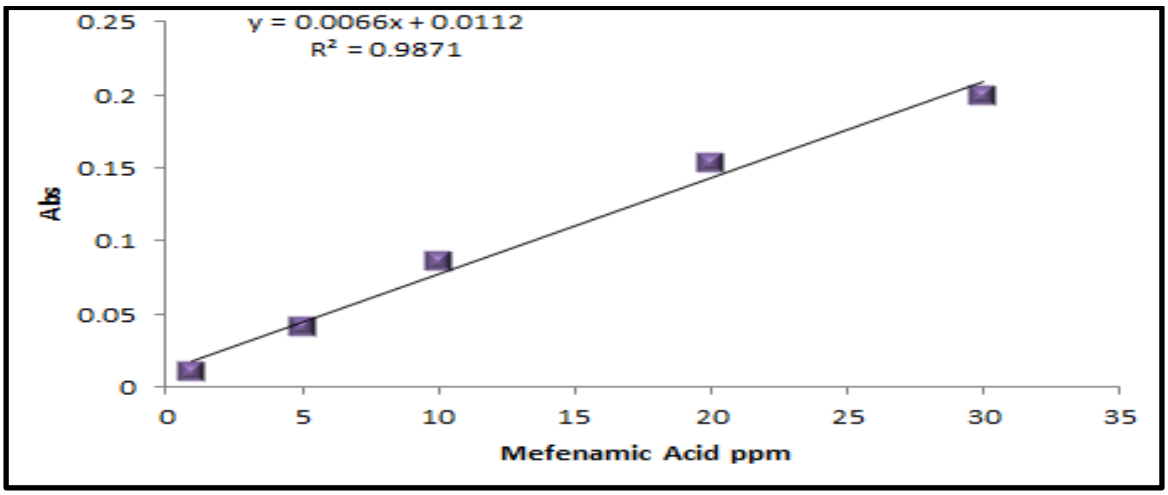

Figure [3.25]: Calibration Curve of MA

The sensitivity and correlation coefficient are shown in Table [3.7].

Table [3.7]: The Effect of MA conc. on the Absorption Peak Height when, NQS conc. = 50 ppm, reaction coil length = 75 cm, NaOH = 0.15 mL to 20 mL MA at room temperature

MA ppm	Abs	QR
1	0.011	0.018
5	0.041	0.044
10	0.086	0.077
20	0.153	0.143
30	0.2	0.209

3.2.1.A.2.6. Repeatability

The relative standard deviation (RSD %) represents the precision of the proposed method has been studied utilizing 30 ppm of MA solution. At the optimum conditions, 6 replicate measurements were carried out for the determined concentration and recorded as shown in Figure [3.26] and Table

[3.8]. The standard deviation value is equal to 0.0019, and the relative standard deviation value is equal to 0.586, indicating the high precision of the suggested method.

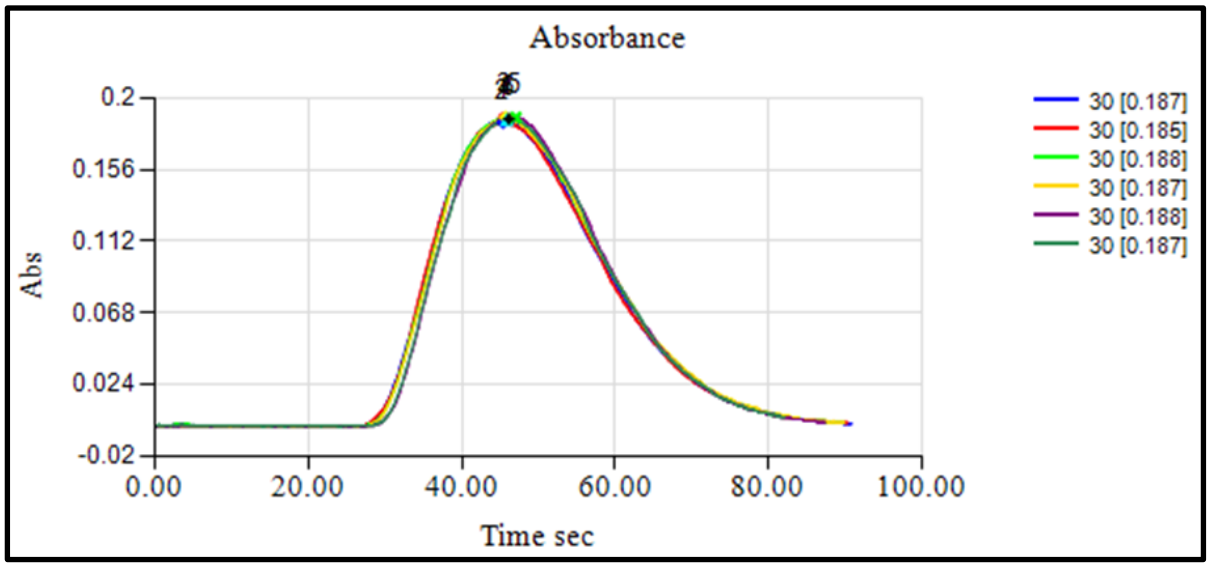

Figure [3.26]: Repeatability of 30 ppm MA Solution by Reverse – Continuous FIA

Table [3.8]: Repeatability Results for 30 ppm MA Solution by Reverse – Continuous FIA

Sample No.	1	2	3	4	5	6	Mean	SD	RSD%
Abs.	0.187	0.185	0.188	0.187	0.188	0.187	0.187	0.0011	0.586

3.2.1.A.2.7. Dead Volume

The quality of the obtained results was examined by performing the dead volume experiment. This experiment includes two steps: in the first step, water instead of NQS was loaded in the valve loop, and in the second step, water instead of the carrier solution represented the mixture of MA and NaOH. The

response to the two experiments was confirmed and was zero, indicating no dead volume, as shown in Figure [3.27].

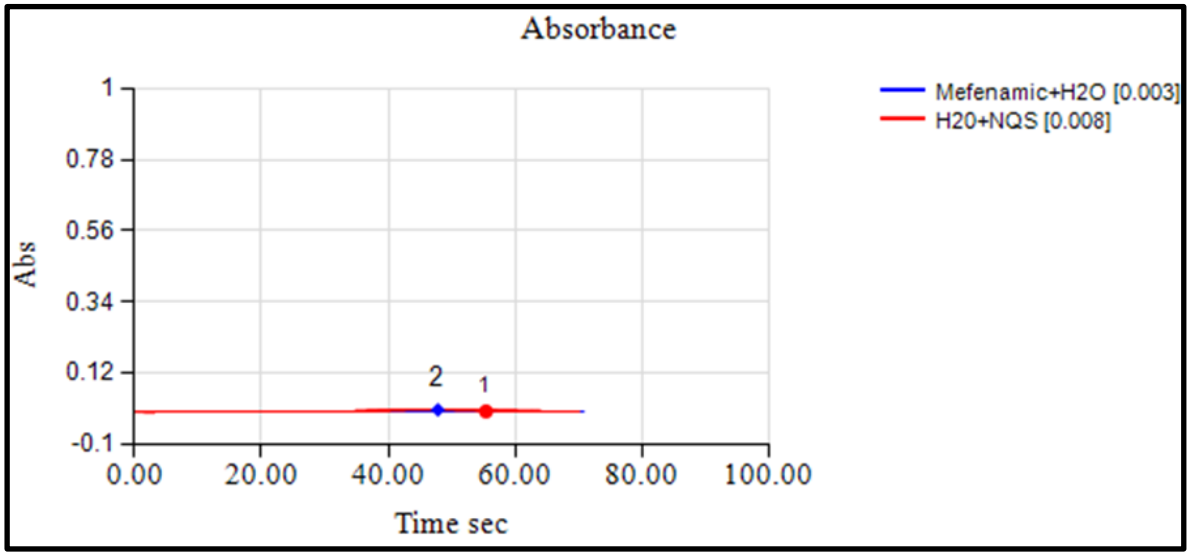

Figure [3.27]: The Dead Volume of MA

3.2.1.A.2.8. The Determination of Dispersion

The dispersion coefficient (dilution factor D) was studied to illustrate the dispersion process extent within the flow injection system from the injection point at the valve to the detecting point at the detector. The dispersion coefficient can be calculated through Equation [1.1] and its equal 1.17.

The dispersion coefficient was studied using one concentration of MA solution within the calibration curve range (30 ppm). In the first step, the reaction between the MA alkaline solution and the NQS solution was implemented inside the FIA system under the defined optimum conditions by measuring the peak height that represents the peak height with the dilution process (H_{max}). In the second step, the reaction between the MA alkaline solution and the NQS solution in appropriate volumes was implemented in a glass beaker and passed the final solution through the system, then measuring

the absorption peak height that takes the plateau shape with a constant height value with the time that represents the peak height without the dilution process (H°). And the obtained results are displayed in Figure [3.28].

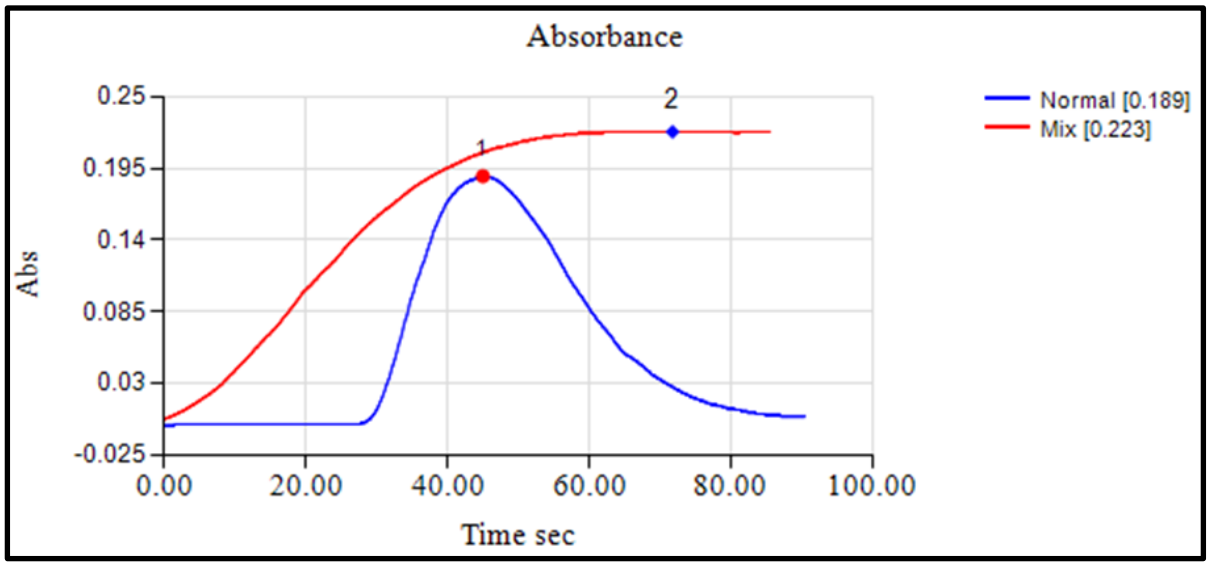

Figure [3.28]: Dispersion Coefficient Study Results for MA Determination FIA System

3.2.1.A.2.9. In Aqueous Solutions, MA can be Determined as follows

Two aqueous solutions were prepared and considered solutions of unknown concentration; then, the absorbance was measured according to the optimum conditions, as shown in Figure [3.29]. Then the solutions' concentration was determined by setting each solution's absorbance on the straight line of the previous calibration curve, as shown in Figure [3.30] and Table [3.9]. The value of the resulting solutions from the calibration curve was very close to the prepared solutions, considering the preparation errors.

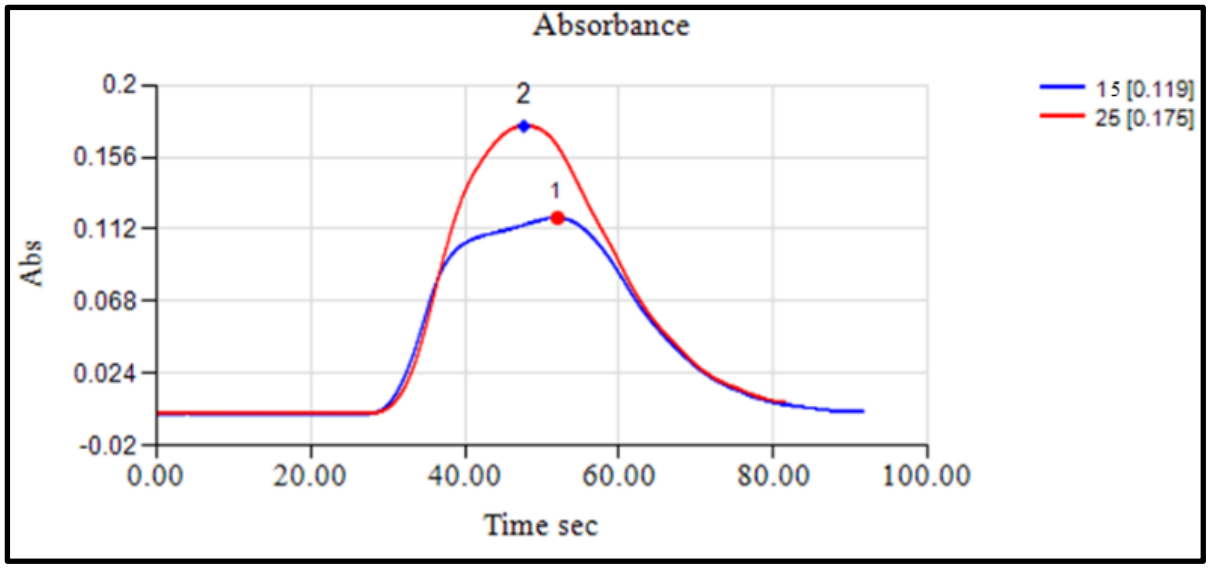

Figure [3.29]: The Spectrum of Possible Applications

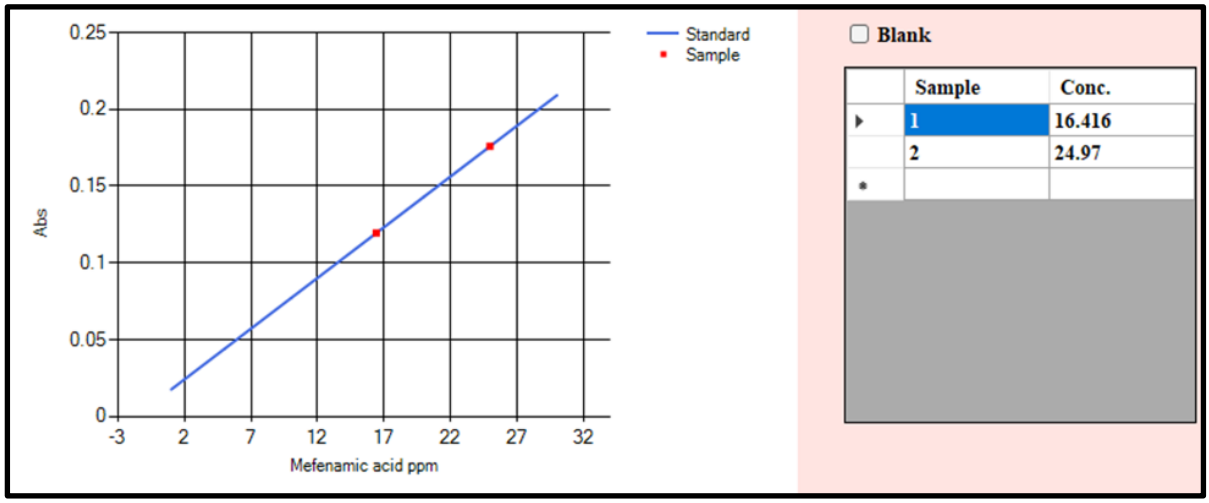

Figure [3.30]: Determination of Unknown Aqueous Solutions

Table [3.9]: Value of Sample Application

Index	Sample ppm (Taken)	MA ppm (Founded)	Peak Height	Recovery
1	15	16.358	0.119	109
2	25	24.889	0.175	99.6

3.2.1.B.1. The Calibration Curve of MA Determination by NQS in the Basic Medium Using the Spectrophotometric Method (Batch method)

The calibration curve of the MA determination method at 477 nm was plotted under the optimum conditions by preparing a series of MA solutions having different concentrations and analyzing each in triplicate, then drawing the reaction product absorbance against the corresponding MA concentration.

The suggested method allows for determining the MA in the linearity range of (0.5-10) ppm, as shown in Table [3.10] and Figure [3.31].

Table [3.10]: The effect of MA concentration on the absorption value when, MA volume = 1mL, NQS conc. = 50 ppm, NQS volume = 1 mL, used base type = NaOH, Base conc. = 0.2M, Base volume = 0.1 mL, at room temperature.

MA conc. ppm	Abs. 1	Abs. 2	Abs. 3	Absorbance means	SD	RSD%
0.5	0.063	0.063	0.062	0.0626	0.00047	0.752
2	0.187	0.186	0.186	0.186	0.00047	0.253
4	0.371	0.371	0.37	0.3706	0.00047	0.127
7	0.654	0.653	0.653	0.653	0.00047	0.072
10	0.919	0.919	0.918	0.9186	0.00047	0.051

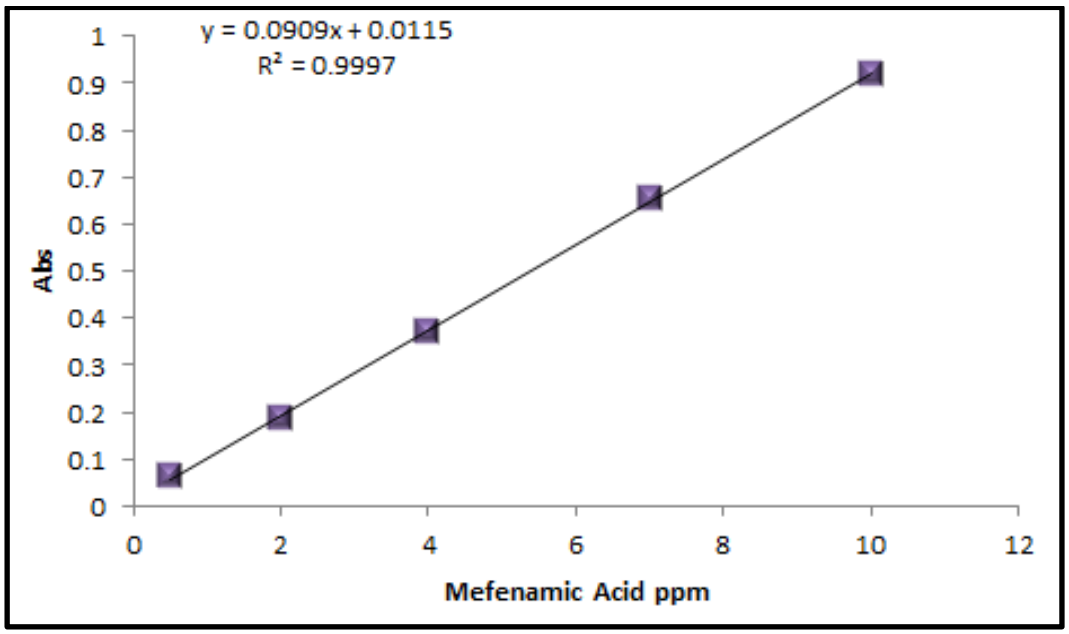

Figure [3.31]: Calibration Curve of MA by Batch Method

3.2.1.B.2. In Aqueous Solutions, MA can be Determined as follows

Three aqueous solutions of unknown concentration were measured, and then their concentration was determined after measuring the absorbance and determined on the calibration curve, as shown in Table [3.11] and Figure [3.32].

Table [3.11]: The Value of the Sample Application

Index	Sample (taken)ppm	Mefenamic acid (founded)ppm	Absorbance	Recovery
1	2	2.2	0.205	110
2	5	5.1	0.476	102
3	6.5	6.7	0.624	103

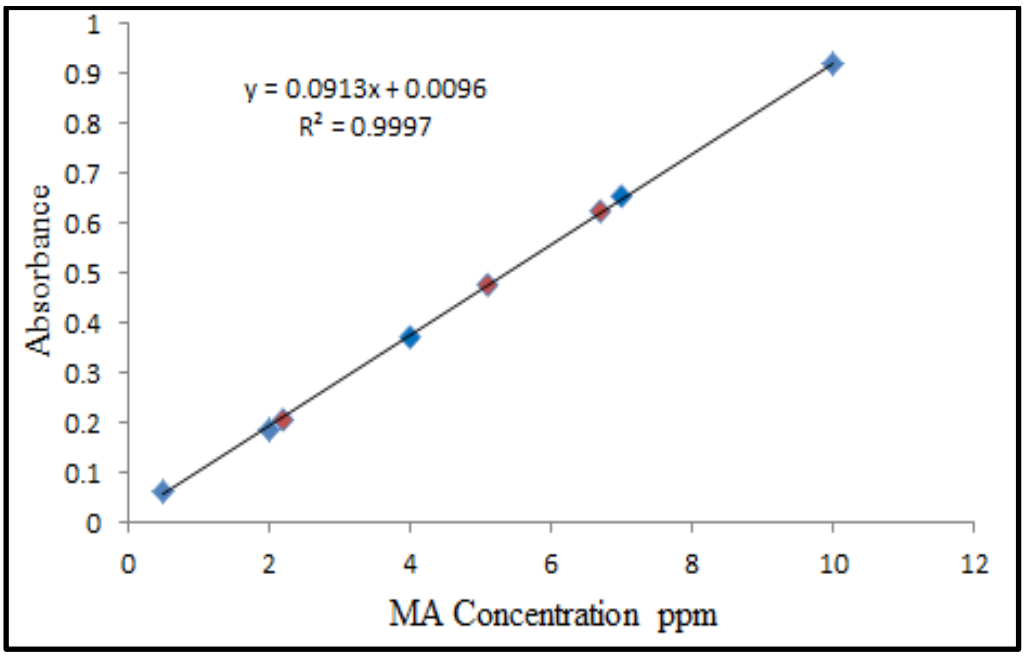

Figure [3.32]: Determination of Unknown Aqueous Solutions

3.2.2.A.1. Spectrofluorometric Method to Determine Procaine Hydrochloride by Merging-Zone FIA

A single parameter was changed to optimize experimental conditions, and the effect on the fluorescence of the species was monitored to identify the best possible testing conditions for the experiment, see Scheme [3.7].

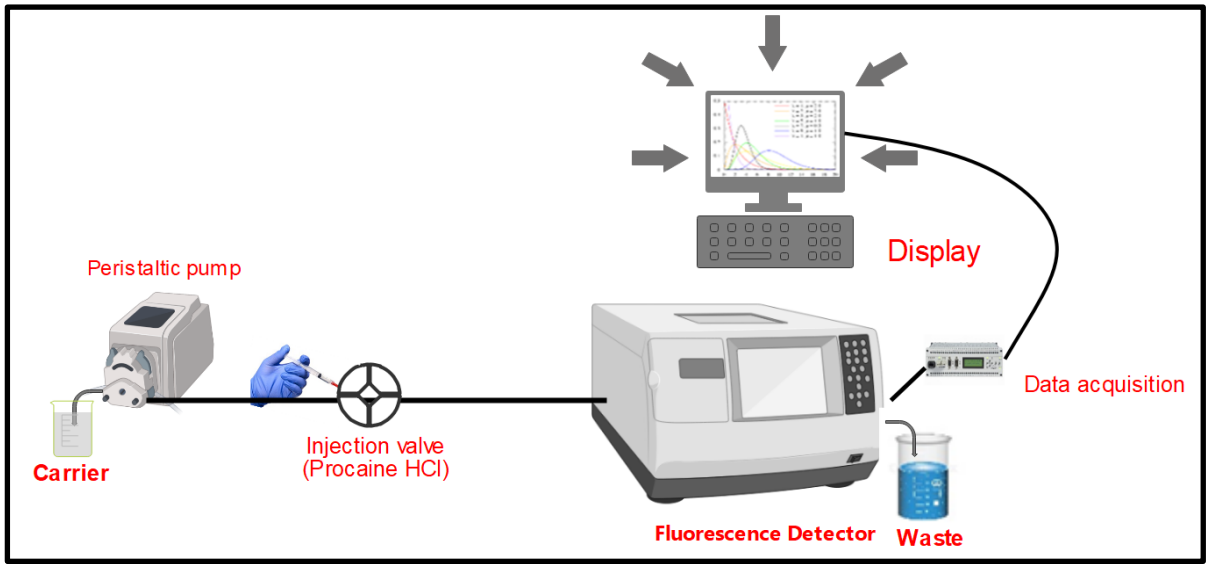

Scheme [3.7]: Design of Merging-Zone FIA with Fluorescence Detector

3.2.2.A.1.1. Determining the Maximum Ex and Em to Procaine HCl

A maximum emission of Procaine was scanned by using a fluorescence spectrophotometer. The fluorescence spectrum of Procaine showed a maximum excitation peak at 285 nm and a maximum emission peak at 362 nm, as shown in Figure [3.33] and Table [3.12].

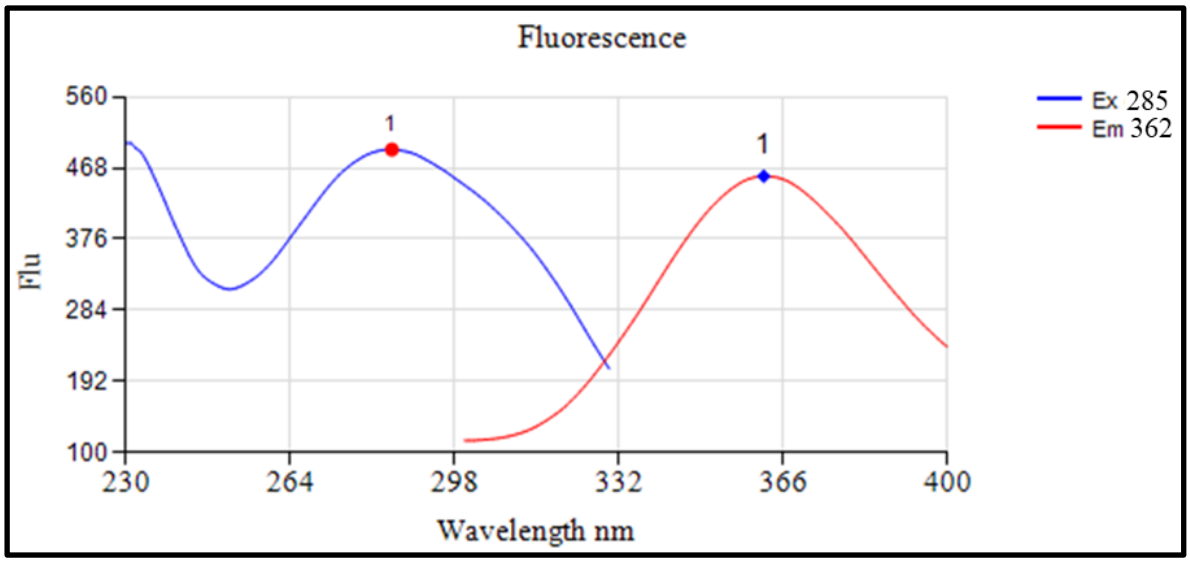

Figure [3.33]: Typical Scanning Fluorescence Spectrum for 300 ppm Procaine Standard of Excitation Spectral (blue line) and Emission Spectral Response (red line) Dissolved in Distilled Water

Table [3.12]: Result of Lambda Max

INDEX	Lembda	Ex
1	285	491.916

INDEX	Lembda	Em
1	362	457.393

3.2.2.A.1.2. The Influence of Flow Rate:

The effect of the flow rate and the selection of the optimum speed for the system interaction was studied. The results in Figure [3.34] show the effect of the pump speed on the response value (peak height) at the conditions mentioned below, as it is noted that the response decreases by increasing the pump speed from 1 to 5, and this matches the theoretical foundations of the effect of speed on response. The third speed, with a response rate of 112.106, is preferred over the fourth and fifth speeds for being the highest value. Also, the third speed is preferable to the slower speeds; although speeds 1 and 2 have the highest response than the third speed, the shape of the peak for those low speeds is broad and not ideal; either the form of the peak of the third speed, which has a flow rate of 1.5 ml per minute, is the best because it is sharp and uniform.

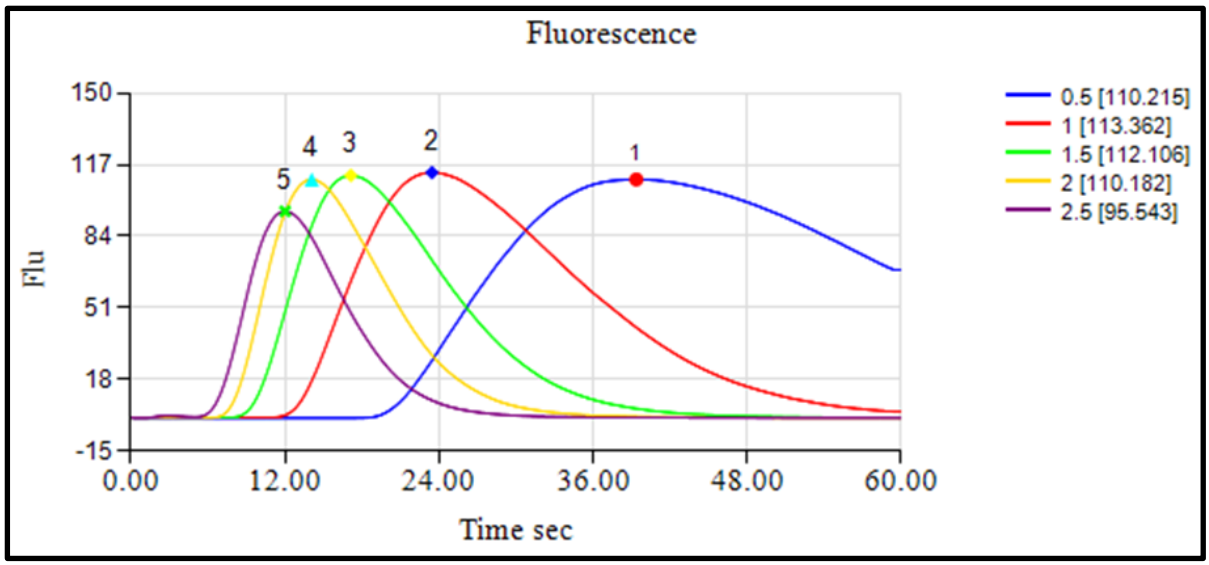

Figure [3.34]: Effect of Flow Rate on the Fluorescence Peak Height when, Procaine conc. = 70 ppm, reaction coil length = zero, at room temperature.

3.2.2.A.1.3. General Procedures and the Calibration Curve

Procaine was quantitatively determined, and the calibration curve was prepared at Ex 285 nm and Em 362 nm by preparing a series of Procaine solutions with different concentrations and analyzing each employing the FIA system. The fluorescence peak height value was plotted against the concentration. The suggested method allows for the determination of Procaine in the range of (1-100) ppm, as shown in Figures [3.35] and [3.36] and Table [3.13].

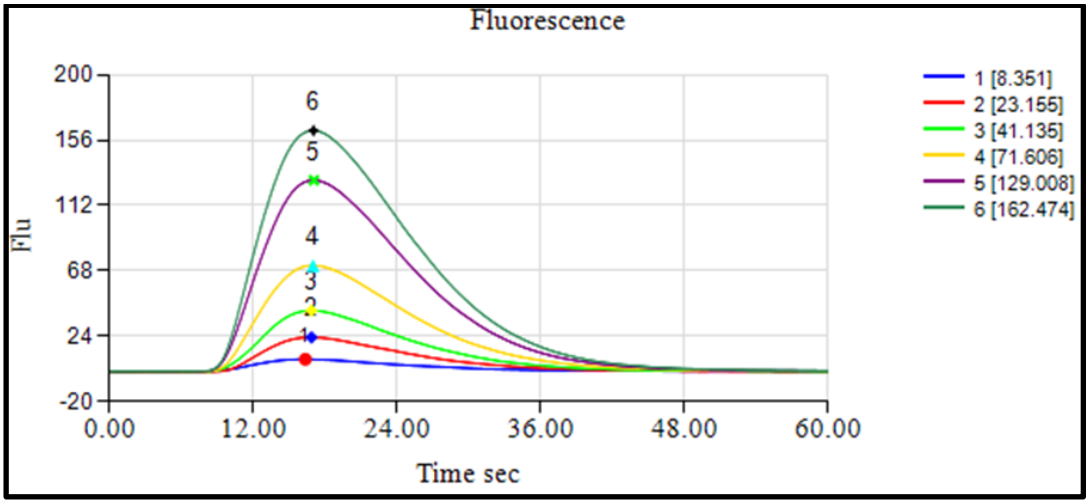

Figure [3.35]: Fluorescence Spectra of Procaine by Merging-Zone FIA

Table [3.13]: The Effect of Procaine conc. on the Fluorescence Peak Height when, flow rate = 1.5 mL/min, carrier = distilled water, reaction coil length = zero, at room temperature

Index	Sample	Procaine HCl ppm	Peak Height
1	1	1	8.351
2	2	5	23.155
3	3	10	41.135
4	4	50	71.606
5	5	75	129.008
6	6	100	162.474

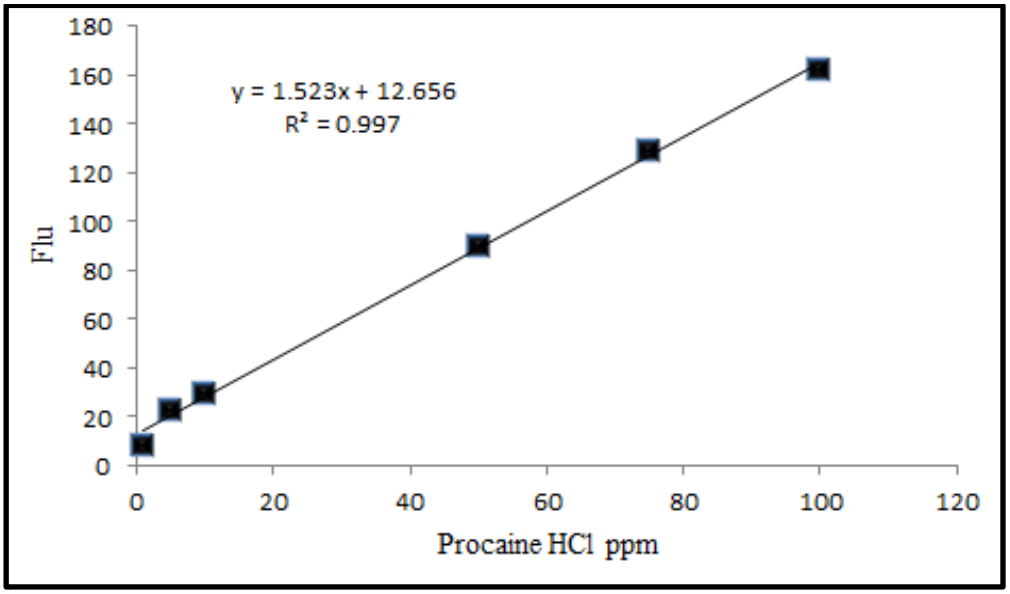

Figure [3.36]: Calibration Curve of Procaine

3.2.2.A.1.4. Repeatability

The relative standard deviation (RSD %) represents the precision of the proposed method has been studied utilizing 70 ppm of Procaine solution. At the optimum conditions, 4 replicate measurements were carried out for the determined concentration and recorded as shown in Figure [3.37] and Table [3.14]. The standard deviation value is equal to 2.378, and the relative standard deviation value is equal to 2.008, indicating the high precision of the suggested method.

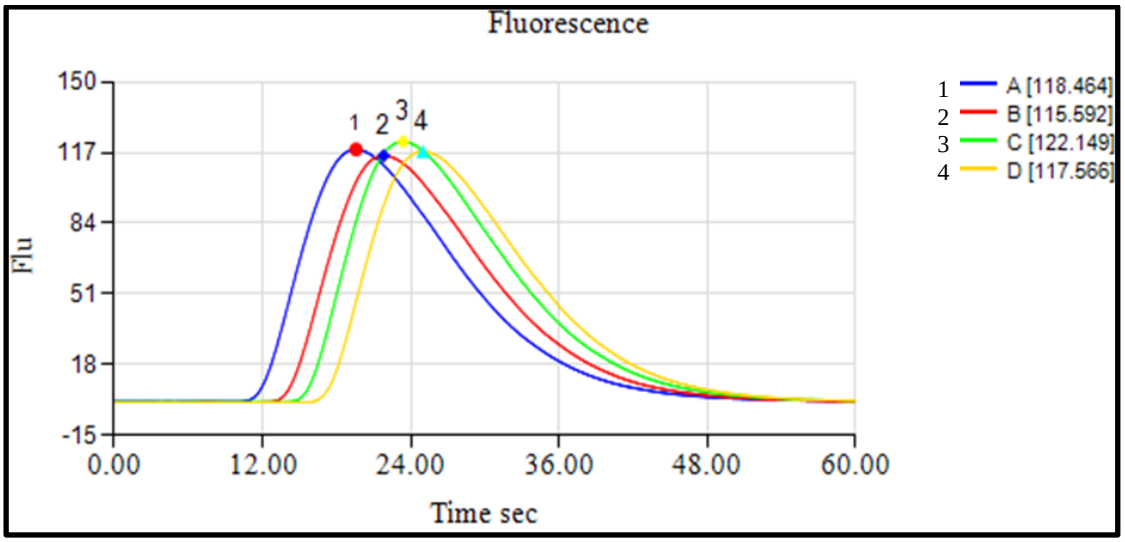

Figure [3.37]: Depicted the Repeatability of Procaine

Table [3.14]: Repeatability Results for 70 ppm Procaine Solution by Merging-Zone FIA

Sample No.	1	2	3	4	Mean	SD	RSD%
Flu.	118.464	115.592	122.149	117.566	118.443	2.378	2.008

3.2.2.A.1.5 The Determination of Dispersion

The dispersion coefficient (dilution factor D) was studied to illustrate the dispersion process extent within the flow injection system from the injection point at the valve to the detecting point at the detector. The dispersion coefficient can be calculated through Equation [1.1] and its equal 1.651.

The dispersion coefficient was studied by using one concentration of procaine solution within the calibration curve range (80 ppm). In the first step, the procaine solution was implemented inside the FIA system under the defined optimum conditions by measuring the peak height that represents the peak height with the dilution process (H max). In the second step, the procaine solution was implemented in a glass beaker and passed the solution through the system, then measuring the fluorescence peak height that takes the plateau shape with a constant height value with the time representing the peak height without the dilution process (H°). The obtained results are displayed in Figure [3.38].

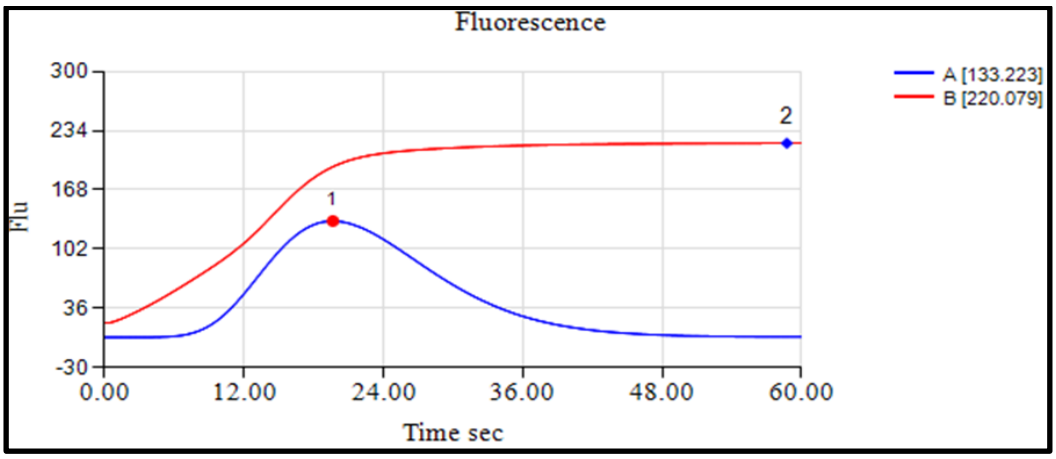

Figure [3.38]: Dispersion Coefficient Study Results for Procaine Determination Merging-Zone FIA

3.2.2.A.1.6. Application in Aqueous Solutions

Three aqueous solutions were prepared and considered solutions of unknown concentration; then, the fluorescence was measured according to the optimum conditions, as shown in Figure [3.39]. Then the solutions' concentration was determined by setting each solution's fluorescence on the straight line of the previous calibration curve, as shown in Figure [3.40] and Table [3.15]. The value of the resulting solutions from the calibration curve was very close to the prepared solutions, considering the preparation errors.

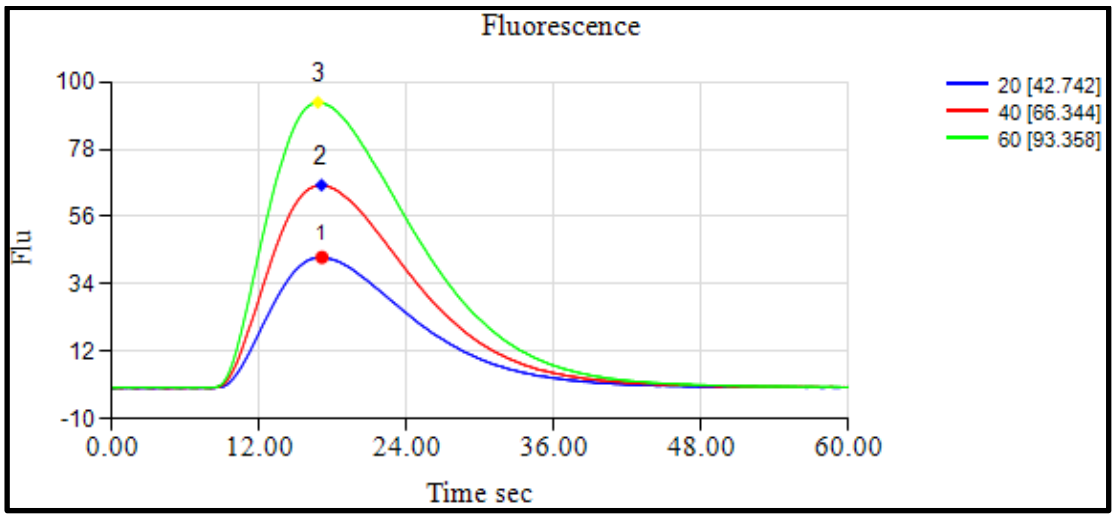

Figure [3.39]: The Spectrum of Possible Applications

Table [3.15]: Value of Sample Application

Index	Sample (taken)	Procaine (founded)	Peak Height	Recovery
1	20	20	42.742	100
2	40	36.5	66.344	91
3	60	54.6	93.358	91

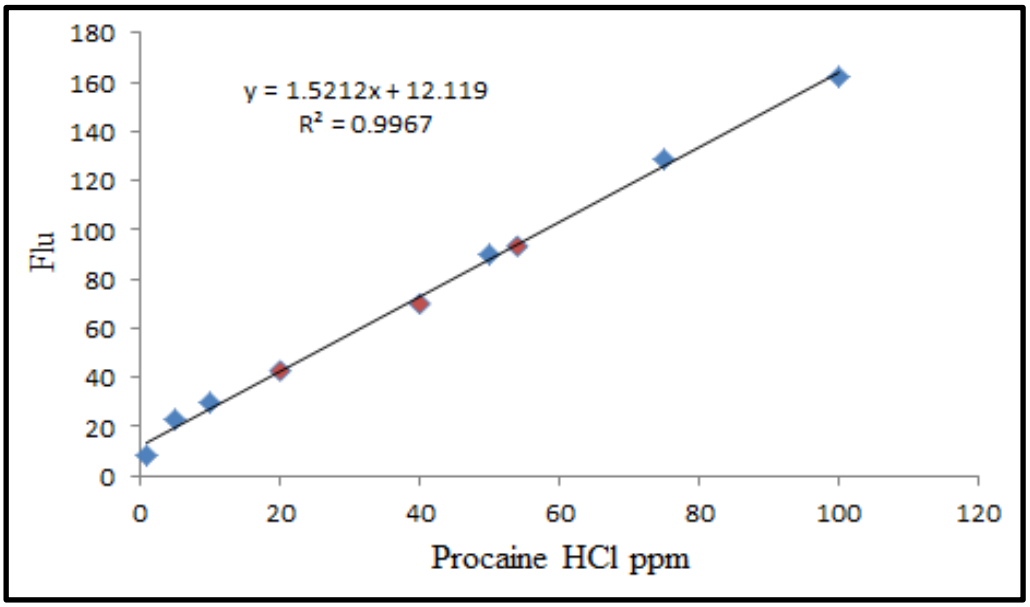

Figure [3.40]: Determination of Unknown Aqueous Solutions

3.2.2.A.2. Spectrofluorometric Method to Determine NQS by Merging-Zone FIA

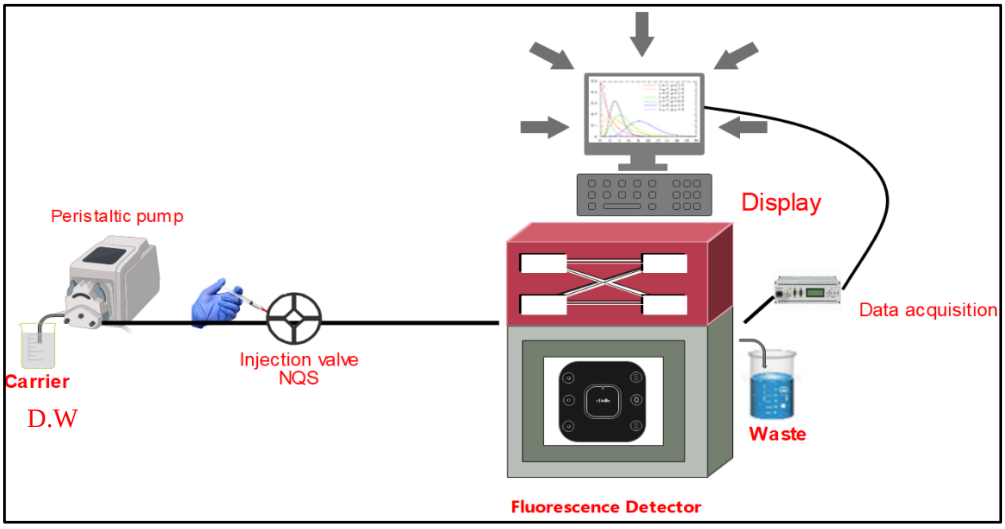

Scheme [3.8]: Design of Merging-Zone FI Unit with Fluorescence Detector

3.2.2.A.2.1. Determining the Maximum Ex and Em to NQS

A maximum emission of NQS was scanned using a fluorescence spectrophotometer. The fluorescence spectrum of NQS showed a maximum excitation peak at 469 nm and a maximum emission peak at 543 nm, as shown in Figure [3.41] and Table [3.16].

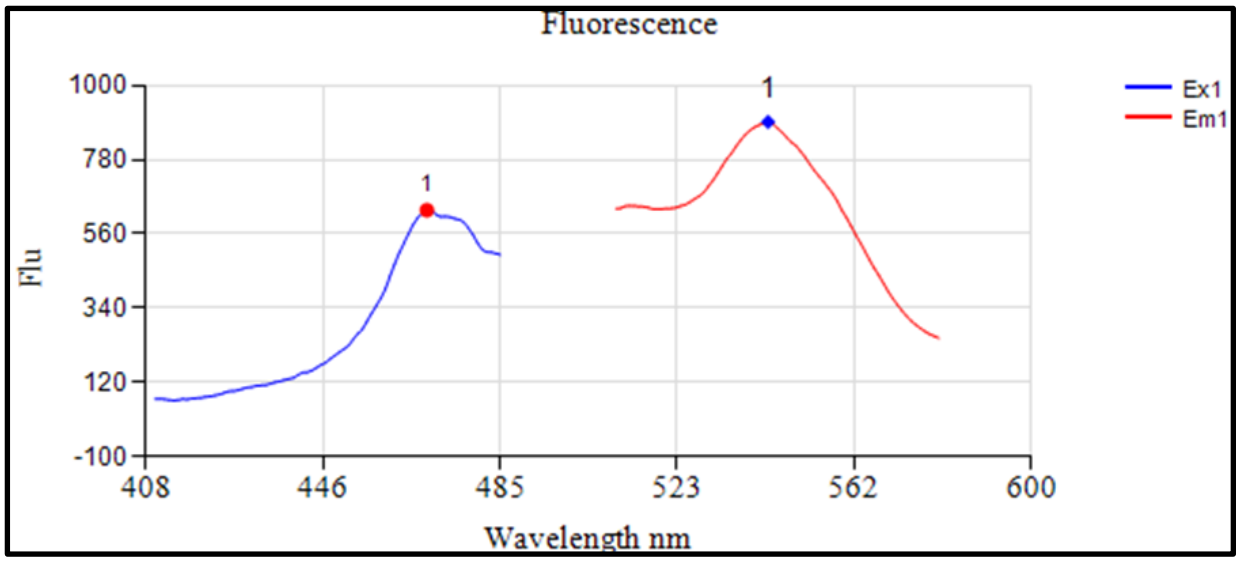

Figure [3.41]: Typical Scanning Fluorescence Spectrum for 80 ppm NQS Standard of Excitation Spectral (blue line) and Emission Spectral Response (red line) Dissolved in Distilled Water

Table [3.16]: Result of Lambda Max

Lembda	Ex1	Lembda	Em1
469	630.21	543	892.058

3.2.2.A.2.2. General Procedures and the Calibration Curve

NQS was quantitatively determined, and the calibration curve was prepared at Ex 469 nm and Em 543 nm by preparing a series of NQS solutions with different concentrations and analyzing each employing the FIA system. The fluorescence peak height value was plotted against the concentration Figure [3.42]. The suggested method allows for the determination of NQS in the range of (5-50) ppm, as shown in Table [3.17] and Figure [3.43].

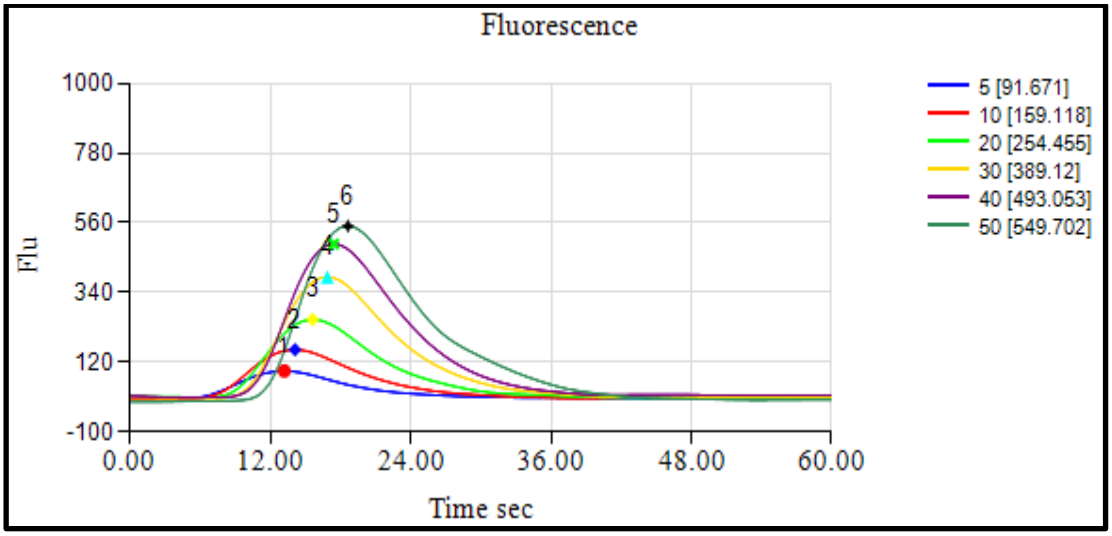

Fig. [3.42]: Fluorescence Spectra of NQS by Merging-Zone FIA

Table [3.17]: The Effect of NQS conc. on the Fluorescence Peak Height when, flow rate = 1.5 mL/min, carrier = distilled water, reaction coil length = zero, at room temperature

Index	Sample	test ppm	Peak Height
1	1	5	91.671
2	2	10	159.118
3	3	20	254.455
4	4	30	389.12
5	5	40	493.053
6	6	50	549.702

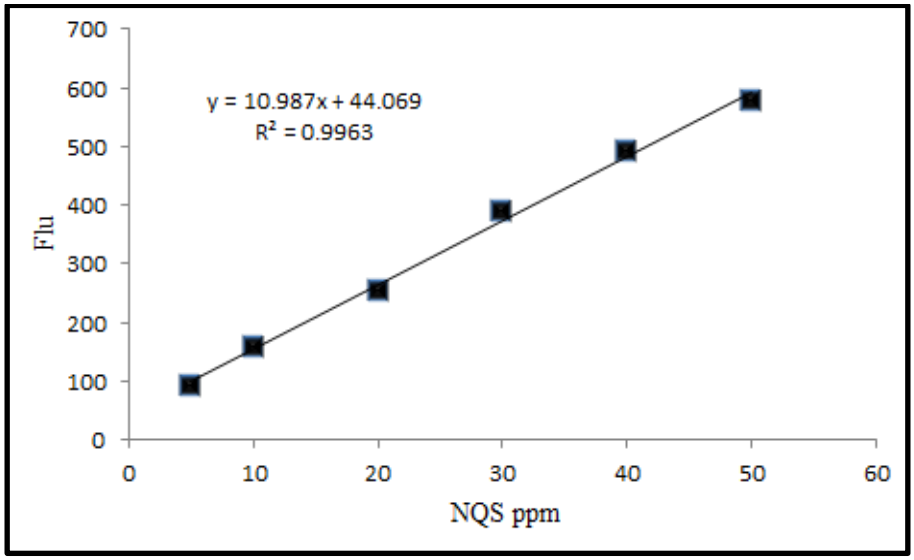

Figure [3.43]: Calibration Curve of NQS

3.2.2.A.2.3. Repeatability

The relative standard deviation (RSD %) representing the precision of the proposed method has been studied utilizing 30 ppm of NQS solution. At the optimum conditions, 6 replicate measurements were carried out for the determined concentration and recorded as shown in Figure [3.44] and Table [3.18]. The standard deviation value is equal to 7.862, and the relative standard deviation value is equal to 1.941, indicating the high precision of the suggested method.

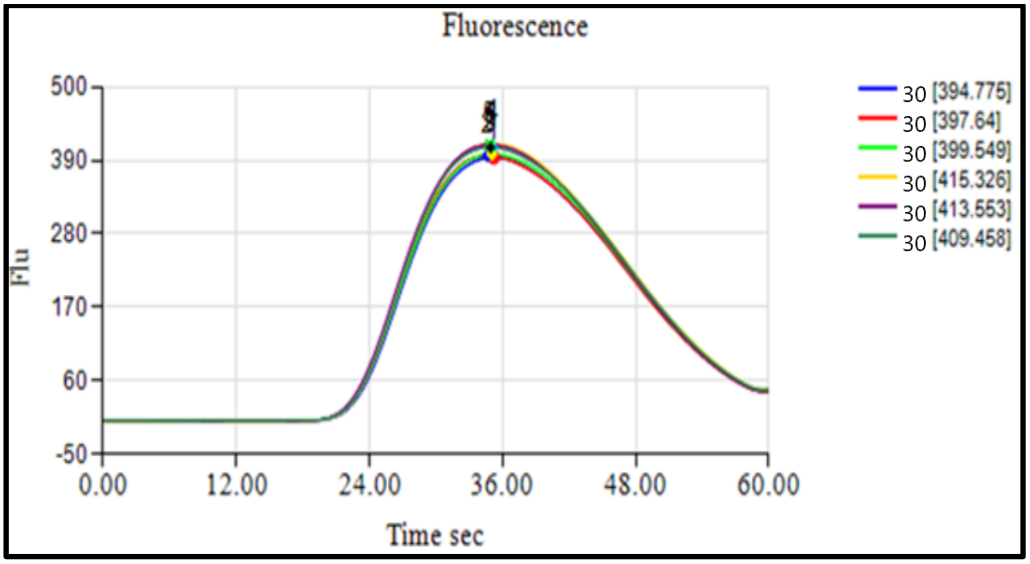

Figure [3.44]: Repeatability of 30 ppm for NQS Solution by Merging-Zone FIA

Table [3.18]: Repeatability Results for 30 ppm NQS Solution by Merging-Zone FIA

Sample No.	1	2	3	4	5	6	Mean	SD	RSD%
Flu.	395	398	400	415	414	409	405	7.862	1.941

3.2.2.A.2.4. Application in aqueous solutions

Three aqueous solutions were prepared and considered solutions of unknown concentration; then, the fluorescence was measured according to the optimum conditions, as shown in Figure [3.45]. Then the solutions' concentration was determined by setting each solution's fluorescence on the straight line of the previous calibration curve, as shown in Figure [3.46] and Table [3.19]. The value of the resulting solutions from the calibration curve was very close to the prepared solutions, considering the preparation errors.

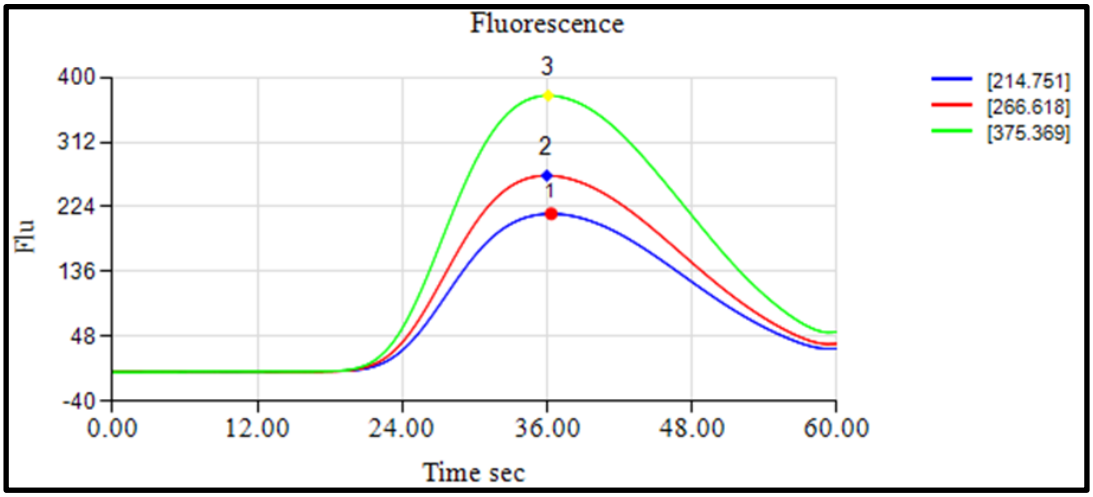

Figure [3.45]: The Spectrum of Possible Applications

Table [3.19]: Value of Sample Application

Index	Sample (taken)ppm	NQS (founded)ppm	Peak Height	Recovery
1	15	15.34	214.751	102
2	20	20.987	266.618	104
3	30	30.03	375.369	100

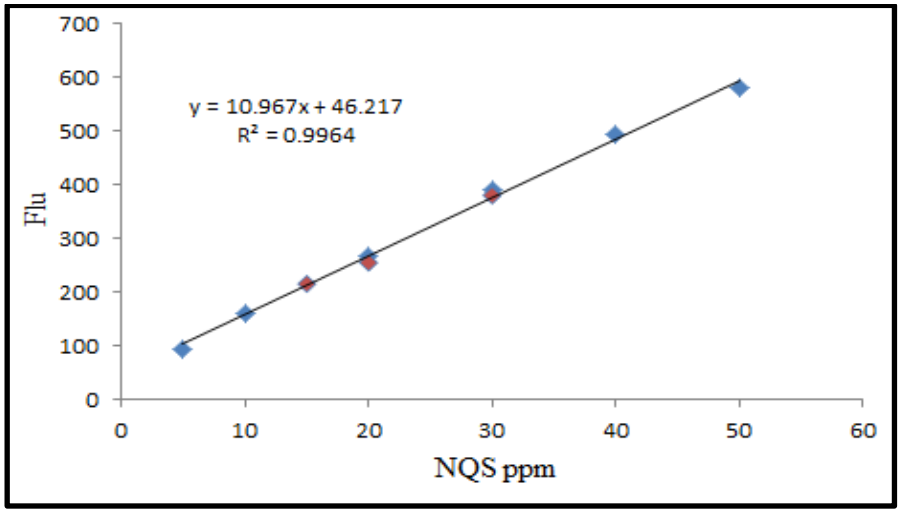

Figure [3.46]: Determination of Unknown Aqueous Solutions

3.2.2.B.1. Batch Spectrofluorometric Method to Determine MA in Terms of NQS

3.2.2.B.1.1. Determining the Maximum Ex &Em to NQS

A maximum emission of 100 ppm NQS was scanned using a fluorescence spectrophotometer. The fluorescence spectrum of NQS showed a maximum emission peak at 477.42 nm, as shown in Figure [3.47].

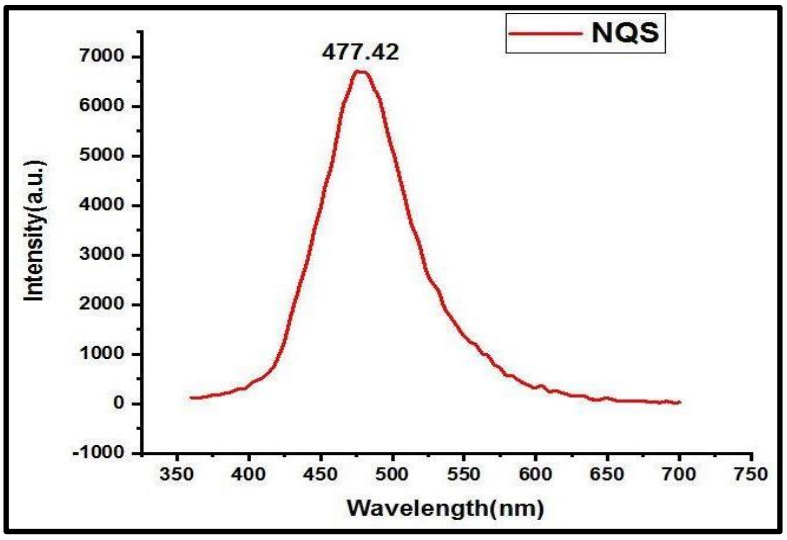

Figure [3.47]: A Maximum Fluorescence Emission Spectrum of NQS

3.2.2.B.1.2. General Procedures and the Calibration Curve

MA was quantitatively determined, and the calibration curve was prepared at Em 477 nm by preparing a series of MA solutions with different

concentrations and analyzing each after mixing with base and reagent. The fluorescence peak height value was plotted against the concentration Figure [3.48]. The suggested method allows for the determination of MA in the range of (1-100) ppm, as shown in Table [3.20] and Figure [3.49].

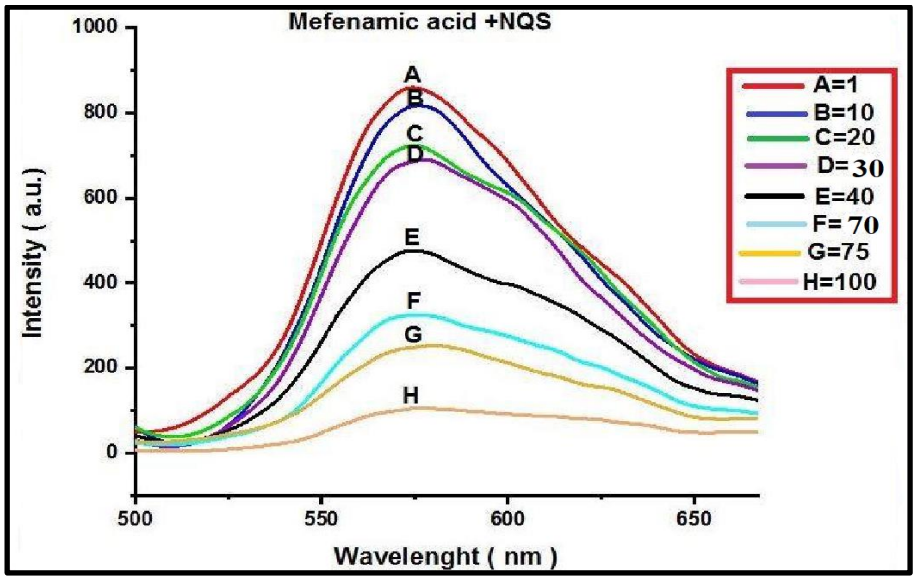

Figure [3.48]: Fluorescence Spectra of MA in Terms of NQS

Table [3.20]: The Effect of MA Conc. on the Fluorescence Peak Height when, NQS conc. = 50 ppm, volume of alkaline medium = 0.1 mL of 0.2 M from NaOH, at room temperature

Index	MA concentration(ppm)	Peak Hight
A	1	880
B	10	805
C	20	730
D	25	690
E	40	590
F	70	330
G	75	290
H	100	90

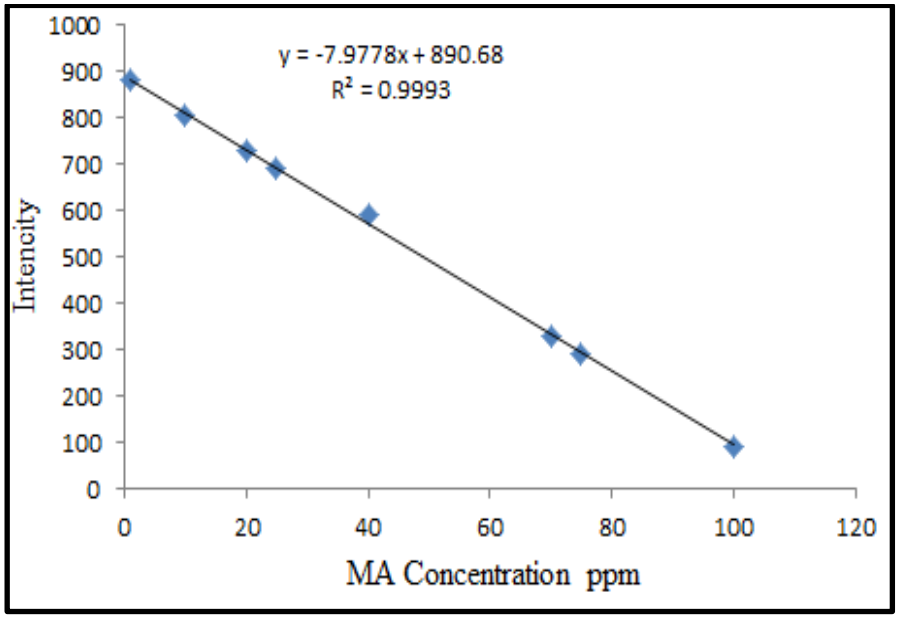

Figure [3.49]: Calibration Curve of MA

3.2.2.B.1.3. Application in aqueous solutions

Three aqueous solutions were prepared and considered solutions of unknown concentration; then, the fluorescence was measured according to the optimum conditions, then the solutions' concentration was determined by setting each solution's fluorescence on the straight line of the previous calibration curve, as shown in Table [3.21] and Figure [3.50]. The value of the resulting solutions from the calibration curve was very close to the prepared solutions, considering the preparation errors.

Table [3.21]: Value of Sample Application

Index	Sample (taken)ppm	MA (founded)ppm	Peak Height	Recovery
1	35	33.4	600	103
2	40	40.9	590.7	101
3	75	77.5	290.41	99

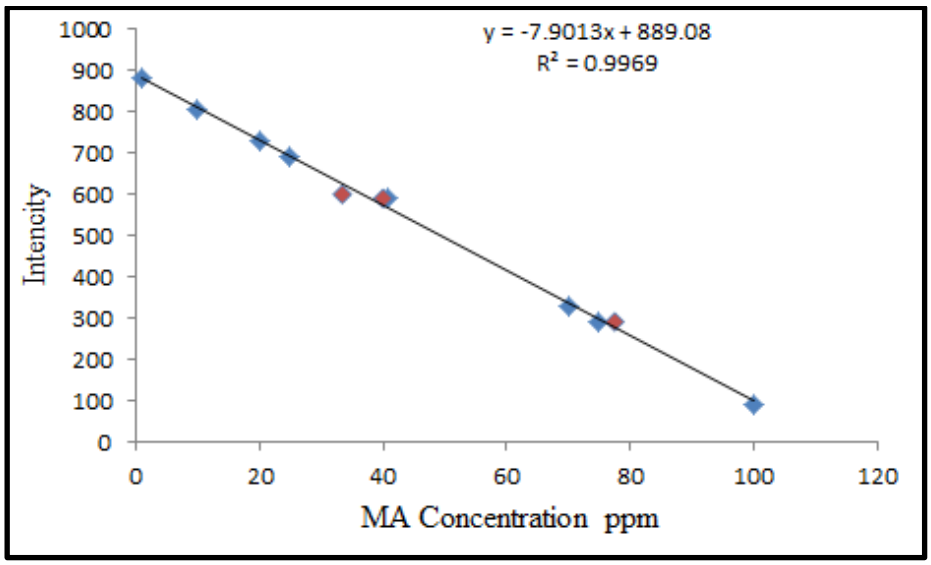

Figure [3.50]: Determination of Unknown Aqueous Solutions

3.2.2.B.2. Batch Spectrofluorometric Method to Determine MA

3.2.2.B.2.1. Determine the Maximum Em of MA

A maximum emission of 100 ppm MA was scanned using a fluorescence spectrophotometer. The fluorescence spectrum of MA showed a maximum emission peak at 295.2 nm, as shown in Figure [3.51].

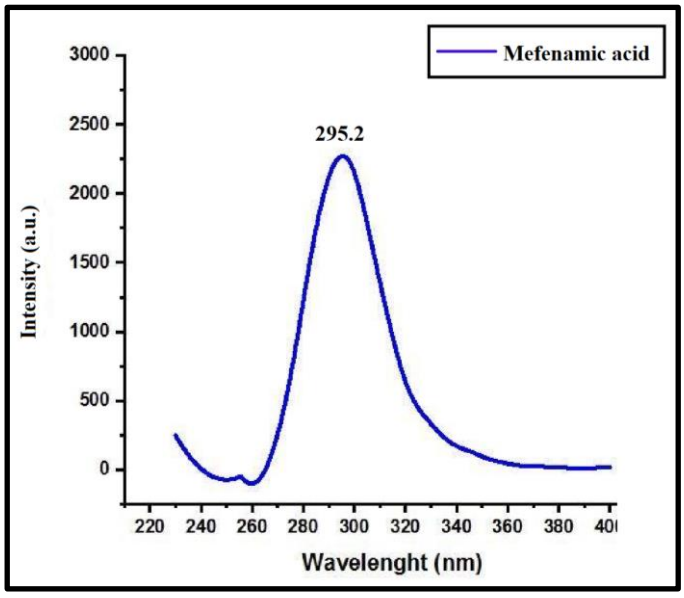

Figure [3.51]: A Maximum Fluorescence Emission Spectrum of MA

3.2.2.B.2.2. General Procedures and the Calibration Curve

MA was quantitatively determined, and the calibration curve was prepared at Em 295.2 nm by preparing a series of MA solutions with different concentrations and analyzing each. The fluorescence peak height value was plotted against the concentration Figure [3.52]. The suggested method allows for the determination of MA in the range of (1-100) ppm, as shown in Table [3.22] and Figure [3.53].

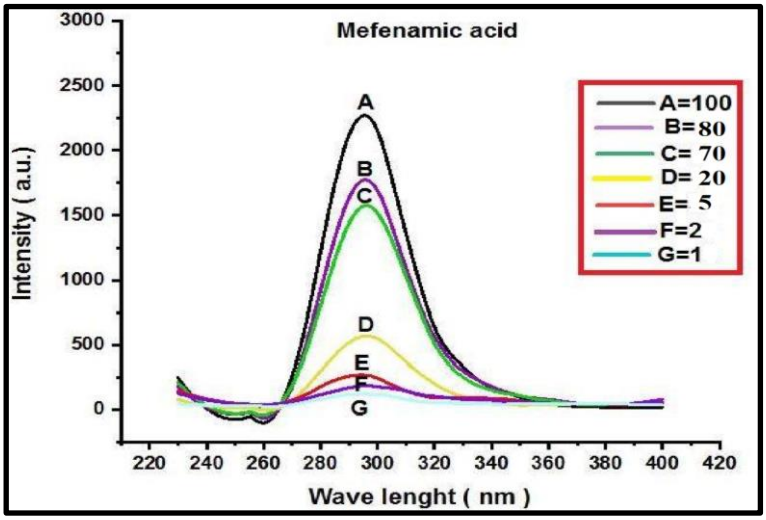

Figure [3.52]: Fluorescence Spectra of MA

Table [3.22]: The Effect of MA Conc. on the Fluorescence Peak Height at room temperature

Index	MA concentration(ppm)	Peak Height
G	1	130
F	2	195
E	5	250
D	20	600
C	70	1600
B	80	1800
A	100	2300

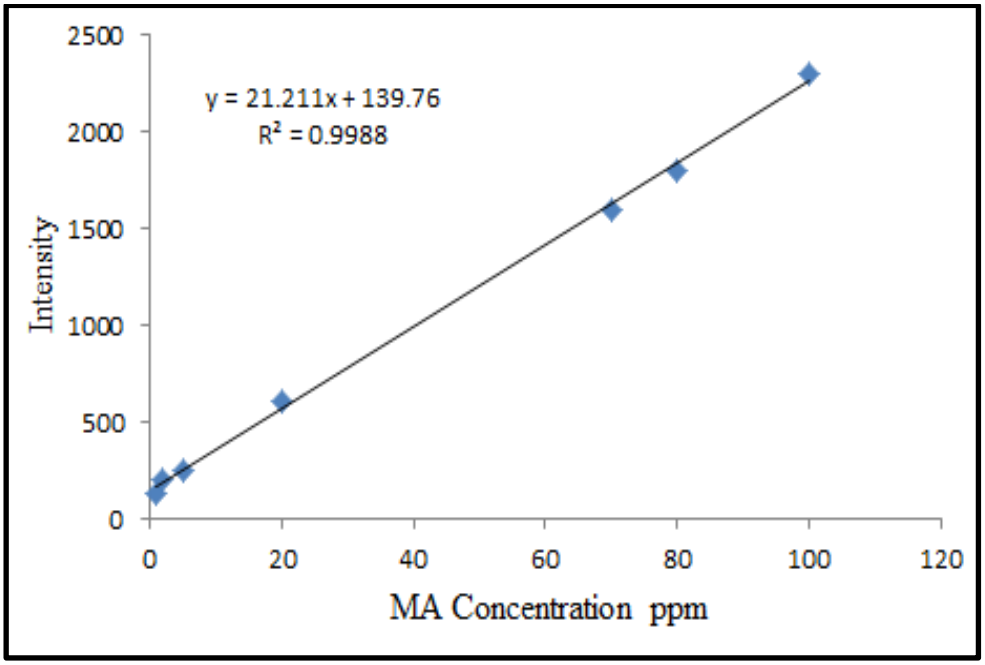

Figure [3.53]: Calibration Curve of MA

3.2.2.B.2.3. Application in aqueous solutions

Three aqueous solutions were prepared and considered solutions of unknown concentration; then, the fluorescence was measured according to the optimum conditions, then the solutions' concentration was determined by setting each solution's fluorescence on the straight line of the previous calibration curve, as shown in Table [3.23] and Figure [3.54]. The value of the resulting solutions from the calibration curve was very close to the prepared solutions, considering the preparation errors.

Table [3.23]: Value of Sample Application

Index	Sample (taken)ppm	MA (founded)ppm	Peak Height	Recovery
1	35	33.4	850.89	95
2	55	40.9	1255.42	98
3	90	77.5	2051.6	101

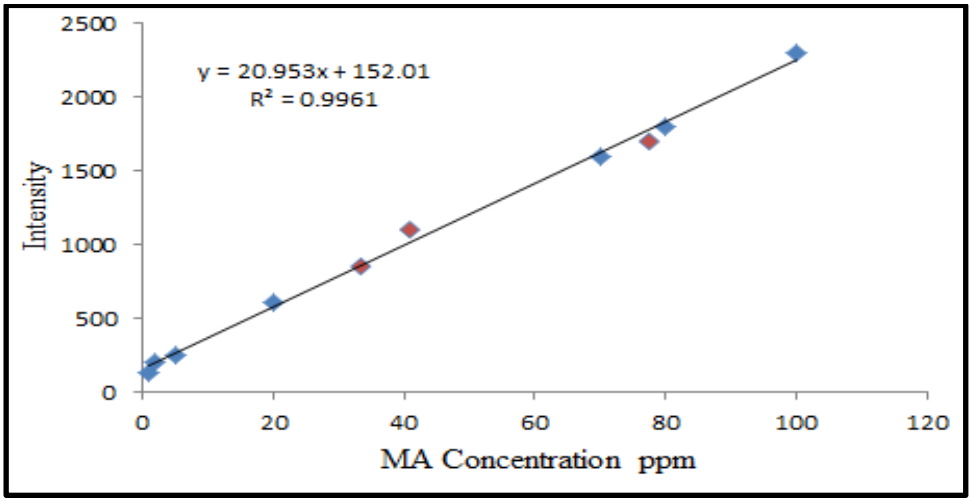

Figure [3.54]: Determination of Unknown Aqueous Solutions

3.3 results of the research and their comparison with previous studies

Table [3.24]: The results of this research

	Method	Reagent	Rang ppm	R^2	Slop	RSD%	Recovery	λ_{max}
Mefenamic acid	Merging zone - FIA	NQS	1-20	0.9999	0.012	1.237	99.5-101.8	477
	Reverse -FIA	NQS	1-30	0.9869	0.007	0.586	99.6-109	477
	Batch	NQS	0.5-10	0.9997	0.0912	0.072	102-110	477
	Fluorescence (Batch)	NQS	1-100	0.9993	7.997	—	99-103	Em(NQS) 477.42
	Fluorescence (Batch) Direct	—	1-100	0.9988	21.211	—	95-101	Em(MA) 295.2
Procaine HCl	Fluorescence + Merging FIA	NQS	1-100	0.9986	1.519	2	91-100	Em(NQS) 362
NQS	Fluorescence + Merging FIA	NQS	5-50	0.9976	10.961	1.941	100-104	Em 573

From the Table [3.24] we note that the MA determination methods have certain properties that are characterized by their range, RSD%, and R. In general, flow injection methods are characterized by low sample size and modeling speed while fluorescence methods are characterized by a wide range.

The RSD%, sensitivity and range of the both merging zone and reverse methods are better than those found in the literature [72, 73, 75-79]in the MA's determination.

As for the determination of procaine, the method is better in terms of range, RSD% and sensitivity compared to [86, 88, 89, 91, 94, 95].

3.4. Conclusions:

1. Amino drugs and reagents under study can be determined using the spectral methods, which can be combined with the flow injection technique. The study has shown that all systems designed are highly efficient.
2. The determination of MA, Procaine and the reagent (NQS) in the flow injection unit is characterized by the rate in analysis and high sensitivity in determination and wide range of concentrations, which is one of the preferred advantages in analytical chemistry.
3. The flow injection system is characterized by not consuming chemicals in large quantities, as it is characterized by the use of tiny volumes and low concentrations of both the reagent and the carrier solution mixture, as well as the small sample size
4. Other benefits of the new systems were high selectivity and recovery, good repeatability, fair relative standard deviation values, high sampling rate, good precision and accuracy, and dead volume equal to zero.
5. The linearity range of the calibration graph is different with the difference in the flow injection or batch system for the same reaction.
6. The proposed methods were applied to determine MA, Procaine, and NQS from aqueous solutions.
7. The fluorescence estimation method is characterized by its wide range and high sensitivity
8. Both NQS and MA reagents were determined by fluorescence using aqueous solutions without needing expensive reagents.

3.5. Recommendations

1-Determining other amino drugs using this technique

2-By FIA methods, other reagents can be identified

3-It is possible to use the UV area directly to identify amino drugs through these systems

4-Linking these techniques to HPLC technology and estimating amino drugs through it

5-Through the results, fluorescence can be linked to the flow injection to determine the amino drugs and organic reagents capable of interacting with primary and secondary amines.

Chapter One

Introduction and Literature Review

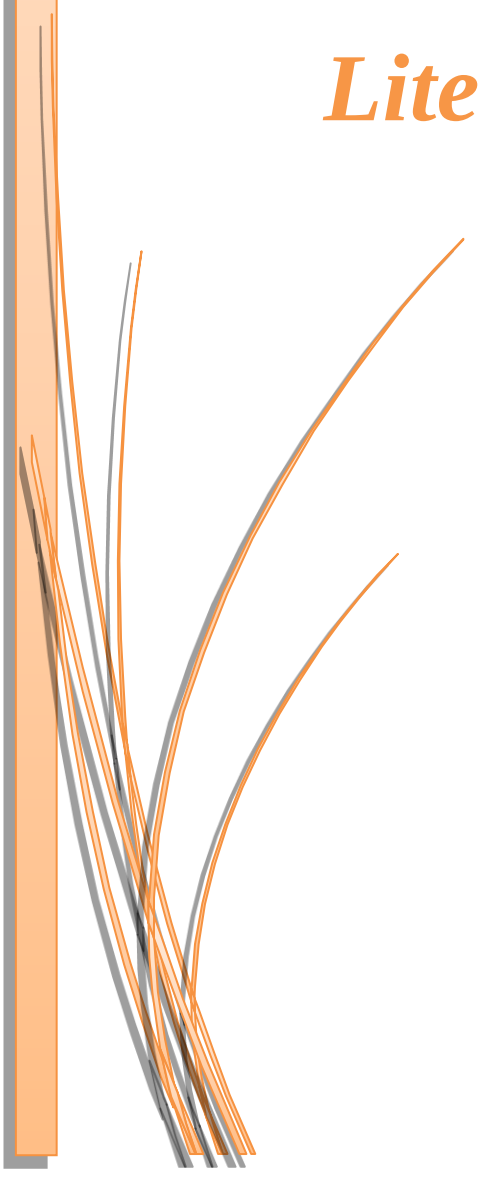

1. Introduction

1.1 Flow Analysis

Flow examination refers to the common name for all investigative techniques that rely on introducing a sample into a flowing liquid, it is referred to as the carrier stream through aspiration or injection into the medium [1].

Flow analysis can be divided into two categories based on two fundamental ideas [2]. It is possible to divide samples into two categories: those introduced continuously and those presented discretely, and those raised in a segmented or an unsegmented manner depending on the flowing media [3-5], as illustrated in Figure [1.1].

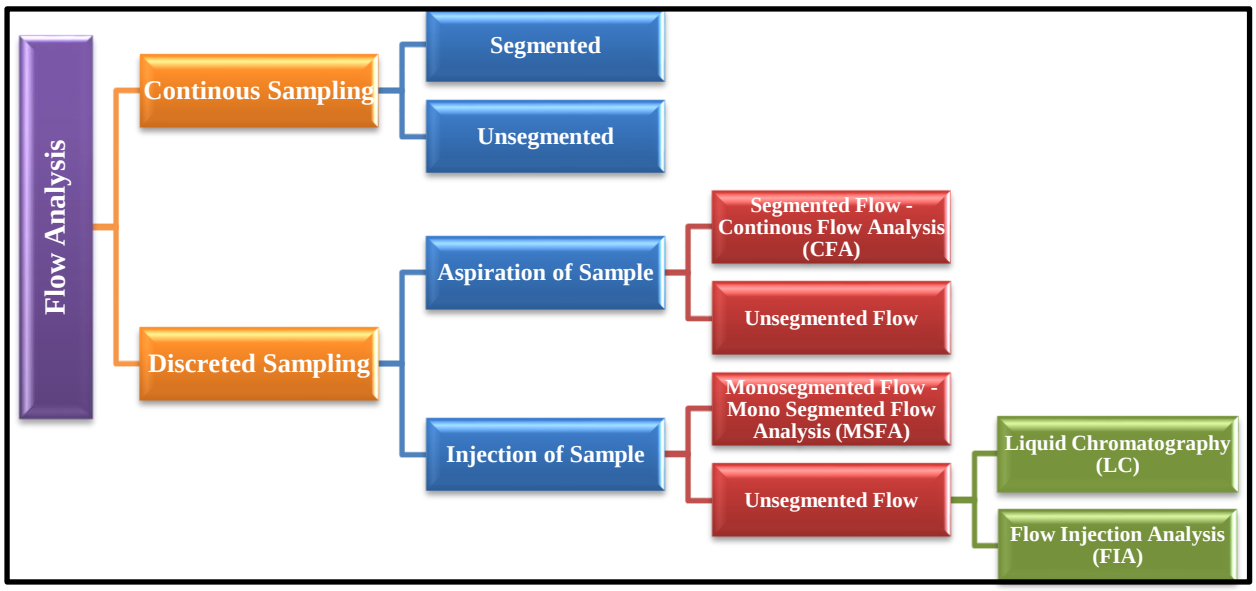

Figure [1.1]: Organization of flow analysis techniques by IUPAC guidelines

The applications of this technique include pharmaceutical analyses [6, 7], insecticide screenings [8, 9], cosmetics evaluations [10-12], and more. In flow injection analysis, many distinct advantages set it apart. These advantages are:

1. They convert open-system reactions (open cups) to closed-system responses.
2. It can reduce the analysis time by substituting mechanical processes instead of manual ones, such as mixing and separating, as it can quickly model at 120 analyzes per hour.
3. Its modern devices are characterized by being small in size.
4. The devices have a speedy response, as the time is between 5 and 200 seconds.
5. The injected sample volume is between 10 and 200 microliters and is not a consuming material. This technique does not require more than half a milliliter of the reagent solution at each analysis.
6. Personal errors are minimal compared to other techniques.
7. This technique appears in high congruence and repetition in the readings.
8. FA is combined with other analytical methods.

1.1.1 Beginnings of Flow Injection Analysis

Even though flow analysis has been around since the 1940s, it is still relatively new. In 1957, Skeggs' seminal work presented the general technique of segmented continuous flow analysis (SCFA) through air-segmented streams, which was later combined with other detection procedures such as redox potential, pH, turbidity, and spectrophotometric absorbance of radiation, as well as the elimination of the sampling stage of the analyzed material [3, 13-15]. These advancements laid the groundwork for the introduction of flow analysis in 2000 . This technique restricts sample longitudinal dispersion along the flow stream, which minimizes sample contact and allows for a more extended residence period of the sample, hence boosting sensitivity and allowing for comparatively slow reactions. However, any air bubbles injected into the liquid stream must be eliminated

before the test[16]. To avoid detection errors, aspirating the bubbles before detection is usual, as shown in Figure [1.2].

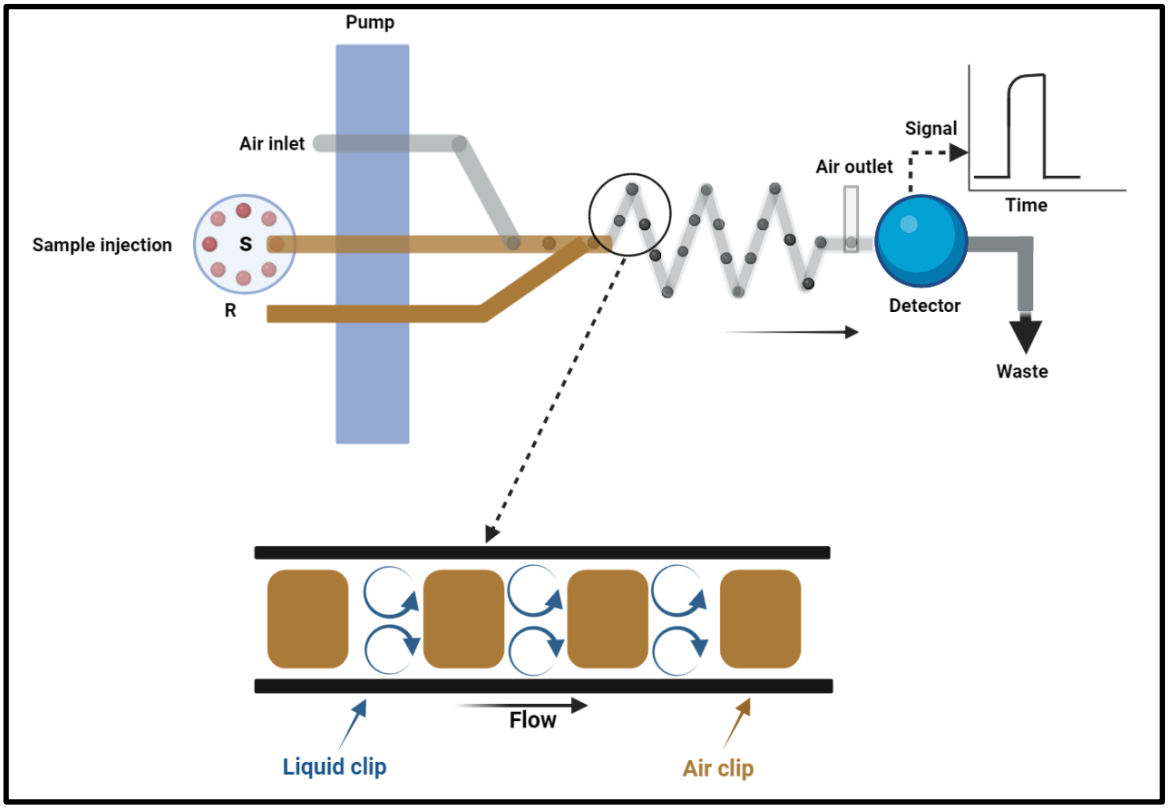

Figure [1.2]: The parts of the SFA analyzer and its mechanics

There are many disadvantages that have been identified from the use of this technique. These are:

1. It isn't easy to control the size of air bubbles.
2. The flow is irregular due to air pressure and rough paths of bubbles.
3. Emptying the air bubbles is required before they reach the cell.
4. The difficulty of completely controlling the movement of the carrier current.
5. The bubble analysis device is large and complex.

In the literature, it is noted that the new idea of continuous flow analysis was simultaneously patented in 1975 by Ruzicka and Hansen in Denmark and Stewart in the United States [4].

A continuous flow injection analysis (CFIA) manifold injects a liquid sample into a non-segmented continuous carrier stream of a suitable liquid using a (CFIA) manifold. This equipment is simple, affordable, and has a high sample rate and dependability while still being easy to use. The residence time of the model in a non-segmented stream is much less than the residence time in an air-segmented system. Following that, several other highly competitive flow injection instruments were created and deployed to various applications in the following years.

The FIA device, which has a column as part of its design, appears superficially to be the HPLC device, with the likeness and convergence in flow velocity and size being preserved in the rest of the device (pump, valve, detector, and recorder) as shown in Figure [1.3]. Because the fluid in HPLC requires a strong thrust force through the column material, the pressure in HPLC is 70 atmospheres, whereas, in FIA, it is 0.5 atmospheres, as a simple peristaltic pump (i.e., a pump with no valves) is used. While these techniques have different purposes, the most significant difference is their focus. FIA is meant to find the most important number of samples with the fewest reagents and sample solutions, while HPLC is about separating and estimating several components in one model.

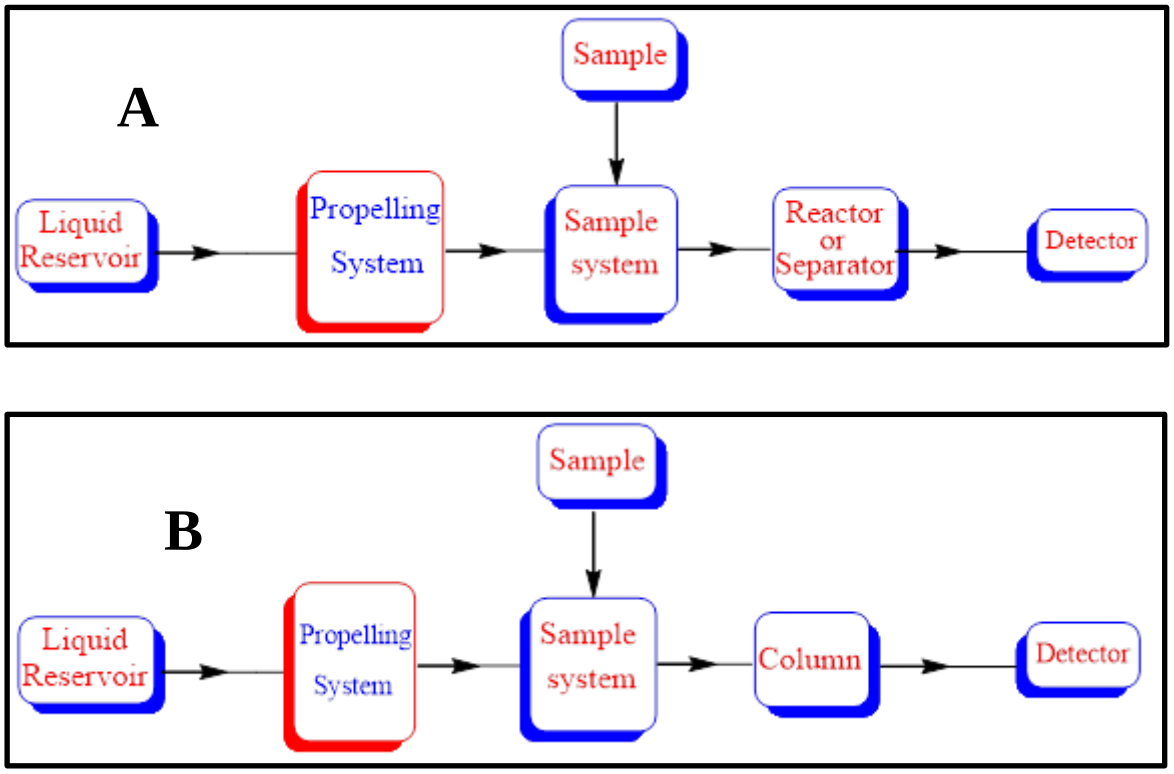

Figure [1.3]: Similarity between (A) FIA. and (B) HPLC.

1.1.2 Technical Modes of Flow Injection Analysis

1.1.2.1 Merging Zones Technique

Bergamin and colleagues were the first to propose merging zones in 1978 . In this way, the problem of continuous flow injection instruments was avoided, which used the reagent endlessly even when there was no sample to analyze. Even though volumes at the CFIA do not exceed a few hundred microliters, the merging zones technique resulted in considerable cost savings, and notably for expensive chemicals such as phenol. This method must inject each sample and reagent separately into the carrier stream, which is accomplished using a twofold injection valve. As a result, the sample-reagent zone is produced, and the sample is then transferred to the detector for analysis[17], as shown in Figure [1.4].

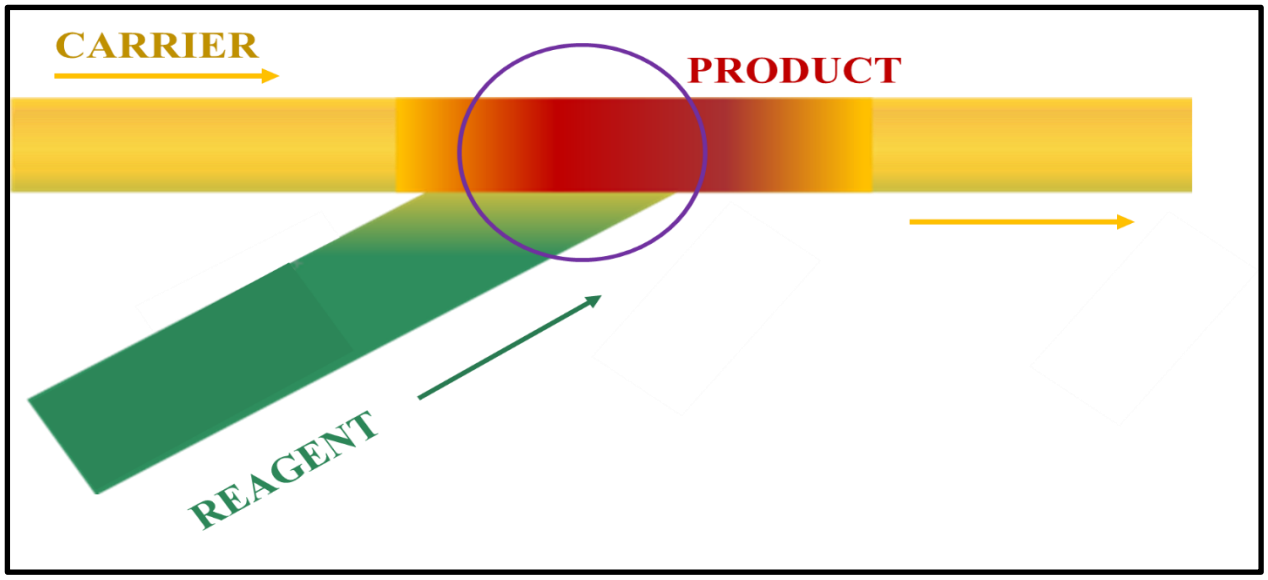

Figure [1.4]: Merging zone technique

1.1.2.2 Stop-Flow Injection Analysis

In 1979, Ruzicka and Hansen proposed stop-flow injection analysis (SFIA) to detect glucose and urea levels in blood serum samples . The injection process is identical to that used in FIA, except that when the sample/reagent zone reaches the flow cell, the carrier stream is terminated, and the flow cell is closed. Selecting and regulating the stopping time improves sensitivity while simultaneously reducing dispersion by extending the residence time of slow reactions without increasing the length of the reaction coil. The waste generation, enabling kinetic studies across a wide range of concentrations and wavelengths, reducing reagent use and waste generation, and enabling kinetic studies across a wide range of concentrations and wavelengths[18], as shown in Figure [1.5].

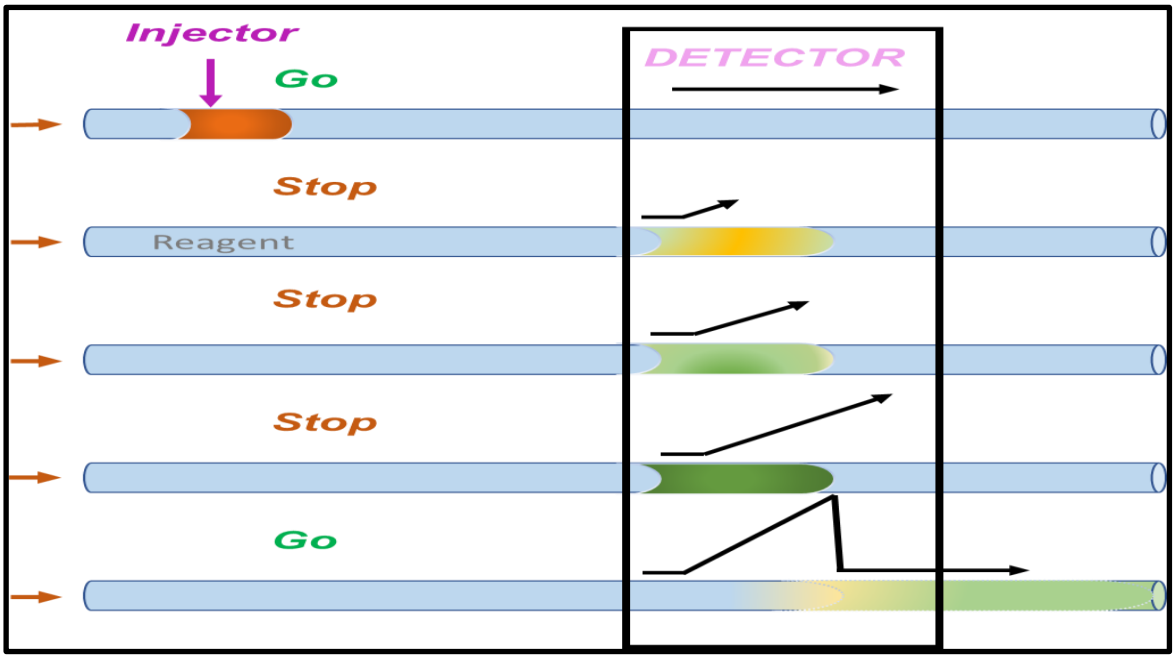

Figure [1.5]: Stop Flow Injection Analysis

1.1.2.3 Reversed Flow Injection Analysis

Johnson and Petty first proposed this technique in 1982 as an early attempt to detect the amount of phosphate in seawater by injecting the reagent into the water . rFIA was utilized, which is a reversed FIA technique. The sample was pumped continuously rather than through a carrier, and a premixed reagent was injected instead of a page; this is partly because dispersion in rFIA is lower than in traditional FIA, which reduces the diluting impact and increases insensitivity[19].

When the reagents used are expensive, and the model is cheap and available in large quantities, it is preferable to reverse the injection process. In rFIA, the reagent solution is injected into the sample solution, as the latter becomes the conductive current. This technology is characterized by being economical because the used detector is small. Still, this technology is flawed as it consumes the sample solution. The valves need a cleaning process at each

analysis, which causes time consumption and reduces the number of analyzed samples.

1.1.2.4 Mono-segmented Flow Analysis

To increase the sample rate and sensitivity of continuous flow measurements, Pasquini and de Oliviera developed mono-segmented continuous flow analysis (MCFA) or (MSFA) in 1985 . The sample zone must be injected between two bubbles of air or inert gas to prevent it from being scattered by the carrier solution. In the absence of chemical reaction or sufficient residence time for the response to approach equilibrium without axial dispersion between the sample/reagent zone and carrier, this technique provides measurements that can be made without interference [20].

1.1.2.5 Sequential Injection Analysis

Ruzicka and Marshall introduced sequential injection analysis in 1990 by publishing the first description (SIA) . The SIA technique is based on the sequential sample injection and reagent into a holding coil and toward the pump via a selection valve. After that, the flow is reversed to propel the piece and reagent-distributed zones through the reaction coil and detector before being changed again [21], as shown in Figures [1.6] and [1.7].

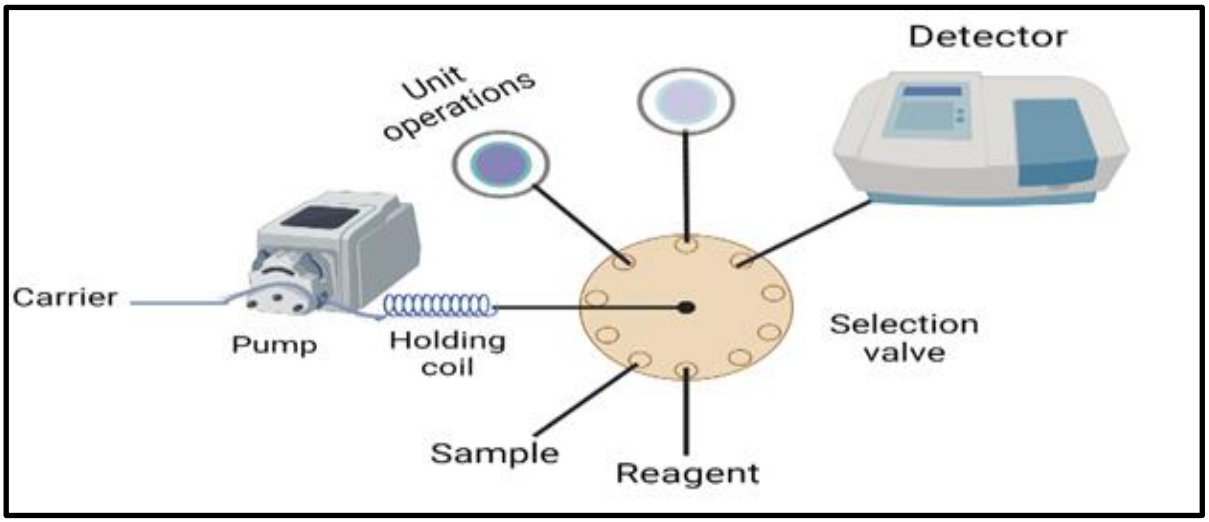

Figure [1.6]: The manifold of Sequential Injection Analysis

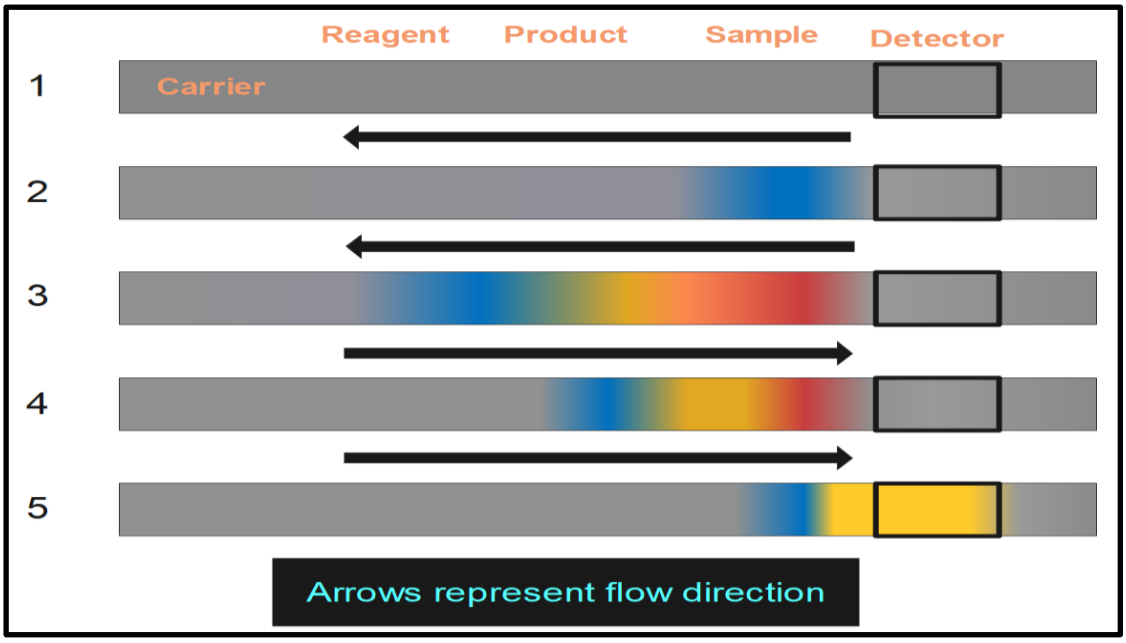

Figure [1.7]: The SIA method is composed of the following steps: (1) satisfying the holding coil (HC) with carrier solution, (2) aspirating the reagent into the HC, (3) aspirating the sample into the HC, (4) fraternization to generate a sample/reagent zone, and (5) measuring the product zone at the detector.

In addition to versatility and comprehensive computer interoperability, SIA offers excellent sample throughput and lower reagent and sample use than other systems.

1.1.2.6 Analyses of Injections Using Multiple Syringes

The multi-syringe flow injection analysis (MSFIA) technique was developed in 1999 as a very speedy and resilient solution for automating many procedures that combined the advantages of both the FIA and SIA techniques. Automatic flow injection systems of this type comprise an auto burette equipped with four syringes for injection. Peristaltic pumps move different liquids at high flow rates, comparable to how they work. Each syringe's head is equipped with a two-way commutation valve, which allows for coupling the needle to the manifold lines of the solution reservoir as desired [22].

1.1.3 Dispersion in FIA

Controlling the dispersion of the sample is one of the principles of FIA, so when designing any FIA system, attention is focused on two things: the amount of the original sample solution that is diluted by diffusion on its way towards the detector and the time it takes for the sample area to cut the distance from the injection valve to the sensor. Distribution occurs at the convergence of two liquids of different concentrations, as the internal penetration of the molecules of a fluid occurs through another fluid in contact with it, which is called dispersion. It contributes to the interaction between the sample material and the detector, increasing insensitivity. Also, it causes the occurrence of a mitigation process that, in turn, reduces sensitivity and increases the breadth of the top area. It is concluded that the dominant chemical reaction causes an increase in sensitivity with an increase in dispersion [23]. Still, sometimes dilution is the main influencing factor, which leads to a decrease in the method's

sensitivity, so it is necessary to control and balance the effects of the chemical reaction and the dilution process.

1.1.3.1 Dispersion Types

A- Axial Dispersion: occurs in the current flow direction and leads to attenuation and widening at the top, more significant than radial dispersion. The axial distribution clearly shows its effect in straight pipes, as shown in Figure [1.8], and the axial dispersion is called laminar flow [24].

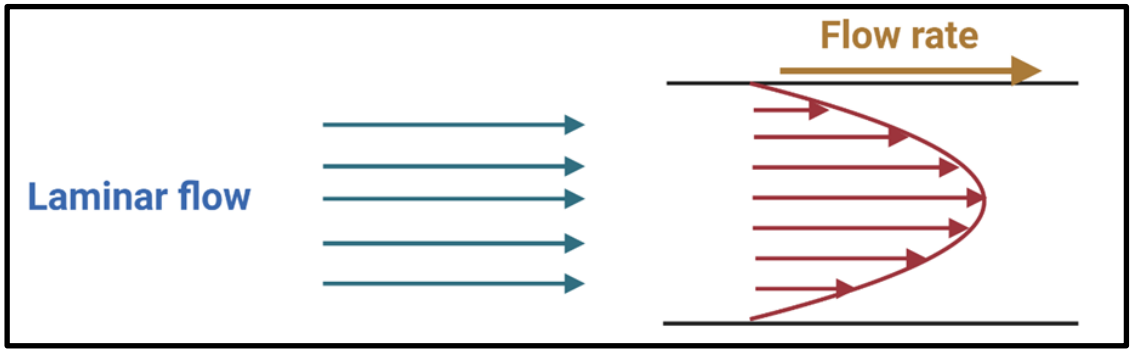

Figure [1.8]: Axial dispersion

B- Radial Dispersion: is produced by the effect of the current flowing, which is usually directed towards the walls, so it causes mixing to occur with the least amount of dilution and expansion in the area of the top. Using coiled tubes and reactors, the bends in the flow path cause greater sensitivity and narrow, sharp peaks. Figure [1.9] shows the flow path's radial dispersion resulting from hooks [25].

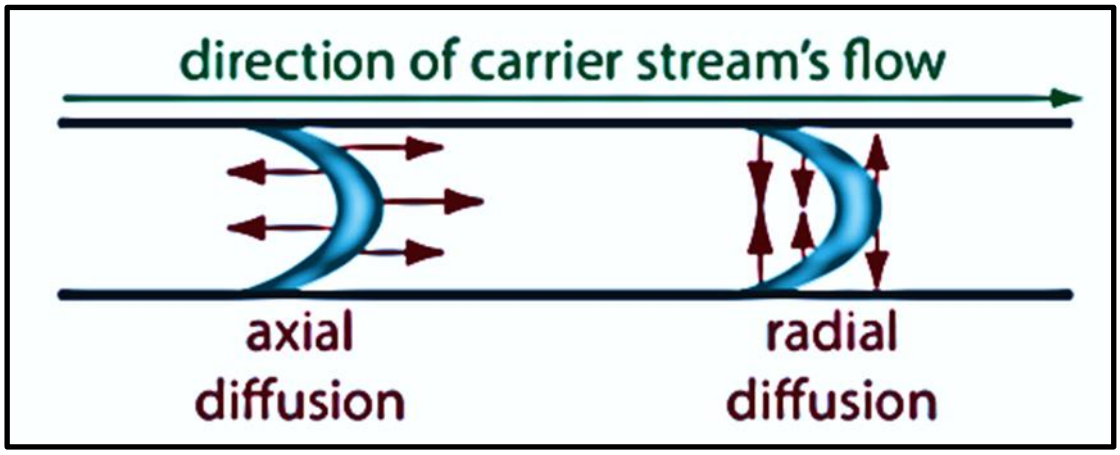

Figure [1.9]: Type of dispersion

1.1.3.2 Dispersion coefficient

The dispersion coefficient (D) is distinct as the ratio between the concentration before and after dilution as shown in Figure [1.10] [26-29].

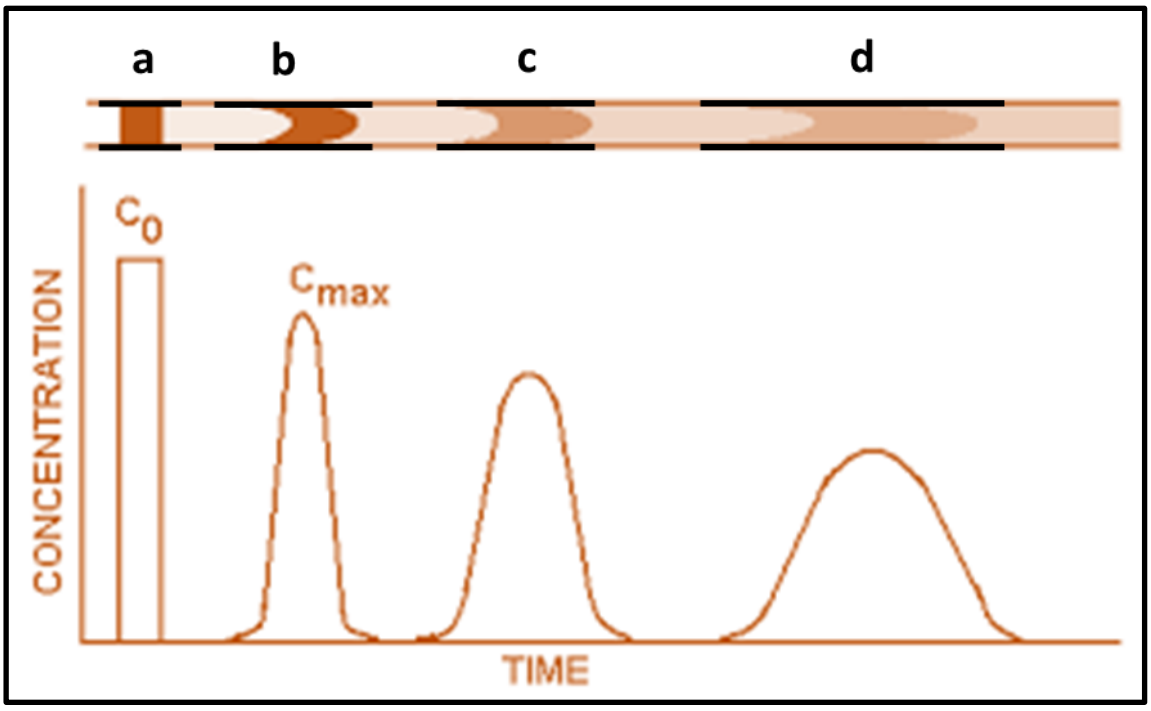

Figure [1.10]: Effect of dispersion on the shape of a sample's flow profile at different times during a flow injection analysis; (a) at injection valve before flow at the manifold ((t_o=0)), (b) when convection dominates dispersion

($((t_1>t_o))$), (c) when convection and diffusion contribute to dispersion($((t_2>t_1))$); and (d) when diffusion dominates dispersion ($((t_2>>))$). (Co= Conc. in injected volume, C= peak conc. at detector).

The dispersion coefficient is given by Equation [1.1].

$$D = C^o / C_{max} = H^o / H_{max} = A^o / A_{max} \ldots\ldots\ldots\ldots\ldots [1.1]$$

C_{max} Concentration after dilution in the recorded curve

C^o Original concentration of the injected form solution

H_{max}, H^o When dealing with the height of the summit as a reading

A_{max}, A^o When dealing with absorbance as a reading

The FIA regulations give dispersion three categories [30-34]**:**

1- When 3 > D > 1, the scattering is low or limited. It is preferred to achieve high analytical sensitivity in coordination with detectors with high sensitivity, such as ionic selective electrodes, atomic spectroscopy, and electrical conductivity.
2- When 10 > D > 3 the classification is as medium dispersion. It is commonly used whenever a special mixing process is required for the sample area with the detector, such as spectroscopic methods.
3- As for the high dispersion systems when D > 10, they are used in cases where parts require intense mixing of the sample area with the reagents, such as flow-injection adjustments and slow reactions that require a long time to complete the response.

1.1.3.3 Method for Calculating the Dispersion Coefficient

The dispersion coefficient is measured by comparing the response resulting from two cases [35, 36]

1- Mixing the sample solution at a specific concentration with the reacting solutions and injecting the resulting solution into the system as the resulting curve reaches a steady-state, which is °H, which is proportional to the concentration of the solution original °C, this response is free from dispersal effects.
2- The other case includes injecting the sample with the same concentration into the line of the carrier solution and recording the response H_{max} is proportional to the concentration C_{max}, as the effect of dispersion emerges, as the reaction here is less than continuous response (°C) and the value of D is calculated through Equation [1.1].

1.1.3.4 Factors Affecting the Dispersion of the Sample Area

The degree of dispersion and the height of the recorded peak is determined by several factors, including the injected sample and the flow channels' geometry, lengths, and flow velocity [37].

1.1.3.4.1 Injected Sample Volume

The injected model is one of the critical factors affecting the dispersion process. It increases the sensitivity size (peak height) as the size of the injected sample increases. Still, with larger volumes of samples, there will be no complete dispersion of the model in the reagent solution; as the increase in the example is relative to a decrease in sensitivity and an increase in time, the

detector may cause a broad peak or may cause a double in height and increase time to analyze necessary [38].

1.1.3.4.2 Volume of Reagents

The change in the volume of reagents through changing the lengths of the model connections plays an essential role in the effect on dispersion and, therefore, sensitivity, which increases directly with the size of the detector to increase the distribution of the sensor in the model. Still, the high volumes when reading the model cause distortion and a double peak. Still, the single-channel system means that the detector is the carrier solution, so the sensor size is ineffective. The latter does not apply to the single-channel system that operates with the inverse gastric injection technique, as the size of the detector becomes the effect mentioned previously [39].

1.1.3.4.3 Engineering Formation of Pipes

Reaction coils and coil-shaped tubes are preferred over straight lines, and this is to increase the degree of mixing with radial dispersion using secondary flow events as a result of centrifugal forces when the solution passes through the twisted areas, and this leads to a radial mixing in the size of the injected sample and thus reduces the axial dispersion [40].

1.1.3.4.4 Dimensions of the Reaction Coil

The scattering of the sample area upsurges with the increase in the internal diameters of the reaction coil, tubes, and channels, as the value of samples and D, is directly proportional to the square of the pipe diameter, so doubling the pipe diameter increases the volume the required reagents are four times. The dispersion of the sample area increases with the increase in the

distance it travels. With the rise in the length of the tubes, the time for diffusion increases, while there is less time for diffusion to occur in short-length tubes. In addition, increasing the length of the coil delays the analysis time, therefore, the number of samples is localized in a specific time, so it is preferable to use smaller lengths. When the output is formed at speed, sometimes it utilizes a high reaction coil lengths case. It is essential when the reaction needs time to complete (slow responses). The latter increases the reaction coil's length to increase the peak's height [41].

1.1.3.4.5 Flow Rate

Ruzica and Hansen explain that dispersal incidence is less at slow flow velocities. Decreasing the flow velocity increases the retention time of the sample before it is transferred to the detector. In this case, the model and sensor interaction reach equilibrium. Then the response will be higher at lower flow velocities. Higher velocities reduce sensitivity than lower velocities. A broad, double, distorted peak appears, increasing the analysis time and thus reducing the number of samples. The proportion of materials mixing and spreading among them may be slow, with an increase in speed. In the loop, the mixing increases at a specific time and, therefore, the height of the top gains [42].

1.1.3.4.6 The Degree of Mixing of Solutions

The mixing ratio of one substance solution varies with another when the sample solution mixes with the reagent quickly; this means that the dispersion is fast and a rapid response appears, but when the mixing is ventilated, the distribution is slow; also, this requires changing other factors that affect mixing and thus dispersion, such as velocity, temperature and length interaction file [43].

1.1.3.4.7 Concentration of Reagents

The reagent concentration is one factor that affects the scattering area and thus sensitivity. Low concentrations from the detector compared to the model's attention gives a low sensitivity. Still, increasing the engagement increases the sensitivity (Peak height). When all the sample quantity is reacted and converted into a product, the reagent concentration increase becomes non-existent effective. The high concentrations of the reagent 1 x 10^{-3} molar in the single-channel system in which the solution is the detector is the carrier current working to produce a noise more significant than the baseline. Therefore, it is preferable to use very dilute concentrations of 1 x 10^{-5} molar so that the noise of the detector signal does not interfere with the peak signal [44].

1.1.4 Components of Flow Injection Units:[45]

1. The pump propels the carrier stream through a narrow tube.
2. Connection tubes.
3. An injection port (injection valve) introduces a minor discrete sample or standard into the carrier stream.
4. Reaction coil: A sample processing step is responsible for the mixing of reagents, samples, and standards, the dilution of the piece, and the enrichment of models for trace study.
5. Detector: important to measure response.

1.2. Fluorescence

At ambient temperature, most molecules are at their lowest vibrational level, known as the ground electronic state, and are promoted to excited states due to light. Simple illustrations of molecule absorption to produce the first, S1,

or second, S2, excited states are shown in the following diagrams in Figure [1.11] [46].

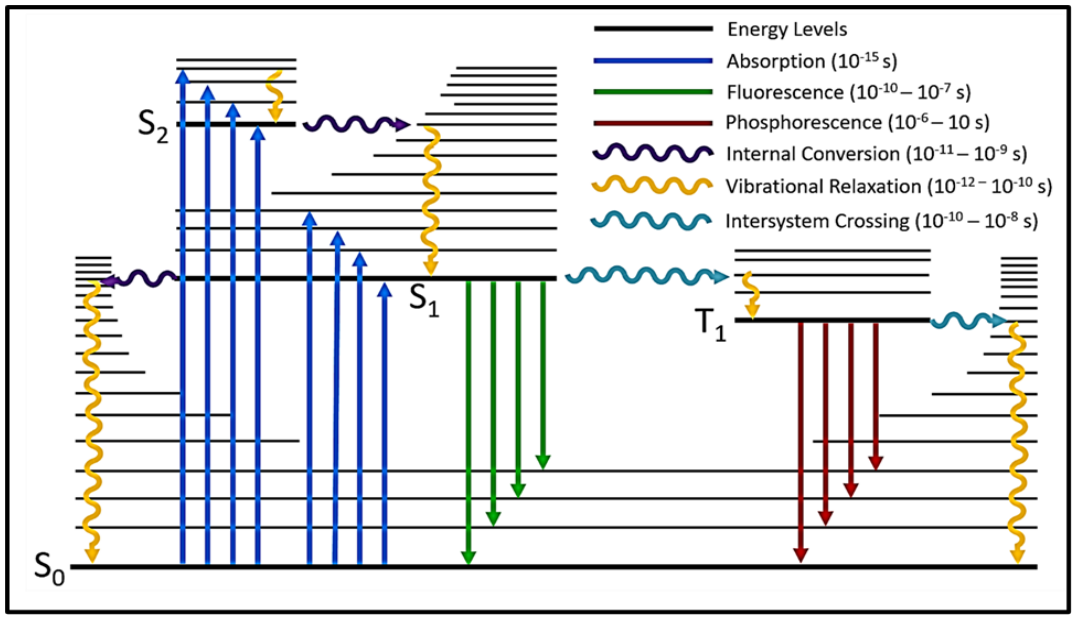

Figure [1.11]: Transitions that contribute to the formation of absorption and fluorescence emission spectra [47, 48]

Excitation can cause the molecule to vibrate at one of the vibrational sub-levels associated with each electronic state, depending on the nature of the excitation. Because the energy is absorbed in discrete quanta, distinct absorption bands are expected to be formed. As previously stated, the simplified picture above does not consider the rotational levels associated with each vibrational level, which generally increases the number of possible absorption bands to the point where individual transitions become challenging to resolve. As a result, most compounds, except those with local rotational levels, have broad absorption spectra (for example, planar and aromatic compounds). After absorbing energy and attaining one of the higher vibrational frequencies of the excited state, the molecule loses all of its surplus vibrational energy due to a collision with another molecule. It decays to the vibrational level that corresponds to the excited state's lowest vibrational level. As a bonus, virtually

every molecule with an electronic structure more significant than the second undergoes internal conversion and transitions with the same energy from its lowest vibrational level to a higher vibrational level of a lower excited state. For the molecules to achieve the lowest vibrational level of their initial excited state, they must continue to lose energy. The molecule can then return to any of the vibrational vibrations of the ground state, generating energy in the form of fluorescence. The quantum efficiency of the solution will be maximized if this step is repeated for all molecules that have absorbed light. If the alternative path is never used, the quantum efficiency of the alternative way will be less than one, and it may even be close to zero. The 0 - 0 transition, which connects the lowest vibrational level of the ground electronic state to the lowest vibrational level of the first excited state, happens in both absorption and emission processes and can be used to distinguish between the two types of methods [49]. All other absorption transitions take significantly more energy than fluorescence emission transitions. Therefore, it may be expected that the emission spectrum will overlap the absorption spectrum at the wavelength associated with the zero-to-zero transition and that the remainder of the emission spectrum will be either lower in energy or longer in wavelength than the absorption spectrum [50] Figure [1.12].

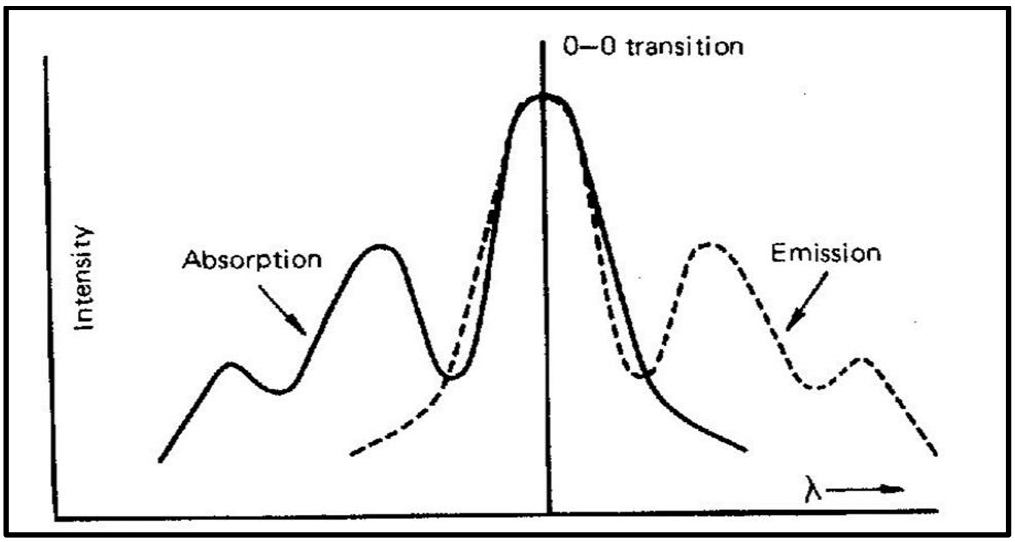

Figure [1.12]: Idealized Absorption and Emission Spectra [51]

The absorption and emission spectra coincide strictly at the spectrum's 0-0 transitions. The discrepancy signifies little energy lost due to the absorbing molecule's interaction with the solvent molecules in the surrounding environment. Due to the energy absorption necessary to reach the initial excited state, the molecule's structure is mostly unaffected. Accordingly, the ground and first excited states have a comparable distribution of vibrational levels. The energy discrepancies between emission and absorption bands will equal their energy disparities [52]. There are numerous instances where the emission spectra are the inverse of the absorption spectra. Because fluorescence emission always originates at the lowest vibrational level of the first excited state, the shape of the emission spectrum remains constant regardless of the wavelength of the stimulating light. The emission spectrum depicts how much light is emitted compared to the excitation wavelength. It is necessary to vary the wavelength of the exciting light while simultaneously charting the emission from the sample as a function of the wavelength of the exciting light to acquire the excitation spectrum. The corrected excitation spectrum is a plot of emission vs. excitation wavelength produced when the intensity of the exciting light remains constant while the wavelength of the light changes.

The quantum efficiency of complex compounds is not dependent on the wavelength of light used, which is valid for the vast majority of such compounds. Except for molecules with a high molecular extinction coefficient, the emission will be proportional to their molecular extinction coefficient. In other words, a substance's corrected excitation spectrum will be similar to its absorption spectrum if the substance does not have a high molecular extinction coefficient [53-55].

1.3. 1,2-Naphthoquinone-4-Sulfonate:

Inorganic amines and amino acids are being determined analytically utilizing 1,2-Naphthoquinone-4-sulfonate (NQS), which is increasingly being used in conjunction with ultraviolet/visible (UV-Vis) spectrophotometric detection methods [56-58]. In 1922, Folin proposed using of NQS as a reagent for the calorimetric determination of amino acids. Initial experiments resulted in the development of an amino acid identification method, in which amino groups are coupled with NQS in an alkaline solution to produce vibrantly colored molecules. Numerous studies have used the reagent to determine the presence of amines, and reddish dyes have been extracted into chloroform using the same method. The quantitative analysis of phenethylamine compounds was carried out using NQS [59]. Extraction of the reaction products was accomplished by thin-layer chromatography [60], which was followed by analysis utilizing a range of techniques, including elemental analysis, nuclear magnetic resonance (NMR), infrared (IR), and mass spectrometry [61] as shown in Figure [1.13].

Figure [1.13]: Image of NQS in nature and Chemical Structure

1.4 Drugs

1.4.1 Mefenamic Acid (MA)

1.4.1.1 Brief Introduction of Mefenamic Acid (MA):

Mefenamic acid, an anthranilic acid derivative, is a non-steroidal anti-inflammatory medication (NSAID) that belongs to the fenamate class [62]. It has a short plasma half-life of 2 hours. Non-steroidal anti-inflammatory drugs are classified into eight classes based on their structural similarities. Among these classes, anthranilic acid derivatives play a significant role. Mefenamic acid treats various types of discomfort, including menstrual cramps. It acts as an anti-inflammatory, analgesic, and antipyretic. Mefenamic, like other NSAIDs, is non-selective. It inhibits the two cyclooxygenase isoforms (COX-1 and COX-2), inhibiting the metabolism of cellular arachidonic acid (AA) and upregulating prostaglandin production, resulting in an increase in vascular permeability, edema, hyperalgesia, pyrexia, and inflammation [63-66]. IUPAC Name: N-(2,3-dimethyl phenyl)-2-aminobenzoic acid. Molecular Formula: $C_{15}H_{15}NO_2$ Figure [1.14]

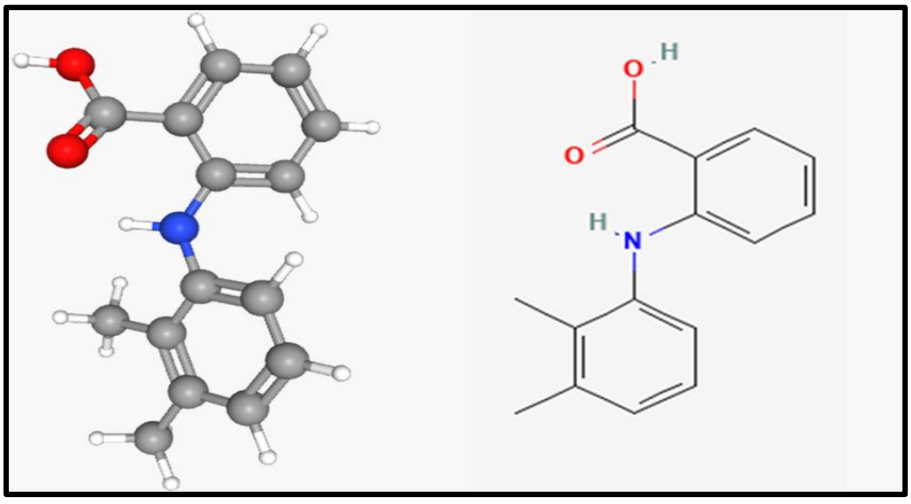

Figure [1.14]: The Chemical Structure of Mefenamic Acid.

1.4.1.2 Chemical and Physical Properties of Mefenamic Acid[65]

- Trade name: Ponstel, Ponstan, many others.
- Molecular Weight: 241.285 g/mol.
- State: Solid (i.e., a white crystalline powder).
- Solubility: It dissolves in dilute solutions of alkali hydroxides. Practically insoluble in water, slightly soluble in ethanol (96 percent), and methylene chloride.
- Pka= 4.2 (at 25℃).
- Elimination half-life: 2–4 hours.
- Melting point= 230 °C.

1.4.1.3 Dosage Forms of Mefenamic Acid [66]

MEF is available in the market as:

- Capsule.
- Tablet.

1.4.1.4 Usage of Mefenamic Acid

Relieve mild to moderate pain, including menstrual pain [63].

1.4.2. Procaine Hydrochloride

1.4.2.1 Brief Introduction of Procaine HCl

Caine is a short-acting ester local anesthetic which is used as a substitute for cocaine as a spinal aesthetic in the early twentieth century. It is also one of the earliest spinal aesthetics, having replaced cocaine as the preferred spinal aesthetic in the early twentieth century. However, due to concerns regarding lidocaine and transient neurologic symptoms (TNS), Procaine has been re-

evaluated as a fast-acting local aesthetic option. However, this medication is not widely used because it has a higher failure rate than lidocaine, causes significantly more nausea, and requires a longer recovery. 135 If used, it is often administered as a hyperbaric drug in dosages ranging from 50 to 200 mg at a 10 percent concentration [67-69]. IUPAC Name**:** 2-(diethylamino) ethyl4-aminobenzoate; hydrochloride. Molecular Formula: $C_{13}H_{21}ClN_2O_2$ Figure [1.15].

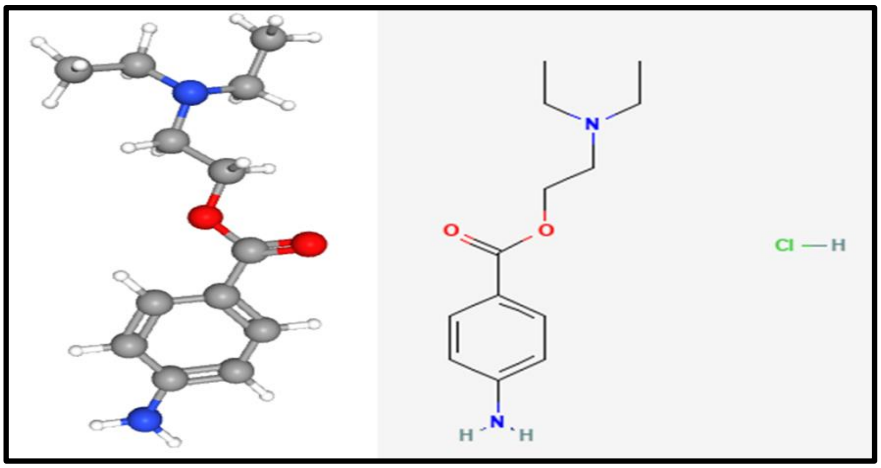

Figure [1.15]: The Chemical Structure of Procaine

1.4.2.2 Chemical and Physical Properties of Procaine [69]

- Trade name: Novocain or Neocene.
- Molecular Weight: 272.77 g/mole.
- State: Solid (i.e., a white crystalline powder).
- Solubility: It dissolves well in water and less in alcohol and is insoluble in ether.
- Elimination half-life: 40–84 seconds.
- Melting point: 155-175 °C.

1.4.2.3 Dosage Forms of Procaine

Procaine is available in the market as a capsule, tablet, and injection.

1.4.2.4 Using of Procaine:

- Local an aesthesia.
- To treat many diseases:
  - Fat.
  - Subscription.
  - Orgasm.
  - Cancer diseases.

1.5 Literature Review of the Analytical Method Used for the Determination of Mefenamic Acid and Procaine HCl

Table [1.1] below represents different methods that are used to determine Mefenamic Acid and Procaine hydrochloride.

Table [1.1]: Different Methods used to Determine Mefenamic Acid and Procaine Hydrochloride

	Reagent	λ_{max} nm	Technology	LOD mg L^{-1}	LOQ mg L^{-1}	R^2	Range mg L^{-1}	RSD	Slope	Recovery %	Ref.
Mefenamic acid	Potassium ferricyanide	465	FI Spectrophotometric	—	—	0.9998	1.00-100	0.82	1.68 $\times 10^{-2}$	—	[70]
	—	280	HPLC	15	25	0.998	25 – 4000 ng/mL	10.6 %	0.0003	110±7.5	[71]
	Ce (IV)	Ex 255 Em 354	Spectrofluorimetric	0.009	—	—	0.03 – 1.5	1.72 %	—	102–109	[72]
	—	300	HPLC	1.5	5.9	0.998	50 – 250	0.090	1.77	99.61	[73]
	—	—	potentiometric	6.2×10^{-7}	—	0.998	10^{-6}– 10^{-2}	1.5	58.9 ± 0.7	100.14	[74]
	Chloranil	540	spectrophotometric	2.16	7.15	0.9996	10 – 60	—	2.4×10^{-2}	—	[75]
	Ferric chloride with o-phenanthroline	510	Indirect Spectrophotometric	0.065	0.195	0.9993	0.4 – 2.0	<2.0	0.048	100 ± 0.92	[76]
	EEM	460	spectrofluorimetric	0.32	—	0.995	0.66 – 10.00	—	—	109.0	[77]

	Reagent	λ_{max} nm	Technology	LOD mg L^{-1}	LOQ mg L^{-1}	R^2	Range mg L^{-1}	RSD	Slope	Recovery %	Ref.
Mefenamic acid	—	220	RP-HPLC	0.39	1.2	0.999	100 – 300	—	866.4	99.7 – 102.2	[78]
	NQS	450	spectrophotometric	0.189	—	0.9995	0.5 – 10.0	1.29– 2.14	0.1409	99.80 – 100.80	[79]
	Astrafloxin	533	extraction – spectrophotometric	0.72	—	0.9988	2.0 – 21.0	—	0.1443	—	[80]
	—	280	extraction and HPLC	0.075	—	0.989	0.7– 100	4.2	—	—	[81]
	—	225	TLC-densitometric RP-HPLC-DAD	—	—	0.9999 , 0.9997	0.3–2 , 7–50	1.134 , 1.389	5207 , 117.11	99.558 ± 0.928 , 99.52 ± 0.346	[82]
	—	282	Developed HPLC	4.88	14.78	0.9999	1.29 – 806	1.07	0.2064	101.10 ± 1.56	[83]
	—	—	Voltametric	1.94 nM	—	0.990	1x 10^{-8} – 3x10^{-6} M	3.7375	—	96.35	[84]
	Metol	533	Spectrophotometric	0.03 mg/ml	0.1 mg/ml	0.9949	2.4 – 24	0.4	—	100.01	[85]

	Reagent	λ_{max} nm	Technology	LOD mg L^{-1}	LOQ mg L^{-1}	R^2	Range mg L^{-1}	RSD	Slope	Recovery %	Ref.
Procaine hydrochloride	4-dimethylaminocinnamaldehyde	547.5	stopped-flow	—	—	0.998	0.5 – 20	0.73	8.41×10^{-3}	—	[86]
	acetone and aged	Ex 402 Em 494	Spectrofluorimetric	7.7	—	0.999	0 –250	2.16	—	—	[87]
	p-dimethylaminobenzalhyde	455	Spectrophotometric	0.1	—	0.9994	0.2–15	1.7	—	92.0–110.0	[88]
	KMnO4	> 390	SIA-CL	0.3	—	0.9998	0.5–50	3.6	—	—	[89]
	pumice modified carbon paste electrode	—	DPV	5.0×10^{-8} M	—	0.995	9.0×10^{-7} – 2.6×10^{-5} M	3.2	5.062×10^{3}	95.2–104.8	[90]
	NQS	484	Spectrophotometric	0.28	—	0.9996	30 – 100	—	19.23	98.0 – 105.2	[91]

	Reagent	λ_{max} nm	Technology	LOD mg L^{-1}	LOQ mg L^{-1}	R^2	Range mg L^{-1}	RSD	Slope	Recovery %	Ref.
Procaine hydrochloride	fluorescamine	Ex 400 Em 494	sequential injection fluorometric	2.6	—	0.9980	10–200	2.1	—	—	[92]
	—	—	FIA using SPCE	6.0×10^{-6} M	—	0.9997	9.0×10^{-6}– 1.0×10^{-4} M	3.2	—	94.8 – 102.3	[93]
	H_2O_2	550	UV-Vis (EI)	3.80×10^{-8} M	—	0.9783	1.50×10^{-7}– 4.15×10^{-6} M	3.05	—	—	[94]
	Phenol	450	Spectrophotometric	1.2931	4.3103	0.9983	2–22	1.651	0.0798	99.82–101.50	[95]
	potassium peroxymonosulfate	—	polarographic	6×10^{-6}	1.9×10^{-6}	0.9996	1×10^{-6}– 5×10^{-5}	1.13	9.1×10^{4}	—	[96]
	Ag-Np	633	SERS	1×10^{-11} M	—	0.9994	10^{-7}– 10^{-10} M	—	216.12	—	[97]

1.5 The Current Work Aims at:

1. Designing new flow injection units to determination Mefenamic acid, Procaine hydrochloride, and NQS.
2. It is determining the optimum conditions for the reaction and studying the physical with chemical variables affecting the estimation, such as Flow rate, Reaction Coil, pH, Volume of buffer, and reagent concentration.
3. Calculating the sampling rate, dispersion coefficient, dead volume, and repeatability.
4. Mefenamic acid, Procaine, and NQS are determined from their aqueous solutions by spectrophotometric with FIA, batch spectrophotometric method, and Spectrofluorimetri

Reference

Reference:

1. van der LINDEN, W.E., Classification and definition of analytical methods based on flowing media (IUPAC Recommendations 1994). Pure and applied chemistry, 1994. 66(12): p. 2493-2500.

2. Tóth, K.S., K Kutner, Wlodzimierz Fehér, Zs Lindner, Erno, Electrochemical detection in liquid flow analytical techniques: Characterization and classification (IUPAC Technical Report). Pure and Applied Chemistry, 2004. 76(6): p. 1119-1138.

3. Skeggs, L.T., An automatic method for colorimetric analysis. American journal of clinical pathology, 1957. 28: p. 311-322.

4. Ruzicka, J.H., EH, Anal Chim Acta 78: 145; Danish Patent Application No. 4846/84, Sept 1974. US Patent, 1975. 4.

5. Růžička, J.S., JWB, Flow injection analysis: Part II. Ultrafast determination of phosphorus in plant material by continuous flow spectrophotometry. Analytica Chimica Acta, 1975. 79: p. 79-91.

6. Soto, C.S., Renato Contreras, David Poza, Cristián Orellana, Sandra Olivares-Rentería, Georgina A, Flow Injection Analysis (FIA) with Thermal Lens Spectrometry (TLS) for the Rapid Determination of Cefoperazone in Urine and Water. Analytical Letters, 2022. 55(12): p. 1932-1944.

7. Setayeshfar, I.R., Hamid Reza Khani, Omid, Application of flow injection analysis-solid phase extraction based on ion-pair formation for selective preconcentration of trace amount of anti-HIV drug. Microchemical Journal, 2022. 177: p. 107245.

8. Ghosh, S.A., Samar Sami Bornman, Charné Apollon, Wilgince Hussien, Aya Misbah Badawy, Ahmed Emad Amer, Mohamed Hussein Kamel, Manar Bakr Mekawy, Eman Ahmed Bedair, Heba, The application of rapid test paper technology for pesticide detection in horticulture crops: a comprehensive review. Beni-Suef University Journal of Basic and Applied Sciences, 2022. 11(1): p. 1-28.

9. Sanches, A.M.C.P., Maiyara Matos, Roberto Tarley, César R Teixeira Medeiros, Roberta A, Flow Injection Analysis System Coupled to Chronoamperometry and Boron-Doped Diamond Electrode for Determination of Synthetic Hormones 17α-Ethinylestradiol and Cyproterone Acetate. Analytical Letters, 2022: p. 1-17.

10. Oyella, D., Assessment of hydroquinone in selected cosmetic products sold on the market within Kampala. 2022, Makerere university.

11. Trojanowicz, M.P., Marta, Flow-Injection Methods in Water Analysis—Recent Developments. Molecules, 2022. 27(4): p. 1410.

12. Negrete, M.A.A.W., Kazimierz Barrientos, Eunice Yanez Escobosa, Alma Rosa Corrales Donis, Israel Enciso Wrobel, Katarzyna, Determination of chromium (III) picolinate in dietary supplements by flow injection-electrospray ionization-tandem mass spectrometry, using cobalt (II) picolinate as internal standard. Talanta, 2022. 240: p. 123161.

13. Betteridge, D.R., J, The determination of glyosbol in water by flow-injection analysis-a novel way of measuring viscosity. Talanta, 1976. 23(5): p. 409-410.

14. Hansen, E.H.R., Jaromir, Flow injection analysis: Part VI. The determination of phosphate and chloride in blood serum by dialysis and sample dilution. Analytica Chimica Acta, 1976. 87(2): p. 353-363.

15. Dutt, V.E.M., Horacio A, Repetitive determination of isonicotinic acid hydrazide in flow-through systems by series reactions. Analytical Chemistry, 1977. 49(6): p. 776-779.

16. Troanowicz, M., Flow Injection Analysis, Instrumentations and applications. 1st. Edition, World Scientific Publishing USA, 2000.

17. Zagatto, E.K., FJ Reis, BF, Merging zones in flow injection analysis: Part 1. Double proportional injector and reagent consumption. Analytica Chimica Acta, 1978. 101(1): p. 17-23.

18. Ruzicka, J.H., EH Ghose, Animesh K Mottola, HA, Enzymic determination of urea in serum based on pH measurement with the flow injection method. Analytical Chemistry, 1979. 51(2): p. 199-203.

19. Johnson, K.S.P., Robert L, Determination of nitrate and nitrite in seawater by flow injection analysis 1. Limnology and Oceanography, 1983. 28(6): p. 1260-1266.

20. Pasquini, C.D.O., Walace A, Monosegmented system for continuous flow analysis. Spectrophotometric determination of chromium (VI), ammonia and phosphorus. Analytical Chemistry, 1985. 57(13): p. 2575-2579.

21. Ruzicka, J.M., Graham D, Sequential injection: a new concept for chemical sensors, process analysis and laboratory assays. Analytica Chimica Acta, 1990. 237: p. 329-343.

22. Martín, V.C.E., Jose Manuel, Multicommutated Flow Injection Analysis, Multisyringe Flow Injection Analysis, and Multipumping Flow Systems. Flow Injection Analysis of Food Additives, 2015. 1: p. 79.

23. Trojanowicz, M., Advances in flow analysis. 2008: John Wiley & Sons.

24. Sherritt, R.G.C., Jamal Mehrotra, Anil K Behie, Leo A, Axial dispersion in the three-dimensional mixing of particles in a rotating drum reactor. Chemical Engineering Science, 2003. 58(2): p. 401-415.

25. Ingram, A.S., JPK Parker, DJ Fan, Xianfeng Forster, RG, Axial and radial dispersion in rolling mode rotating drums. Powder technology, 2005. 158(1-3): p. 76-91.

26. Kato, T.K., Yasushi Nishimura, Masayuki, Temperature dependence of chromatic dispersion in various types of optical fiber. Optics Letters, 2000. 25(16): p. 1156-1158.

27. Aubin, J.P., L Xuereb, Catherine Gourdon, Christophe, Effect of microchannel aspect ratio on residence time distributions and the axial dispersion coefficient. Chemical Engineering and Processing: Process Intensification, 2009. 48(1): p. 554-559.

28. Njeng, A.B.V., Stéphane Clausse, Marc Dirion, J-L Debacq, Marie, Effect of lifter shape and operating parameters on the flow of materials in a pilot rotary kiln: Part I. Experimental RTD and axial dispersion study. Powder Technology, 2015. 269: p. 554-565.

29. Wells, M.S., DE, The effects of crossing trajectories on the dispersion of particles in a turbulent flow. Journal of fluid mechanics, 1983. 136: p. 31-62.

30. Rastegar, S.O.G., Tingyue, Empirical correlations for axial dispersion coefficient and Peclet number in fixed-bed columns. Journal of Chromatography A, 2017. 1490: p. 133-137.

31. Parsaie, A.H., Amir Hamzeh, Predicting the longitudinal dispersion coefficient by radial basis function neural network. Modeling earth systems and environment, 2015. 1(4): p. 1-8.

32. Rubio, F.C.M., A Sánchez García, MC Cerón Camacho, F García Grima, E Molina Chisti, Y, Mixing in bubble columns: a new approach for characterizing dispersion coefficients. Chemical Engineering Science, 2004. 59(20): p. 4369-4376.

33. Liu, H., Predicting dispersion coefficient of streams. Journal of the Environmental Engineering Division, 1977. 103(1): p. 59-69.

34. Caldeweyher, E.B., Christoph Grimme, Stefan, Extension of the D3 dispersion coefficient model. The Journal of chemical physics, 2017. 147(3): p. 034112.

35. Jiemchooroj, A.N., Patrick Sernelius, Bo E, Complex polarization propagator method for calculation of dispersion coefficients of extended π-conjugated systems: The C 6 coefficients of polyacenes and C 60. The Journal of chemical physics, 2005. 123(12): p. 124312.

36. Ruiz-Capillas, C.N., Leo ML, Flow injection analysis of food additives. Vol. 1. 2015: CRC Press.

37. Ruzicka, J.H., Elo Harald, Flow injection analysis. Vol. 104. 1988: John Wiley & Sons.

38. Weng Larsen, S.L., Claus, Critical factors influencing the in vivo performance of long-acting lipophilic solutions—impact on in vitro release method design. The AAPS journal, 2009. 11(4): p. 762-770.

39. Lapa, R.A.L., José LFC Reis, Boaventura F Santos, João LM Zagatto, Elias AG, Multi-pumping in flow analysis: concepts, instrumentation, potentialities. Analytica Chimica Acta, 2002. 466(1): p. 125-132.

40. Whitson, M., Glossary of fusion energy. 1985, USDOE Office of Scientific and Technical Information, Oak Ridge, TN.

41. Kovacev, N.L., Sheng Zeraati-Rezaei, Soheil Hemida, Hassan Tsolakis, Athanasios Essa, Khamis, Effects of the internal structures of monolith ceramic substrates on thermal and hydraulic properties: additive manufacturing, numerical modelling and experimental testing. The International Journal of Advanced Manufacturing Technology, 2021. 112(3): p. 1115-1132.

42. Osborne, O.D.P., Allan Lenehan, Claire E, A simple colorimetric FIA method for the determination of pyrite oxidation rates. Talanta, 2010. 82(5): p. 1809-1813.

43. Bourne, J.K., F Rys, P, Mixing and fast chemical reaction—I: Test reactions to determine segregation. Chemical Engineering Science, 1981. 36(10): p. 1643-1648.

44. Zagatto, E.A.G.A., MAZ Jacintho, Antonio Octavio Mattos, IL, Compensation of the Schlieren effect in flow-injection analysis by using dual-wavelength spectrophotometry. Analytica Chimica Acta, 1990. 234: p. 153-160.

45. Shiundu, P.M., Automated methods development in flow injection analysis. 1991.

46. Hammond, G.S.T., Nicholas J, Organic Photochemistry: The study of photochemical reactions provides new information on the excited states of molecules. Science, 1963. 142(3599): p. 1541-1553.

47. Wachtler, M.S., Adolfo Gatterer, Karl Fritzer, Harald P Ajo, David Bettinelli, Marco, Optical properties of rare-earth ions in lead germanate

glasses. Journal of the American Ceramic Society, 1998. 81(8): p. 2045-2052.

48. Bejaoui, S.M., Xavier Desgroux, Pascale Therssen, Eric, Laser induced fluorescence spectroscopy of aromatic species produced in atmospheric sooting flames using UV and visible excitation wavelengths. Combustion and Flame, 2014. 161(10): p. 2479-2491.

49. Cartwright, D.C., Vibrational populations of the excited states of N2 under auroral conditions. Journal of Geophysical Research: Space Physics, 1978. 83(A2): p. 517-531.

50. Vandewal, K.B., J Nikolis, VC, How to determine optical gaps and voltage losses in organic photovoltaic materials. Sustainable Energy & Fuels, 2018. 2(3): p. 538-544.

51. Fan, C.H.S., Peipei Su, Tsu-Hui Cheng, Chien-Hong, Host and dopant materials for idealized deep-red organic electrophosphorescence devices. Advanced Materials, 2011. 23(26): p. 2981-2985.

52. Dorenbos, P., The 4fn↔ 4fn− 15d transitions of the trivalent lanthanides in halogenides and chalcogenides. Journal of luminescence, 2000. 91(1-2): p. 91-106.

53. Ishida, H.T., Seiji Hasegawa, Yasuchika Katoh, Ryuzi Nozaki, Koichi, Recent advances in instrumentation for absolute emission quantum yield measurements. Coordination chemistry reviews, 2010. 254(21-22): p. 2449-2458.

54. Würth, C.G., Markus Pauli, Jutta Spieles, Monika Resch-Genger, Ute, Relative and absolute determination of fluorescence quantum yields of transparent samples. Nature protocols, 2013. 8(8): p. 1535-1550.

55. Brouwer, A.M., Standards for photoluminescence quantum yield measurements in solution (IUPAC Technical Report). Pure and Applied Chemistry, 2011. 83(12): p. 2213-2228.

56. Al-Tamimi, S.A.A.-M., Norah Sultan Abdulaziz Aly, Fatma Ahmed, Utility of Spectroscopic Studies for Quantification of Cefditoren Pivoxil in Commercial Samples. Journal of the Chemical Society of Pakistan, 2021. 43(4).

57. Kazemipour, M.F., Iman Ansari, Mehdi, Gabapentin Determination in Human Plasma and Capsule by Coupling of Solid Phase Extraction, Derivatization Reaction, and UV-Vis Spectrophotometry. Iranian Journal of Pharmaceutical Research: IJPR, 2013. 12(3): p. 247.

58. Elbashir, A.A.A., Abir Abdalla Ali Ahmed, Shazalia M Aboul-Enein, Hassan Y, 1, 2-Naphthoquinone-4-sulphonic acid sodium salt (NQS) as an analytical reagent for the determination of pharmaceutical amine by spectrophotometry. Applied Spectroscopy Reviews, 2012. 47(3): p. 219-232.

59. Hashimoto, Y.E., Masaru Tominaga, Keiko Inuzuka, Shigeko Moriyasu, Masataka, Quantitative analysis of phenethylamine derivatives by thin layer chromatography. Determination of psychotropic drugs and ephedra bases. Microchimica Acta, 1978. 70(5): p. 493-504.

60. Farrell, B.J., TM, An investigation of high-performance liquid chromatographic methods for the analysis of amphetamines. Journal of Chromatography B: Biomedical Sciences and Applications, 1983. 272: p. 111-128.

61. Darwish, I.A.A., Heba H Amer, Sawsan M Al-Rayes, Lama I, Spectrophotometric study for the reaction between fluvoxamine and 1, 2-naphthoquinone-4-sulphonate: Kinetic, mechanism and use for determination of fluvoxamine in its dosage forms. Spectrochimica Acta Part A: Molecular and Biomolecular Spectroscopy, 2009. 72(4): p. 897-902.

62. Choi, K.C., Jung-Kap Yoo, Gyurng-Soo, Spectrophotometric determination of amantadine sulfate after ion-pairing with methyl orange. Archives of Pharmacal Research, 1991. 14(4): p. 285-289.

63. de Abajo, F.J.R., Luis Alberto García Montero, Dolores, Association between selective serotonin reuptake inhibitors and upper gastrointestinal bleeding: population based case-control study. Bmj, 1999. 319(7217): p. 1106-1109.

64. Kuznetsova, L.A.C., W Terence, Applications of ultrasound streaming and radiation force in biosensors. Biosensors and Bioelectronics, 2007. 22(8): p. 1567-1577.

65. J, d.A.F., Effects of selective serotonin reuptake inhibitors on platelet function. Drugs & aging, 2011. 28(5): p. 345-367.

66. Sowjanya, K.T., JC Gurupadayya, BM Indupriya, M, Spectrophotometric determination of pregabalin using Gibb's and MBTH reagent in pharmaceutical dosage form. Der Pharma Chemica, 2011. 3(1): p. 112-122.

67. Steindler, A.L., JV, Differential diagnosis of pain low in the back: allocation of the source of pain by the procaine hydrochloride method. Journal of the American Medical Association, 1938. 110(2): p. 106-113.

68. Outland, T.H., CR, The use of procaine hydrochloride as a therapeutic agent. Journal of the American Medical Association, 1940. 114(14): p. 1330-1333.

69. Chapman, C.C., P Nielsen, IL Sitaram, BR Huntington, PJ, The role of procaine in adverse reactions to procaine penicillin in horses. Australian veterinary journal, 1992. 69(6): p. 129-133.

70. García, S.S.-P., Concepción Albero, Isabel García, Concepción, Flow-injection spectrophotometric determination of diclofenac or mefenamic acid in pharmaceuticals. Microchimica Acta, 2001. 136(1): p. 67-71.

71. Rouini Mohammad-Reza Asadipour Ali Ardakani, Y.H.A., Fakhredin, Liquid chromatography method for determination of mefenamic acid in human serum. Journal of Chromatography B, 2004. 800(1-2): p. 189-192.

72. Ahad, B.-T., A Simple Spectrofluorimetric Method for Determination of Mefenamic Acid in Pharmaceutical Preparation and Urine. Bulletin of the Korean Chemical Society, 2006. 27.

73. Jaiswal, Y.T., Gokul Surana, Sanjay, Application of HPLC for the simultaneous determination of ethamsylate and mefenamic acid in bulk

drugs and tablets. Journal of liquid chromatography & related technologies, 2007. 30(8): p. 1115-1124.

74. Santini, A.P., Helena Redigolo Pezza, Leonardo, Development of a potentiometric mefenamate ion sensor for the determination of mefenamic acid in pharmaceuticals and human blood serum. Sensors and Actuators B: Chemical, 2007. 128(1): p. 117-123.

75. Raza, A., Spectrophotometric determination of mefenamic acid in pharmaceutical preparations. Journal of Analytical Chemistry, 2008. 63(3): p. 244-247.

76. M Al-mufty, Z.R.A., Nief, Indirect spectrophotometric method for the determination of mefenamic acid in pharmaceutical formulations. Rafidain journal of science, 2009. 20(6): p. 39-47.

77. Madrakian, T.A., Abbas Mohammadnejad, Masoumeh, Second-order advantage applied to simultaneous spectrofluorimetric determination of paracetamol and mefenamic acid in urine samples. Analytica chimica acta, 2009. 645(1-2): p. 25-29.

78. Havaldar, F.H.V., Dharmendra L, Simultaneous determination of paracetamol, acetyl salicylic acid, mefenamic acid and cetirizine dihydrochloride in the pharmaceutical dosage form. E-Journal of Chemistry, 2010. 7(S1): p. S495-S503.

79. Dikran, S.B.M., Ala Karim al-Jabburi, Muin Iskandar Nasir, Ahmad Saib, Spectrophotometric determination of mefenamic acid in pharmaceutical

preparations. Ibn al-Haitham Journal for Pure and Applied Science, 2014(Vol. 27, Issue 3 (31 Dec. 2014), pp.339-349, 11 p.): p. 11.

80. Kormosh, Z.A.M., O. Yu Bazel', Ya R., Extraction-spectrophotometric determination of mefenamic acid in pharmaceutical preparations. Journal of Analytical Chemistry, 2014. 69(10): p. 960-964.

81. Kahkha, M.R.R.K., Massoud Afarani, Mahdi Shafiee Sepehri, Zahra, Determination of mefenamic acid in urine and pharmaceutical samples by HPLC after pipette-tip solid phase microextraction using zinc sulfide modified carbon nanotubes. Analytical Methods, 2016. 8(30): p. 5978-5983.

82. Morcoss, M.M.A., Nada S Ali, Nouruddin W Elsaady, Mohammed T, Different chromatographic methods for simultaneous determination of mefenamic acid and two of its toxic impurities. Journal of chromatographic science, 2017. 55(7): p. 766-772.

83. ATIPAIRIN, A.S., SOMCHAI, DETERMINATION OF MEFENAMIC ACID IN A TOPICAL EMULGEL BY A VALIDATED HPLC METHOD. International Journal of Applied Pharmaceutics, 2019: p. 86-90.

84. Malode, S.J.S., Nagaraj P Kulkarni, Raviraj M, Voltammetric detection and determination of mefenamic acid at silver-doped TiO2 nanoparticles modified electrode. Materials Today: Proceedings, 2019. 18: p. 671-678.

85. Rashad, I.Q.B., Mohsin Hamza. Spectrophotometric Determination of Mefenamic acid using Metol reagent by Oxidative Coupling Reaction. in IOP Conference Series: Materials Science and Engineering. 2021. IOP Publishing.

86. Carmona, M.S., Manuel Pérez-Bendito, Dolores, A selective and sensitive kinetic method for the determination of procaine and benzocaine in pharmaceuticals. Journal of pharmaceutical and biomedical analysis, 1992. 10(2-3): p. 145-152.

87. Carretero, A.S.C.-B., C Peinado, S Fernández El Bergmi, R Gutiérrez, A Fernández, Fluorimetric determination of procaine in pharmaceutical preparations based on its reaction with fluorescamine. Journal of pharmaceutical and biomedical analysis, 1999. 21(5): p. 969-974.

88. Liu, L.D.L., Yuan Wang, Huai You Sun, Yue Ma, Li Tang, Bo, Use of p-dimethylaminobenzalhyde as a colored reagent for determination of procaine hydrochloride by spectrophotometry. Talanta, 2000. 52(6): p. 991-999.

89. Paseková, H.P., Miroslav, Determination of procaine, benzocaine and tetracaine by sequential injection analysis with permanganate-induced chemiluminescence detection. Talanta, 2000. 52(1): p. 67-75.

90. Wang, C.Y.H., Xiao Ya Di Jin, Gen Leng, Zong Zhou, Differential pulse adsorption voltammetry for determination of procaine hydrochloride at a pumice modified carbon paste electrode in pharmaceutical preparations and urine. Journal of pharmaceutical and biomedical analysis, 2002. 30(1): p. 131-139.

91. Xu, L.X.S., Yun Xiu Wang, Huai You Jiang, Ji Gang Xiao, Yan, Spectrophotometric determination of procaine hydrochloride in pharmaceutical products using 1, 2-naphthoquinone-4-sulfonic acid as the chromogenic reagent. Spectrochimica Acta Part A: Molecular and Biomolecular Spectroscopy, 2003. 59(13): p. 3103-3110.

92. Chen, X.-W.S., Xin Wang, Jian-Hua, A sequential injection fluorometric procedure for the determination of procaine in human blood and pharmaceuticals. Analytical and bioanalytical chemistry, 2006. 385(4): p. 737-741.

93. Bergamini, M.F.S., André L Stradiotto, Nelson R Zanoni, Maria Valnice B, Flow injection amperometric determination of procaine in pharmaceutical formulation using a screen-printed carbon electrode. Journal of pharmaceutical and biomedical analysis, 2007. 43(1): p. 315-319.

94. Chen, Y.-H.T., Feng-Shou Song, Mao-Ping, Spectrophotometric determination of procaine hydrochloride with hemoglobin as catalyst. Journal of analytical chemistry, 2009. 64(4): p. 366-370.

95. Al-Uzri, W.A., Spectrophotometric Determination of Procaine Hydrochloride in Pharmaceutical Preparations via Diazotization-Coupling Reaction with Phenol. Asian Journal of Chemistry, 2015. 27(12).

96. Plotycya, S.S., Oksana Pysarevska, Solomiya Blazheyevskiy, Mykola Dubenska, Liliya, A new approach for the determination of benzocaine and procaine in pharmaceuticals by single-sweep polarography. International Journal of Electrochemistry, 2018. 2018.

97. Abdulazeez, I.P., Saheed A Saleh, Tawfik A Al-Saadi, Abdulaziz A, Spectroscopic, DFT and trace detection study of procaine using surface-enhanced Raman scattering technique. Chemical Physics Letters, 2019. 730: p. 617-622.

98. Bülbül, B.B., Seda, Developing of buffer-precipitation method for lead metaborate (Pb (BO2)(2) center dot H2O) nanostructures. 2020.

99. Attia, K.A.E.-O., Ahmed Ramzy, Sherif Abdelazim, Ahmed H Hasan, Mohamed A Abdel-Kareem, Rady F, Simultaneous determination of elbasvir and grazoprevir in their pharmaceutical formulation by synchronous fluorescence spectroscopy coupled to dual wavelength method. Spectrochimica Acta Part A: Molecular and Biomolecular Spectroscopy, 2021. 248: p. 119157.

100. Chayavanich, K.T., Pattara Imyim, Apichat, Biocompatible film sensors containing red radish extract for meat spoilage observation. Spectrochimica Acta Part A: Molecular and Biomolecular Spectroscopy, 2020. 226: p. 117601.

101. Aupoil, J.C., Jean-Baptiste de Lacaillerie, Jean-Baptiste d'Espinose Poulesquen, Arnaud, Interplay between silicate and hydroxide ions during geopolymerization. Cement and Concrete Research, 2019. 115: p. 426-432.